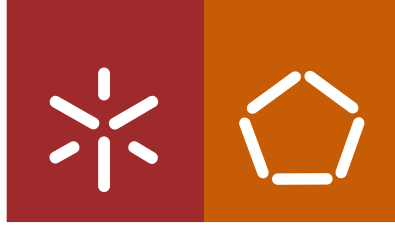




Universidade do Minho
Escola de Engenharia

Cristiano da Silva Leal

Operation and monitoring of a sequencing batch reactor with aerobic granular biomass in the presence of pharmaceutically active compounds using quantitative image analysis and chemometric techniques



Universidade do Minho
Escola de Engenharia

Cristiano da Silva Leal

Operation and monitoring of a sequencing batch reactor with aerobic granular biomass in the presence of pharmaceutically active compounds using quantitative image analysis and chemometric techniques

Tese de Doutoramento
Doutoramento em Engenharia Química e Biológica

Trabalho efetuado sob a orientação da
Professora Doutora Daniela Patrícia Bernardino Mesquita
e do
Professor Doutor António Luís Pereira do Amaral

DIREITOS DE AUTOR E CONDIÇÕES DE UTILIZAÇÃO DO TRABALHO POR TERCEIROS

Este é um trabalho académico que pode ser utilizado por terceiros desde que respeitadas as regras e boas práticas internacionalmente aceites, no que concerne aos direitos de autor e direitos conexos. Assim, o presente trabalho pode ser utilizado nos termos previstos na licença abaixo indicada. Caso o utilizador necessite de permissão para poder fazer um uso do trabalho em condições não previstas no licenciamento indicado, deverá contactar o autor, através do RepositóriUM da Universidade do Minho.

Licença concedida aos utilizadores deste trabalho



Atribuição-NãoComercial-SemDerivações
CC BY-NC-ND

<https://creativecommons.org/licenses/by-nc-nd/4.0/>

AGRADECIMENTOS

Gostaria de agradecer a todos os que acompanharam a realização deste trabalho.

Primeiramente gostaria de agradecer aos meus orientadores Doutora Daniela Patrícia Bernardino Mesquita e Doutor António Luís Pereira do Amaral pela confiança disponibilidade e apoio neste caminho. O entusiasmo demonstrado e a partilha de conhecimento em muito contribuiu para a melhoria desta Tese.

Quero também agradecer ao Professor Doutor Eugénio Campos Ferreira a disponibilidade e a oportunidade de desenvolver trabalho no grupo BIOSYSTEMS.

Agradeço à Doutora Cristina Quintelas a preciosa ajuda e as palavras de motivação durante este caminho.

Agradeço à Doutora Angeles Val del Rio o apoio incondicional, a motivação e ajuda durante todos estes anos, mas especialmente numa fase inicial deste Doutoramento durante a sua estadia no Centro de Engenharia Biológica. Sem dúvida que as suas palavras me motivaram na altura certa desta caminhada.

Agradeço a todos os colegas do Laboratório de Bioprocessos e Bioprodutos Sustentáveis (LBBS) e do Laboratório de Biotecnologia Ambiental (LBA) pela disponibilidade de partilha de equipamentos.

Agradeço ao René Benevides pelas preciosas discussões que certamente contribuíram para a construção desta Tese e pelo suporte durante as atividades experimentais.

Agradeço à Natércia a ajuda as palavras de apoio e confiança sem dúvida o caminho ficou mesmo menos tortuoso assim!!

Ao Yves, à Martine e à Isabel pelo suporte durante a minha passagem pelo Instituto Superior de Engenharia de Coimbra (ISEC).

Agradeço à Sandra as sugestões! Mesmo distante acompanhaste o trabalho de perto!!!

Finalmente agradeço à Ana, à minha família e amigos a paciência e confiança depositada em mim, extremamente importante durante estes anos, a vós vos dedico o empenho destes anos.

The work presented in this thesis was financially supported by a doctoral advanced training (call NORTE-69-2015-15) funded by the European Social Fund under the scope of Norte2020 - Programa Operacional Regional do Norte.

DECLARAÇÃO DE INTEGRIDADE

Declaro ter atuado com integridade na elaboração do presente trabalho académico e confirmo que não recorri à prática de plágio nem a qualquer forma de utilização indevida ou falsificação de informações ou resultados em nenhuma das etapas conducente à sua elaboração.

Mais declaro que conheço e que respeitei o Código de Conduta Ética da Universidade do Minho.

Operação e monitorização de um reator descontínuo sequencial com biomassa granular aeróbia na presença de compostos farmacologicamente ativos utilizando análise quantitativa de imagem e técnicas quimiométricas

Sumário

Nesta tese foi operado um reator descontínuo sequencial, inoculado com AGS (SBR-AGS) proveniente de um sistema granular à escala real, para o tratamento de água residual sintética, primeiramente sem qualquer adição de fármaco e posteriormente adicionando os estrogénios 17 β -estradiol (E2) e 17 α -etinilestradiol (EE2) e o antibiótico sulfametoxazol (SMX). Foram ainda desenvolvidas e otimizadas novas metodologias de amostragem e separação das frações baseadas no conteúdo em sólidos suspensos, de aquisição em microscopia de campo claro e em lupa binocular, para a fração de flocos e grânulos, respetivamente, assim como os necessários programas de processamento e análise quantitativa de imagens (QIA). Foram ainda aplicadas diferentes técnicas quimiométricas, incluindo a regressão linear múltipla (MLR), análise de componentes principais (PCA), árvores de decisão (DT) e análise discriminante (DA) aos dados relativos à estrutura e morfologia da biomassa, assim como aos parâmetros operacionais do reator. O sistema de SBR-AGS, após um processo de maturação da biomassa aeróbia, apresentou um claro predomínio da fração granular sobre a fração flocular, caracterizado por uma predominância de grânulos de elevado tamanho (superiores a 2.5 mm em diâmetro), robustos, estruturalmente estáveis e com uma boa sedimentabilidade. Adicionalmente verificou-se o predomínio da fração orgânica nos agregados, face à inorgânica, não tendo sido verificados fenómenos de *bulking* no sistema. A aplicação de PCA aos dados obtidos permitiu isolar claramente os *clusters* correspondentes aos períodos operacionais com a biomassa madura e com a adição dos diferentes fármacos e identificar as principais correlações entre os parâmetros estudados. No tocante à previsão por MLR dos sólidos suspensos (totais – TSS e voláteis – VSS) de ambas as frações, da densidade da biomassa e do índice volumétrico de lamas, foram obtidos resultados promissores. A aplicação de DA e DT aos dados obtidos permitiu distinguir, com sucesso, os diferentes períodos operacionais e identificar as amostras contendo PhACs.

Palavras-chave: análise quantitativa de imagem, biomassa granular aeróbia, compostos farmacologicamente ativos, técnicas quimiométricas

Operation and monitoring of a sequencing batch reactor with aerobic granular biomass in the presence of pharmaceutically active compounds using quantitative image analysis and chemometric techniques

Summary

In this thesis, a laboratory scale sequencing batch reactor (SBR) inoculated with AGS from a full-scale WWTP was operated for the treatment of a synthetic wastewater, first in the absence of PhACs and later in the presence of the 17β -estradiol (E2) and 17α -ethinylestradiol (EE2) steroid estrogens and the sulfamethoxazole (SMX) sulphonamide antibiotic. New methodologies for sampling and biomass granular and floccular fractions separation, based on the suspended solids content, as well as bright field and stereomicroscopy monitoring and image acquisition, were also developed and optimized, as well as the necessary quantitative image analysis (QIA) routines. In order to best comprehend the collected data, different chemometric tools were also applied, including multilinear regression (MLR), principal component analysis (PCA), discriminant analysis (DA) and decision trees (DT) to the morphological and structural parameters of the biomass and the main operational parameters of the SBR. The SBR-AGS system, after a maturation process of the aerobic biomass, showed a clear predominance of the granular fraction over the floccular one, characterized by a predominance of granules of large size (larger than 2.5 mm in diameter), robust, structurally stable and with good settling properties. Additionally, there was a predominance of the organic fraction in the aggregates, compared to the inorganic one, with no bulking phenomena being observed in the system. The performed PCA allowed to clearly isolate the clusters corresponding to the experimental periods with mature AGS and E2, EE2 and SMX addition, and enlighten the studied parameters interrelationships. Regarding the MLR forecast of both fractions total (TSS) and volatile (VSS) suspended solids, biomass density and sludge volumetric index, promising results were obtained. Besides, the application of DA and DT allowed to identify the different operational periods, and successfully classify the samples in the presence and in absence of the PhAC.

Keywords: Aerobic granular sludge, chemometric tools, pharmaceutically active compounds, quantitative image analysis

TABLE OF CONTENTS

Chapter 1 – Context, aim and outline.....	1
1.1. Context.....	1
1.2. Research aim	2
1.3. Outline of the thesis.....	3
Chapter 2 – Introduction.....	4
2.1. Aerobic granular sludge systems.....	4
2.1.1. Context.....	4
2.1.2. Structure and microbiology of aerobic granules	4
2.1.3. Mature granules properties	5
2.1.4. Factors affecting the stability of AGS.....	6
2.1.5. Application of AGS to toxic compounds' removal from wastewater.....	7
2.2. Pharmaceutical active compounds.....	7
2.2.1. Sulfonamides.....	9
2.2.2. Steroid estrogens.....	11
2.3. PhACs removal in biological WWT systems	12
2.3.1. Granular based technologies	16
2.4. AGS structure and morphology monitoring	18
2.4.1. AGS sampling.....	18
2.4.2. Microscopy observation.....	19
2.5. Quantitative image analysis methodologies.....	20
2.5.1. Application of QIA in WWT systems	20
2.6. QIA procedures description	21
2.6.1. Image acquisition.....	22
2.6.2. Image treatment (processing).....	22
2.6.3. Segmentation and debris elimination.....	23
2.6.4. Image analysis.....	23

2.6.5. Shape and size descriptors	23
2.7. Chemometric tools	24
2.7.1. Principal component analysis.....	24
2.7.2. Decision trees.....	25
2.7.3. Discriminant analysis	25
2.7.4. Multilinear regression.....	26
2.8. Concluding remarks.....	26
Chapter 3 – Material and methods.....	28
3.1. Experimental set-up	28
3.1.1. Reactor operation	28
3.1.2. PhAC concentrations.....	30
3.2. Physicochemical analyses.....	31
3.3. Sludge sampling and image acquisition.....	31
3.4. Quantitative image analysis methodologies.....	32
3.5. Chemometric tools	34
3.6. Statistical analysis	35
Chapter 4 - Performance of the SBR-AGS	36
4.1. Introduction	36
4.2. Results and discussion	36
4.2.1. SBR performance with stable and mature AGS	36
4.2.2. SBR performance in the presence of PhAC.....	37
4.2.3. Suspended and granular fractions structure of mature AGS	39
4.2.4. Suspended and granular fractions structure of AGS in the presence of PhAC.....	43
4.3. Conclusions.....	51
Chapter 5 - Validation of the QIA methodology.....	53
5.1. Introduction	53
5.2. Results and discussion	53
5.2.1. Compliance of the sample volumes for the AGS characterization.....	53

5.2.2. Granular and suspended (floccular) fractions sieving	56
5.2.3. Triplicates analysis.....	59
5.3. Conclusions.....	62
Chapter 6 - Application of chemometric tools for the SBR-AGS assessment.....	63
6.1. Introduction	63
6.2. Biomass contents and settling ability analysis by PCA.....	63
6.3. Biomass contents and settling ability prediction by MLR	71
6.4. PhAC monitoring and identification.....	79
6.4.1. Use of Discriminant Analysis	79
6.4.2. Use of Decision Trees	86
6.5. Conclusions.....	89
Chapter 7 – Final conclusions and suggestions	92
7.1. Conclusions.....	92
7.2. Suggestions for future work.....	94
REFERENCES.....	97
SCIENTIFIC OUTPUT	129
APPENDICES.....	130

LIST OF FIGURES

Figure 1 Thesis structure.....	3
Figure 2 Worldwide distribution of full-scale WWTP with AGS (Nereda ©2020).....	4
Figure 3 Diagram of an aerobic granule (adapted from (Wilén et al., 2018; Nancharaiah and Reddy 2018))	5
Figure 4 SMX, E2 and EE2 in different environment compartments (Ting and Praveena, 2017)	8
Figure 5 Example of a workflow for a QIA procedure (adapted from (Costa et al., 2013))	21
Figure 6 Experimental set up of the employed SBR-AGS.....	28
Figure 7 Experimental set up and sampling methodology of the SBR-AGS.....	29
Figure 8 Evolution of concentrations of the studied PhAC during the monitoring period.....	30
Figure 9 Workflow for the QIA assessment of AGS a) floccular fraction b) granular fraction.....	34
Figure 10 COD, TIN and TP removal efficiencies for the SBR-AGS throughout the monitoring period.	37
Figure 11 Evolution of the reactor performance for the E2, EE2 and SMX experiments monitoring period. a) COD, b) TIN and c) TP removal efficiencies.	38
Figure 12 a) TSS and b) VSS evolution for the suspended (Floc) and granular (Gran) biomass c) TSS and VSS (Floc+ Gran) and AGS settling properties (SVI_5) and d) SVI_{30}/SVI_5 evolution.	40
Figure 13 Evolution of the (a) TA_{flocs}/Vol and (b) % Area for the F1, F2 and F3 fractions; (c) TL/TA_{floc1} , TL/TSS and TL ratios.	41
Figure 14 Evolution of (a) TV_{gran}/Vol and (b) % Vol for the G1, G2 and G3 fractions.	42
Figure 15 Evolution of the robustness for (a) F1, F2, F3 fractions, (b) G1, G2, G3 fractions and eccentricity, for (c) F1, F2, F3 fractions, (d) G1, G2, G3 fractions.	43
Figure 16 Evolution of the TSS and VSS for the granular and floccular fractions for the E2, EE2 and SMX experiments monitoring period. a) TSS_{total} (floccular+granular), b) VSS_{total} (floccular + granular), c) TSS_{floc1} d) VSS_{floc1} e) TSS_{gran1} f) VSS_{gran1} g) TSS_{gran1}/TSS_{total1} h) VSS_{gran1}/VSS_{total1} and i) VSS/TSS	45
Figure 17 Evolution of the AGS physical properties for the E2, EE2 and SMX experiments monitoring period. a) density, b) SVI_5 , and c) SVI_{30}/SVI_5	47
Figure 18 Evolution of the percentages in area (for flocs) and in volume (for granules) according to the size class for the E2, EE2 and SMX experiments monitoring period. a) F1-%A, b) G1-%V, c) F2-%A, d) G2-%V, e) F3-%A and f) G3-%V.	50
Figure 19 Evolution of TL, (a) TL/TA_{floc1} (b) TL/TSS_{floc} (c) and TL/VSS_{floc} (d) for the E2, EE2 and SMX experiments monitoring period.....	51
Figure 20 TSS contents in SBR-AGS for each sampling period.	54
Figure 21 Average and standard deviations criteria values behavior, for the granules diameter, with the granules number increase, for the first monitored day of the EE2 experiment.....	55

Figure 22 Total monitored granules and minimum representative number (nb) of granules according to the average and standard deviation criteria.....	55
Figure 23 Total monitored granules and complying intervals according to the average and standard deviation criteria.....	56
Figure 24 Aggregates percentage above and below 250 μm in equivalent diameter for the granular and floccular fractions.....	57
Figure 25 Stratification analysis presenting the percentage of the aggregates (quantified as granules) below 250 μm collected in the 500 μm sieve.	58
Figure 26 Average diameter and standard deviation of the granular and floccular fractions.....	59
Figure 27 . Standard deviation percentage with respect to the size ranges for the granular and floccular fractions diameter.....	60
Figure 28 PCA with the mature AGS dataset. a) Operational periods and b) AGS structure, contents and settling parameters.....	64
Figure 29 Variable importance for PC1 and PC2, regarding the PCA with the mature AGS dataset.....	65
Figure 30 PCA with the biomass density dataset. a) Operational periods and b) AGS structure, contents and settling parameters.....	67
Figure 31 Variable importance for PC1 and PC2, regarding the PCA with the biomass density dataset.....	68
Figure 32 PCA with the: sludge physicochemical parameters a) including and b) excluding the biomass density; QIA based morphology and structural parameters of the AGS for the c) floccular fraction and d) granular fraction.....	70
Figure 33 Correlations between the observed and predicted VSS for the suspended fraction. a) using the mature AGS dataset b) using the biomass density dataset.	72
Figure 34 Correlations between the observed and predicted floccular TSS values. a) using the mature AGS dataset b) using the biomass density dataset.....	73
Figure 35 Correlations between the observed and predicted granular VSS. a) using the mature AGS dataset b) using the biomass density dataset.....	74
Figure 36 Correlations between the observed and predicted granular TSS. a) using the mature AGS dataset b) using the biomass density dataset.....	75
Figure 37 Correlations between observed and predicted density values. a) based on TSS b) based on VSS.	76
Figure 38 Correlations between observed and predicted SVI_5 values. a) using the biomass density dataset b) using the mature AGS dataset.....	78
Figure 39 Correlations between the observed and predicted SVI_5 based on TSS a) using the biomass density dataset b) using the mature AGS dataset.....	79

Figure 40 DA with AGS and QIA data, using the mature AGS dataset, for the operational periods discrimination.	80
Figure 41 DA with AGS and QIA data, using the mature AGS dataset, for PhAC addition discrimination.	81
Figure 42 DA with AGS and QIA data, using the biomass density dataset, for the operational periods discrimination.	81
Figure 43 DA with AGS and QIA data, using the biomass density dataset, for PhAC addition discrimination.	82
Figure 44 DA for operational periods identification with the: sludge physicochemical parameters a) including and b) excluding the biomass density; QIA based morphology and structural parameters of the AGS for the c) floccular fraction and d) granular fraction.	84
Figure 45 DA for PhAC addition discrimination with the: sludge physicochemical parameters a) including and b) excluding the biomass density; QIA based morphology and structural parameters of the AGS for the c) floccular fraction and d) granular fraction.	85
Figure 46 DT performed using the mature AGS dataset identification of a) operational periods and b) samples with, or without, PhAC addition; and using the biomass density dataset identification of c) operational periods and d) samples with, or without, PhAC addition	87
Figure 47 DT for identification operational periods and samples with, or without, PhAC addition a) operational periods with physicochemical parameters including density; b) samples with, or without, PhAC addition with physicochemical parameters including density; c) operational periods with physicochemical parameters excluding density; d) samples with, or without, PhAC addition with physicochemical parameters excluding density; e) Operational periods with floccular fraction QIA parameters; f) Samples with, or without, PhAC addition with floccular fraction QIA parameters; g) Operational periods with granular fraction QIA parameters; h) Samples with, or without, PhAC addition with with floccular fraction QIA parameters.	88

LIST OF TABLES

Table 1 Reported concentrations of SMX, E2 and EE2 in aquatic systems.....	9
Table 2 Reported PNEC and LOEC of SMX, E2 and EE2 in the literature.....	9
Table 3 Studies encompassing SMX, E2 and EE2 removal in full-scale WWTP.....	14
Table 4 Studies of SMX, E2 and EE2 in granular based technologies	17
Table 5 Studies encompassing sieving methodologies for separation of fractions of AGS	19
Table 6 Concentrations (in mg L ⁻¹) of the studied PhAC entering and leaving the SBR-AGS.....	30
Table 7 Aggregates number percentage with respect to size ranges for granular and floccular fractions within 175 to 250 µm.....	58
Table 8 Standard deviation percentage with respect to the size range for the granular and floccular fractions and main parameters	61

LIST OF SYMBOLS AND ABBREVIATIONS

- A²/O – Anaerobic/anoxic/oxic reactor
- AGS – Aerobic granular sludge
- AOB – Ammonia-oxidizing bacteria
- AQDS – Anthraquinone-2,6-disulfonate
- ARG – Antibiotic resistant genes
- AS – Activated sludge
- BOD – Biochemical oxygen demand
- BPA – Bisphenol A
- CANON – Completely autotrophic nitrogen-removal over nitrate
- CAS – Conventional activated sludge
- CCD – Charge coupled device
- CLSM – Confocal laser scanning microscopy
- CMOS – Complementary metal-oxide semiconductor
- CONT – Control experiment
- CT – Chemometric tools
- CW – Constructed wetlands
- DA – Discriminant analysis
- DDD – Defined daily dose
- Deq – Equivalent diameter
- DO – Dissolved oxygen
- DT – Decision trees
- E1 – Estrone
- E2 – 17 β -estradiol
- E3 – Estriol
- EE2 – 17 α -ethinylestradiol
- EMR – Enzymatic membrane reactors
- EPS – Extracellular polymeric substances
- EU – European Union
- F1 – Flocs with equivalent diameter below 25 μ m
- F2 – Flocs with equivalent diameter between 25-250 μ m
- F3 – Flocs with equivalent diameter above 250 μ m

FBR – Fixed bed reactor

FISH – Fluorescent in situ hybridization

G1 – Granules with equivalent diameter below 0.25 mm

G2 – Granules with equivalent diameter between 0.25-2.5 mm

G3 – Granules with equivalent diameter above 2.5 mm

GAO – Glycogen accumulating organism

GMBR – Granular membrane bioreactor

HRT – Hydraulic retention time

HS – Hybrid systems

LOEC – Lowest observed effect concentration

MBBR – Moving bed biofilm reactor

MBR – Membrane reactor

MF – Microfiltration

MLR – Multilinear regression

MLSS – Mixed liquor suspended solids

MRI – Magnetic resonance imaging

mRNA – Messenger ribonucleic acid

N – Nitrogen

N/A – Nitritation-anammox

NF – Nanofiltration

NH₄⁺-N – Ammonium nitrogen

NMR – Nuclear magnetic resonance

NO₂⁻-N – Nitrite

NO₃⁻-N – Nitrate

NOB – Nitrite-oxidizing bacteria

OD – Oxidation ditch

OLR – Organic load rate

OTC – Oxytetracycline

P – Phosphorous

PAO – Phosphorous accumulating organism

PCA – Principal component analysis

PHA – Polyhydroxyalkanoates

PhAC – Pharmaceutically active compound
PN/A – Partial nitritation anammox
PNEC – Predicted no-effect concentration
QIA – Quantitative image analysis
RBC – Rotating biological contactor
rCOD – Readily biodegradable chemical oxygen demand
RGB – Red green and blue channels
RO – Reverse osmosis
RPD – Residual prediction deviation
SBD/SV – Sludge bed volume per sample volume
SBR – Sequencing batch reactor
SECV– Standard error of cross validation
SEM – Scanning electron microscopy
SGV – Superficial gas velocity
SMX – Sulfamethoxazole
SMX-TP – Sulfamethoxazole transformation products
SRT – Solids retention time
SVI₃₀ – Sludge volume index at 30 min
SVI₅ – Sludge volume index at 5 min
TA – Total microbial aggregates area per volume
TEM – Transmission electron microscopy
TIN – Total inorganic nitrogen
TL/TA – Total filament length per total aggregates area
TL/TSS – Total filament length per total suspended solids ratio
TL – Total filament length per volume
TN – Total nitrogen
TP – Total phosphorous
TSS – Total suspended solids
TSS/TA_{floc} – Floccs apparent density
TSS_{floc} – Total suspended solids for the floccular biomass
TSS_{gran} – Total suspended solids for the granular biomass
TSS_{total} – Total suspended solids for the overall biomass

TV_{gran}/Vol – Total volume of granules per volume of sample

UASB – Upflow anaerobic sludge blanket

VSS – Volatile suspended solids

VSS_{loc} – Volatile suspended solids for the floccular biomass

VSS_{gran} – Volatile suspended solids for the granular biomass

VSS_{total} – Volatile suspended solids for the overall biomass

VTG – Vitellogenin

WSP – Waste stabilization ponds

WTP – Water treatment plants

WWT – Wastewater treatment

WWTP – Wastewater treatment plant

Chapter 1 – Context, aim and outline

1.1. Context

Recently, several pharmaceutically active compounds (PhACs), among which the 17 β -estradiol (E2) and 17 α -ethinylestradiol (EE2) steroid estrogens and the sulfamethoxazole (SMX) sulphonamide, have received wide attention due to the increasing concern on their release in the environment. This is accentuated by the fact that the effect of these compounds remains relatively unknown, due to the lack of standard methods for their quantification, considered as a main challenge in water resources management. It is known that most of the PhACs found in several environmental compartments, such as surface waters, could be related to inefficient removal in wastewater treatment plants (WWTPs). However, there is still a lack of legal requirements addressing the levels of discharge of compounds such as SMX, E2, and EE2 in watercourses (Geissen *et al.*, 2015; Leal *et al.*, 2020a).

In wastewater treatment (WWT), one of the most critical steps is the biological treatment, with activated sludge (AS) systems being the most applied worldwide for that purpose. On the other hand, aerobic granular sludge (AGS) systems have been seen as a promising technology for biological WWT and replacing AS systems due to smaller footprint, compactness of the system and resistance to shock and toxic loads (Bengtsson *et al.* 2019). Such aerobic granules present a mixed microbial community that further allow the simultaneous removal of nitrogen (N) and phosphorous (P) nutrients, with the microorganisms responsible for P and N removal having different locations within the granule due to different oxygen diffusion gradients (Nancharaiah *et al.*, 2018; Nancharaiah and Sarvajith 2019; Van den Berg *et al.*, 2020; Mosquera-Corral *et al.*, 2005).

Nonetheless, the stability of aerobic granules was found to be dependent on several conditions, including the hydrodynamic shear stress and settling time (Qin *et al.*, 2004). Due to the complexity of the AGS systems itself, and to the nature of the wastewater, several dysfunctions may affect the granules, ultimately leading to their disintegration (Yuan *et al.*, 2017). Traditional techniques to monitor the AGS, in order to prevent such occurrences, include microscopic investigation of the AGS morphology and diameter assessment (Cyzdik-Kwiatkowska *et al.*, 2013). As a result, many studies have been developed for the automatic assessment of the morphology and structure of biological WWTP biomass using quantitative image analysis (QIA) (Grijnsperdt and Verstraete 1997; Amaral 2003; Amaral and Ferreira 2005), paramount to remove the subjectivity of human analysis and extract quantitative data (Amaral and Ferreira 2005). In fact, QIA has already been applied for the identification of different types of bulking in AS systems and, more recently, to assess the effect of ferric chloride in

AS flocs (Mesquita, *et al.*, 2011a; Asensi *et al.*, 2019). QIA has also been applied to monitor dysfunctions in anaerobic granular sludge systems during shock loads of toxic compounds (Costa *et al.*, 2010). However, studies addressing the morphology and structural assessment of AGS are still scarce, and the effect of PhACs, such as E2, EE2 and SMX, in AGS morphology and structure is still poorly understood.

Due to the large amount of data provided by QIA, the use of chemometric tools (CT) to treat and organize such information were found to be crucial. In this sense, principal component analysis (PCA), for instance, is considered one of the most important multivariate statistical technique used for biological WWTPs monitoring either using operational parameters, performance indicators and/or morphological and structural parameters of the sludge (Mesquita 2010). Also, decisions trees (DT) were already used to predict foaming events in full-scale WWTPs based on the microscopic observation of AS and morphological and structural parameters of flocs obtained by QIA (Leal *et al.*, 2016). DT were useful for the identification and prediction of bulking events in full-scale WWTPs using operational parameters and filamentous bacteria communities information by Fluorescent in situ hybridization (FISH) techniques (Deepnarain *et al.*, 2019). Moreover, discriminant analysis (DA) has also been used for the identification of protozoa species in AS systems by QIA (Ginoris *et al.* 2007a, 2007b, 2007c).

Thus, it is clear that, in the near future, with the increase of new and emergent technologies, QIA and CT may contribute for timely decisions in full-scale WWTP, bringing new insights to the biomass morphology and structure, and contributing to process optimization.

1.2. *Research aim*

The current thesis reports the study of a lab-scale sequencing batch reactor (SBR) treating a synthetic wastewater, including the morphological and structural assessment of the inoculated AGS through QIA. Further experiments were conducted with mature AGS in the presence of different PhACs, including E2, EE2 and SMX, to assess their effect on the biomass with both the floccular and the granular fractions of the AGS (separated with a mesh sieve of 500 μm) being evaluated by microscopy and stereomicroscopy techniques, respectively. For that purpose, QIA techniques were employed resulting in large datasets of morphological parameters. As a result, CT were next employed including PCA to enlighten the studied parameters interrelationships, DA and DT for the identification of the E2, EE2 and SMX operational periods and samples in the presence or absence of PhACs, and multilinear regression (MLR) to predict the settling ability and suspended solids of mature AGS.

1.3. Outline of the thesis

The outline of this thesis is presented in Figure 1. Chapter 1 presents the research aim, context and outline of the thesis and chapter 2 provides a general introduction to biological WWT systems for PhACs removal and the main impacts of the studied PhACs, as well as the applicability of AGS. In chapter 3 the material and methods are presented. Chapter 4 presents the performance of the SBR-AGS in terms of chemical oxygen demand (COD), total inorganic nitrogen (TIN) and total phosphorus (TP) removal and biomass structural properties. The validation of the QIA approach for AGS assessment in the presence of PhACs is discussed in chapter 5. In chapter 6 the main CT applied for the assessment of the SBR-AGS is emphasized and, finally, the general conclusions of this work, and main suggestions for future work, are presented in chapter 7.

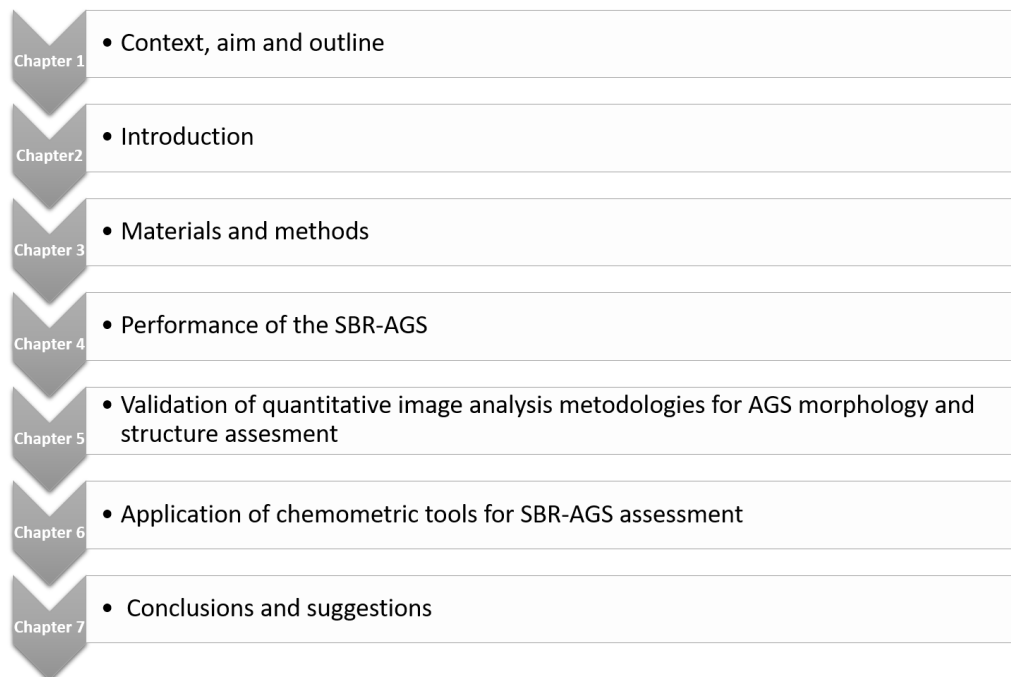


Figure 1 Thesis structure

Chapter 2 – Introduction

2.1. Aerobic granular sludge systems

2.1.1. Context

The aerobic granular sludge (AGS) technology for biological WWT has been developed by the Delft University of Technology in the Netherlands and scaled up under the trade name Nereda®. At the moment 67 projects of Nereda®, are currently either in operation, under construction or in design (Nereda ®2020). This technology is now present worldwide in countries such as The Netherlands, Portugal, Ireland, Brazil, South Africa and Australia, among others. In fact, full-scale operation of AGS for industrial WWT has been reported since 2006 and for domestic sewage since 2009 (Pronk *et al.*, 2015). Among these, 60 systems were projected to treat municipal wastewaters (domestic and industrial) and 7 for industrial WWT (Nereda ®2020). In Portugal 2 full-scale WWTP operate with AGS in Frielas and Faro-Olhão, both treating municipal wastewaters. The world distribution of AGS systems in full-scale operation is presented in Figure 2.



Figure 2 Worldwide distribution of full-scale WWTP with AGS (Nereda ®2020)

Taking Figure 2 into consideration, AGS can be considered a growing technology in terms of full-scale implementation for different WWT applications. Thus, the development and application of monitoring techniques for AGS is of major interest.

2.1.2. Structure and microbiology of aerobic granules

Aerobic granules can be considered a self-immobilized type of biofilm, that have been replacing the AS systems worldwide, presenting denser and more compact granules than AS flocs (Bengtsson *et al.*,

2019). In fact, the AGS has proven to be more energy efficient, as well as presenting a smaller footprint (Sarma and Tay, 2018). Also, it is known that AGS is suitable for recalcitrant organic matter and simultaneous removal of N and P from wastewater (Winkler *et al.*, 2018). Aerobic granules are a technology with the different granular microbial layers established based on the oxygen concentration (Nancharaiah and Reddy, 2018). Furthermore, extracellular polymeric substances (EPS) are also differently distributed in the granules and play a major role in the formation, stability and morphology of AGS (McSwain *et al.*, 2005; Pronk *et al.*, 2017).

In the outer layer of the granule an aerobic microenvironment is created favoring organic matter removal and nitrification, whereas in the intermediate layer the anoxic conditions favor denitrification and biological P removal, and the more internal layer is constituted by an anaerobic zone (Wilén *et al.*, 2018). The oxygen based internal stratification of the granular sludge effects the microbial landscape, thus, a natural distribution of microorganisms in the granule is established. Denitrifying organisms are located in the outer layer due to the higher dissolved oxygen availability, while denitrifying, phosphorous accumulating organisms (PAOs) and glycogen accumulating organisms (GAOs) are located in the inner zones due to anoxic/anaerobic conditions (Nancharaiah and Reddy, 2018). Moreover, biologically induced precipitation of mineral compounds can also occur in the anaerobic zone of granules (Manas *et al.*, 2012).

The main internal layers and microbial composition in an aerobic granule are presented in Figure 3.

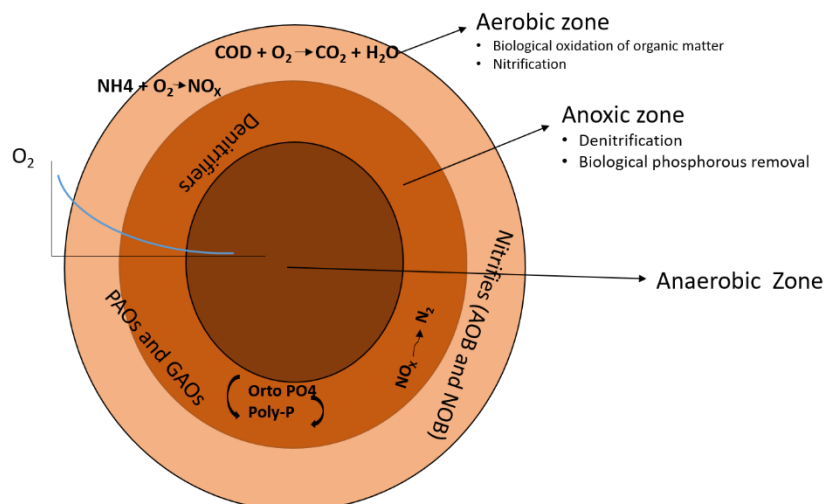


Figure 3 Diagram of an aerobic granule (adapted from Wilén *et al.*, 2018; Nancharaiah and Reddy 2018)

2.1.3. Mature granules properties

It is well known that aerobic granules present improved settling properties compared with AS, including higher settling velocities and lower sludge volume index at 30 min (SVI₃₀) (Etterer and Wilderer, 2001; Nor Anuar *et al.*, 2007; Gao *et al.*, 2011). Since AGS settles faster than AS, the sludge volume

index at 5 min (SVI_5) and SVI_5 per SVI_{30} ratio is used to assess the settling properties and AGS stability (Corsino *et al.*, 2016). The stability of mature granules can also be inferred by the VSS per TSS ratio, mainly ranging from 85% to 95% (Corsino *et al.*, 2016).

Several references can be found in literature assessing the maturation of granules, based on size (diameters over 200 μm in 90% of the aggregates) and SVI_5 to SVI_{30} differences lower than 10% (Liu and Tay, 2007; Verawaty *et al.*, 2012). For the particular case of fish canning wastewaters treatment, the formation of mature granules occurred in a SBR after 75 days of operation resulting in 3.4 mm diameter granules, SVI_{30} of 30 mL g^{-1} VSS and density around 60 g VSS $\text{L}_{\text{granule}}^{-1}$ (Figuroa *et al.*, 2008). In fact, a number of works already revealed that density could be an important property regarding the stability of AGS systems (Corsino *et al.*, 2016; Czarnota *et al.*, 2020).

2.1.4. Factors affecting the stability of AGS

The granular stability is one of the most critical issues regarding AGS systems, mainly due to the large amount of variables that influence the process: reactor configuration (e. g. height/diameter ratio), hydrodynamic shear stress conditions in the reactor (e. g. superficial gas velocity – SGV), organic load, pH and feed composition, among others (Awang and Shaaban, 2016; Lashkarizadeh 2015).

Hydrodynamic conditions are a triggering factor for microbial auto-immobilization (granule formation) affecting also its size and morphology (Zhu *et al.*, 2015). Zhu *et al.* (2015) demonstrated that during the operation of a sequential batch airlift reactor, under low shear rate (SGV ranging from 0.6 to 1.2 $\text{cm}\cdot\text{s}^{-1}$) small granules were obtained and a dominant community of filamentous bacteria and granules instability was observed in long-term operation. On the other hand, under high shear stress, severe changes were observed in the reactor. Also, an organic load rate (OLR) of 6 $\text{kg COD m}^{-3}\text{day}^{-1}$ affected the aerobic granules stability, resulting in small granules that disintegrated and were washed out in a SBR (Zheng *et al.*, 2006). It has also been found that an OLR of 21.3 $\text{kg COD m}^{-3}\text{day}^{-1}$ led to the aerobic granules breakdown in a SBR operated with acetate as carbon source (Adav *et al.*, 2010).

In fact, disintegration of granules during long-term operation of reactors seems to be one of the most challenging issues for the application of AGS technology, with additional factors affecting granule stability during the operation, including particulate substrates in the influent, toxic feed components, aerobic feeding and too short famine periods (Franca *et al.*, 2018). More recently, the effect of availability of readily biodegradable COD in the aerobic phase on the morphology and structure of AGS was also investigated, with the results showing that high aerobic loads of acetate ($8 \text{ mg COD g VSS}^{-1} \text{ h}^{-1}$)

caused filamentous outgrowth, decreasing the settling ability properties and provoking the loss of biomass (Haaksman *et al.*, 2020).

2.1.5. Application of AGS to toxic compounds' removal from wastewater

AGS is considered a promising WWT technology, already being used in the petrochemical, pulp and paper industries, and hypersaline, oily, sulfur-laden, recalcitrant (from membranes industry) and heavy metals rich wastewaters, among others (Corsino *et al.*, 2016; Caluwé *et al.*, 2017; Xue *et al.*, 2017; Wei *et al.*, 2017; Farooqi and Basheer 2017; Guo *et al.*, 2020; Paulo *et al.*, 2021). In the particular case of PhACs removal, it has already been shown that these compounds can be largely biosorbed onto AGS (Mihciokur and Oguz, 2016). In fact several references can be found in literature reporting AGS as a suitable technology for PhACs removal from wastewaters including steroid estrogens and antibiotics (Kent and Tay, 2019; Mendes Barros *et al.*, 2021).

2.2. Pharmaceutical active compounds

PhACs are an emerging concern worldwide. The European Union (EU) is the second biggest consumer in the World, with 24% of the total consumption, just a little less than the United States of America. Consumption per capita in EU ranges from 50 to 150 g year⁻¹ for human medical products (BIO Intelligence Service, 2013). About 4000 PhACs are used worldwide for a diversity of purposes, with production rates for several reaching up to 100,000 tons year⁻¹ (IWW, 2014).

Considering just the antibiotics use, the total amount is estimated between 100,000 and 200,000 ton year⁻¹ with approximatively 50% being used for veterinary purposes (sulfonamides being one of the most common) and as growth promoters (Kümmerer, 2003; Danner *et al.*, 2019; Sarmah *et al.*, 2006a). Furthermore, the antibiotics consumption increased 65% between 2000 and 2015, from 21.1 to 34.8 billion daily doses with the consumption rate increasing 39% (from 11.3 to 13.7 defined daily doses – DDDs inhabitant⁻¹ day⁻¹, (Klein *et al.*, 2018). Regarding the total amount of discharged natural steroid estrogens (estrone – E1, estriol – E2 and 17 β -estradiol – E3), it is estimated at 29.5 tons year⁻¹ (considering the world's population of 6.7 billion inhabitants). Moreover, 720 kg year⁻¹ of synthetic estrogens (17 α -ethinylestradiol – EE2) are also released solely by the use of contraceptive pills (Combalbert and Hernandez-Raquet, 2010).

It is known that SMX, E2 and EE2 can flow into WWTPs from hospital activities, clinical analysis laboratories, industrial activities (such as pills production in the pharmaceutical industry), wastewater discharge and reuse (Cui *et al.*, 2006; Avberšek, *et al.*, 2011; Zhou *et al.*, 2012). Moreover, the surface

waters distributed to the urban environment, even when treated in water treatment plants (WTP), may still contain considerable amounts of these PhACs (Ting and Praveena, 2017), which later contaminate soils and aquifers. Figure 4 shows the main sources of SMX, E2 and EE2 flowing into a WWTP, as well as the dissemination of these compounds in different environmental compartments, including water, wastewater, soil and aquatic biota.

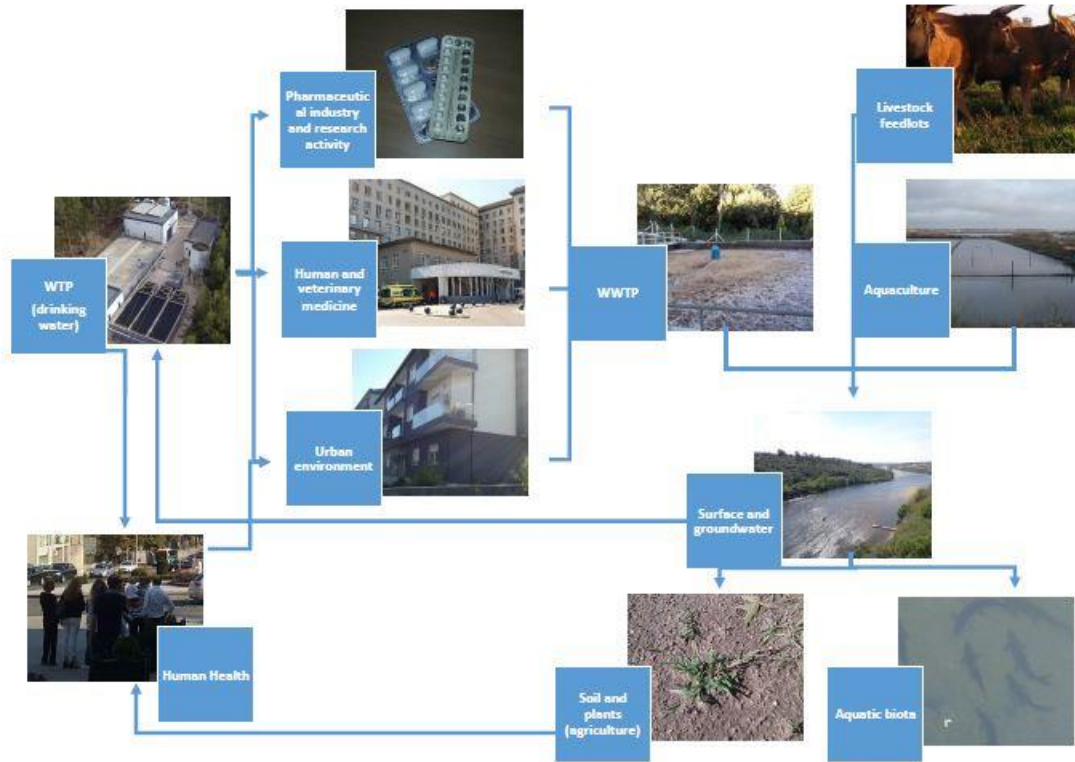


Figure 4 SMX, E2 and EE2 in different environment compartments (Ting and Praveena, 2017)

PhACs are commonly found in ground waters, surface waters, treated wastewaters and even drinking waters, in concentrations up to tens of nanograms per liter for E2, hundreds of nanograms per liter for SMX and up to 1 mg L⁻¹ for EE2. Some reported concentrations of SMX, E2 and EE2 in aquatic systems are presented in Table 1.

Table 1 Reported concentrations of SMX, E2 and EE2 in aquatic systems

PhAC	Concentration	Type of water	References
SMX	Around 410 ng L ⁻¹	Groundwater	(Sacher <i>et al.</i> , 2001)
	Around 480 ng L ⁻¹	Surface water	(Radjenović <i>et al.</i> , 2009; Hirsch <i>et al.</i> , 1999)
	Around 66 ng L ⁻¹	Drinking water Discharged wastewater	(Mucker, 2006)
E2	1 to 22 ng L ⁻¹	WWTP	(Pal <i>et al.</i> , 2010)
	0 to 4.5 ng L ⁻¹	River water	(Pal <i>et al.</i> , 2010)
EE2	0 to 9 µg L ⁻¹	Treated wastewater	(Baronti <i>et al.</i> , 2000)
	831 µg L ⁻¹ (max.) and 73 µg L ⁻¹ (avg.)	Stream water	(Kolpin <i>et al.</i> , 2002)

The ecotoxicity of PhACs is usually assessed by means of the Lowest Observed Effect Concentration (LOEC) and Predicted No-Effect Concentration (PNEC). Table 2 gives further information about the PNEC and the LOEC for the toxicity assessment of SMX, E2 and EE2. With respect to the PNEC, values as low as a few nanograms per liter for E2 (Anderson *et al.*, 2012), and even lower for EE2 (Laurenson *et al.*, 2014), were found for the aquatic life, with LOEC values of 28.8 and 1 ng L⁻¹ for fathead minnow, respectively (Seki *et al.*, 2006; Pawlowski *et al.*, 2004). SMX also has low PNEC values, below 1 µg L⁻¹, for the aquatic life (Straub 2016), while presenting a LOEC of 1.97 nmol L⁻¹ for river biofilms (Yergeau *et al.*, 2010, 2012). However, the toxicity values of PhACs reported in the literature should be carefully analyzed since the results are strongly dependent on the species involved, and whether *in vitro* or *in vivo* assays are used (Laurenson *et al.*, 2014).

Table 2 Reported PNEC and LOEC of SMX, E2 and EE2 in the literature

PhAC	LOEC	PNEC	References
SMX	n. a.	0.59 µg L ⁻¹ for aquatic life	(Straub, 2016)
	n. a.	0.89 µg L ⁻¹ for aquatic life	(Huang <i>et al.</i> , 2018)
	1.97 nmol L ⁻¹ for river biofilms communities	n. a.	(Yergeau <i>et al.</i> , 2010, 2012)
E2	n. a.	5 ng L ⁻¹ (short-term on fish)	(Anderson <i>et al.</i> , 2012)
	n. a.	2 ng L ⁻¹ (long-term on fish)	(Anderson <i>et al.</i> , 2012)
	Below 8.94 ng L ⁻¹ , below 28.8 ng L ⁻¹ and below 85.9 ng L ⁻¹ for medaka, fathead minnow, and zebrafish respectively	n. a.	(Seki <i>et al.</i> , 2006)
	n. a.	2 ng L ⁻¹	(Caldwell <i>et al.</i> , 2012)
EE2	n. a.	0.1 ng L ⁻¹ for aquatic life	(Pawlowski <i>et al.</i> , 2004)
	1 ng L ⁻¹ for fathead minnow	n. a.	(Laurenson <i>et al.</i> , 2014) (Pawlowski <i>et al.</i> , 2004)

n.a.: not available

2.2.1. Sulfonamides

Sulfonamides, including SMX, are widely prescribed and used to treat animals and humans for bronchitis, prostatitis and urinary tract infections (Lipman, 1993; Cavallucci, 2007), with its acetylated

and conjugated compounds posing an environmental risk (Hruska and Franek, 2012). Although (Andreozzi *et al.*, 2003) report that direct and indirect photodegradation can be an important process for the elimination of SMX, these compounds are only partially degraded in the environment. As a result, they are likely to accumulate in water bodies such as ground, surface and drinking waters in amounts up to hundreds of nanograms per liter (Table 1). Moreover, the concentrations of these antibiotics in WWTPs varies according to the consumption patterns, as well as the treatment methodology (Michael *et al.*, 2013).

The effects of SMX in aquatic life remains poorly understood, and information is lacking on the potential consequences of this antibiotic in the environment (Watkinson *et al.*, 2007). Nonetheless, it is known that the long-term persistence of antibiotics (even at low concentrations) in the environment can promote the proliferation of antibiotic resistant bacteria in river streams and, thus, stimulate microorganism drug resistance (Martinez, 2008; Watkinson *et al.*, 2009). Indeed, the detection of sulfonamide resistance genes in river microorganisms and aquatic biofilm communities (Luo *et al.*, 2010; Koczura *et al.*, 2016; Aubertheau *et al.*, 2017), alongside the prevalence of SMX-resistant bacteria in aquaculture environments (Gao *et al.*, 2012), have been correlated to the total SMX concentration, among other sulfonamides, in those environments.

SMX exposure can also lead to changes in higher life forms, such as on zebra fish livers (Madureira *et al.*, 2012) and been related to pericardial edema, York sac edema hemagglutination, tail deformation and swim-bladder defects (Lin *et al.*, 2013). SMX and SMX-transformation products (SMX-TP) resulting from the SMX biodegradation, photolysis or hydrolysis in the aquatic environment can also have acute effects on *Vibrio fischeri*, leading to the inhibition of luminescence (Majewsky *et al.*, 2014).

Besides their impact in aquatic biota, SMX, among others sulfonamides, were also found in soil (Wang *et al.*, 2015) affecting soil-plant systems such as radish and pakoi cultures regarding seed germination and up-ground plant growth (Wang *et al.*, 2016), root elongation during plant germination and growth, temporal changes on soil respiration and inhibiting soil phosphatase activity (Liu *et al.*, 2009). However, these authors also considered that the expected effects regarding plant growth and soil microbial activities may be mild and show a quick recovery due to loss and/or binding of SMX onto soil components.

Regarding human health, and as a result of chronic exposure to environmental antibiotics, Hamscher *et al.*, (2003) have stressed that a large number of antibiotics can induce allergic reactions. Indeed, with respect to sulfonamides, a number of studies have reported allergic effects from sulfamethazine (Hjorth and Roed-Petersen, 1980; Choquet-Kastylevsky *et al.*, 2002), Although no SMX

sole effects have been reported, Pomati *et al.* (2006) refer to the inhibition of human embryonic kidney cells at concentrations of nanograms per liter for a mixture of antibiotics containing SMX. On the other hand, Straub (2016) stated that no risk is apparent for indirect human exposure to SMX through drinking water and food, whereas Uslu *et al.* (2013) came to the same conclusion regarding water bodies. However, this is not the case for sulfamethazine, which has the potential to increase thyroid gland follicular adenoma (Leung *et al.*, 2013).

2.2.2. Steroid estrogens

Steroid hormones are a group of biologically active compounds synthesized from cholesterol and with a common cyclopentane-perhydro phenanthrene ring (Ying, *et al.*, 2002). Four of the estrogens most commonly found in wastewater include 3 natural steroids (17 β -estradiol – E2, estrone – E1 and estriol – E3) and one synthetic compound (17 α -ethinylestradiol – EE2) (Racz and Goel, 2010). E2 is a naturally occurring steroid hormone, being the major female sex hormone, and an essential factor in the regulation of the menstrual cycle, in the development of puberty and in secondary female sex characteristics (Drugbank, 2016a). E2 may also be present in hormone therapy products for reduced estrogen production (menopausal and peri-menopausal symptoms), treatment of hypoenestrogenism, palliative treatment of breast and prostate cancer, as well as for transgender hormone therapy (Drugbank, 2016b). On the other hand, EE2 is used mainly for the treatment of vasomotor symptoms associated with the menopause, female hypogonadism, prostatic carcinoma-palliative therapy, treatment of breast cancer and contraceptive purposes (Drugbank, 2016b).

WWTPs effluents could be seen as one of the major sources of E2 and EE2 in surface and ground waters (Table 1) due to its inefficient removal (Braga *et al.*, 2005), alongside livestock manure and aquaculture (Sarmah *et al.*, 2006b; Kolodziej *et al.*, 2004). In fact, several studies have shown that a considerable fraction of the polar metabolites of E2 and EE2 can be cleaved in WWTPs, resulting in discharge of the initial compounds (Panter *et al.*, 1999; D'Ascenzo *et al.*, 2003; Ternes *et al.*, 1999). Consequently, the disposal of animal manure, wastewater, and sewage sludge to agricultural land can lead to the transfer of steroid hormones, including E2 and EE2, into soils, surface and ground waters (Stumpe and Marschner, 2007). Another major source of steroid estrogens comes from the urban environment, mainly from human excretion, being released into WWT systems in either conjugated or unconjugated forms at micrograms per person and day levels (Johnson and Sumpter, 2001; Johnson and Williams, 2004). Indeed, human excretion is a major source of the estrogens found in domestic wastewaters, with the amount of excreted estrogens, and namely EE2, depending on several factors,

including gender, hormonal and menstrual state, pregnancy and contraceptive use (Johnson and Sumpter, 2001).

Estrogens, present in the environment in concentrations up to hundreds of micrograms per liter, can have a large impact on human and animal health (Stumpe and Marschner, 2007). Consequently, several environmental impacts could be related to exposure to E2 and EE2 affecting aquatic biota, soils, surface and ground waters (among others). Indeed, water bodies with high estrogen levels, including downstream WWTPs effluents, may have a pronounced effect on aquatic species, leading to fish being feminized (McAvoy, 2008). Estrogens can deregulate and interfere with normal biological responses by mimicking natural hormones and disrupting signal pathways, like endocrine disruptors. Chronic exposure of fathead minnows (*Pimephales promelas*) to low E2 concentrations (5 to 6 ng L⁻¹) feminize males through the production of vitellogenin (VTG) mRNA (evidenced by intersex changes in males), impact on gonadal development, and altered oogenesis in females (Kidd *et al.*, 2007). EE2 was also found to have the same effect (Bila and Dezotti, 2007). Moreover, estrogens (including E2 and EE2) and their mimics can cause severe damage to fish populations, as shown by the rapid decrease fish stocks in contaminated lakes (Bila and Dezotti, 2007; Kidd *et al.*, 2007) with the fish reproductive rate being reduced over 3 generations (Cripe *et al.*, 2009).

Concerning the effect of the chronic exposure to contaminant estrogens in water and food products on humans, Swan *et al.* (2007) found that hormones (used as growth promoters) were responsible for the reduction of the sperm count in the male offspring of women with a high red meat regime during gestation. Furthermore, contaminant estrogens, with relevance to EE2, are thought to induce some diseases, such as uterus, breast and prostate cancer, male fertility reduction, abnormal sexual development, abnormal thyroid glands, increased polycystic ovaries incidence, disturbances in ovarian functions, fertilization and pregnancy, endometriosis and neurobehavioral effects (Soto *et al.*, 1991; Adeel *et al.*, 2017; Verbinnen *et al.*, 2010; Birnbaum and Fenton, 2003; Coleman *et al.*, 2005; Solomon and Schettler, 2000; Gray, 1998; Daston *et al.*, 1997). Finally, Sodr  *et al.* (2007) emphasized that the embryonic stage is much more susceptible to estrogens compared to adults. Indeed, exposure at early stages of development can change developmental processes themselves, whereas at a more advanced stage they can solely interfere with reproduction or affect the offspring (Arcand-Hoy and Benson, 1998).

2.3. PhACs removal in biological WWT systems

PhACs are commonly present in domestic sewages with sulfonamide antibiotics and steroid estrogens of particular interest and concern, due to their extensive use in human health. Some of these

compounds are hardly, or not metabolized at all, during their therapeutic use and are excreted unchanged (Mohapatra *et al.*, 2014). The main metabolic pathways, physical and chemical properties of the studied PhAC can be found in Section 1 of Appendices. Indeed, PhACs are nowadays considered as an emerging environmental problem due to their continuous release and persistence in aquatic ecosystems, even at low concentrations (Carabin *et al.*, 2015), with the extent of their effects remaining relatively unknown due to lack of standard methods for quantification. Consequently, PhACs are now considered a major challenge in water resources management (Geissen *et al.*, 2015).

The increasing concern about the environmental and human health risks of PhACs led to the development of several technologies for the removal of these compounds (Badia-Fabregat and Oller, 2017). Studies have already shown that conventional activated sludge (CAS) systems in WWTPs are inefficient for the removal of a large number of PhACs (Hirsch *et al.*, 1999; Joss *et al.*, 2006). Based on this information, different technologies have been already studied and applied to obtain a suitable removal of PhACs, including membrane reactors (MBR), moving bed biofilm reactor (MBBR), enzymatic membrane reactors (EMR), hybrid systems (HS, involving a number of different systems, such as biofilms and suspended biomass), granular sludge based technologies and treatment with the *Trametes versicolor* fungi, among others (Salgado *et al.*, 2012; Mohapatra *et al.*, 2014; Petrie *et al.*, 2014; Grandclément *et al.*, 2017; Tiwari *et al.*, 2017; Beshia *et al.*, 2017; Ahmed *et al.*, 2017). A significant number of studies have tried to determine the removal efficiencies of PhACs in full-scale WWTPs, and a literature survey of the main studies encompassing SMX, E2 and EE2 removal efficiencies in full-scale WWTPs is presented in Table 3.

Table 3 Studies encompassing SMX, E2 and EE2 removal in full-scale WWTP

PhAC	Concentration	Load	Process type	Removal efficiency	References
SMX	average of 430 ng L ⁻¹	n. a.	AS	67%	(Göbel <i>et al.</i> , 2005)
	0.21 to 2.8 µg L ⁻¹	n. a.	1 AS (two stage with a nitrification tank), 1 extended aeration, 1 RBC, 1 pure oxygen AS	48% to 75%	(Batt <i>et al.</i> , 2007)
	230 to 570 ng L ⁻¹	n. a.	CAS / MBR* / FBR*	60% to -138%	(Göbel <i>et al.</i> , 2007)
	139 ng L ⁻¹	n. a.	1 MBR*, 1 NF, 1 RO	Above 95% for NF and RO; MBR inefficient	(Kim <i>et al.</i> , 2007)
	n.a	40 mg day ⁻¹ per 1000 inhabitants	3 AS, 1 AS + UV	No removal	(Zuccato <i>et al.</i> , 2010)
	below 10 ³ ng L ⁻¹	n. a.	MBR	66%	(Kim <i>et al.</i> , 2014)
	4 to 8 to 3180 ng L ⁻¹	Maximum load of 447 µg d ⁻¹ per person	2 A ² /O, 1 cyclic AS, 1 OD	7.5% to 61%	(Yan <i>et al.</i> , 2014)
	maximum of 641 ng L ⁻¹	n. a.	WWTP1 (OD + UV) WWTP2 (A ² /O-CIO ₂ -UV)	No removal in WWTP1 and 99% in WWTP2	(Estrada-Arriaga <i>et al.</i> , 2016)
	below 5.3 µg L ⁻¹	n. a.	AS	51% to 70%	(de Jesus Gaffney <i>et al.</i> , 2017)
0.245 to 1.15 µg L ⁻¹ in CAS and 0.019 µg L ⁻¹ in CW**	n. a.	1 CAS, 1 CW	99.6 to 99.8% in CAS and negative (-100 %) removal in CW	(Afonso-Olivares <i>et al.</i> , 2017)	
E2	1 to 30 ng L ⁻¹	n. a.	4 WWTP with no biological treatment, 6 AS, 1 AS + biosorption, 3 TF, 1 biorotor, 2 AS + N removal, 1 TF/AS, 2 TF/AS + N removal	58% to 99% removal	(Svenson <i>et al.</i> , 2003)
	above 1.0 ng L ⁻¹	n. a.	1 MBR*, 1 NF, 1 RO	Above 95% for NF and RO; MBR inefficient	(Kim <i>et al.</i> , 2007)
	1.0 to 4.2 ng L ⁻¹	n. a.	1 CAS, 2 OD, 1 with bioreactors, 1 with aerobic lagoons	47% to 68%	(Ying, <i>et al.</i> , 2008)
	maximum of 1,1 ng L ⁻¹	n. a.	1 AS N/D/P, 1 AS N/D	Above 90%	(Koh <i>et al.</i> , 2009)
	119 ng L ⁻¹	n. a.	CAS	70% to 100%	(Manickum and John, 2014)
	maximum of 44 ng L ⁻¹	n. a.	WWTP1 (OD + UV) WWTP2 (A ² /O-CIO ₂ -UV)	99% and 100% in WWTP1 and WWTP2, respectively	(Estrada-Arriaga <i>et al.</i> , 2016)
EE2	0.003 µg L ⁻¹	n. a.	AS	Maximum of 85 %	(Baronti <i>et al.</i> , 2000)
	1 to 30 ng L ⁻¹	n. a.	4 WWTP with no biological treatment, 6 AS, 1 AS + biosorption, 3 TF, 1 biorotor, 2 AS + N removal, 1 TF/AS, 2 TF/AS + N removal	58% to 99%	(Svenson <i>et al.</i> , 2003)
	1.3 ng L ⁻¹	n. a.	1 MBR*, 1 NF, 1 RO	Above 95% for NF and RO; MBR inefficient	(Kim <i>et al.</i> , 2007)
	0.1 to 1.3 ng L ⁻¹	n. a.	1 AS + 6 lagoons for tertiary treatment 1 with 2 OD + chlorination 1 AS+ UV 1 with 10 anaerobic lagoons + 8 aerobic lagoons	No removal	(Ying <i>et al.</i> , 2008)
	maximum of 0,2 ng L ⁻¹	n. a.	1 AS N/D/P, 1 AS N/D	Above 90%	(Koh <i>et al.</i> , 2009)
	30 ng L ⁻¹	n. a.	CAS	90%	(Manickum and John, 2014)

n.a. – not available; AS – activated sludge; A²/O – Anaerobic/anoxic/oxic reactor; CAS – conventional activated sludge; FBR – Fixed bed reactor; RBC – Rotating biological contactor; WSP – Waste stabilization ponds; NF – Nanofiltration; OD– Oxidation ditch; UV – Ultraviolet; TF –Trickling filter; N/D – Nitrifying/denitrifying system N/D/P – Nitrifying/denitrifying with phosphorous removal system; RO – Reverse osmosis; CW – Constructed wetlands; * lab-scale; ** concentrations data reported to sample points after grinding, for all WWTP

The elimination of SMX has been investigated in full-scale WWTPs with different biological WWT systems by (Göbel *et al.*, 2005, 2007) and (Polesel *et al.*, 2016) among others. Removal of SMX in full-scale WWTPs occurs mainly by biotransformation, though deconjugation of metabolites back to the parent form can have a negative effect on the removal efficiency (Polesel *et al.*, 2016). In this sense, the most commonly studied conjugated metabolite of SMX in full-scale WWTPs is N4-acetyl-SMX (Göbel *et al.* 2007), and the sorption of this metabolite can be considered negligible due to its chemical properties (Polesel *et al.*, 2016).

With respect to estrogens, removal efficiencies above 90% for E2 and EE2 in municipal WWTPs were obtained under both aerobic and anaerobic conditions (Joss *et al.*, 2004). However, whereas E2 was oxidized and further eliminated by a CAS system, EE2 remained mainly persistent (Ternes *et al.*, 1999). On the other hand, Ternes *et al.* (2002) stressed that adsorption of steroid estrogens to sludge plays an important role in their removal from wastewaters. In addition, research evaluating different full-scale WWTPs technologies were crucial for a deeper understanding of the removal process of estrogens. Braga *et al.* (2005) found that the removal efficiencies of estrogens were higher in WWTPs with microfiltration (MF), reverse osmosis (RO) and chlorination/dichlorination compared to the WWTP with FeCl₃ addition. Taking into account the relatively low solids concentration in the enhanced primary treatment, the degree of estrogens partitioning in the organic fraction was thought to be responsible for the difference between the two plants. Miège *et al.* (2009) reported greater removal efficiencies for steroid estrogens in AS systems with nitrogen removal and membrane bioreactors. In addition, EE2 removal in fixed biomass reactors and waste stabilization ponds occurred predominantly in the liquid phase, under high SRT conditions. Johnson *et al.* (2005) compared the concentration of steroid estrogens (E1, E2 and EE2) in treated effluents from different WWTPs presenting diverse WWT technologies, finding that the lowest estrogen removals occurred in the WWTP with solely a primary chemical treatment, whereas higher efficiencies were seen in WWTPs with AS and oxidation ditch (OD) systems.

With the purpose of understanding the behavior and the removal efficiencies of estrogens in a full-scale WWTP in Australia, Ying *et al.* (2008) showed that the removal rates of estrogens were consistent with the biochemical oxygen demand (BOD), mixed liquor suspended solids (MLSS) and ammonia removal efficiencies. Higher BOD, MLSS and ammonia values resulted in lower removal efficiencies of

estrogens. Moreover, this study pointed out that the least efficient studied WWTP consisted of a series of anaerobic and aerobic lagoons whereas the most efficient were CAS and OD systems.

2.3.1. Granular based technologies

AGS is considered one of the most promising technologies in WWT systems regarding the removal of sulfonamides and steroid estrogens, with a few references in literature addressing this issue.

SMX can be largely removed (average of 90% removal) in SBR-AGS treating biogas slurry and above 90% in operation under low C/N ratios (Liao *et al.*, 2019; Yu *et al.*, 2020), although its effect in SBR-AGS microbial communities, as well as other antibiotics (sulfadiazine, fluoxetine and oxytetracycline - OTC), is also reported in literature (Kang, *et al.*, 2018a; Wan *et al.*, 2018; Moreira *et al.*, 2015; Ferreira *et al.*, 2016; Wang *et al.*, 2019). Moreover, it was also shown that these compounds can be highly biosorbed into AGS, and further metabolized (Mihciokur and Oguz, 2016). In other antibiotics, such as tetracycline, it has also been found that the removal occurred by adsorption (fast) and biodegradation (slower) processes in a nitrifying granular reactor (Shi *et al.*, 2011).

Regarding steroid estrogens, EE2 was found to be largely removed mainly by adsorption. Ternes *et al.* (2002), and Zheng *et al.* (2016) showed that E2 can be adsorbed more easily onto AGS when compared to AS (Zheng *et al.*, 2016). Good removal efficiencies of E2 and EE2 were also obtained on a lab-scale SBR-AGS treating municipal wastewater, obtaining 84% and 85% of average removal efficiencies, respectively (Balest *et al.*, 2008). In addition, bisphenol A (BPA), a xenoestrogen, was successfully removed from wastewaters using AGS, where *Sphingomonadaceae* and *Pusillimonas* sp. were found to be direct BPA-degraders in BPA-exposed granules (Cyzdik-Kwiatkowska *et al.*, 2017).

More recently, Amorim *et al.* (2018) showed that the load of different PhACs in a SBR-AGS led to changes in the abundance of ammonia-oxidizing bacteria (AOB), nitrite-oxidizing bacteria (NOB) and polyphosphate-accumulating organisms (PAO) (Amorim *et al.*, 2018). AGS has also been used in membrane bioreactors (MBR), as well for the removal of a number of different PhACs, with their effect in the microbial communities present in these reactors also exploited in several studies. According to Xia *et al.* (2015), *Firmicutes* sp., *Aeromonas* sp. and *Nitrospira* sp. were found to be crucial for antibiotics removal in a granular membrane bioreactor (GMBR) (Xia *et al.*, 2015). Furthermore, in a GMBR was found a SMX removal efficiency of 80%, and *Zoogloea*, *Tolomonas*, *Arcobacter*, *Terrimonas* and *Singulisphaera* were pointed out as the functional bacteria able to degrade these compounds (Wang *et al.*, 2016).

With respect to other granular sludge systems, it should be noticed that the granules from a completely autotrophic nitrogen-removal over nitrate (CANON) reactor became more compact and dominated by the multi-resistant fungus *Scedosporium boydii* when exposed to high concentrations of SMX (Rodriguez-Sanchez *et al.*, 2017). Also Zhang *et al.* (2019) showed that SMX and OTC inhibited the performance of an anammox system and the dissemination of antibiotic resistant genes (ARG). Chen *et al.* (2017) found that the specific denitrification activity of denitrifying granules decreased with the increase on SMX concentration in batch tests. On the other hand, no inhibition was reported in continuous-flow experiments in an upflow anaerobic sludge blanket (UASB) reactor with 100 mgL⁻¹ of SMX (Chen *et al.*, 2017). In another study, a SMX removal efficiency of 70% was achieved in a combined nitrification-anammox (N/A) biomass system in optimal conditions for nitrifying bacteria (Kassotaki *et al.*, 2018). Similar results were obtained for the treatment of black (sanitary) waters using a partial nitrification-anammox (PN/A) system combined with an UASB reactor (de Graaff *et al.*, 2011). Regarding steroid estrogens removal, it was found that most of the E2 removal during the separate treatment of synthetic urine using a PN/A system was due to adsorption onto the biomass and biodegradation (transformation of E2 to E1, followed by slow degradation of E1 to other metabolites) (Huang *et al.*, 2016). The studies addressing the removal of the SMX, EE2 and E2 are presented in Table 4.

Table 4 Studies of SMX, E2 and EE2 in granular based technologies

PhAC	Concentration	System	Main achievements	References
EE2	530 µg. L ⁻¹	SBR with AGS	77% of removal efficiency (average)	(Kent and Tay, 2019)
E2	9 µg. L ⁻¹	UASB	82.17% of biodegradation efficiency after 4.5 days	(Zhao <i>et al.</i> , 2020)
	2µg. L ⁻¹	Anoxic/anaerobic/oxic SBR with AGS	84% of removal efficiency	(Kang <i>et al.</i> , 2018b)
	200 µg. L ⁻¹	SBR with AGS	60% of removal efficiency without AQDS 95% of removal efficiency with AQDS addition	(Mendes Barros <i>et al.</i> , 2021)
SMX	50 µg. L ⁻¹	SBR with AGS	>60% of removal	(Zhao <i>et al.</i> , 2015)
	125 µgL ⁻¹ VSS ⁻¹	SBR with AGS	Glycerol enhanced the biotransformation of SMX	(Mery-Araya <i>et al.</i> , 2019)
	n. a.	SBR with AGS	Highest removal of 91 ± 9% (values in average)	(Liu <i>et al.</i> , 2019)
	0.5-1.0 mgL ⁻¹	Anammox reactor	The performance of OTC or SMX was lower than that sum of their independent effects.	(Zhang <i>et al.</i> , 2019)

n. a. Not available; SBR – Sequencing batch reactor; AGS – aerobic granular sludge; UASB – Upflow Anaerobic Sludge Blanket; OTC – Oxytetracycline; AQDS – Anthraquinone-2,6-disulfonate

2.4. AGS structure and morphology monitoring

The AGS structure was found to be essential for process control, and for that purpose, the granules size assessment is gaining increasing attention (Verawaty *et al.*, 2013; Zhang *et al.*, 2015; Long *et al.*, 2019). Literature already reports the relevance of optimizing the granules size distribution in such reactors (Zhou *et al.*, 2016). Other studies revealed that a granule-size based discharge could enhance the stability and control of AGS processes (Li *et al.*, 2006; Sheng *et al.*, 2010; Zhu *et al.*, 2013). Also, it was previously found that the granules size can influence the reactor performance, particularly, phosphorous and nitrogen compounds' removal from wastewaters (Li *et al.*, 2019). More recently, the granules size was found to be correlated with the content and composition of EPS in AGS systems (Rusanowska *et al.*, 2019) and might have impact in nitrification ability (Nguyen *et al.*, 2021).

Several methods in literature already report a number of different AGS structure assessment methodologies directed to granules: (i) freezing microtome sections; (ii) dissolved oxygen (DO) microelectrode (to assess microbial density in granules through DO profiles in the granules); (iii) confocal laser scanning microscopy (CLSM); (iv) ultra-high-field NMR; as well as for separated flocs and granules fractions: (v) magnetic resonance imaging (MRI) (Li *et al.*, 2014; Kirkland *et al.*, 2020; Ranzinger *et al.*, 2020). Quantitative image analysis (QIA) can be considered a less invasive technique when compared to DO microelectrode and freezing microtome sections methods. When compared with NMR and MRI, QIA can provide a more in-depth analysis of the aggregates structure and morphology.

2.4.1. AGS sampling

AGS sampling for structure and morphology assessment is now considered challenging regarding sample representativeness. Furthermore, other challenges are related to differences in the biomass features at different depth of the reactor (stratification issues) due to different hydraulic stress (Fan *et al.*, 2019). On the other hand, physical handling and washing processes may change the AGS structure and morphology. It is known that the stability of the AGS process is quite dependent on the balance between the floccular and granular fractions in the system (Aqeel *et al.*, 2019). Moreover, several studies could be found in literature relating to sludge fractionation, including the use of different sieves size and different sludge volumes for fractions separation (Pronk *et al.*, 2015; Cheng *et al.*, 2018; Jahn *et al.*, 2019). In this sense, the development of adequate sampling procedures for both flocs and granules morphological and structural assessment is of major interest. The main sampling methodologies encompassing AGS sieving methodologies for flocs and granules fractions' separation are presented in Table 5.

Table 5 Studies encompassing sieving methodologies for separation of fractions of AGS

References	Sieving methodology	Reactors scale
(Cheng <i>et al.</i> , 2018)	0.3 mm sieving and washed three times with tap water	Lab-scale
(Cydzik-Kwiatkowska <i>et al.</i> , 2018)	mesh sizes of 2 mm, 1 mm, 710 μ m, 500 μ m, 355 μ m, 125 μ m and 90 μ m	Full-scale
(Dahalan <i>et al.</i> , 2015)	mesh sieve 0.2, 0.4, and 0.6 mm	Lab-scale
(Xu <i>et al.</i> , 2018)	2 mm, 0.925 mm, 0.76 mm, 0.59 mm and 0.23 mm sieves	Lab-scale
(Jing-Feng <i>et al.</i> , 2012)	0.18 mm, 0.18 – 0.45 mm, 0.45 – 0.6 mm, 0.6 – 0.9 mm and .0.9 mm sieves	Granular and flocculent lab-scale MBR
(Kishida <i>et al.</i> , 2010)	125, 250 and 420 μ m sieves	Lab-scale
(Nor Anuar <i>et al.</i> , 2008)	0.2, 0.4 and 0.6 mm sieves	Lab-scale
(de Graaff <i>et al.</i> , 2018)	granules were sieved and washed on a 1.6 mm sieve	Full-scale
(Truong <i>et al.</i> 2018a; 2018b)	less than 0.15 mm, 0.15 - 0.4 mm, 0.4 - 1.0 mm, 1.0 - 2.0 mm, and larger than 2.0 mm	Lab-scale
(Liu <i>et al.</i> , 2014)	100 mL of mixed sludge was taken out from the reactor and filtered by a sieve with an aperture of 0.1 mm	Lab-scale
(Liu <i>et al.</i> , 2017)	100 mL samples mixed liquor were taken at the end of the aeration period were filtered through a series of sieves with apertures of 1 mm, 0.55 mm, 0.38 mm, and 0.21 mm.	Lab-scale
(Choerudin <i>et al.</i> , 2018)	wet sieve analysis with opening 0.3 mm, 0.425 mm, 0.8 mm, and 2.0 mm	Lab-scale
(Jahn <i>et al.</i> , 2019)	mesh size of 500 μ m to divide into flocculent and granulated fractions	Lab-scale
(Pronk <i>et al.</i> , 2015)	approximately 1,500 mL of reactor volume was washed over a 212 mm and 600 mm sieve	Full-scale
(Franca <i>et al.</i> , 2015)	sieving mixed liquor samples through 0.65 mm and 0.25 mm net sieves	Lab-scale

2.4.2. Microscopy observation

Microscopy observation of AGS is usually performed by (i) bright-field microscopy, (ii) scanning electron microscopy (SEM), (iii) transmission electron microscopy (TEM), and (iv) CLSM combined with fluorescence in-situ hybridization (FISH) for microbial structure assessment (Tay *et al.*, 2001; Jang *et al.*, 2003; Meyer *et al.*, 2003; Lemaire, *et al.*, 2008; Weissbrodt *et al.*, 2013). More recently stereo and bright-field microscopy were used for the morphology assessment of AGS (Val del Rio *et al.*, 2012; Corsino *et al.*, 2018) and the composition of mineral deposits in the granules was conducted by SEM coupled with energy dispersive X-ray (Pishgar *et al.*, 2020).

Taking the above into consideration, the application of microscopic and stereomicroscopic techniques for the observation, and quantitative assessment, of the sludge floccular and granular fractions in the presence of PhAC (such as SMX, E2 and EE2) can be considered of major interest. Furthermore, as traditional AGS microscopy monitoring address mainly the assessment of the sludge

granules' fraction with a scarce amount of quantitative morphology descriptors, the use of QIA techniques allows for a deeper understanding of the biomass structure.

2.5. Quantitative image analysis methodologies

2.5.1. Application of QIA in WWTP systems

A number of AS monitoring procedures using QIA rely on microscopy monitoring and image acquisition of unstained samples, with particular interest on the evaluation of AS systems malfunctions (filamentous and viscous bulking, pin-point flocs formation, dispersed growth and foaming) (Mesquita *et al.*, 2009; Mesquita, *et al.*, 2011b; Liwarska-Bizukojc *et al.*, 2014; Leal *et al.*, 2016). It should also be stressed that these studies have gone beyond the lab-scale monitoring and are currently performed in full-scale WWTP. Furthermore, the determination of the AS systems biota component, such as protozoa and metazoa, has already been performed by the use of semi-automatic QIA procedures (Amaral *et al.*, 2004; Ginoris *et al.* 2007a, 2007b; Amaral *et al.*, 2008). In some cases, staining procedures are indispensable for the proposed monitoring objective. In this context, several works have already been conducted involving QIA of stained samples, mainly for bacteria Gram status determination (Pandolfi and Pons, 2004) and viability and physiological state evaluation (Amaral *et al.*, 2013; Mesquita *et al.* 2013, 2014, 2015).

QIA has also been used to predict settling ability properties in AS, addressing mainly filamentous bacteria and floc aggregates (Molina *et al.*, 2020). Moreover, several references could be found in literature regarding the importance of QIA for full-scale WWTP monitoring and modelling purposes (Khan *et al.*, 2018). For instance, QIA has been found useful in determining microbial aggregates and colloidal contents, size and morphology in raw and treated wastewaters in a full-scale WWTP treating palm oil effluents (Khanam *et al.*, 2016). One of the major field of applications, in that regard, refers to biological aggregates monitoring with QIA already being used to investigate the effect of ferric chloride in AS flocs morphology (Asensi *et al.*, 2019) and of AS morphology in the oxygen transfer ratio (Campbell *et al.*, 2019). QIA tools have also been used for monitoring filamentous bacteria such as the specific filaments length (SFL) in assessing the effect of surfactants and establish a direct correlation between SFL and the apparent viscosity in AS systems (Campbell *et al.*, 2020). By coupling the biological aggregates and filamentous bacteria monitoring, the settling ability of AS biomass has been assessed (Molina *et al.*, 2020), and a number of dysfunctions were identified, and even predicted, including different types of bulking.

The applicability of QIA procedures in anaerobic granular sludge has been previously verified through the evaluation of structural changes during the revival process of anaerobic granules, as well as to monitor several dysfunctions related to the presence of organic solvents and other toxic compounds (Abreu *et al.*, 2007; Costa *et al.* 2009, 2009a). More recently, size and morphological parameters obtained with QIA were also used for predicting the biomass settling velocity in UASB reactors (Tassew *et al.*, 2019) and an automated QIA procedure was developed for assessing the effect of ultrasonication process in the size and morphology of hydrogen producing granules (Shin *et al.*, 2019).

However, works encompassing the structural and morphological assessment of AGS systems are still unexplored, thus, its study can be considered of major interest. An in-depth characterization of the AGS structure, both under stable conditions and possible dysfunctions related to the presence of PhAC (such as E2, EE2 and SMX) by QIA, can be seen as quite valuable.

2.6. QIA procedures description

QIA techniques usually encompass several procedures crucial for the successful application of this tool, beyond microscopic observation and sludge sampling, namely image acquisition, image treatment (processing) and image analysis. The main steps of a QIA procedure are presented in Figure 5 and further described.

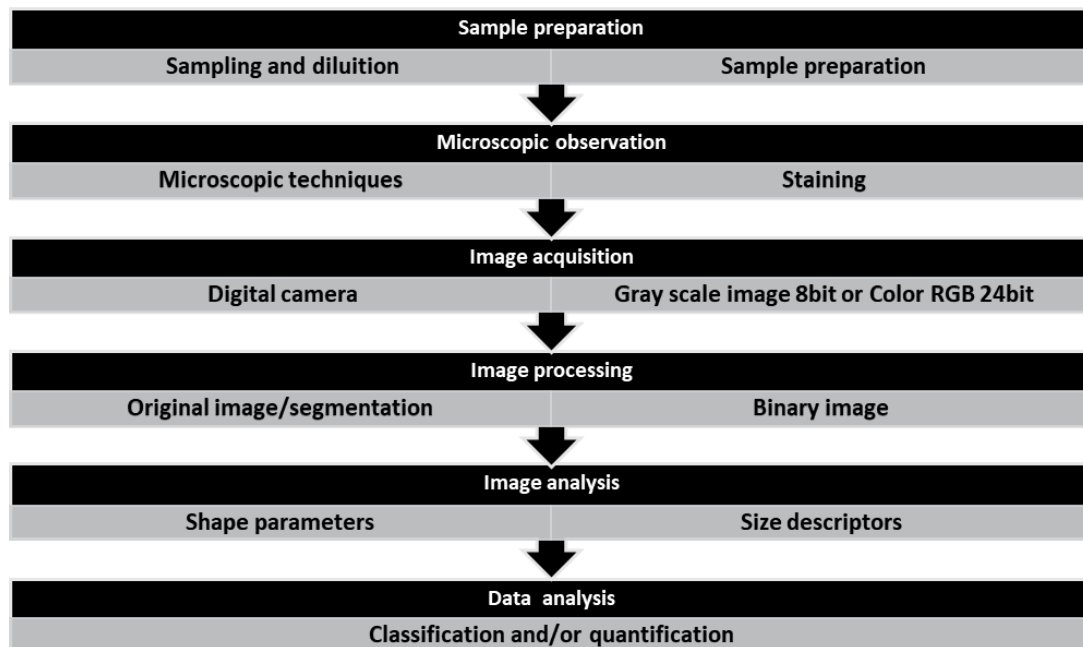


Figure 5 Example of a workflow for a QIA procedure (adapted from (Costa *et al.*, 2013))

2.6.1. Image acquisition

The image acquisition is, in most cases, performed using digital cameras, mostly fit with CCD (Charge Coupled Device) or CMOS (Complementary Metal-Oxide Semiconductor) sensors. The signal produced from the digital camera leads to the formation of a matrix of picture elements (called pixels), proportional to the light intensity received by each sensor (Russ, 2002). In such cameras, the number of bits allocated to each pixel, in a given image, determines the number of color shades (or levels) of the image. For instance, in grayscale images (mostly acquired in bright field or phase contrast microscopy) usually 8 bits are allocated to each pixel, corresponding to 256 linear levels of brightness (Mesquita *et al.*, 2013). On the other hand, in color imaging it is possible to determine changes in color channels that cannot be identified by the sole use of a single 8-bit gray scale intensity channel. Therefore, this type of images is usually digitized as 24-bit RGB (red, green, and blue channels), meaning that 8 bits or 256 (linear) levels of brightness for red, green, and blue are stored.

2.6.2. Image treatment (processing)

After image acquisition, images are then processed to obtain the final image (grey scaled, labeled or binary) containing the necessary information for a given application (Amaral, 2003). The first image processing procedure usually focuses on background determination and light differences removal. Two of the main approaches reside on either using a previously acquired background image or in the use of an image processing methodology to estimate the background image. In the first case, the background image must be obtained *a priori* upon the acquisition of the images, and in the later obtained *a posteriori* from the image(s) by the use of low pass filters or a series of grey-scale closing and opening operations (Amaral, 2003). In either case the background image can be used to be subtracted or divided from the original image.

Furthermore, contrast enhancement may also be performed to improve the object's perceptibility by enhancing the brightness difference between the object and the background (McAndrew, 2005). Regarding that purpose, several techniques have been applied based on histogram equalization, edge enhancement and detection methodologies and high pass filters, among others (Kotkar and Gharde, 2013). Noise elimination, or attenuation, may also be required for some images and, for this purpose, a series of smoothing filters, both linear and non-linear, can be applied (Amaral, 2003).

2.6.3. Segmentation and debris elimination

Segmentation is one of the crucial steps of a QIA procedure and consists in the labeling of the image in regions representing the objects of interest (Khan *et al.*, 2014). This includes the separation between objects and background originating labeled, mask or binary images. Typically, a grey scale image is converted in a binary image (pixel value 1 for object and 0 for the background), by defining a given threshold using segmentation algorithms. However, if two different classes of objects are to be segmented in the final image, such as the identification of flocs, on one hand, and filaments, on the other, different threshold values (or even methodologies) may need to be defined for each (Jenné *et al.*, 2003).

2.6.4. Image analysis

This step is performed once the final (either binary, labeled or mask) images from the processing step are obtained. The most common parameters determined in AS systems are related to the microbial aggregates Euclidean morphology, such as (projected) area, number, perimeter, length, width, compacity, convexity, eccentricity, roundness, and extend, among many others. Also, the determination of the filaments numbers, length and contents are crucial when monitoring sludge dysfunction events. However, in some cases, the complex shape of a given structure may set the basis for fractal dimensions to be used.

2.6.5. Shape and size descriptors

As previously referred, several authors have already studied the application of QIA procedures to WWTP systems, in order to monitor the aggregated biomass characteristics, mainly in terms of the aggregated and filamentous bacteria contents and structure. These parameters have been, for the most part, related to the aggregates morphology, such as the Euclidian geometry parameters described in Amaral (Amaral, 2003). Furthermore, some parameters originated from the QIA data, such as the total microbial aggregates area per volume (TA), total filament length per volume (TL), total filament length per total aggregates area ratio (TL/TA) and total filament length per total suspended solids ratio (TL/TSS), have already proven to be helpful in WWTP monitoring.

The most common determined shape parameters, for QIA based WWTP monitoring, can be found in Section 2 of the appendices.

2.7. Chemometric tools

2.7.1. Principal component analysis

Principal component analysis (PCA) allows the determination of linear combinations of the original variables, called principal components (PCs) which are used to visualize latent structures and phenomena in the data. The original data is projected into a new coordinate system with the objects being described by scores and the variables by loadings (Einax *et al.*, 1997). PCA works by decomposing the data matrix X as the sum of the outer product of T (containing the scores) and P (containing the loadings) plus a residual matrix E :

$$X=TP^t+E$$

Each resulting PC captures the maximum variation not explained by the former PCs, i.e., the first PC maximizes the covariance in the raw data and the subsequent PCs maximize the covariance in the residual matrices, after extracting the former PCs. This dimensional reduction is achieved by the PCs being orthogonal and, hence, uncorrelated.

PCA has been used in several studies encompassing WWTP systems monitoring (Amaral and Ferreira, 2005; Mesquita *et al.*, 2008; Leal *et al.*, 2016). In fact, PCA was used in AS disturbances studies such as filamentous bulking, pinpoint floc formation and viscous bulking (Amaral *et al.*, 2013), and for the identification of protozoa and metazoa in AS systems by QIA (Amaral *et al.*, 1999; Motta *et al.*, 2001). In addition, a number of full-scale WWTPs pollutants studies were also performed with PCA (Singh *et al.*, 2005), encompassing the assessment of the plant performances and the enlightenment of the latent relationships between operational parameters (Avella *et al.*, 2011; Platikanov *et al.*, 2014; Ebrahimi *et al.*, 2017; Wang *et al.*, 2017). Moreover, PCA has also proven to be helpful for the identification of the factors affecting filamentous bacteria communities in nutrient removal full-scale WWTPs (Milobeldzka *et al.*, 2016) and for polyhydroxyalkanoates (PHA) inclusions quantification in SBR under different operational conditions (Amaral *et al.*, 2017). With respect to AGS systems PCA has already been used for microbial community analysis in AGS systems inoculated with sludge adapted to mild-low temperatures (Muñoz-Palazon *et al.*, 2018).

Regarding the particular case of PhACs removal in WWT systems, PCA has been already used to study the correlations between their concentrations and removal rates, and the characterization of influent wastewaters parameters and WWTP control design parameters (Santos *et al.*, 2009). Furthermore, the relationships between physical and chemical properties of target compounds and their removal efficiency in a full-scale constructed wetland (CW) were also determined with PCA (Vystavna *et*

al., 2017). In fact, PCA also proved to be helpful to understand the transport phenomena of PhACs, and their metabolites, between water and sediments, and further potential exposure to aquatic biota (Koba *et al.*, 2018).

2.7.2. Decision trees

A decision tree (DT) is a powerful prediction method feeding an input data (variables) matrix to a series of consecutive yes/no queries in order to predict a predefined response vector (Breiman *et al.*, 1984). To that effect, the size of the tree (the number of branches) should be carefully chosen in order to avoid overfitting the response data by pruning using, for instance, k-fold cross-validation (Krzywinski *et al.*, 2017).

DT has been used in several studies encompassing WWT systems monitoring, namely in prediction of foaming events in full-scale WWTP based on flocs morphology and structure parameters, protozoa, metazoa and filamentous bacteria communities (Leal, *et al.*, 2016). Moreover, DT has also been useful in the identification of bulking phenomena in full-scale WWTP using operational parameters and filamentous bacteria communities data (Deepnarain *et al.*, 2019). In fact, protozoa and metazoa communities were also important for the characterization of full-scale WWT systems using DT (Amaral *et al.*, 2018), and identification of protozoa and metazoa species based on QIA (Ginoris *et al.*, 2007a). DT was also used for the prediction of odor properties in full-scale WWTPs (Byliński *et al.*, 2019)

2.7.3. Discriminant analysis

Discriminant analysis (DA) is used to determine the best variables discriminating between two, or more, naturally occurring groups (Singh *et al.*, 2005). This technique is based on the definition of discriminant functions as linear orthogonal combinations of the original variables, organized in decreasing order of group separation ability (Einax and Zwanziger, 1997). The resulting discriminant functions can be further used to allocate new observation within one of the predefined groups (Kim *et al.*, 2011). One of the major differences between the use of PCA and DA relies on the need of the second for foreknowledge about the dataset groups (by means of feeding training data). (Singh *et al.* 2005)

DA has already been used in the recognition of protozoa and metazoa in AS systems (Ginoris *et al.*, 2007a), monitoring wastewater quality of a full-scale WWTP (Sulthana *et al.*, 2014), identification and diagnosis of problems in full-scale WTP (Garcia-Alvarez *et al.*, 2009; Flores-Alsina *et al.*, 2010) and identification of antibiotic resistance genes and fecal contamination in an urban catchment (Carroll *et al.*, 2009).

2.7.4. Multilinear regression

The multilinear regression (MLR) analysis is a linear regression method for estimating dependent variables (Y data) from a set of explanatory variables (X data). The MLR calculates the explanatory variables coefficients (β) by minimizing the sum of the residuals (differences between observed and predicted Y values) squares in a given dataset. An MLR model can be represented by the following equation:

$$Y = \beta_0 + \sum \beta_i x_i + \varepsilon \quad (\text{Eq. 1})$$

where x_i represents an explanatory variable of Y (the dependent variable), β_i is the coefficient associated to the explanatory variable x_i , and ε is the residual (Park *et al.*, 2015).

MLR has already been used in WWT systems for the prediction of BOD_5 , COD and removal of trace organic compounds from wastewaters (Kwak *et al.*, 2013; Abba and Elkiran, 2017; Park *et al.*, 2015) and for the prediction of total nitrogen (TN) of effluents from a full-scale WWTP (Lee *et al.*, 2014). Regarding the particular case of AGS, MLR has already been applied for performance prediction in a SBR performing a granulation process (Gong, 2018), and for determining the interrelationships between cell hydrophobicity and EPS contents in AGS cultivation with hypersaline and oily wastewaters (Corsino *et al.*, 2015).

2.8. Concluding remarks

Different aerobic biological WWT systems can be found in WWTP, with AS systems, mainly constituted by microbial (floc-forming and filamentous bacteria) aggregates, protozoa and metazoa, being the most widely operated. However, these systems fall short regarding the treatment of emergent PhACs, including sulfonamides and estrogens, widely present nowadays in municipal sewage. Indeed, both AS and MBR systems, the most widely operated, have shown to be, for the most part, inefficient in the removal of PhACs, with serious consequences to aquatic life and human health.

Thus, concern over the development of new sustainable removal technologies is increasing, with the main commonly employed biological WWT systems for PhACs removal being addressed. One of the most promising technologies, to that effect is AGS, which was employed within an SBR in the current research. Indeed, the use of AGS-based systems is expanding due to its smaller environmental footprint comparing with conventional systems (e.g., AS systems), increased resistance to organic load shocks and adequateness for toxic compounds removal. It should be stressed, though, that the AGS properties are intrinsically dependent on its structure, which must be carefully monitored and, traditionally, rely on human-based visual inspection.

Complementing the microscopy survey of WWT systems, QIA has proved to be a powerful tool for monitoring and control. In fact, its ability to provide quantitative data, in comparison to human-based qualitative assessment, is a determining factor for the increasing acceptance of this methodology. As such, QIA methodologies are increasingly used to estimate WWT systems effluent quality and predict disturbances. More recently, QIA has been applied for AGS assessment in mature and stable conditions.

Given the large amount of data provided by QIA, chemometric techniques have been successfully employed to make sense of such large databases. Expanding on the above, in the current work a QIA methodology has been employed to study the effect of PhACs (SMX, E2 and EE2) presence in the biomass of an SBR-AGS system. In the current work, it could be validated the usefulness of QIA, coupled with chemometrics, as a suitable tool for the assessment of the SBR-AGS biomass in the presence of PhACs.

Chapter 3 – Material and methods

3.1. Experimental set-up

The experimental set-up includes a SBR with a volume of 5 L with AGS inoculated from a full-scale WWTP (with aerobic granules) from Portugal. The work volume was 2.5 L, the feeding was provided by a *Watson Marlow 101 R* pump (*Watson Marlow, Wilmington, USA*) and the treated effluent by a *Watson Marlow 323* pump (*Watson Marlow, Wilmington, USA*). The air supply was controlled with an *Aalborg GCF17* mass flow controller (*Aalborg, Aalborg, Denmark*) the pH of synthetic wastewater and temperature of mixed liquor was monitored with a *Consort C1010* multiparameter analyzer (*Consort, Turnhout, Belgium*). Timers were used in aeration, feeding and discharge pumps allowing to control the SBR cycles. The experimental set-up of the SBR-AGS used during the experiments is presented in Figure 6.

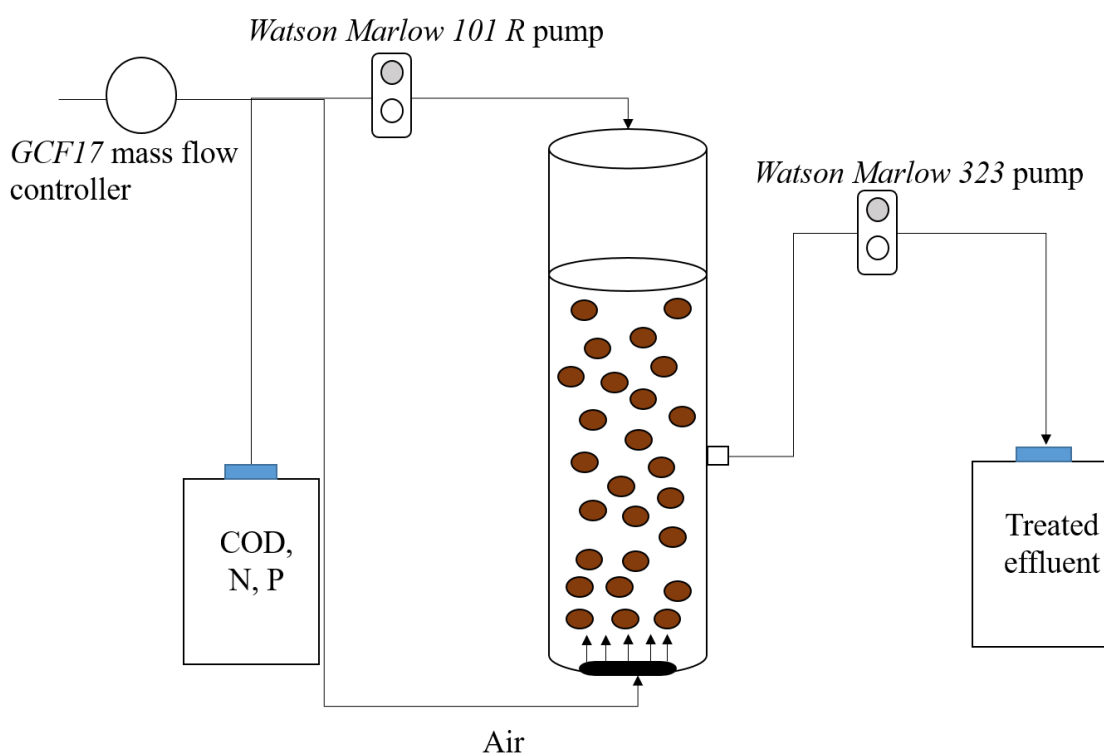


Figure 6 Experimental set up of the employed SBR-AGS

3.1.1. Reactor operation

The 5L SBR-AGS was operated for the treatment of a synthetic wastewater containing 5.168 g L⁻¹ of C₂H₃O₂Na·3H₂O; 0.887 g L⁻¹ of MgSO₄·7H₂O; 0.35 g L⁻¹ of KCl; 0.596 g L⁻¹ of Na₂HPO₄; 0.286 g L⁻¹ of KH₂PO₄; 1.894 g L⁻¹ of NH₄Cl. A volume of 10 mL L⁻¹ of a trace elements solution was added containing 1.5 g L⁻¹ of FeCl₃·6H₂O; 0.15 g L⁻¹ of H₃BO₃; 0.03 g L⁻¹ of CuSO₄·5H₂O; 0.18 g L⁻¹ of KI; 0.12 g L⁻¹ of

$\text{MnCl}_2 \cdot 4\text{H}_2\text{O}$; 0.06 g L^{-1} of $\text{Na}_2\text{MoO}_4 \cdot 2\text{H}_2\text{O}$; 0.12 g L^{-1} of $\text{ZnSO}_4 \cdot 7\text{H}_2\text{O}$, and 0.15 g L^{-1} of $\text{CoCl}_2 \cdot 6\text{H}_2\text{O}$ (adapted from (De Kreuk *et al.*, 2005)). The experiments with PhACs were conducted operating the SBR-AGS in the presence of environmentally relevant concentrations of steroid estrogens, namely E2 and EE2, and the sulphonamide SMX.

In order to characterize the mature AGS, a prior experiment was conducted for 49 days in the absence of PhAC, acting as a control (CONT). Furthermore, the inoculated biomass was set to acclimate for a period of 22 days before the E2, EE2 and SMX experiment data collection. Each operational cycle in the SBR lasted for 6 h encompassing 120 min of feeding, 232 min of aeration, 3 min of settling and 5 min of withdrawal, with a hydraulic retention time of 12 h. Care was taken to allow the AGS attaining somewhat similar characteristics, mainly in terms of the overall removal performance and granular biomass (fraction and large granules size), in the beginning of the monitoring period for all experiments (CONT, E2, EE2, and SMX). For that purpose, the AGS was allowed to recover to the initial steady-state conditions, between experiments, for a period of roughly one month without any PhAC addition. The SBR was operated at room temperature ($18\text{-}23^\circ\text{C}$), with an air flow of 7.50 L min^{-1} , resulting in a superficial air velocity kept above 1.8 cm s^{-1} allowing to keep the granules mixture in suspension during the monitoring period. The experimental setup, encompassing the sludge sampling methodology, is presented in Figure 7.

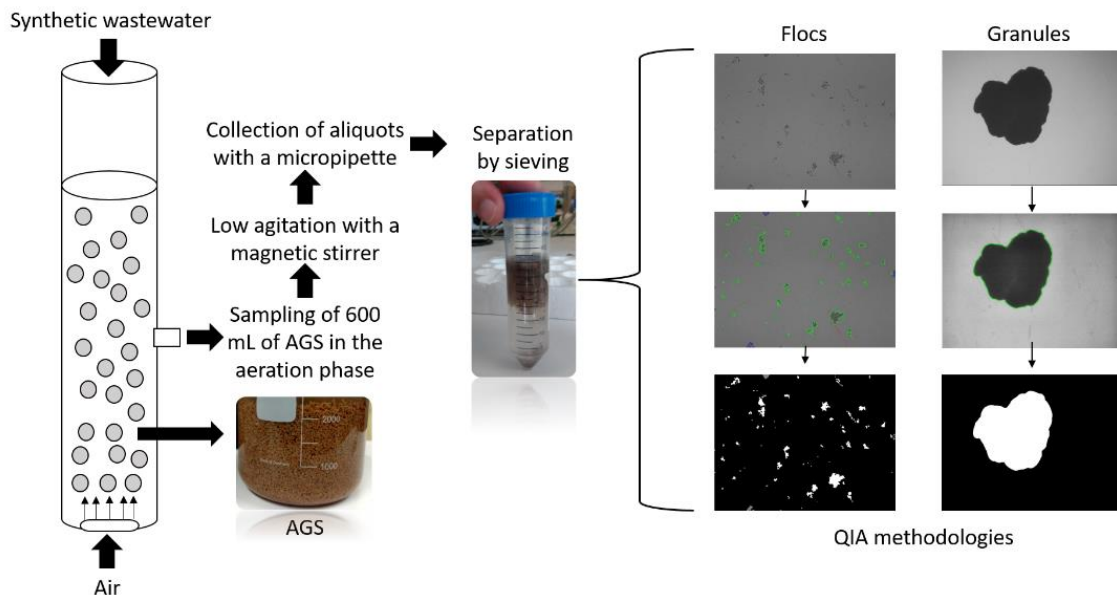


Figure 7 Experimental set up and sampling methodology of the SBR-AGS

3.1.2. PhAC concentrations

The PhACs feeding was performed each other week with the addition of the studied PhACs in the SBR-AGS assessed by collecting samples in the synthetic feed (INLET, entering the reactor). In accordance, the studied PhACs concentrations entering the reactor, during the monitoring period, can be found in Table 6. The average INLET values were somewhat similar between the studied PhACs (0.221, 0.278 and 0.290 mg L⁻¹ for E2, EE2, and SMX respectively). The most relevant differences were found to be in the maximum concentrations, and standard deviation, and in both cases the highest values were determined for the EE2 steroid estrogen (1.258 mg L⁻¹ and 0.493 mg L⁻¹, respectively). Given the SBR chosen operational strategy, the E2, EE2 and SMX concentrations entering the reactor were null each other week.

Table 6 Concentrations (in mg L⁻¹) of the studied PhAC entering and leaving the SBR-AGS

INLET				
PhAC	Minimum	Average	Maximum	Standard deviation
[E2]	0.000	0.221	0.564	0.204
[EE2]	0.000	0.278	1.258	0.493
[SMX]	0.000	0.290	0.537	0.197
OUT				
PhAC	Minimum	Average	Maximum	Standard deviation
[E2]	0.000	0.000	0.000	0.000
[EE2]	0.000	0.003	0.017	0.007
[SMX]	0.000	0.000	0.000	0.000

The evolution of the E2, EE2 and SMX concentrations entering the reactor during the monitoring periods are presented in Figure 8.

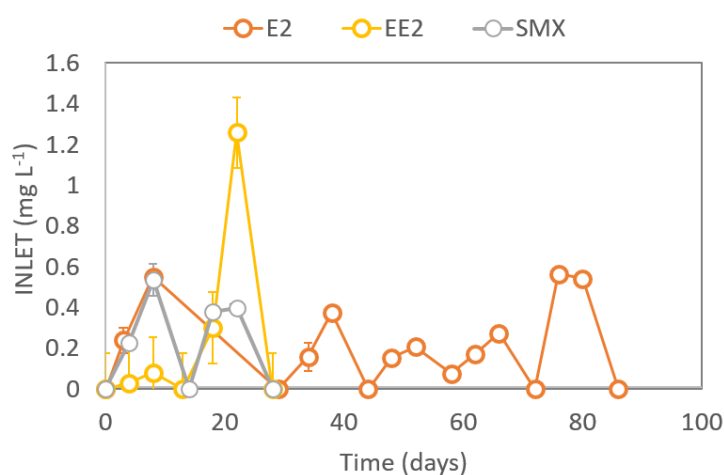


Figure 8 Evolution of concentrations of the studied PhAC during the monitoring period

3.2. Physicochemical analyses

Chemical oxygen demand (COD), ammonium nitrogen (N-NH_4^+), nitrite (N-NO_2^-), nitrate (N-NO_3^-) and phosphorus (P) concentrations were determined with Hach Lange cell tests (*Hach Lange, Dusseldorf, Germany*). The total inorganic nitrogen (TIN) concentration in the influent was assumed to be equal to the ammonium concentration, while the TIN in the effluent was determined as the sum of ammonia, nitrite, and nitrate concentrations.

The total and volatile suspended solids for the overall biomass ($\text{TSS}_{\text{total}}$ and $\text{VSS}_{\text{total}}$), floccular (TSS_{floc} , VSS_{floc}) and granular (TSS_{gran} , VSS_{gran}) fractions, as well as the SVI at 5 (SVI_5) and 30 minutes (SVI_{30}), were determined according to standard methods (*APWA, 2017*). The aggregates density (Dens.) was determined with Blue dextran by the method described by Beun *et al.* (2002). Blue dextran was acquired from GE Healthcare Biosciences.

The chromatographic analysis of E2, EE2 and SMX was performed for the synthetic feeding entering the reactor (INLET) and for the treated effluent (OUT). The analysis was performed using a Shimadzu Corporation apparatus (*Shimadzu, Tokyo, Japan*) consisting of a Nexera UHPLC with a multi-channel pump (LC-30 CE), an autosampler (SIL-30AC), an oven (CTO-20AC), a diode array detector (M-20A) and a system controller (CBM-20A) with built-in software (LabSolutions), according to (Quintelas *et al.*, 2019; Fonseca *et al.*, 2013). The collected samples were centrifuged at 8000g and filtered with a 0.2 μm filter prior to HPLC analysis. The mobile phase, with a flow rate of 0.8 mL min^{-1} , consisted of water (pump A) and acetonitrile (pump B) and the isocratic mode (55% A and 45% B), was used. The diode array detector, ranging from 190 to 400 nm, was used for quantification at 220 nm. E2, EE2 and SMX (98%) were acquired from Sigma Aldrich.

3.3. Sludge sampling and image acquisition

It is known that the AGS collected from within the reactor is not exempt of representativeness issues regarding its structural analysis, particularly at lab-scale. With the aim of minimizing this problem the following sampling methodology was proposed.

A sludge volume of 600 mL was collected at mid-point depth in the reactor, to obtain homogeneous and representative biomass samples, in the beginning of the aeration stage at regular time intervals. Furthermore, the sludge bed volume per sample volume (SBD/SV) on the collected samples was also surveyed in order to be proportional to the SBD/SV in the reactor, with the sampling procedure being repeated otherwise (Pronk *et al.*, 2014). These samples were kept under low agitation conditions to avoid settling and promote the mixture between the solid and liquid phases on one hand,

and to avoid changes in the sludge morphology and structure by high shear stress conditions, on the other. Such a high sampling volume (12% of the reactor volume) was collected to avoid representativeness issues. Furthermore, the aliquots were collected with a micropipette with a sectioned tip (allowing larger aggregates to flow) for the separation of fractions prior to the QIA procedure, and the remaining volume was reintroduced in the reactor.

The separation of the granular and suspended (floccular) mature AGS was obtained using a 500 μm sieve, allowing for the floccular aggregates to pass through, and with the retained granules carefully picked up by rinsing with distilled water (Leal *et al.*, 2020a) to avoid physical disruption. Care was also taken to avoid the formation of a filtration cake by carefully pouring the sampled volume throughout the available filtration area. This procedure was employed with the aim of minimizing possible alterations in the biomass morphology and structure during the physical handling. The granular fraction TSS were determined according to standard methods (APWA, 2017).

Aliquots of a standardized volume were employed for the granules QIA analysis, based on the TSS of the granular fraction. For samples with TSS lower than 15 g L^{-1} , a 35 mL sample aliquot was used, whereas for TSS higher than 15 g L^{-1} , a 10 mL aliquot was employed, in order to avoid significantly incrementing the time spent on image acquisition. The separated granular biomass fraction was further deposited in a Petri dish. Images from the entire set of granules present in each aliquot volume were acquired through the use of an *Olympus SZ 40* stereomicroscope (*Olympus*, Shinjuku, Japan) under a total magnification of $15\times$. For the particular case of the SMX experiment, a *Leica S8APO* stereomicroscope was used under a total magnification of $16\times$. The number of acquired granules averaged from $840 (\pm 380)$ for the 35 mL aliquots to $394 (\pm 104)$ for the 10 mL aliquots.

Regarding the suspended (floccular) biomass, aliquots of 10 μL (in triplicate) were collected with a micropipette, with a sectioned tip to allow larger aggregates to flow through, deposited onto a slide and let to air-dry. Images were further acquired in bright field microscopy with an *Olympus BX51* microscope (*Olympus*, Shinjuku, Japan) or a *Nikon Eclipse Ci-L* (*Nikon*, Minato, Japan) under a total magnification of $40\times$ for the CONT and E2 experiments and $100\times$ for the EE2 and SMX experiments, resulting in a total of 150 images (average of 11,200 flocs) per sample.

3.4. *Quantitative image analysis methodologies*

The employed QIA methodology was based on the identification and characterization of the aerobic granular and floccular biomass using the previously developed routines, run on Matlab 7.8.0 (The

Mathworks, Natick, MA). A more detailed description of the employed QIA methodology can be found in (Amaral, 2003).

The QIA routine for the granules identification first performs a background correction (with or without the use of a previously acquired background image) in order to correct for non-uniform light differences. A contrast enhancement step is next performed, based on a Canny edge detection algorithm, to sharpen the granules edges and facilitate border recognition. Granules segmentation is then achieved based on a thresholding algorithm, in order to separate them from the background. Debris elimination is the subsequent step and is based mainly in a size morphological opening operation. The minimum equivalent diameter for a granule not to be considered debris or floccular material trapped in the sieve, was set to 175 μm , taking also into account the limitations posed by the higher magnification used for the granules image acquisition, which resulted in less than 2% of the acquired aggregates falling below this threshold. The segmented granules image is then stored, coding the granules entirely within the image limits as 1, the granules cut-off by the image borders as 0.5 and the background as 0.

With respect to the QIA routine for the flocs identification, following an initial background correction, an histogram equalization and a low pass filter are next applied to enhance the aggregates borders. Flocs segmentation is then achieved through the use of a thresholding algorithm, followed by debris elimination considering a size based morphological operation. The minimum equivalent diameter for a floc not to be considered debris was set to 9 μm , taking also into account that smaller structures are likely to be composed by a number of bacterial cells hardly composing a full floccular structure. As for the granules, the segmented flocs image is then stored, coding the flocs as well.

In WWT systems monitoring, the QIA data analysis step usually encompasses the quantification and/or classification of the microbial aggregates structure (aggregated and filamentous biomass) based on the previously identified parameters. In this context, one of the most commonly performed data pre-processing step is based on the microbial aggregates division into three equivalent diameter (Deq) size classes: small (micro)flocs (F1, below 0.025 mm), intermediate (meso)flocs (F2, between 0.025 and 0.25 mm), and large (macro)flocs (F3, above 0.25 mm). In accordance, the granules were also divided into three size classes based on their Deq: small granules (G1, below 0.25 mm), intermediate granules (G2, between 0.25 and 2.5 mm) and large granules (G3, above 2.5 mm). Furthermore, a study of the aggregates retained on the sieve and below 250 μm was also performed for continuity analysis purposes.

The QIA based morphological characterization routine was next performed on the resulting images of the identification step and allowed for the determination of each granule and floc morphology and size parameters, identified in the section 1 of Appendices. Further information regarding the parameters' calculation can be found in Amaral (2003). The QIA workflow for the AGS floccular and granular fractions is presented in Figure 9.

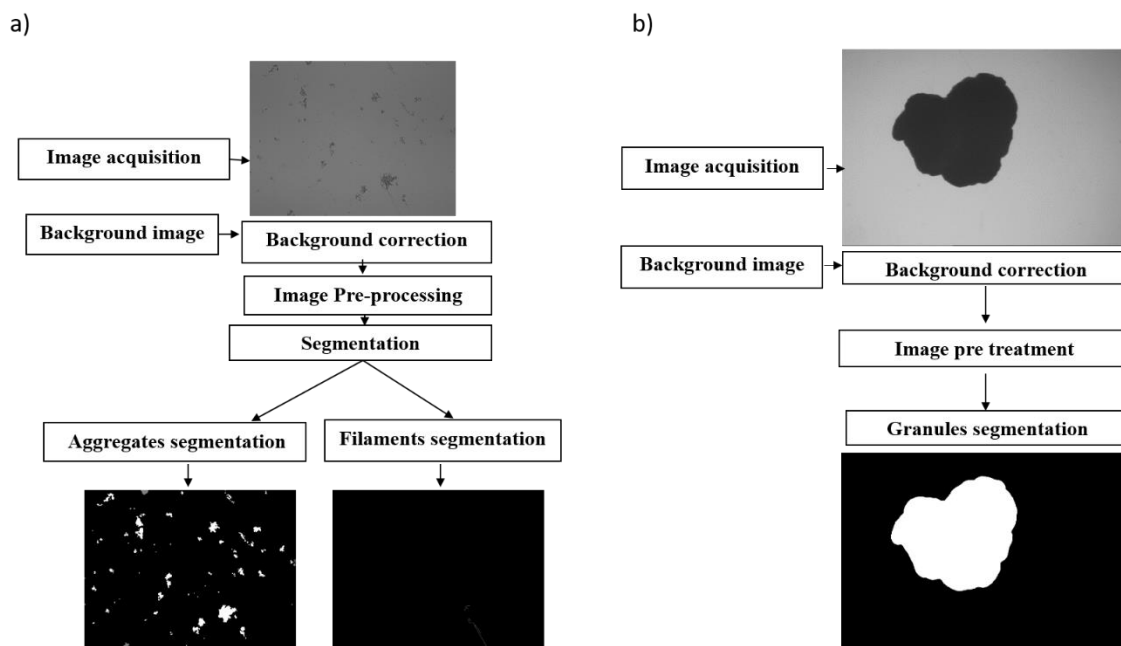


Figure 9 Workflow for the QIA assessment of AGS a) floccular fraction b) granular fraction

3.5. Chemometric tools

In the current study, PCA and MLR were performed for the ensemble CONT, E2, EE2 and SMX experiments regarding the SBR physicochemical parameters (with and without density) and the main QIA morphological parameters of both granular and floccular AGS fractions. A total of 34 observations and 140 variables were employed for these analyses including the sludge density, whereas 28 observations and 139 variables were employed otherwise. For both PCA, DA and DT, ensemble and separate analyses were performed for the floccular and granular fractions, and for the sludge physical and settling properties. Matlab 7.3 (*The Mathworks, Inc. Natick, USA*) was used to perform all the above analyses.

The main objective of the employed PCA focused on the establishment of the key interrelationships between, and within, the physicochemical and morphological parameters, as well as with the found naturally occurring clusters. Regarding the employed DA and DT, the main focus was set on selecting the best physicochemical and/or morphological parameters (or orthogonal combinations with respect to the DA), for the separation and/or identification of each experiment group and samples containing

PhACs. Lastly, MLR was employed to obtain linear model fits for TSS and VSS (both for the suspended and granular biomass), SVI_5 , and biomass density (Y dataset) from the QIA based data (X dataset).

3.6. *Statistical analysis*

A statistical runs test (Bradley, 1968) was applied to the granules QIA data obtained for each day of the different experiments, in order to determine the corresponding z-value. An α -value of 0.05 (95% confidence) was used, and the obtained z-values were compared with the Critical z-value (1.96) for the chosen α -value. In accordance, it could be assumed that the data exhibits random behavior for a z-value below 1.96, exhibiting nonrandom behavior otherwise. For that purpose, a *runstest* was performed in Matlab 7.3 (*The Mathworks, Inc. Natick, USA*) for the number of up or down runs on the sequence of observations of the granules QIA parameters to test the hypothesis that the values appear in random order.

Chapter 4 - Performance of the SBR-AGS

4.1. Introduction

AGS systems are considered robust for both nutrient removal and organic matter removal. However, the removal efficiencies reported in literature are quite dependent on a number of variables (Purba *et al.*, 2020). AGS has proven to be suitable for simultaneous removal of COD, P-PO₄ and N in long-term operation of SBR treating low C/N domestic wastewater with, respectively, 84%, 96% and 71% of removal efficiencies being reported (Campo *et al.*, 2020). Regarding synthetic wastewaters, 93%, 58% and 100% average removal efficiencies were achieved for COD, N and P, respectively, in a SBR-AGS with SRT of 15 days operated, although when the SRT was not controlled the P removal efficiency decrease to 15% (Castellanos *et al.*, 2021).

With respect to the performance of AGS in the presence of PhACs, average COD removal above 92%, and N-NH₃ and P around 99%, were obtained during the treatment of EE2 4-nonylphenol and carbamazepine (Kent and Tay, 2019). On the other hand, lower performances were obtained in the presence of 2 µg L⁻¹ of SMX, in a SBR operated with HRT of 12h, regarding COD, TN and TP removal, averaging 96%, 44% and 89% respectively (Kang *et al.*, 2018b). Again, the SBR-AGS performance in the presence of PhAC could be dependent of several variables namely the specific PhAC, respective concentration and mixtures, among other operational variables.

4.2. Results and discussion

4.2.1. SBR performance with stable and mature AGS

In this subsection, the performance of the SBR with stable and mature AGS will be discussed. For that purpose, an operational period of 66 days was allowed for the stabilization and maturation of granules, with the VSS/TSS ratio being used to assess the maturation of AGS presenting a value of 0.87 in the end of the stabilization period. The performance of the reactor, assessed by the COD, TIN and TP removal efficiencies, throughout the monitoring period, is presented in Figure 10.

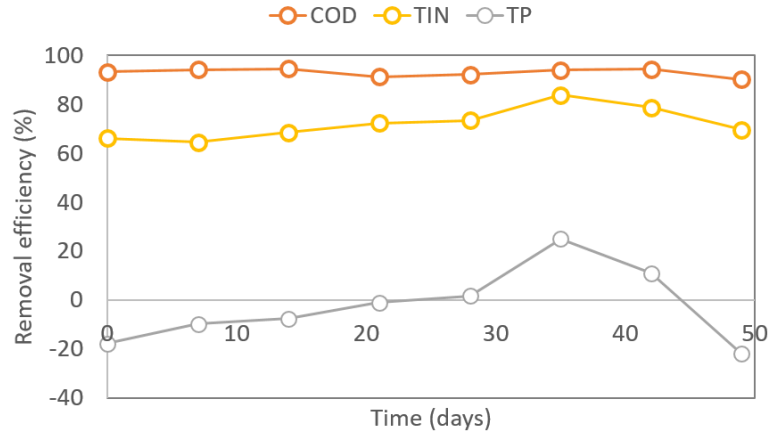


Figure 10 COD, TIN and TP removal efficiencies for the SBR-AGS throughout the monitoring period.

The SBR performance, in the period upon obtaining mature AGS showed high and relatively constant removal efficiencies (Figure 10) regarding the COD (above 90%, with an average value of 93 ± 2 %) and ammonia oxidation (above 90%, with an average value of 94 ± 2 % - data not shown). In addition, during the entire operational period, the TIN removal efficiency remained somewhat constant with an average value of 72 ± 7 %. On the other hand, the TP removal efficiency remained, for the most part of the monitoring period, quite low or even negative. The negative TP removal efficiency could be related to the interference of nitrates on PAO metabolism. Nitrate can inhibit phosphorus release in anaerobic conditions and uptake in the aerobic ones (Zou *et al.*, 2006). Several references can be found in literature reporting similar results of COD and TIN removal efficiencies in lab-scale, pilot scale, and full-scale AGS systems, respectively (Bassin *et al.*, 2012; Long *et al.*, 2019; Pronk *et al.*, 2015; Świątczak and Cydzik-Kwiatkowska, 2018). Moreover, poor TP removal efficiencies (around 15%) were also obtained in the first days of operation of a lab-scale AGS system under high temperature (Ab Halim *et al.*, 2016).

4.2.2. SBR performance in the presence of PhAC

The SBR-AGS performance, in terms of pollution removal, was also evaluated through the COD, TIN and TP removal efficiencies in the presence of PhACs. Thus, the evolution of these parameters, during the monitoring period, is presented in Figure 11. Also, the nitrification process (in section 3 of the appendices) was evaluated.

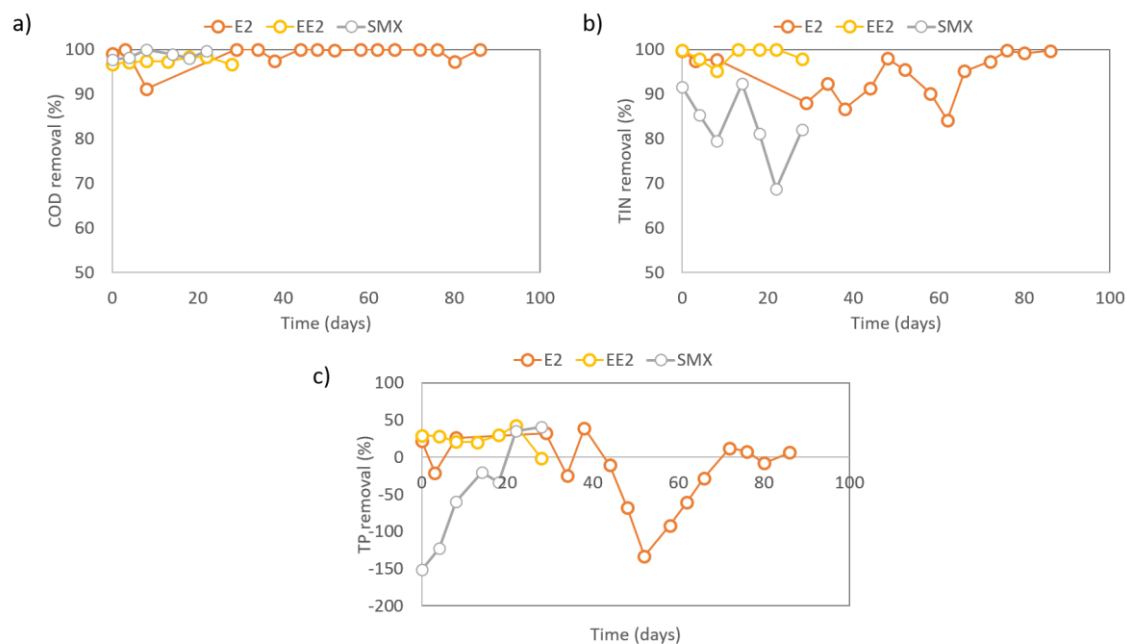


Figure 11 Evolution of the reactor performance for the E2, EE2 and SMX experiments monitoring period. a) COD, b) TIN and c) TP removal efficiencies.

Regarding the COD removal efficiency (Figure 11a), it was found that the values were tendentially constant throughout the experiments, ranging from 97.2% to 100.0% for the E2 experiment (except for day 8 with 91.1%) and averaging 99.6% ($\pm 0.9\%$) without day 8, from 96.6 to 98.3% for the EE2 experiment and averaging 97.4% ($\pm 0.7\%$) and from 97.8% to 99.9% for the SMX experiment and averaging 98.7% ($\pm 0.9\%$). Similar results of COD removal was found in a SBR with AGS treating pharmaceuticals and personal care products including SMX (Yu *et al.*, 2020).

With respect to the nitrogen removal, assessed by the TIN (Figure 11b), an oscillating behavior was found for the E2 experiment, ranging from 84.1% to 99.7%, and averaging 94.5% ($\pm 5.1\%$), although recovering to the initial values at the end of the experiment. Larger average values were obtained for the EE2 experiment (98.7% $\pm 1.8\%$), within a smaller range (95.2% to 100.0%). Regarding the SMX experiments, the TIN removal ability was more affected, ranging from 68.7% to 92.4%, and averaging 82.9% ($\pm 8.1\%$), with an oscillating decreasing trend. Again, similar results were found in the literature for SBR operating with AGS and under alkalinity conditions (Yao *et al.*, 2014; Gao *et al.*, 2020). In fact these results could be also partially explained by the effect of continuous dosing of SMX on abundance of ammonia oxidizing bacteria (AOB) and nitrite oxidizing bacteria (NOB) and in nitrification ability (Katipoglu-Yazan *et al.*, 2016).

On the other hand, the TP removal (Figure 11c) was quite poor during all experiments, often presenting negative values and never surpassing 42.6% in all cases. Regarding the E2 experiment, an

oscillating behavior was found, ranging from -132.6% to 38.8% , and averaging $-18.8\% (\pm 48.1\%)$. The behavior of the EE2 experiment was much more regular ranging from 20.0% to 42.6% (except for the last day with -1.8%) and averaging $28.3\% (\pm 8.2\%)$ without the last day. With respect to the SMX, and although presenting an average of $-44.5\% (\pm 73.0\%)$, an increasing behavior could be found, ranging from -151.1% up to 40.3% , in the end. These results could be related to the effect of nitrate and nitrite in the metabolism of phosphate accumulating organisms (PAO) (Zou *et al.*, 2006; Zheng *et al.*, 2013). Moreover, similar results of phosphorous removal were also found in a AGS system operated under stress caused by high salinity conditions (He *et al.*, 2020).

Comparing the results obtained for the COD removal ability, with respect to the TIN and TP (at day 0 and throughout the experiments), the obtained sludge seems to present better performances in removing the organic matter (maintaining the initial removal ability). This may point to a more resilient COD removal ability, regarding the studied PhAC presence, when compared to TIN and TP (which fluctuated more). These results are in accordance with previous works addressing the removal of SMX and oxytetracyclines (OTC) in SBR-AGS (Yu *et al.*, 2020; He *et al.*, 2021). Indeed, it can be inferred that the COD removal efficiency was not strongly affected by the addition of E2, EE2 and SMX, with the removal values remaining somewhat constant throughout the experiments (above 91%).

On the other hand, the studied PhAC had a more pronounced effect on the TIN removal efficiencies, presenting a larger fluctuation throughout the experiments. In that respect, the SMX effect seems more pronounced leading to a decreasing trend in the TIN removal ability. The TP removal efficiency was quite poor during all experiments, often presenting negative values and never surpassing 42.6% in all cases. EE2 seems to least affect (within the studied PhAC) the TP removal efficiency taking into consideration its somewhat stable values throughout this experiment. On the other hand, the TP removal fluctuated more with the addition of E2, although recovering at the end. Interestingly, the SMX presence seems to even improve the TP removal ability. However, care should be taken when assessing the TP removal ability in the present case, since this process is quite dependent of a number of other conditions.

4.2.3. *Suspended and granular fractions structure of mature AGS*

The VSS concentration inside the SBR varied between 4.6 and 6.2 g VSS L⁻¹ (average value of 6.1 ± 0.7 g VSS L⁻¹) whereas the TSS varied between 5.1 and 6.9 g TSS L⁻¹ (average value of 5.4 ± 0.7 g TSS L⁻¹). The obtained high organic fraction (VSS/TSS average ratio of 0.89 ± 0.01) reflected the last

stages of the dynamic granules' maturation process in the current experiment, and could be expected given the synthetic feed used in this experiment (Corsino *et al.*, 2016). Figure 12 presents the evolution of the suspended and granular biomass fractions throughout the monitoring period. Regarding the suspended solids (TSS and VSS) (Figure 12,b), the granular biomass fraction predominated throughout the monitoring period, presenting an average value of 4.3 ± 0.8 g TSS L⁻¹ and 4.0 ± 0.7 g VSS L⁻¹, around two and a half times larger than the suspended biomass fraction counterpart (with average values of 1.7 ± 0.4 g TSS L⁻¹ and 1.5 ± 0.4 g VSS L⁻¹). Furthermore, a shift towards an increased content in granular biomass (both in terms of TSS and VSS) occurred from day 14 to day 23, and from that day onwards the granular biomass solids concentration remained stable (average values of 4.9 ± 0.2 g TSS L⁻¹ and 4.5 ± 0.2 g VSS L⁻¹, respectively). On the other hand, from day 14 onwards, both the TSS and VSS concentrations of the suspended biomass steadily decreased until the end of the monitoring period (1.0 g TSS L⁻¹ and 0.9 g VSS L⁻¹ in the last day of the monitoring period). Regarding the biomass physical characteristics, the SVI₅ varied between 36 and 67 mL gTSS⁻¹, decreasing in the first part of the monitoring period but remaining tendentially stable from day 14 onwards, indicating an AGS with a good settling ability (average value of 47.2 ± 11.0 mL gTSS⁻¹) and presenting an SVI₃₀/SVI₅ ratio close to 1 (average value of 0.93 ± 0.05) (Figure 12d). The obtained values can be considered in accordance with several references found in the literature regarding the expected SVI of stable and mature AGS (Etterer and Wilderer, 2001; Pronk *et al.*, 2015).

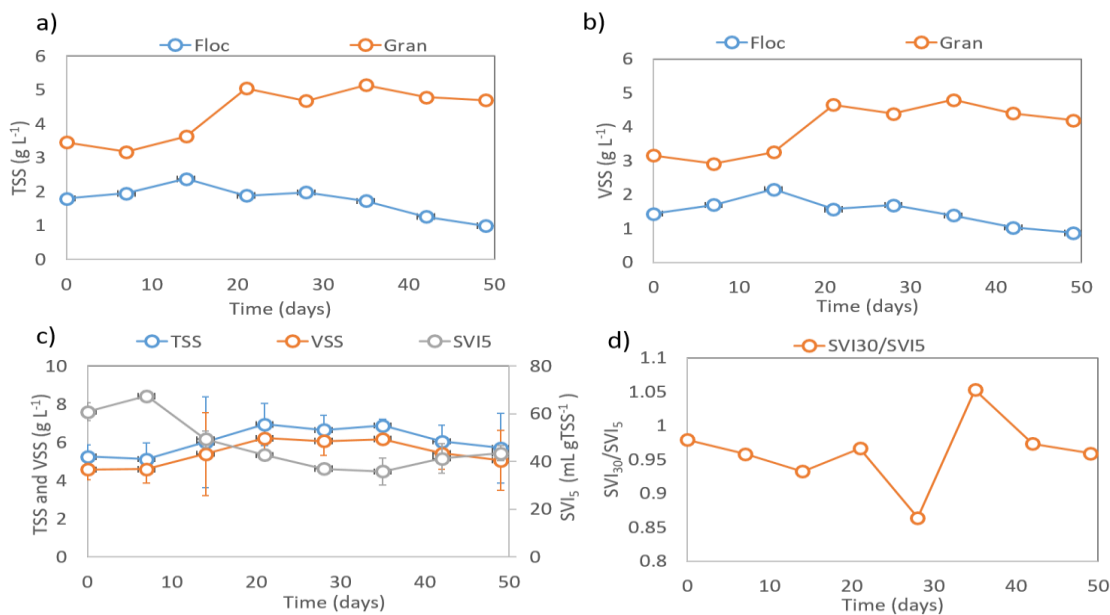


Figure 12 a) TSS and b) VSS evolution for the suspended (Floc) and granular (Gran) biomass c) TSS and VSS (Floc+Gran) and AGS settling properties (SVI₅) and d) SVI₃₀/SVI₅ evolution.

The evolution of the TA_{flocs}/Vol and % Area for the F1, F2 and F3 fractions, and of the TL/TA_{flocs} , TL/TSS and TL ratios throughout the monitoring period are presented in Figure 13. The suspended aggregated (flocs) biomass amount (Figure 13a), in terms of projected area per sample volume, steadily decreased from day 87 ($1408 \text{ mm}^2 \text{ mL}^{-1}$) onwards ($876 \text{ mm}^2 \text{ mL}^{-1}$ in the last day of the monitoring period), in line with the flocs TSS and VSS decrease. Within the flocs biomass, the intermediate (F2, 25-250 μm) flocs predominated (70% or above with an average of $74.8 \pm 5.6\%$) throughout the entire monitoring period, followed by the large (F3, $>250 \mu\text{m}$) flocs (average value of $17.5 \pm 7.6\%$). On the other hand, the small (F1, $<25 \mu\text{m}$) flocs (average value of $7.7 \pm 4.7\%$) did not surpass, except from one occasion, the 10% barrier (Figure 13b).

Regarding the filamentous contents of the samples (Figure 13c), and although a significant variation in relative terms was determined (average value of $2.8 \pm 1.5 \text{ m mL}^{-1}$ for TL , $2.4 \pm 1.1 \text{ mm mm}^2$ for TL/TA_{flocs} and $0.48 \pm 0.28 \text{ m mg}^{-1}$ for TL/TSS), in absolute terms the obtained values were found to be quite lower than the filaments threshold able to lead to filamentous bulking problems (20 m mL^{-1} for TL , 15 mm mm^2 for TL/TA_{flocs} and 7 m mg^{-1} for TL/TSS (Mesquita *et al.*, 2008)).

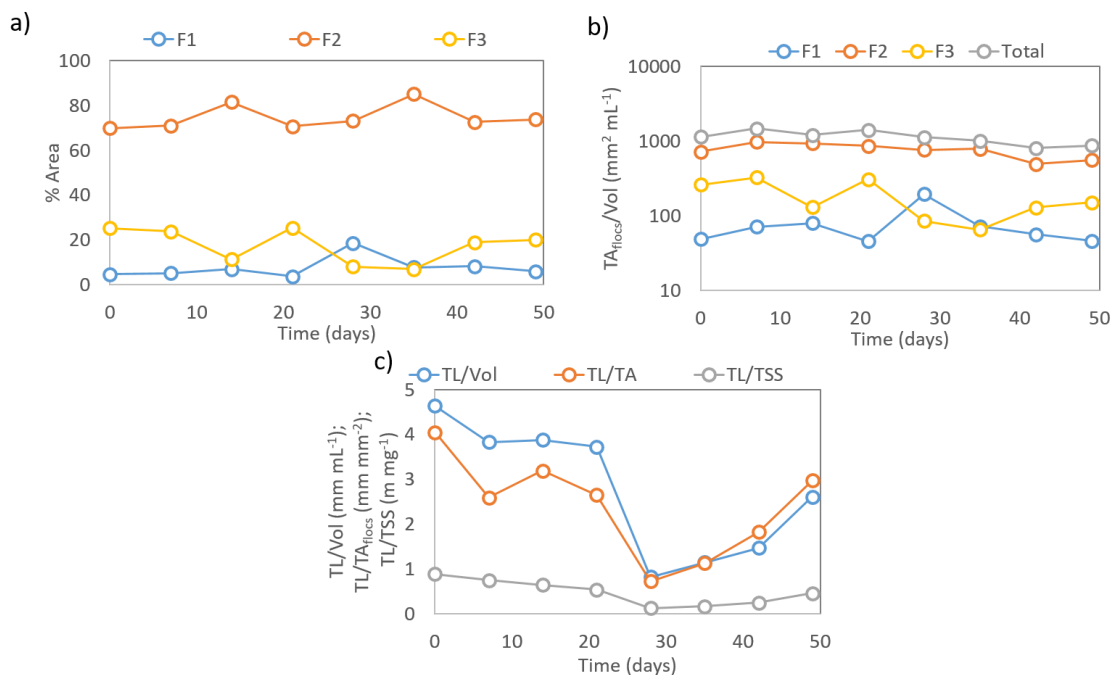


Figure 13 Evolution of the (a) TA_{flocs}/Vol and (b) % Area for the F1, F2 and F3 fractions; (c) TL/TA_{flocs} , TL/TSS and TL ratios.

The evolution throughout the monitoring period, of the TV_{gran}/Vol and % Vol for the G1, G2 and G3 fractions is presented in Figure 14. The granular biomass amount, in terms of estimated volume per sample volume (average value of $383 \pm 59 \text{ mm}^3 \text{ mL}^{-1}$), slightly oscillated during the monitoring period (Figure 14a). Within the granular biomass, the large granules (G3, $>2.5 \text{ mm}$) predominated (68% or

above with an average value of $80.7 \pm 8.4\%$) throughout the entire monitoring period (Figure 14b), followed by the intermediate (G2, 0.25-2.5 mm) granules (average value of $19.3 \pm 8.4\%$). On the other hand, the small (G1, <0.25 mm) granules (average of $0.006 \pm 0.004\%$) could be considered almost negligible. Furthermore, with the increased solids concentration in granular biomass (TSS and VSS) that occurred from day 14 to day 23, the small granules practically disappeared.

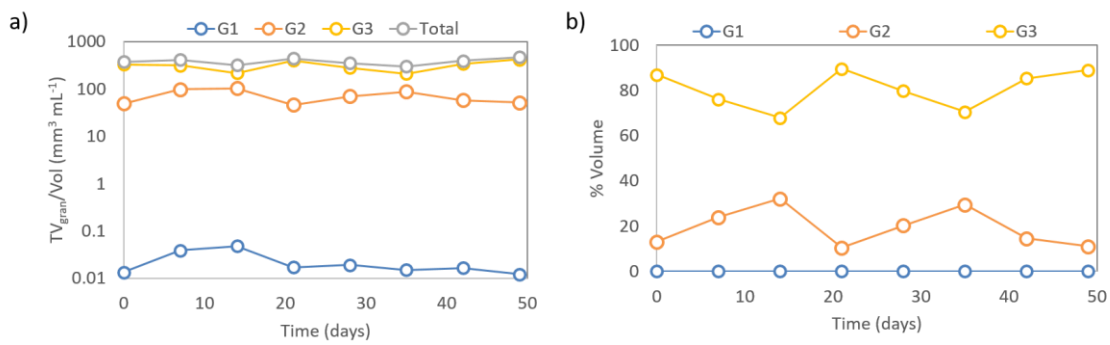


Figure 14 Evolution of (a) TV_{gran}/Vol and (b) % Vol for the G1, G2 and G3 fractions.

Figure 15 presents the evolution of the robustness and eccentricity morphological descriptors for the F1, F2, F3, G1, G2 and G3 fractions throughout the monitoring period.

The evolution of the overall aggregated (flocs) biomass morphology (in terms of robustness and eccentricity) was found to be quite dependent on the small flocs due to the fact that this fraction was highly predominant in terms of their numbers (above 73% in average). And, although the intermediate flocs (predominant in terms of projected area) presented a somewhat stable morphology (robustness average value of 0.63 ± 0.03 and eccentricity of 0.75 ± 0.02) throughout the monitoring period, an overall decreasing trend in the aggregates robustness (Figure 15a) and increasing trend in their eccentricity (Figure 15c), representative of the flocs deterioration, could be found from day 30 onwards.

Regarding the granular biomass, the obtained 0.74 ± 0.02 overall values for the robustness (Figure 15b) and 0.72 ± 0.02 for the eccentricity (Figure 15d), indicate the presence of robust, yet slightly elongated, structures. Furthermore, both the overwhelming intermediate and large granular biomass morphology was found to be quite stable during the entire monitoring period.

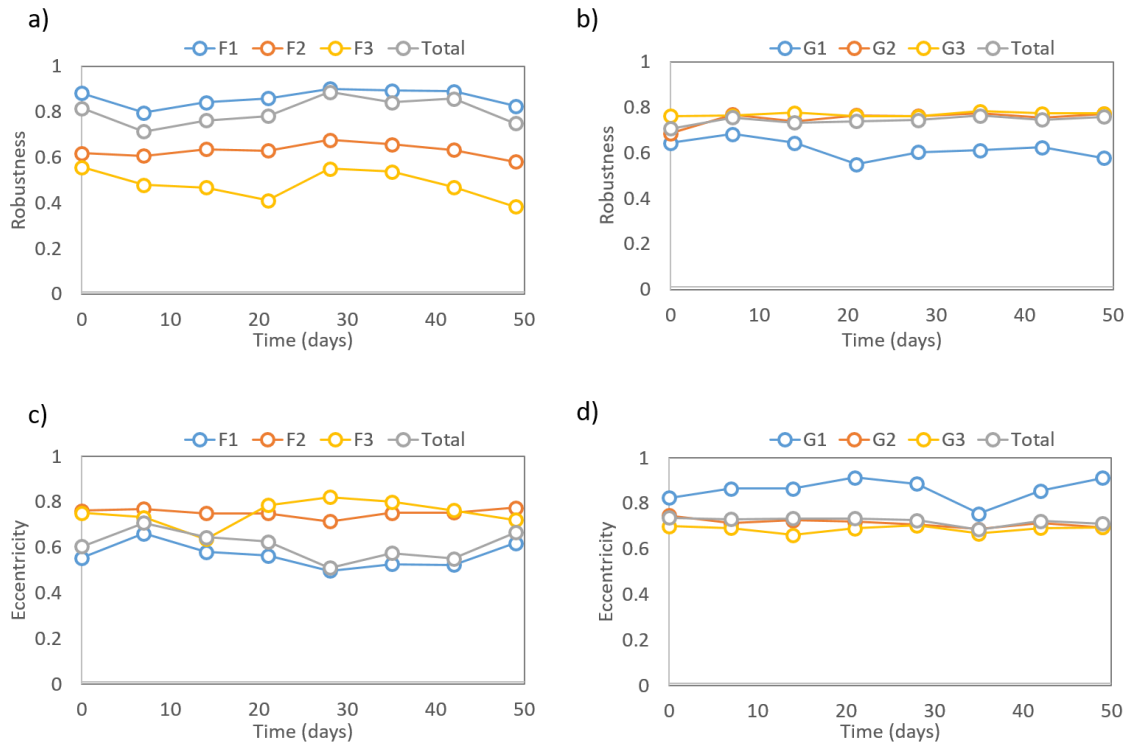


Figure 15 Evolution of the robustness for (a) F1, F2, F3 fractions, (b) G1, G2, G3 fractions and eccentricity, for (c) F1, F2, F3 fractions, (d) G1, G2, G3 fractions.

4.2.4. Suspended and granular fractions structure of AGS in the presence of PhAC

4.2.4.1. Biomass physical characteristics

The SBR-AGS biomass characterization throughout the monitoring period, in terms of the TSS and VSS, for the granular and floccular fractions, is presented in Figure 16 for the studied PhACs.

The total VSS (Figure 16b) in the E2 experiment varied between 6.3 and 21.7 g L⁻¹ (average of 15.6 ± 5.0 g L⁻¹) and the total TSS (Figure 16c) between 7.6 and 24.6 g L⁻¹ (average of 17.7 ± 5.7 g L⁻¹), resulting in a VSS/TSS ratio of 0.88 (± 0.03). With respect to the EE2 experiment, the total VSS varied from 18.0 to 23.2 g L⁻¹ (average of 19.7 ± 2.0 g L⁻¹) and the total TSS between 18.9 and 24.5 g L⁻¹ (average of 20.7 ± 2.2 g L⁻¹), resulting in a VSS/TSS ratio of 0.95 ± 0.01. Slightly higher contents were obtained for the SMX experiment, with the total VSS varying from 20.6 to 25.2 g L⁻¹ (average of 23.2 ± 1.9 g L⁻¹) and the total TSS between 21.7 and 26.6 g L⁻¹ (average of 24.4 ± 2.0 g L⁻¹), resulting in a VSS/TSS ratio of 0.95 ± 0.00. The obtained solids contents were found to be similar to a hybrid granular sludge system operating under low hydraulic pressure (Lang *et al.*, 2015), whereas similar VSS/TSS values were obtained in the start-up period of a pilot scale granular sludge reactor treating low strength wastewaters (Isanta *et al.*, 2012).

Both solids (TSS and VSS) contents (Figure 16 a-b) at the beginning of the E2 experiment were quite lower than for the EE2 and SMX experiments due to the reuse of each experiment final biomass in the reactor for the next experiment (E2, EE2 and SMX in sequence). However, mid-point at the E2 experiment monitoring period (around day 34) the solids contents increased toward similar values to the EE2 and SMX and, from that day on, stabilized around that value. Regarding the EE2 experiment, after a slight increase, the biomass contents returned to the initial values at the end of the monitoring period. On the other hand, and although fluctuating, an increasing solids trend was found in the SMX experiment. The VSS/TSS ratio (Figure 16i) allowed establishing a high, and relatively constant, organic fraction of the aggregates, for the EE2 and SMX experiments. On the other hand, regarding the E2 experiment this ratio increased during the monitoring period until reaching similar values to the EE2 and SMX experiments in the end.

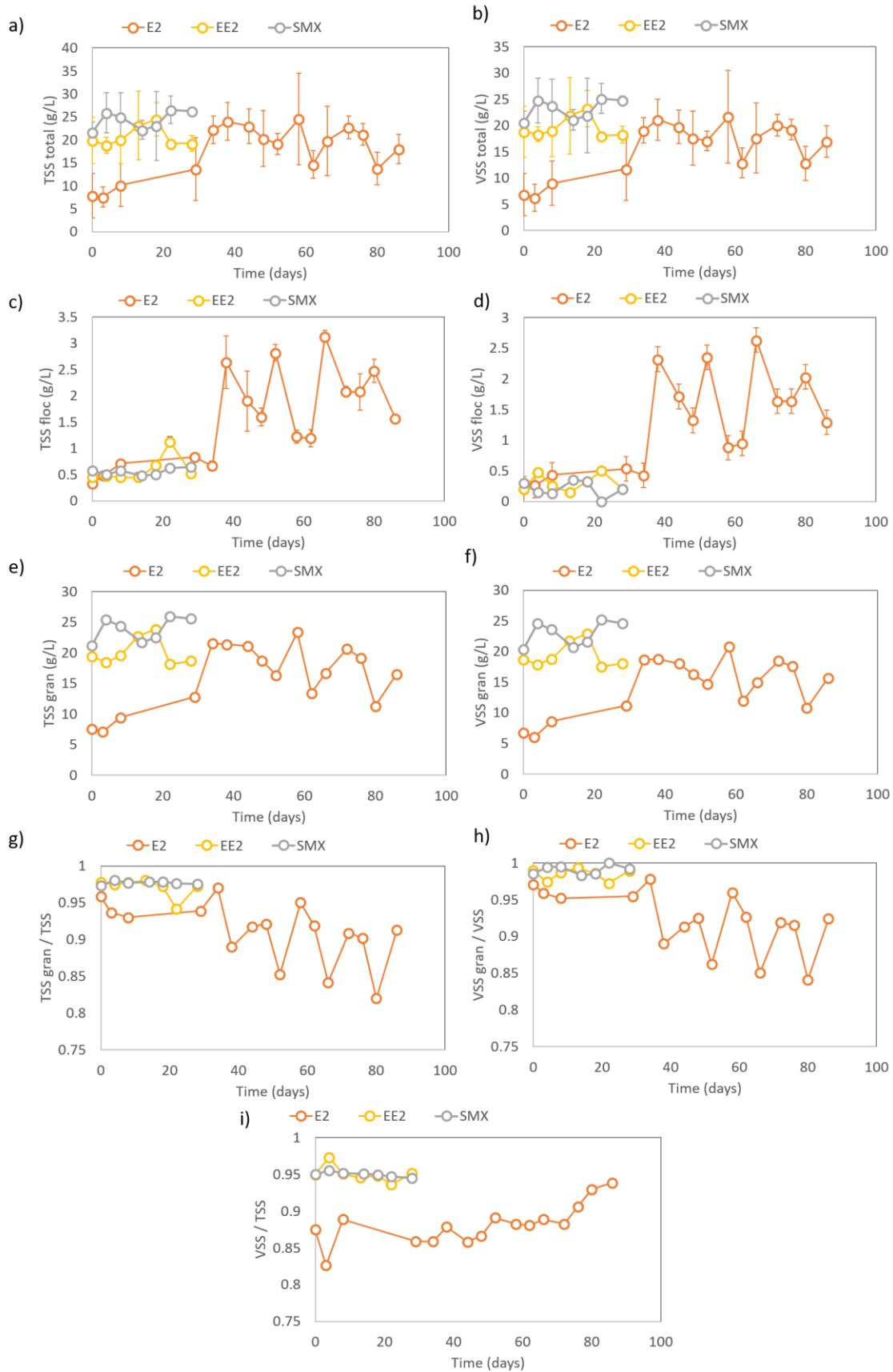


Figure 16 Evolution of the TSS and VSS for the granular and floccular fractions for the E2, EE2 and SMX experiments monitoring period. a) TSS_{total} (floccular+granular), b) VSS_{total} (floccular + granular), c) TSS_{floc}, d) VSS_{floc}, e) TSS_{gran}, f) VSS_{gran}, g) TSS_{gran}/TSS_{total}, h) VSS_{gran}/VSS_{total} and i) VSS/TSS.

With respect to the floccular fraction of the biomass, the VSS_{floc} in the E2 experiment varied between 0.2 and 2.6 g L⁻¹ (average of 1.3 ± 0.8 g L⁻¹) and the TSS_{floc} between 0.3 and 3.1 g L⁻¹ (average of 1.6 ± 0.9 g L⁻¹) (Figure 16c-d). Regarding the EE2 experiment these values varied between 0.2 and 0.5 g L⁻¹ (average of 0.3 ± 0.1 g L⁻¹) for the VSS_{floc} and between 0.4 and 1.1 g L⁻¹ (average of 0.6 ± 0.2 g L⁻¹) for the TSS_{floc} . Somewhat similar results were found for the SMX experiment with the VSS_{floc} varying between 0.1 and 0.3 g L⁻¹ (average of 0.2 ± 0.1 g L⁻¹) and the TSS_{floc} between 0.5 and 0.7 g L⁻¹ (average of 0.6 ± 0.1 g L⁻¹). The VSS_{floc} and TSS_{floc} were somewhat similar presenting lower values (around 3% of the TSS and VSS of total biomass (flocs + granules)) when compared to the granular fraction throughout the monitoring period of the EE2 and SMX experiments, and up until day 34 of the E2 experiment. From that day onwards they sharply increased and become oscillating for this PhAC, varying from 4 to 18% of the TSS of total biomass (flocs + granules).

On the other hand, for the granular fraction, the VSS_{gran} in the E2 experiment varied between 6.0 and 20.8 g L⁻¹ (average of 14.3 ± 4.6 g L⁻¹) and the TSS_{gran} between 7.1 and 23.4 g L⁻¹ (average of 16.1 ± 5.2 g L⁻¹) (Figure 16e-f). Regarding the EE2 experiment these values varied between 17.5 and 22.9 g L⁻¹ (average of 19.4 ± 2.1 g L⁻¹) for the VSS_{gran} and between 18.1 and 23.8 g L⁻¹ (average of 20.1 ± 2.2 g L⁻¹) for the TSS_{gran} . With respect to SMX experiment, slightly larger granular contents were found with the VSS_{gran} varying between 20.3 and 25.2 g L⁻¹ (average of 22.9 ± 2.0 g L⁻¹) and the TSS_{gran} between 21.1 and 25.9 g L⁻¹ (average of 23.8 ± 2.0 g L⁻¹). The granular fraction behavior, given its clear predominance in the total biomass (discussed below), was found to mimic the total solids contents.

Taking into account the total biomass, it could be found that the granular fraction represented, on average, 91.1% (± 4.2%), 97.1% (± 1.3%) and 97.7% (± 0.2%) in TSS terms, 92.1% (± 4.2%), 98.4% (± 0.8%) and 99.1% (± 0.6%) in VSS terms, for the E2, EE2 and SMX experiments, respectively (Figure 16g-h). From these values it was evident that, for all experiments, the granular fraction clearly predominated, being slightly higher for the EE2 and SMX experiments. Furthermore, from day 34 onwards, this ratio dropped in the E2 experiment and become fluctuating.

Analyzing the above set of results, the TSS and VSS contents ended up situating in a range around 26 g TSS L⁻¹ and 25 g VSS L⁻¹ for the SMX, and 18 g TSS L⁻¹ and 17 g VSS L⁻¹ for the E2 and EE2, with a granular content higher for the EE2 and SMX (around 98%) than for the E2 (around 92%). In accordance, it seems that the SMX experiment led to larger final granular biomass contents, whereas the E2 led to the opposite. And, although, in absolute terms, all experiments presented high granular biomass contents, regarding the relative granular/biomass ratio, in the E2 experiment a small decrease could be found towards the end of the experiment. These results might indicate that the E2 caused a

more pronounced effect in the AGS system compared with the other studied PhAC (despite the SVI_{30}/SVI_5 value of 1) for this experiment (discussed below).

The SBR-AGS biomass settling characteristics (SVI_5 and SVI_{30}/SVI_5) and aggregates density for the studied PhAC monitoring period are presented in Figure 17.

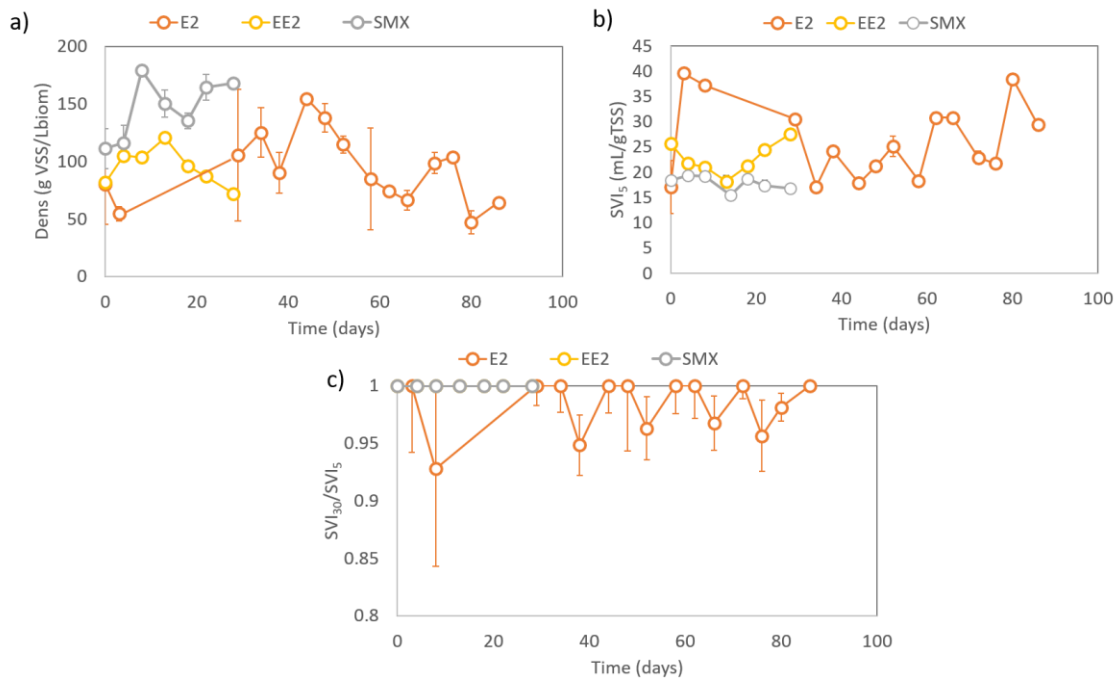


Figure 17 Evolution of the AGS physical properties for the E2, EE2 and SMX experiments monitoring period. a) density, b) SVI_5 , and c) SVI_{30}/SVI_5 .

The biomass density (Figure 17a) fluctuated throughout the monitoring period between 47 and 155 g VSS L⁻¹ biomass for the E2 experiment, with an average of 93.4 (± 30.9) g VSS L⁻¹ biomass, and between 71 and 120 g VSS L⁻¹ biomass for the EE2 experiment, with an average of 95.1 (± 16.4) g VSS L⁻¹ biomass. No significant differences were found between the biomass density for these two compounds. Additionally, the aggregates density increased up until mid-point of these experiments (days 34 from E2 and 13 from EE2, respectively) whilst decreasing from that point onwards until the experiments end. It seems, thus, that after the initial period when it first increased, the biomass density become affected by the presence of these PhAC and started to gradually decrease. Regarding the SMX experiment, the biomass density was higher than for the estrogens, showing an increasing trend throughout the monitoring period, ranging from 111 and 180 g VSS L⁻¹ biomass, with an average of 146.4 (± 26.4) g VSS L⁻¹ biomass. These results seem to indicate that the addition of SMX might have caused an increase on aggregates density over time (opposite behavior compared to the E2 and EE2).

The obtained lower density values are within the published studies in the literature for AGS pulsed aerated operation and granules disintegration in long term AGS systems operation (Carrera *et al.*, 2019; Yuan *et al.*, 2017), whereas the higher values are in the range of continuous AGS systems operation when performing nitrification and simultaneous biodegradation of p-nitrophenol (Jemaat *et al.*, 2013).

The SVI_5 (Figure 17b) varied between 17.1 and 39.6 mL g⁻¹ TSS for the E2, with an average of 26.4 (± 7.7) mL g⁻¹ TSS, and an oscillating increasing trend from the mid-point (day 34) onwards. Regarding the EE2 experiment, an opposite trend from the biomass density was observed, with the SVI_5 showing a decreasing trend up until day 13 and increasing from that day onwards, ranging from 18.2 and 27.6 mLg⁻¹ TSS and averaging of 22.8 (± 3.2) mL g⁻¹ TSS. Regarding the SMX experiment, the SVI_5 presented the smaller values, decreasing very slightly from 19.3 to 16.8 mLg⁻¹ TSS with an average of 17.9 (± 1.4) mL g⁻¹ TSS. In all cases, the presented values allowed to infer a biomass with globally good settling characteristics. In fact, similar SVI results have already been found for SBR-AGS systems, during the treatment of sulfonamides, including SMX and tetracyclines (Liu *et al.*, 2006; Liu *et al.*, 2019; Mendes Barros *et al.*, 2021).

Taking into account that possible AGS systems dysfunctions may be evaluated by the SVI_{30}/SVI_5 ratio (Figure 17c), it could be inferred a quite stable system regarding the E2 and SMX experiments, presenting a constant value of 1, and a slight instability for the EE2, ranging from 0.93 to 1.00 (average of 0.98 ± 0.02).

Analyzing the above set of results, the density ended up situating in a range around 70 g SSV L⁻¹ biomass for the E2 and EE2, and 165 g SSV L⁻¹ biomass for the SMX, the SVI_5 around 28 mLg⁻¹ TSS for the E2 and EE2 and 17 mL g⁻¹ TSS for the SMX, and an SVI_{30}/SVI_5 ratio of 1 for the EE2 and SMX and 0.98 for the E2. Regarding the two estrogens, the end values report a small increase in the SVI_5 , although presenting still good settling properties, accompanied by a small decrease in the aggregates' density towards the end of the experiment. On the contrary, the SMX experiment led to an increase on the sludge density, while maintaining a high settling ability.

4.2.4.2. AGS morphological and structural properties

The evolution of the percentages in area (for flocs) and in volume (for granules) according to the size class in the studied PhACs experiments is presented in Figure 18. Analyzing this (Figure 18a-c-e) the intermediate F2 (25-250 μ m) class of flocs predominated throughout the EE2 monitoring period ranging from 61.4% to 84.2% (averaging $72.5\% \pm 7.4\%$) and presenting a slight increasing trend, followed by the small F1 flocs (<25 μ m) averaging $18.3\% \pm 7.7\%$. On the other hand, the largest F3 flocs (>250 μ m) did not surpassed the 20.8% throughout the monitoring period, averaging $12.8\% (\pm$

5.2%). With respect to the E2 experiment, the F2 class predominated until day 34, and in day 48, 76 and 86, ranging from 29.7% to 83.5% (averaging $48.0\% \pm 16.5\%$). With an opposite trend, the F3 class predominated from day 38 onwards ranging from 0.0% to 64.5% (averaging $42.6\% \pm 18.3\%$, without the last day). Except for the first monitoring day, the F1 class did not surpassed 17.1% throughout the monitoring period, averaging $8.7\% (\pm 4.6\%)$ (first day excluded). Regarding the SMX experiment, an oscillating increasing trend was found for the intermediate F2 flocs, ranging from 50.8% to 81.6% and averaging $64.0\% (\pm 10.3\%)$ opposite to the trend followed by the larger F3 flocs, ranging from 6.6% to 38.6% and averaging $18.4\% (\pm 12.5\%)$. Also, the small F1 class presented a slightly increasing trend ranging from 10.7% to 26.9% and averaging $17.6\% (\pm 5.8\%)$.

In accordance, it could be established that the E2 experiment, apart from the first and last days, presented a higher fraction of the large flocs, and lower for the intermediate and small flocs, than the EE2 and SMX experiments. These results could also partially explain the SVI_5 and SVI_{30} values for these periods in the E2 experiment.

Likewise the flocs area percentage, the granular volume percentage (Figure 18-b-d-f) has also been found relevant in assessing AGS systems (Leal *et al.*, 2020a). Regarding the EE2 experiment, there was a clear predominance of the large G3 (>2.5 mm) granules throughout the monitoring period, which oscillated between 89.8% to 94.1% (average of $92.5\% \pm 1.4\%$). The remaining granules mostly belong to the intermediate G2 (0.25-2.5 mm) class, ranging from 5.9% to 10.2% (average of $7.5\% \pm 1.4\%$), whereas the small granules (G1) never surpassed 0.1%. With respect to the E2 experiment, the large G3 granules also predominated throughout the monitoring period, oscillating between 82.9% to 95.0% (averaging $91.3 \pm 3.3\%$). Again, the remaining granules mostly belong to the G2 class, ranging from 5.0% to 11.9% (average of $8.2\% \pm 2.5\%$) (first day excluded), given that the small granules never surpassed 0.1%. Regarding the SMX experiment, the large G3 granules were, again, overwhelming ranging from 95.3% to 97.0% and averaging $96.3\% (\pm 0.7\%)$, followed by the intermediate G2 granules, between 3.0% to 4.7% (average of $3.7\% \pm 0.7\%$). In addition, the small G1 class never surpassed the 0.1% throughout the monitoring period.

Comparing the E2 and EE2 experiments no significant differences could be found between the granular fractions, both presenting slightly smaller granules than the SMX experiment.

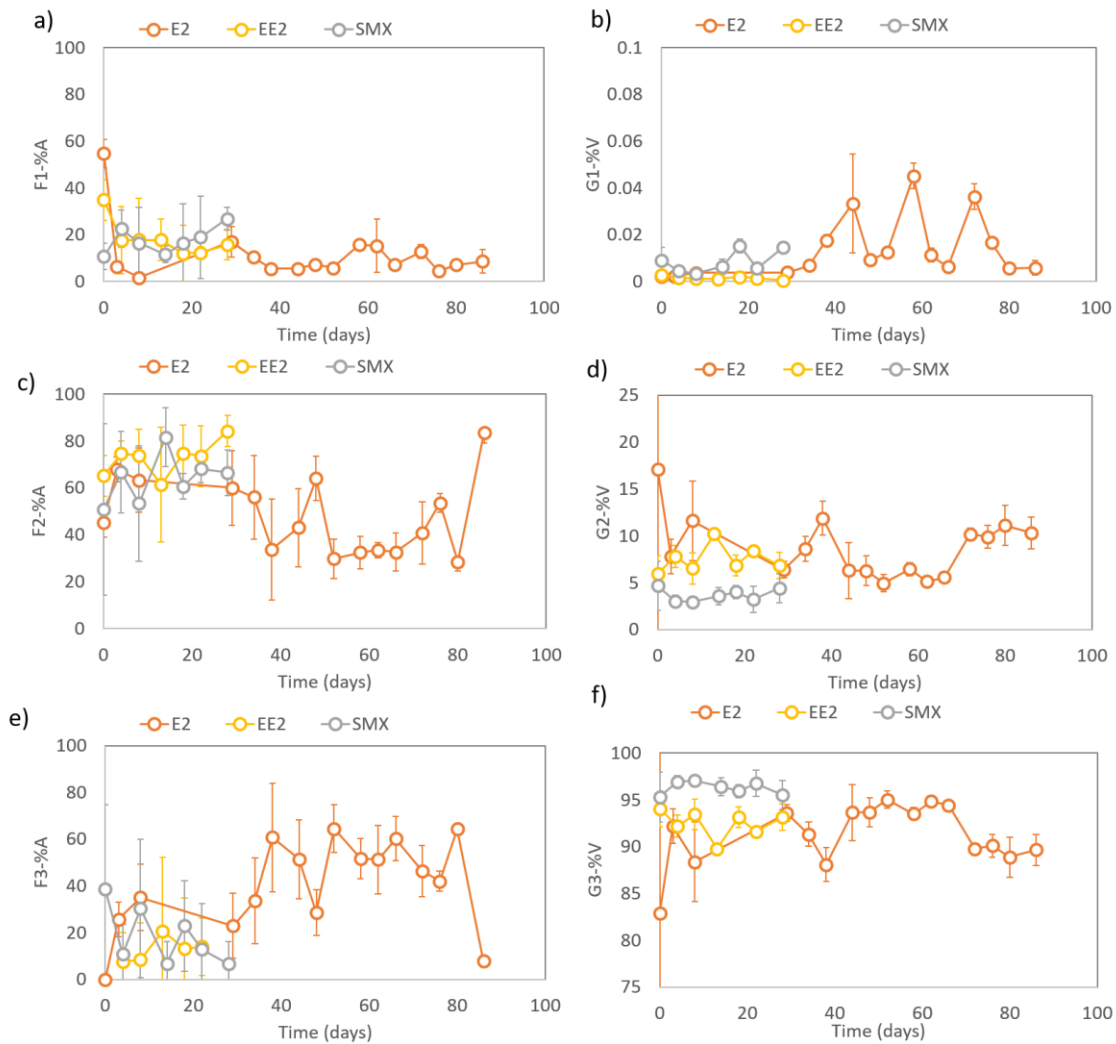


Figure 18 Evolution of the percentages in area (for flocs) and in volume (for granules) according to the size class for the E2, EE2 and SMX experiments monitoring period. a) F1-%A, b) G1-%V, c) F2-%A, d) G2-%V, e) F3-%A and f) G3-%V.

The filamentous bacteria presence in the reactor was monitored through the determination of the TL , TL/TA_{floc} , TL/TSS_{floc} and TL/VSS_{floc} during the monitoring period and is presented in Figure 19. In all cases, the values of these parameters were found to be quite lower than the set of values for bulking conditions in conventional activated sludge (CAS) (20 m mL^{-1} for TL , $15 \text{ mm} \cdot \text{mm}^{-2}$ for TL/TA_{floc} and $7 \text{ mm} \cdot \text{mg}^{-1}$ for TL/TSS_{floc} according to (Mesquita *et al.*, 2008). The lowest values were presented by the E2 experiment, corroborated by the lack of filamentous bacteria presence through microscopic inspection in that period. It should also be noticed that even for the EE2 experiment filamentous peak at day 13, no bulking conditions could be inferred by the presented values.

In fact, the average values for the TL , TL/TA_{floc} , TL/TSS_{floc} and TL/VSS_{floc} (Figure 19 a-b-c-d) were of $0.34 (\pm 0.31) \text{ m mL}^{-1}$, $0.09 (\pm 0.23) \text{ mm mm}^{-2}$, $0.39 (\pm 0.79) \text{ m mg}^{-1} \text{ TSS}$ and $0.60 (\pm 1.30) \text{ m mg}^{-1} \text{ VSS}$ for the E2, $0.92 (\pm 0.31) \text{ m mL}^{-1}$, $2.22 (\pm 2.44) \text{ mm mm}^{-2}$, $1.82 (\pm 1.92) \text{ m mg}^{-1} \text{ TSS}$ and $4.31 (\pm 6.03) \text{ m mg}^{-1} \text{ VSS}$ for the EE2 and $0.97 (\pm 0.45) \text{ m mL}^{-1}$, $2.47 (\pm 1.39) \text{ mm mm}^{-2}$, $1.80 (\pm 1.00) \text{ m mg}^{-1} \text{ TSS}$

and $4.70 (\pm 2.28) \text{ m mg}^{-1} \text{ VSS}$ for the SMX. Analyzing the obtained results, the EE2 and SMX experiments presented very similar and slightly higher values than the E2 experiment.

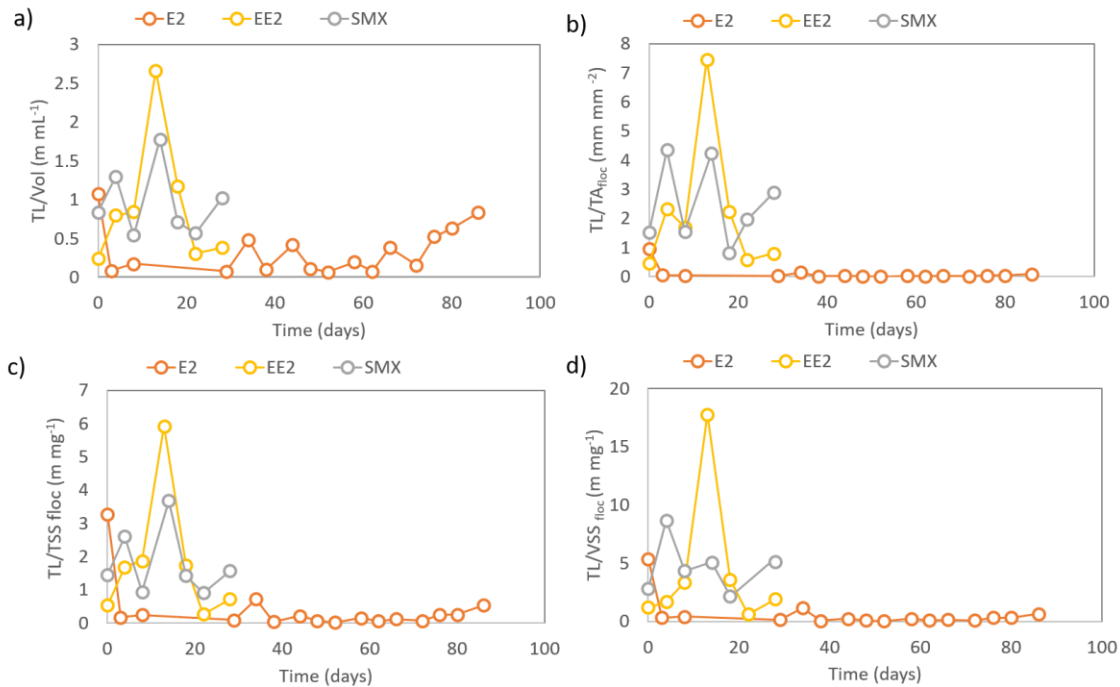


Figure 19 Evolution of TL, (a) TL/TA_{floc} , (b) TL/TSS_{floc} , (c) and TL/VSS_{floc} (d) for the E2, EE2 and SMX experiments monitoring period.

4.3. Conclusions

The COD and TIN removal performances could be considered as being consistently good during the monitoring period of the mature AGS experiment, opposite to the poor TP removal during the experiment. Both the sludge organic fraction (VSS/TSS ratio) and the biomass settling ability (SVI_5) indicate that mature granules were obtained in CONT AGS experiment. Furthermore, the high and constant SVI_{30}/SVI_5 values reflected the stability of the biomass in this period. This is in accordance with the predominant granular biomass fraction, throughout the monitoring period, presenting an average value around two and a half times larger than the suspended biomass fraction counterpart.

Within the granular biomass, the large granules (G3, $>2.5 \text{ mm}$) predominated throughout the entire monitoring period, followed by the intermediate (G2, $0.25\text{-}2.5 \text{ mm}$) granules, presenting a robust, yet slightly elongated, stable structure. Regarding the flocs biomass, the intermediate (F2, $25\text{-}250 \mu\text{m}$) flocs predominated throughout the entire monitoring period, followed by the large (F3, $>250 \mu\text{m}$) flocs. Moreover, no bulking events were inferred by the filamentous bacteria contents within the reactor nor detected by the SVI_5 monitoring.

In general, it could be inferred that the COD removal efficiency was not strongly affected by the addition of E2, EE2 and SMX. Indeed, the obtained sludge seemed to present better performances in removing the organic matter than the inorganic. On the other hand, the PhACs, and mainly SMX, have shown to possess a more pronounced effect on the TIN removal efficiencies. Regarding the TP removal efficiencies, EE2 seems to least affect the TP removal efficiency whereas SMX seems to even improve the TP removal ability. These results revealed that the microorganisms within the studied SBR-AGS able to degrade organic (COD) matter showed to be more resistant to the PhACs presence, compared to those responsible for inorganics (TIN and TP) matter removal.

A high, and relatively constant, organic fraction (VSS/TSS) of the aggregates was obtained for the EE2 and SMX experiments, whereas, regarding the E2 experiment, this ratio increased during the monitoring period until reaching similar values to the EE2 and SMX experiments in the end. Furthermore, the total solids content was found to mimic the predominant granular fraction behavior in all experiments. Both estrogens, led to a small increase in the SVI_5 by the end of the experiment, although presenting still good settling properties, accompanied by a small decrease in the aggregates' density mid-point from the experiment onwards. On the contrary, the SMX experiment led to an increase on the sludge density, while maintaining a high settling ability. The SVI_{30}/SVI_5 ratio indicated a quite stable system regarding the E2 and SMX experiments, presenting a constant value of 1, and a slight instability for the EE2.

For all PhACs experiments, the granular fraction clearly predominated, being slightly higher for the EE2 and SMX experiments. Furthermore, the E2 experiment seemed to cause a small decrease in the relative granular/biomass ratio towards the end of the experiment. These results might indicate that the E2 caused a more pronounced effect in the AGS system, with that regard, than the other studied PhAC. Within the granular biomass fraction, the large (>2.5 mm) granules clearly predominated, whereas the small (<0.25 mm) granules were negligible. Both the E2 and EE2 experiments presented slightly smaller granules than the SMX experiment. Furthermore, intermediate (25-250 μm) flocs were found to predominate, within the floccular biomass, although from mid-point onwards in the experiment the large flocs (>250 μm) started to predominate in the E2 experiment. Analyzing the obtained results for the filamentous bacteria contents, the EE2 and SMX experiments presented very similar and slightly higher values than the E2 experiment. However, no significant filamentous bacteria contents, neither filamentous bulking events, were found during the experiments either with mature AGS or in the presence of SMX and steroid estrogens.

Chapter 5 - Validation of the QIA methodology

5.1. Introduction

Aerobic granular sludge (AGS) is considered a promising technology for wastewater treatment (WWT), being compact, cost-effective, highly resistant to toxic compounds and potentially capable to remove nutrients, toxic, and recalcitrant compounds. For that reason is now replacing activated sludge (AS) systems in several countries (Nancharaiah and Reddy, 2018; Maszenan *et al.*, 2011; Bengtsson *et al.*, 2019). However, the stability of the AGS process is dependent on the balance between the floccular and granular fractions in the system (Aqeel *et al.*, 2019). Moreover, several studies could be found in literature relating to sludge fractionation, including the use of different sieves size and different sludge volumes for fractions separation (Pronk *et al.*, 2015; Cheng *et al.*, 2018; Jahn *et al.*, 2019). In this sense, the application of techniques for both flocs and granules specific morphological and structural assessment is of major interest.

Recently, QIA coupled with chemometric analysis was successfully used for mature and stable AGS systems' monitoring, evaluating both granular and suspended (floccular) biomass (Leal *et al.*, 2020a). However, studies encompassing the validation of these techniques, in terms of floccular and granular continuity under transient conditions (after fractions separation by sieving), in the presence of PhACs, are still scarce. Furthermore, a number of representativeness issues may arise from the use QIA techniques and correspondent small sample volumes required. Taking the above into consideration, the main objective of this section is to evaluate the representativeness of an AGS sampling methodology for the QIA assessment of the morphology and structure of aerobic granules treating PhAC, including the steroid estrogens 17 β -estradiol (E2) and 17 α -ethinylestradiol (EE2) and the antibiotic sulfamethoxazole (SMX). These different experiments were included in order to validate the adequateness and robustness of the proposed methodology for a wide variety of granular and floccular aggregates separated with a 500 μ m mesh sieve.

5.2. Results and discussion

5.2.1. Compliance of the sample volumes for the AGS characterization

First, an evaluation of the employed aliquot volumes adequateness was performed, regarding the representativeness of the monitored number of granules, for the assessment of the size, morphology and structure of the AGS with the proposed QIA methodology. In accordance, the evolution of the granular TSS contents in the reactor, during the different experiments, is presented in Figure 20.

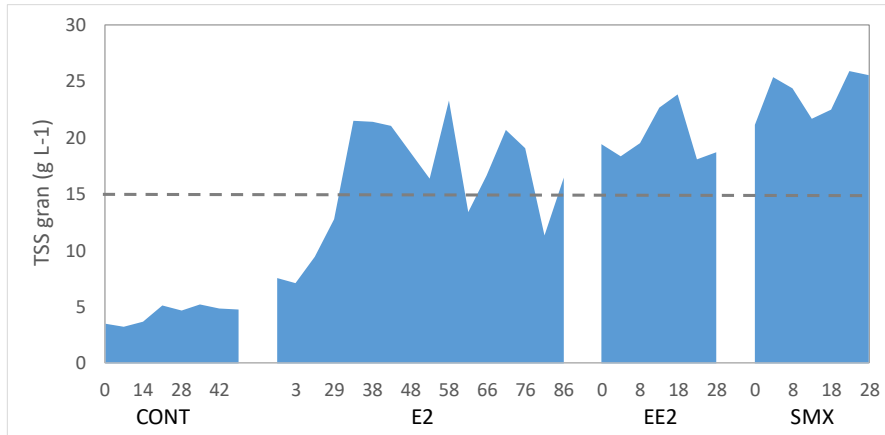


Figure 20 TSS contents in SBR-AGS for each sampling period.

A 35 mL aliquot was used for the experiments with a granular fraction TSS under 15 g L⁻¹ (CONT and E2), whereas a 10 mL aliquot was employed when the TSS was above 15 g L⁻¹ (EE2 and SMX). The reduced volume employed for the experiments presenting larger granular TSS was due to the fact that, for higher biomass contents, the 35 mL aliquots lead to the acquisition of an excessive number of granules, significantly incrementing the time needed for image acquisition.

First, the sequence of observations of the granules QIA parameters was tested (up and down runs test) for the hypothesis that the values appear in random order. The obtained results confirmed that, with the exception of 16 out of 234 (6.8%) datasets regarding the parameters used in this analysis (and 3 out of the 39 for the diameter), a completely random behavior was observed (z-value below 1.96).

Next, the averages and standard deviation values of the selected parameters for sample representativeness (equivalent diameter, length, width, convexity, eccentricity and robustness) were determined throughout an increasing number of monitored granules (unitary steps) and compared with the respective average and standard deviation values for the entire granules number and each studied sample. A variation lower, or equal, to 5% in the average and standard deviations (regarding the entire number of granules) was considered as the goal for the aliquot sample representativeness. As an example, the behavior of the average and standard deviations criteria values, for the granules diameter, throughout the increasing number of included granules of the EE2 experiment for the first monitored day is presented in Figure 21.

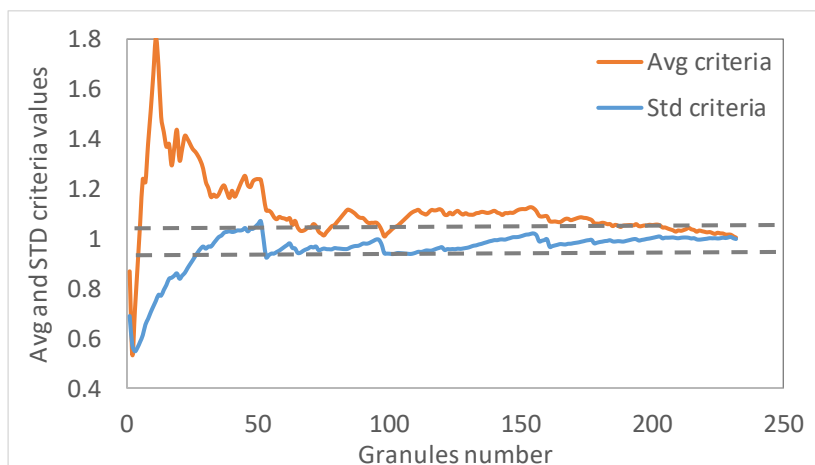


Figure 21 Average and standard deviations criteria values behavior, for the granules diameter, with the granules number increase, for the first monitored day of the EE2 experiment.

Thereafter, the minimum number of granules that allowed for the average value and standard deviation value criteria to drop below 5% (0.05 difference), regarding the entire granules number, was determined for all experiments. In accordance, the number of monitored granules, and the minimum representative number of granules according to the average and standard deviation criteria, is presented in Figure 22.

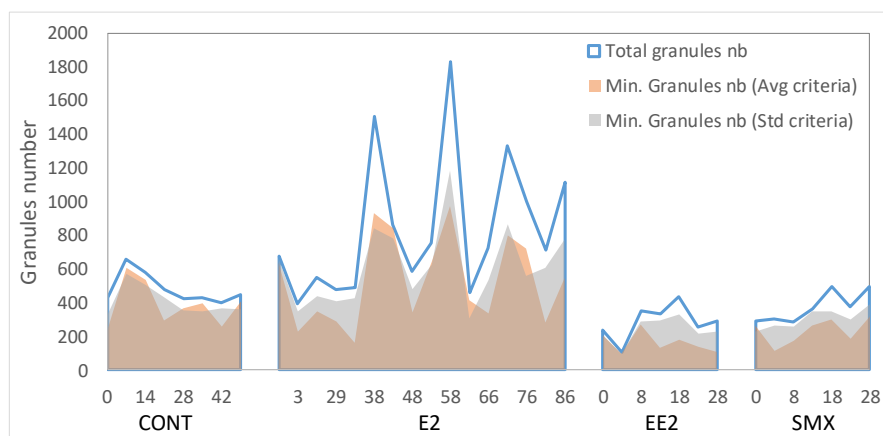


Figure 22 Total monitored granules and minimum representative number (nb) of granules according to the average and standard deviation criteria.

Analyzing Figure 22, it can be inferred that, according to the average and standard deviation criteria and for all cases, the employed aliquot volume allowed for a representative sample with respect to all the studied parameters. For the CONT and E2 experiments (35 mL aliquot), a variation of less than 5% in the average and standard deviation values, regarding the entire number of granules, was obtained for an average of 570 granules (with a complying interval averaging 150 granules). That is, the number of

acquired granules was, on average, 150 granules higher than the minimum number needed to be representative. Regarding the EE2 and SMX experiments (10 mL aliquot), the necessary number of granules averaged 273 granules (with a complying interval averaging 55 granules). The complying interval data is presented in Figure 23.

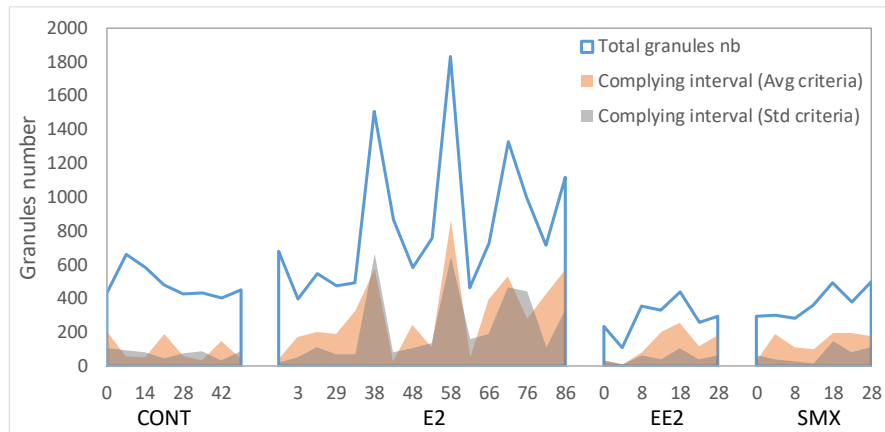


Figure 23 Total monitored granules and complying intervals according to the average and standard deviation criteria.

Taking the above into consideration, it can be inferred that the methodology used to select the granular fraction aliquot volumes, for all cases, was found to be adequate for the QIA assessment of AGS under the employed conditions. Furthermore, it could also be established that the standard deviation criteria was more stringent needing, on average, 18.0% more granules to be complied than the average criteria.

With respect to the floccular biomass fraction, the employed methodology has already been proven representative in the studies of Mesquita *et al.* (2010a, 2010b).

5.2.2. Granular and suspended (floccular) fractions sieving

With the objective of determining the effectiveness of the sieving (500 μm mesh) biomass separation, the size distribution of the granular and suspended (floccular) fractions was studied. For that purpose, the aggregates above and below 250 μm in equivalent diameter (simultaneously the studied largest floccular fraction and smallest granular fraction) of the granular and floccular fractions were compared and are presented in Figure 24. The floccular biomass fraction (passing through the 500 μm sieve) overwhelmingly presented aggregates below 250 μm in diameter. On the other hand, with respect to the granular fraction, in some cases a significant percentage ($15.5\% \pm 9.9\%$) consisted on aggregates with an equivalent diameter below 250 μm trapped in the sieve. As a result, when

considering the granular fraction, as well as for the floccular fraction, the granules separation into size classes is paramount for further enlightenment.

Taking the above into consideration, the granular biomass characterization was, thereafter, performed in three different size classes, namely: below 250 μm (in equivalent diameter) – G1; ranging from 250 to 2500 μm – G2; and above 2500 μm – G3. Concurrently, also for the floccular biomass it has been already proven that its stratification in size classes is of major importance towards their characterization (Mesquita *et al.*, 2011a). In accordance, three different size classes were also employed: below 25 μm (in equivalent diameter) – F1; ranging from 25 to 250 μm – F2; and above 250 μm – F3.

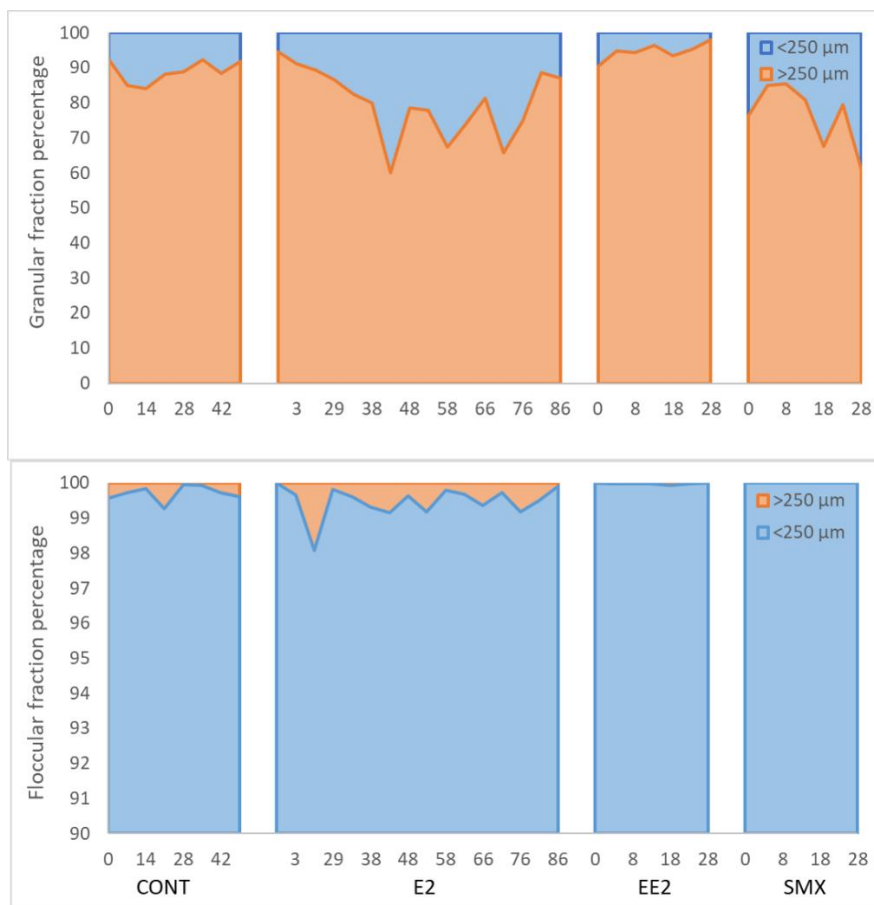


Figure 24 Aggregates percentage above and below 250 μm in equivalent diameter for the granular and floccular fractions.

A stratification analysis (Figure 25) regarding the smallest size class (< 250 μm) of the granules collected in the 500 μm sieve (granular biomass fraction), subjected to the 175 μm (debris) cut-off value, allowed to establish a predominance of the 175-200 μm class for all experiments, followed by the 200-225 μm . On the other hand, for most experiments, the percentage of aggregates retained in the sieve below 175 μm was negligible (<2%). From this analysis, it seems clear a large distribution of

size ranges (even quite below 250 μm) for the aggregates quantified as granules (trapped by the employed sieve).

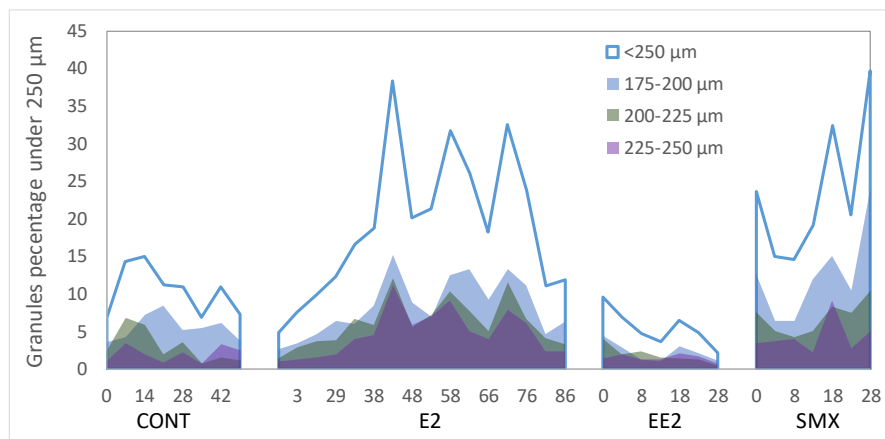


Figure 25 Stratification analysis presenting the percentage of the aggregates (quantified as granules) below 250 μm collected in the 500 μm sieve.

Addressing the continuity analysis, upon determining the flocs distribution within the same range (175 to 250 μm), and comparing with the one obtained for the granules, it results clear a similitude between both fractions. In fact, the 175 to 200 μm size class was predominant for both aggregates (Table 1) (47.3% to 54.8% for the ensemble), followed by the 200 to 225 μm size class (30.7% to 31.4%) and finally by the 225 to 250 μm size class (13.8% to 22.0%). Taking into account the similitude of the three studied size fractions in the lower bound of the granular biomass with the same size fractions of the floccular biomass, this suggests a good agreement between the two acquisition methodologies (flocs and granules), ensuring a continuity in the aggregates determined by them, which reinforces the adequateness of the combined methodology regarding the monitoring purposes.

Table 7 Aggregates number percentage with respect to size ranges for granular and floccular fractions within 175 to 250 μm

Fraction		175 – 200 μm	200 – 225 μm	225 – 250 μm
Granules	CONT	52.5	28.6	18.9
	E2	43.5	32.1	24.4
	EE2	40.5	33.2	26.3
	SMX	52.7	29.1	18.2
	All	47.3	30.7	22.0
Flocs	CONT	50.6	31.4	18.0
	E2	59.2	28.2	12.7
	EE2	55.2	32.2	12.6

SMX	54.4	33.8	11.8
All	54.8	31.4	13.8

5.2.3. Triplicates analysis

For both granular and floccular fractions, triplicates were acquired and processed by QIA. The obtained results of these triplicates were, thereafter, used to determine the average and standard deviation for each experiment sample. The validation of this approach was performed taking first into account the aggregates diameter parameter and later expanded to the most representative parameters. Accordingly, the average diameters and standard deviations for all experiments and size classes are presented in Figure 26. Analyzing the obtained results, it could be established that the standard deviations, with a few exceptions (day 38 of the E2 experiment and day 18 of the SMX experiment, due to the large flocs – F3 low presence, and day 7 of the CONT experiment and days 13 to 28 of the EE2 experiment, due to the low small granules – G1 range), do not encompass, nor significantly affect, the validity of the variation found in the parameters.

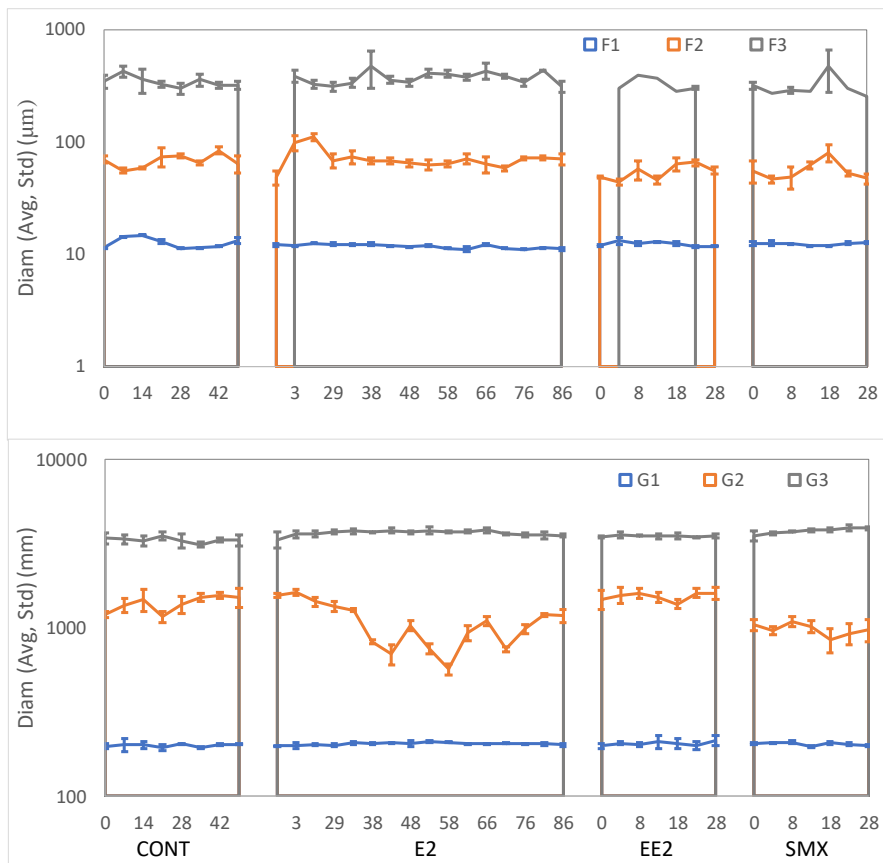


Figure 26 Average diameter and standard deviation of the granular and floccular fractions.

When normalized by the variation range of the diameters average (for each experiment and size class, represented in Figure 27), the standard deviation represented, on average, solely 16.6% of the diameters range variation for the CONT, 11.7% for the E2, 15.8% for the EE2 and 15.5% for the SMX experiments, resulting in a 14.3% average overall. Furthermore, both the granular and floccular biomass were tendentially in accordance, in average terms, with this behavior, attaining 12.1% for the flocs and 16.5% for the granules. With respect to the different studied size classes, the small granules (G1), followed by the large floccular (F3) and granular (G3) aggregates, presented the larger standard deviation (24.3%, 19.5%, and 16.4%, respectively) on the aggregates diameter, due to the following main factors: i) the size range within the small granules (175-250 μm) is, comparably, the tighter range of all classes; ii) the large aggregates are not bounded by an upper limit, with the exception of the image size itself; iii) the aggregates number of the large aggregates, within each aggregates type, is the lowest, thus leading to more discrepancies. On the opposite, and given their high numbers, the small F1 flocs presented the lowest standard deviation (7.2%).

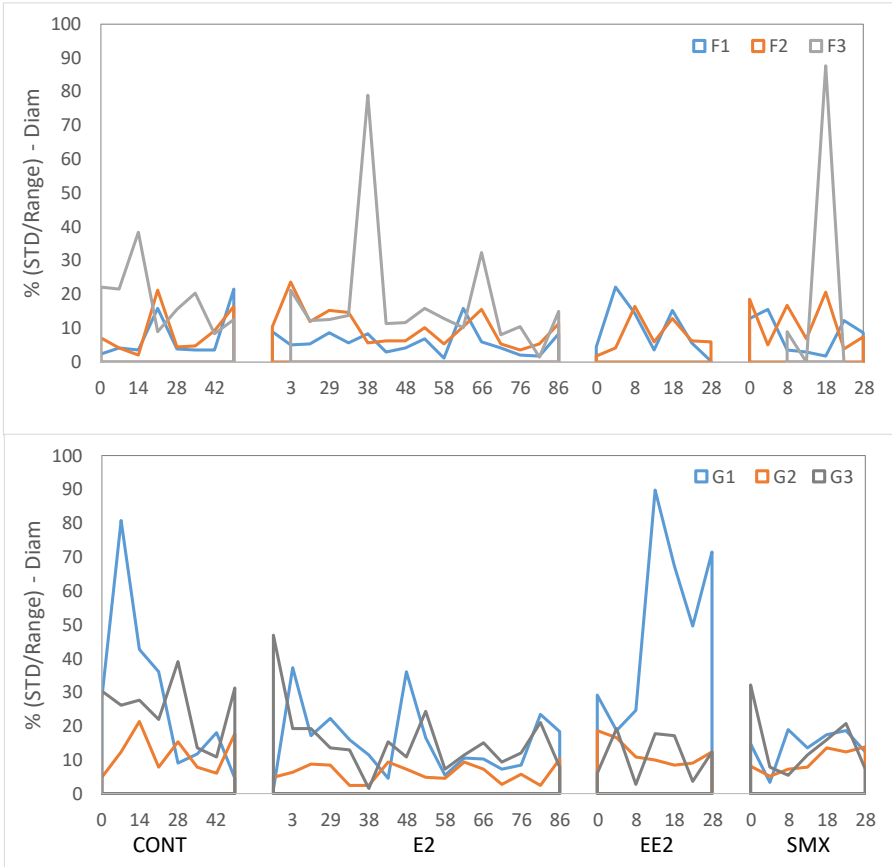


Figure 27. Standard deviation percentage with respect to the size ranges for the granular and floccular fractions diameter.

Table 8 Standard deviation percentage with respect to the size range for the granular and floccular fractions and main parameters

Parameter	Experiment	F1	F2	F3	G1	G2	G3
Diameter	CONT	7.2	8.6	18.4	11.9	11.5	25.0
	E2	5.9	10.0	17.8	6.3	5.9	15.3
	EE2	9.3	7.5	4.9	20.6	12.0	11.2
	SMX	8.1	11.3	35.7	14.0	9.6	14.3
	All	7.2	9.5	19.5	24.3	8.9	16.4
Length	CONT	7.9	9.4	12.7	20.8	12.8	22.8
	E2	13.8	9.9	19.1	7.9	5.6	15.4
	EE2	10.4	8.3	1.5	30.2	12.1	15.1
	SMX	11.6	12.4	21.8	14.2	8.2	16.6
	All	11.5	10.0	16.9	17.6	8.8	17.1
Width	CONT	5.6	8.6	18.9	38.9	11.6	28.2
	E2	6.6	10.3	18.6	10.5	6.1	17.3
	EE2	10.5	7.9	3.5	32.0	12.6	10.7
	SMX	8.4	11.2	42.2	14.6	9.8	13.7
	All	7.5	9.6	20.7	21.9	9.1	17.7
Convexity	CONT	4.8	6.1	18.2	26.9	8.1	11.6
	E2	3.0	8.2	11.2	11.6	6.6	8.4
	EE2	20.1	14.3	29.2	31.2	5.1	9.7
	SMX	21.3	12.9	18.2	18.7	15.7	14.4
	All	9.9	9.7	14.8	19.7	8.3	10.4
Eccentricity	CONT	7.3	6.6	15.2	41.9	7.1	42.1
	E2	6.3	10.9	17.0	13.3	7.6	22.5
	EE2	7.7	17.1	0.1	33.6	14.8	28.4
	SMX	6.8	17.1	17.9	18.9	12.9	19.3
	All	6.8	12.3	16.0	24.1	9.8	27.1
Robustness	CONT	5.5	6.1	24.4	24.6	8.7	16.0
	E2	3.1	9.9	10.5	9.0	5.2	13.5
	EE2	8.6	10.9	0.4	25.9	7.0	18.3
	SMX	9.4	11.0	54.0	14.8	12.6	13.1
	All	5.8	9.5	19.1	16.5	7.6	14.8

With respect to the remaining studied parameters, presented in Table 8 the behavior of each parameter standard deviation, regarding the experiments range followed the established by the diameter parameter. The average values, regarding the ensemble size ranges were somewhat similar

for the diameter (14.3%), length (13.7%), width (14.4%), convexity (12.1%), eccentricity (16.0%), and robustness (12.2%). Analyzing in terms of the size fractions, once again the F3 fraction presented the larger values, regarding the ensemble, within the flocs (ranging from 14.8% to 20.7%) and the F1 fraction the lowest values (ranging from 5.8% to 11.5%). On the other hand, both the granules G1 and G3 fractions presented similar larger results, ranging from 16.5% to 24.3% (G1) and 10.4% to 27.1% (G3), regarding the ensemble.

In conclusion, it seems feasible to infer that the obtained ensemble average values truly represent the samples real values, within the accuracy ranges presented above. Indeed, in most cases, variations on average of less than 15% of the studied parameter range, within the experiment, can be obtained.

5.3. *Conclusions*

In this work, the adequateness of a QIA based methodology, including the establishment of the sample volume, the granular and floccular fractions sieving process, the fractions size cut-off and the image acquisition method was evaluated, taking into account the AGS size, structure and morphology in synthetic wastewaters containing E2, EE2, and SMX. For that purpose, an approach based on a 5% variation criteria for a sample average and standard deviation value was employed. The results proved that the employed aliquot volumes, based on the TSS of the granular fraction, were found adequate for the intended purpose. Furthermore, the performance of the sieving process (500 μm sieve), in successfully separating the biomass granular and suspended (floccular) fractions, was also assessed. As a result, a lower bound cut-off granules size of 175 μm was established for the employed sieve. Next, a comparison between the 175-250 μm overlapping size range on the floccular and granular biomass proved the continuity of the performed methodology. Since the samples image acquisition was performed in triplicate, a final analysis on the obtained average and standard deviation values was employed. This analysis allowed showing that the experiments variations for the studied parameters could be adequately monitored using triplicates.

Chapter 6 - Application of chemometric tools for the SBR-AGS assessment

6.1. Introduction

Given that the assessment of both AGS fractions, by QIA, resulted in large datasets, CT are indispensable for data organization and analysis. In this sense, the main objective of this chapter is to discuss the obtained results regarding the application of: i) PCA for the enlightenment of the interrelationships between, and within, the physicochemical and morphological parameters, as well as with naturally occurring clusters; ii) DA and DT to identify the different operational periods and samples in the presence/absence of PhAC and; iii) MLR for the suspended solids contents and biomass density and settling ability predictions. The main parameters, extracted by QIA, are related to the size, contents, morphology and apparent density of the granular and floccular sludge fractions (see in section 2 of the appendices). Moreover, the sludge physical properties, namely suspended solids, biomass density and settling parameters were also determined. Furthermore, the evolution of most relevant parameters during the monitoring period, resulting from the application of the previous CT can be found in section 4 of the appendices.

6.2. Biomass contents and settling ability analysis by PCA

The results of the main performed PCA for the PhAC (E2, EE2 and SMX) dataset, including the mature AGS experiment (acting as a control – CONT) when feasible, is next addressed. The PCA addressed the SBR-AGS biomass (filamentous, suspended and granular) structure (assessed by QIA), contents and settling ability, and was performed both with and without the biomass density, due to the fact that no data regarding this parameter could be obtained for the mature AGS experiment.

The PCA performed with the inclusion of the mature AGS experiment data, thus excluding density, is presented in Figure 28.

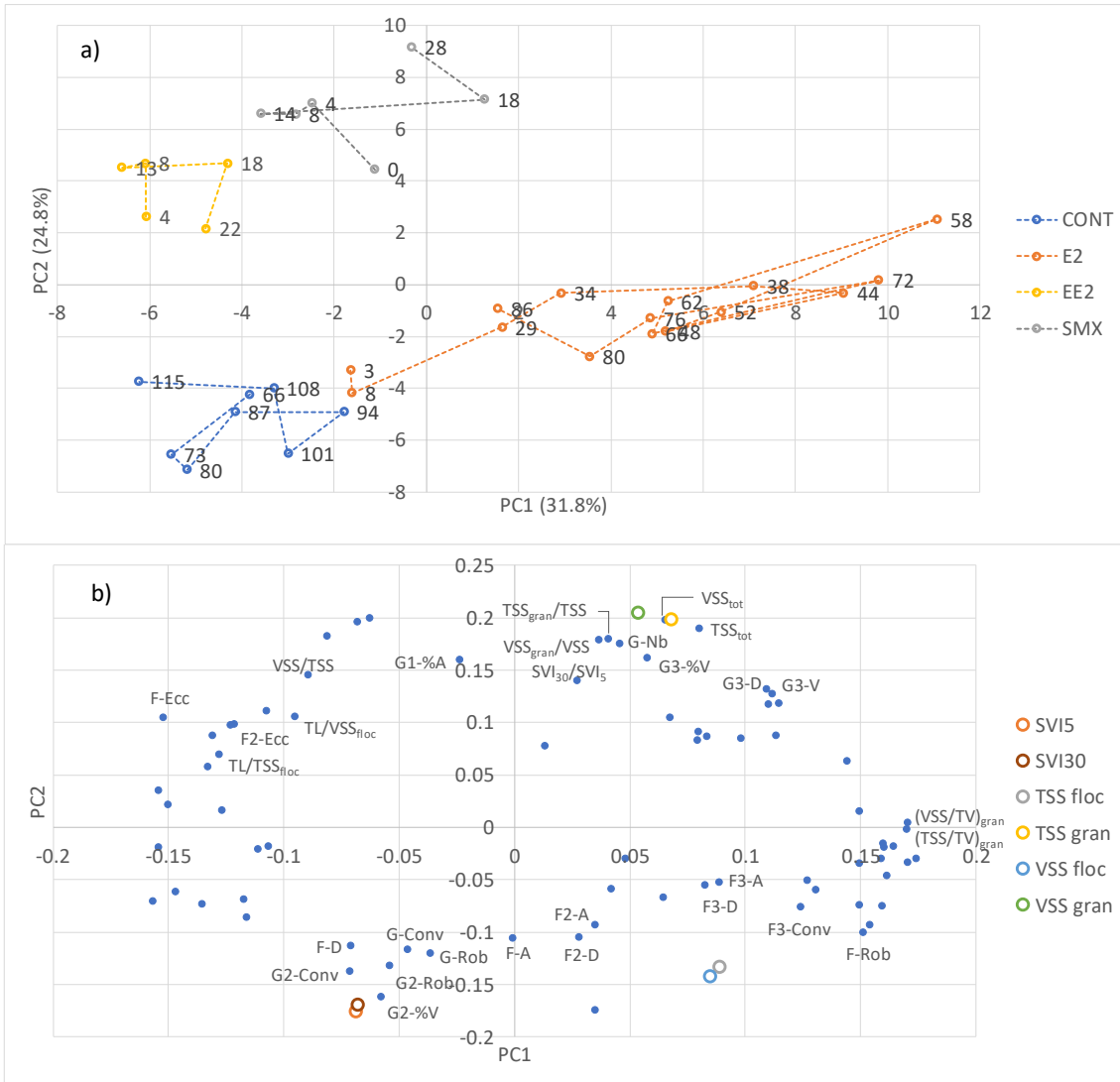


Figure 28 PCA with the mature AGS dataset. a) Operational periods and b) AGS structure, contents and settling parameters.

The results presented in Figure 28a revealed four naturally occurring clusters, corresponding to the experiments with mature AGS (CONT), and in the presence of E2, EE2 and SMX, through the use of PC1 and PC2 (explaining 31.8% and 24.8% of the original dataset variance, respectively). The E2 experiment was characterized by presenting positive PC1 values, with exception of the initial period, and slightly negative PC2 values (except for days 58 and 72). On the other hand, positive values for PC2 could be inferred for the SMX and EE2 operational periods. Moreover, both operational periods showed also mainly negative PC1 values (except for day 18 of the SMX experiment). In fact, these results could be explained by a somewhat similar biomass behavior in terms of morphology and structure during both operational periods. In addition, in the bottom left quadrant, the CONT experiment was characterized by negative values for both PC1 and PC2.

With respect to the variables importance, shown in Figure 29, it should be stressed that PC1 was positively influenced by the large (F3) and total flocs contents (F3-TA, F3-Nb, F-TA and F-Nb), and by the granules apparent density ($(VSS/TV)_{gran}$ and $(TSS/TV)_{gran}$). These values can be correlated to the high flocs' contents, with *Zoogloea* predominance, and higher granules apparent density found for the E2 experiment.

On the other hand, the PC2 was positively influenced by the overall and granular biomass (TSS_{total} and VSS_{total} , TSS_{gran} , VSS_{gran} and G-TV) and large granules (G3-TV and G3-Nb) contents and negatively influenced by the SVI_5 . These results are in accordance with the mature AGS experiment biomass and large granules values (the lowest among all experiments) and the SVI_5 values (the highest among all experiments). In addition, the difference between the SMX and EE2 clusters could be explained by the SMX experiment higher biomass and granules contents (TSS_{total} , VSS_{total} , TSS_{gran} and VSS_{gran}), higher granules apparent density ($(VSS/TV)_{gran}$ and $(TSS/TV)_{gran}$) and slightly lower SVI_5 values.

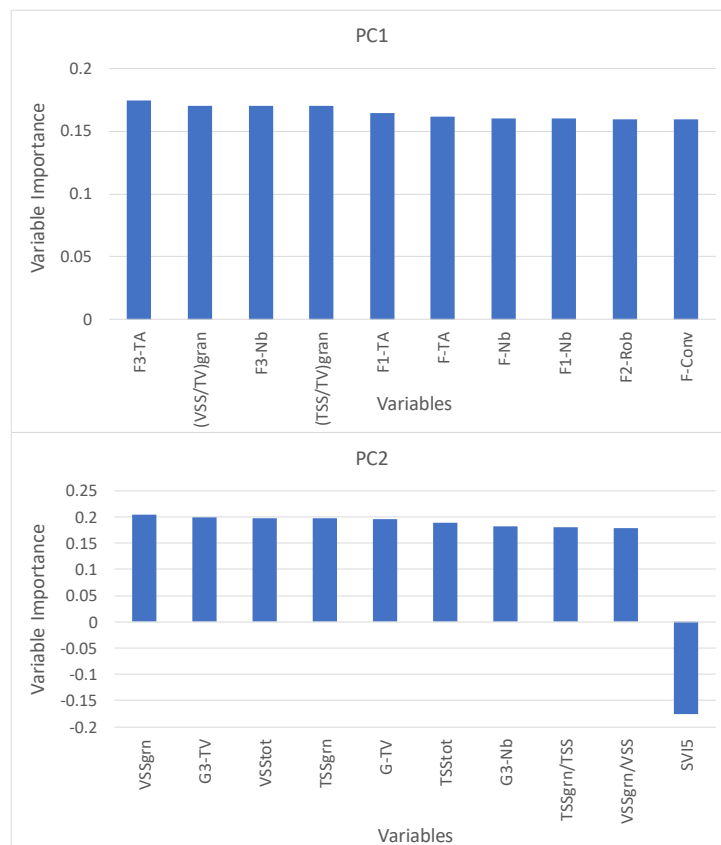


Figure 29 Variable importance for PC1 and PC2, regarding the PCA with the mature AGS dataset.

Regarding the AGS structure, contents and settling ability, presented in Figure 28b, the SVI_5 and SVI_{30} were situated opposite to the granular biomass (TSS_{gran} and VSS_{gran}) contents. Furthermore, the results showed a close relationship of the SVI_5 with the total flocs size (F-D and F-A, quite dependent on

the F1 values), intermediate granules fraction (G2-%V, opposite to G3-%V) and overall and intermediate granules regularity (G-Rob, G-Conv, G2-Rob and G2-Conv). In accordance, an opposite behavior was found between these parameters and the granular biomass (TSS_{gran} and VSS_{gran}) contents.

On the other hand, the granular biomass contents were found to show a close relationship with the overall biomass (TSS_{tot} and VSS_{tot}), biomass stability properties (SVI_{30}/SVI_5 ratio), granular biomass fraction (TSS_{gran}/TSS and VSS_{gran}/VSS), granules (G-Nb) contents and large granules fraction (G3-%V) and size (G3-V and G3-D). In accordance, an opposite behavior was found between these parameters and the SVI values.

With respect to the floccular biomass (TSS_{floc} and VSS_{floc}), the results showed a close relationship with the intermediate and large flocs size (F2-A, F2-D, F3-A and F3-D) and regularity (F-Rob and F3-Conv). On the other hand, an opposite behavior was found regarding the biomass organic fraction (VSS/TSS ratio), filamentous bacteria contents per floccular biomass (TL/TSS_{floc} and TL/VSS_{floc}), overall and intermediate flocs irregularity (F-Ecc and F2-Ecc) and small flocs fraction (F1-%A).

Aiming to understand the biomass density (Dens.) relationship with the AGS morphology and structure, a second PCA was performed, including this parameter in the dataset (and excluding the CONT samples that presented no data for this parameter). The main results of the second PCA are presented in Figure 30.

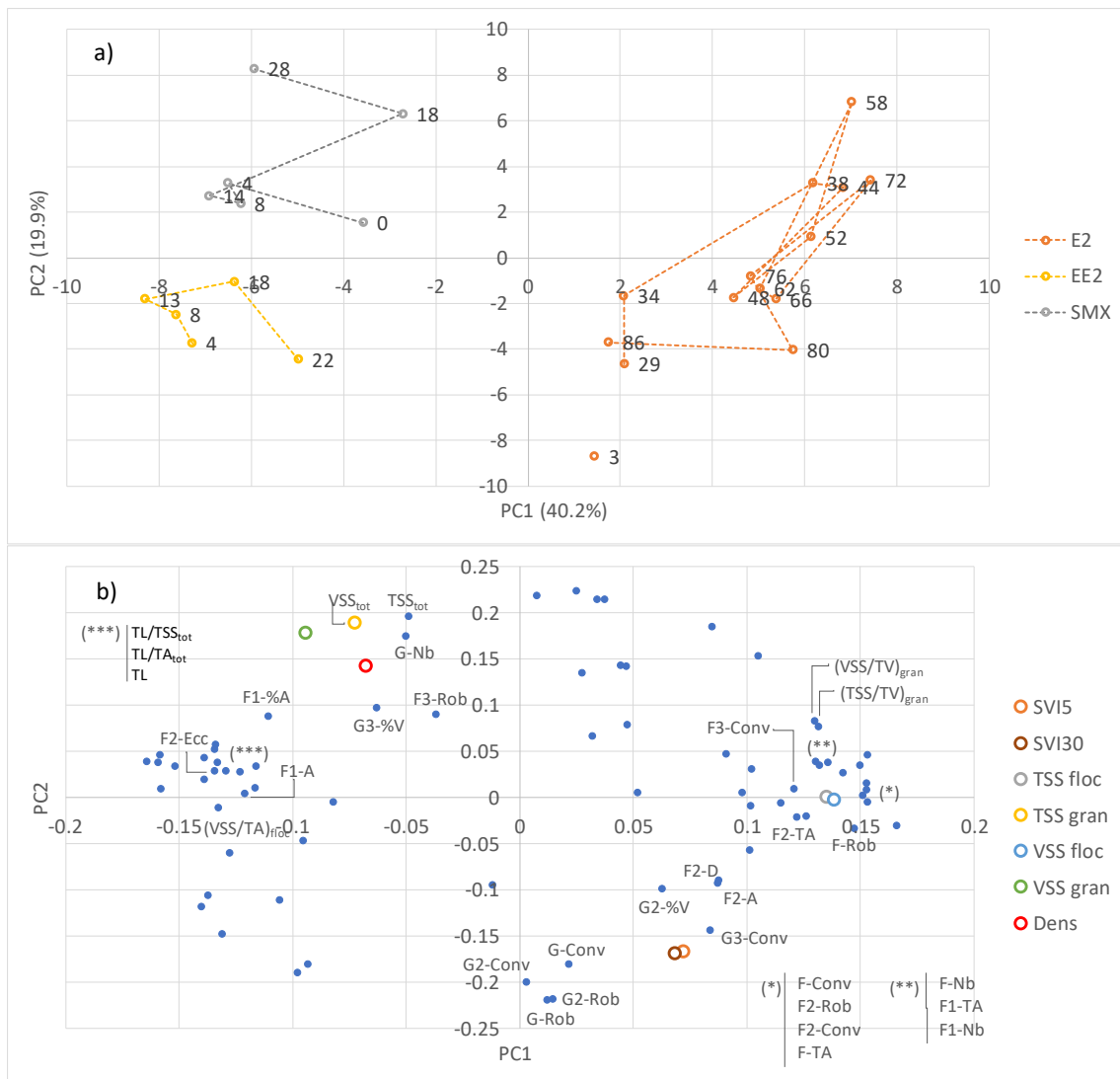


Figure 30 PCA with the biomass density dataset. a) Operational periods and b) AGS structure, contents and settling parameters.

Analyzing Figure 30a, three naturally occurring clusters can be clearly found, representing the three (E2, EE2 and SMX) experiments, by the use of PC1 and PC2 (explaining, respectively, 40.2% and 19.9 % of the original dataset variance). The E2 experiment is characterized by positive PC1 values, contrary to the EE2 and SMX. Regarding the EE2 experiment, both PC were found to be negative, whereas the SMX experiment presented negative PC1 values but positive PC2 values. Again, the EE2 and SMX experiments are not too far apart in the PCA analysis, explained by a somewhat similar biomass behavior in terms of morphology and structure during both operational periods.

Regarding the variables importance, shown in Figure 31 the most relevant variables for PC1 were found to be the large, intermediate and total flocs regularity (F3-Rob, F2-Rob, F2-Conv and F-Conv) and large flocs contents (F3-TA), with a positive influence. On the other hand, with a negative influence, the

most important are the total and large granules contents (G-TV, G3-TV and G3-Nb) and the flocs apparent density ($(TSS/TA)_{floc}$). These results confirm, and add, to the previous analysis, and can be related to the high flocs contents (at the expense of the granules contents) and overall flocs regularity (though presenting lower apparent density) in the E2 experiment.

Regarding PC2, the most important variables were found to be the total and small granules contents (TSS_{total} , TSS_{gran} , G1-TV and G1-Nb), with a positive influence. In fact, these results are in accordance with the presence of a higher small granules contents in the SMX and in the second part of the E2 experiments. Although somewhat conflicting, the total and intermediate granules structure (G-Ecc, G-Rob, G2-Ecc, G2-Rob and G2-Conv) could be also found important for PC2. Interestingly, with the absence of the CONT samples, the biomass settling ability and the large granules contents lost some significance regarding the most important PC.

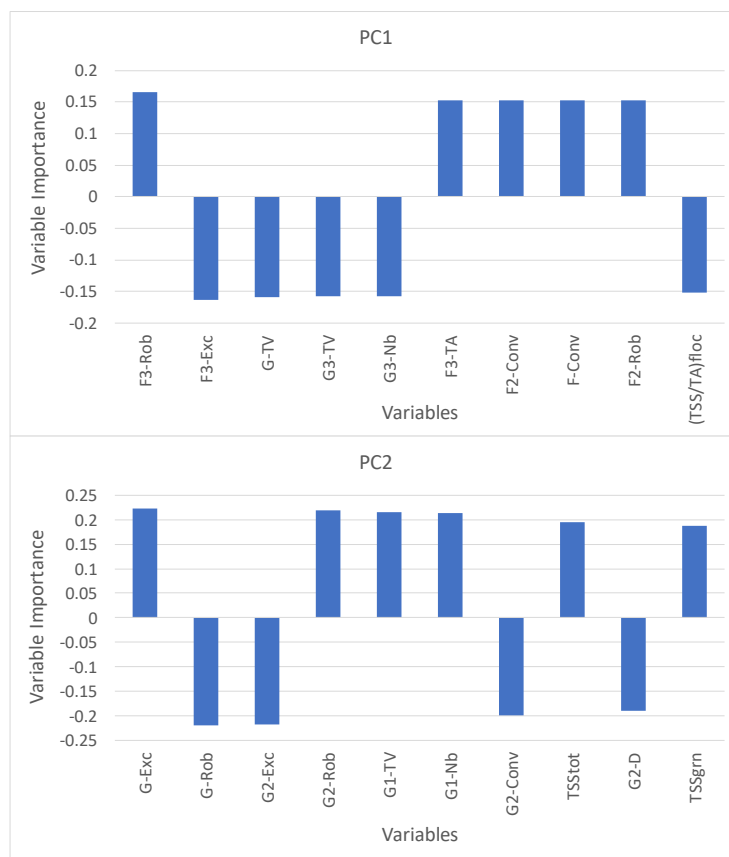


Figure 31 Variable importance for PC1 and PC2, regarding the PCA with the biomass density dataset.

Taking into consideration Figure 30b, some interesting results can be inferred, namely regarding the biomass density, which can be positively related to the granular biomass contents (TSS_{gran} , VSS_{gran}) and negatively to the SVI_5 and SVI_{30} . The granular biomass contents and density correlate with the overall biomass (TSS_{total} and VSS_{total}) and granules (G-Nb) contents, large granules fraction (G3-%V), small

flocs fraction (F1-%A) and the large flocs regularity (F3-Rob). In accordance an opposite behavior was found between these parameters and the SVI. On the other hand, the AGS settling properties (SVI_5 and SVI_{30}) were found to correlate positively with the intermediate granules fraction (G2-%V, opposite to G3-%V), intermediate flocs size (F2-D and F2-A) and granules regularity (G-Rob, G-Conv, G2-Rob, G2-Conv and G3-Conv). In accordance, an opposite behavior was found between these parameters and the granular biomass contents and overall density.

With respect to the floccular biomass contents (TSS_{floc} and VSS_{floc}), the results showed a close relationship with the overall, small and intermediate flocs contents (F-TA, F-Nb, F1-TA, F1-Nb, F2-TA and F2-Nb) and overall, intermediate and large flocs regularity (F-Conv, F-Rob, F2-Conv, F2-Rob and F3-Conv). On the other hand, an opposite behavior was found regarding the flocs apparent density ($(VSS/TA)_{floc}$), small flocs size (F1-A), intermediate flocs irregularity (F2-Ecc), filamentous bacteria contents (TL , TL/TSS_{floc} and TL/TA_{floc}) and granular biomass fraction (VSS_{gran}/VSS , opposite to the flocs biomass fraction).

Comparing the obtained results with the former PCA analysis, the establishment of the parameters influencing the overall density, including the small flocs fraction and large flocs irregularity, and the importance of the intermediate flocs size on the AGS settling properties is of notice. Furthermore, it could also be inferred a correlation of the floccular biomass with the flocs' contents (projected area and number) and flocs biomass fraction (although indirectly).

Aiming to evaluate the influence of the different data groups, four different PCA analyses were performed with: the sludge physicochemical parameters i) including and ii) excluding the biomass density (Figure 32 a,b); the QIA based morphology and structural parameters of the AGS for the iii) floccular fraction (Figure 32 c) and iv) granular fraction (Figure 32d).. Regarding the use of solely the physicochemical parameters, although the CONT and E2 operational periods could be relatively well isolated in the PC1-PC2 space, no clear distinction between the EE2 and SMX periods could be obtained (Figure 32a,b). Also the sole use of the floccular fraction parameters (Figure 32c) was able to isolate the CONT and E2 operational periods, contrary to the EE2 and SMX. However, in this case the operational period closer to the EE2 and SMX was found to be the mature granules control, instead of the E2 period. On the other hand, the use of solely the granular fraction parameters (Figure 32d) resulted in the isolation of the EE2 and SMX operational periods, unlike the CONT and the E2 periods.

The use of solely the granular fraction parameters (Figure 32d) reflected more accurately the initial PCA analysis with all parameters (although not fully separating the CONT and E2 periods), stressing the

importance of the granular fraction structure enlightenment to characterize the different operational periods. On the other hand, the use of the physicochemical parameters seems crucial to separate the mature granules period (in accordance with the lowest SVI_5 values during the mature granules period). Still addressing the operational periods *clustering* ability, the E2 period was most isolated by the use of the floccular fraction parameters (in accordance with the high floc's contents presented).

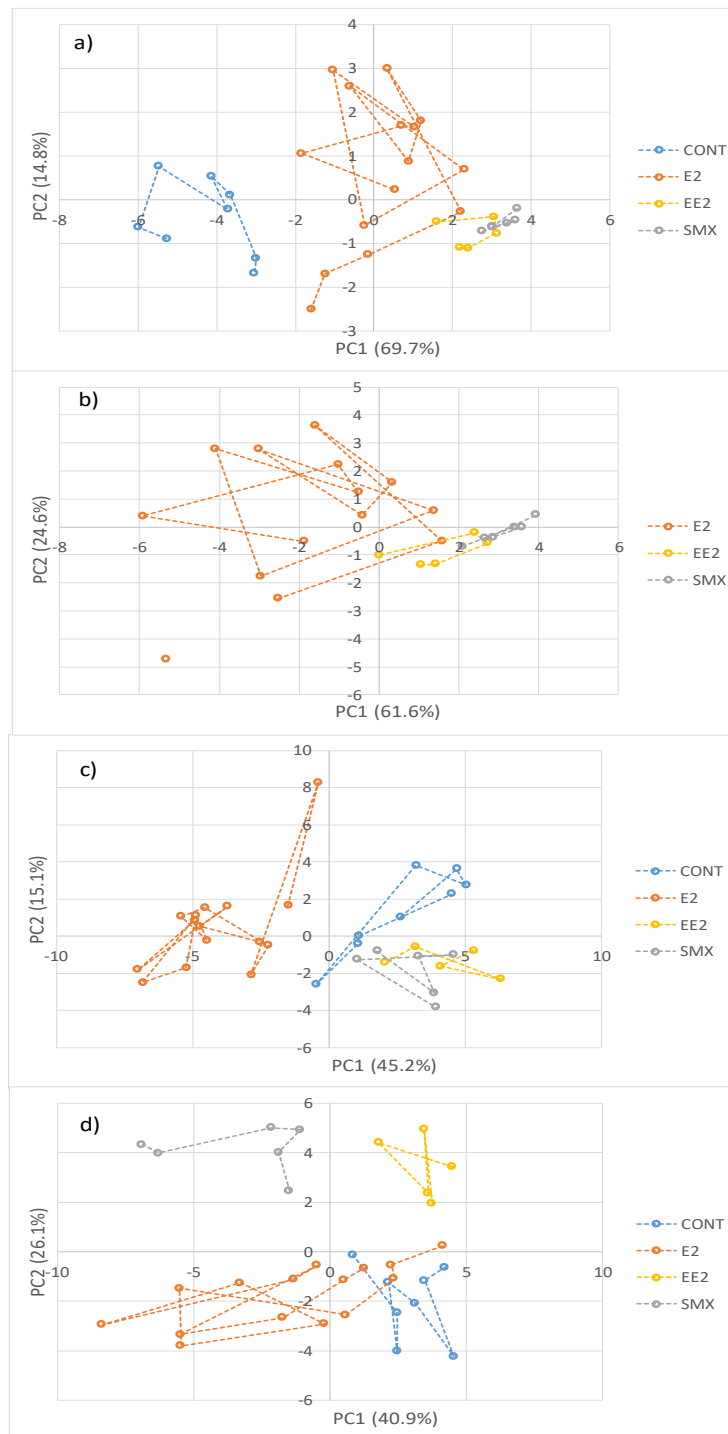


Figure 32 PCA with the: sludge physicochemical parameters a) including and b) excluding the biomass density; QIA based morphology and structural parameters of the AGS for the c) floccular fraction and d) granular fraction.

6.3. Biomass contents and settling ability prediction by MLR

The prediction of VSS, TSS, density and SVI₅ was performed by MLR taking into consideration the biomass (filamentous, suspended, and granular) structure (assessed by QIA), contents and settling ability. Moreover, different models, including the mature AGS data or the biomass density, were performed for SVI₅, VSS and TSS, respectively. Taking into consideration that no biomass density could be obtained for the mature biomass, the use of one of these datasets led to the exclusion of the other. Given that the stability of AGS systems is dependent on the balance between the suspended and granular fractions, the prediction of VSS and TSS was performed separately for both fractions. In all cases two thirds of the collected database were used for training purposes and one third for validation purposes.

The obtained prediction abilities were evaluated taking into account the ensemble (training and validation) data, in terms of the coefficient of determination (R²), p-value, root mean square error (RMSE) the residual predictive deviation (RPD, reflecting the ratio between the population standard deviation – SD, and the prediction standard error of cross validation – SECV). An RPD value above 3 is recommended for screening purposes (Fearn 2002).

With respect to the VSS of the suspended fraction, using the mature AGS dataset, a R² value of 0.914 (p-value<0.01, RMSE of 0.216 g L⁻¹ (8.6% of the studied range) and RPD of 3.50) was obtained for the prediction model shown in Equation 2, based on the overall and small flocs contents, intermediate flocs fraction, intermediate and large flocs size, and overall flocs morphology.

$$\text{VSS}_{\text{floc}} = -3.091 + 8.35 \times 10^{-5} (\text{TA}_{\text{floc}}) + 6.40 \times 10^{-4} (\% \text{Nb}_{\text{F}_2})^2 + 6.48 (\text{Rob}_{\text{floc}}) - 8.56 \times 10^{-8} (\text{Nb}_{\text{F}_1}) - 5.84 \times 10^{-8} (\text{Area}_{\text{F}_2})^2 + 1.98 \times 10^{-11} (\text{Area}_{\text{F}_3})^2 + 0.00134 (\text{Diam}_{\text{F}_2})^2 + 0.0929 (\text{Diam}_{\text{F}_2}) \quad (\text{Eq. 2})$$

With respect to the suspended fraction VSS using the biomass density dataset, shown in Equation 3, the most important parameters were found to be related with the overall and large flocs contents, intermediate flocs fraction, overall, intermediate and large flocs size, and overall flocs morphology. For this prediction a R² value of 0.948 (p-value<0.01, RMSE of 0.195 g L⁻¹ (7.8% of the studied range) and RPD of 4.13) was obtained.

$$\text{VSS}_{\text{floc}} = -4.25 + 9.22 \times 10^{-5} (\text{TA}_{\text{floc}}) + 2.89 \times 10^{-7} (\text{Area}_{\text{floc}})^2 - 9.42 \times 10^{-9} (\text{Area}_{\text{F}_2})^2 + 8.26 \times 10^{-12} (\text{Area}_{\text{F}_3})^2 - 0.569 (\% \text{Nb}_{\text{F}_3}) + 5.029 (\text{Conv}_{\text{floc}}) - 1.091 \times 10^{-8} (\text{TA}_{\text{F}_3})^2 \quad (\text{Eq.3})$$

The correlations between the observed and predicted VSS of the suspended fraction, either using the biomass density or the mature AGS datasets, are presented in Figure 33.

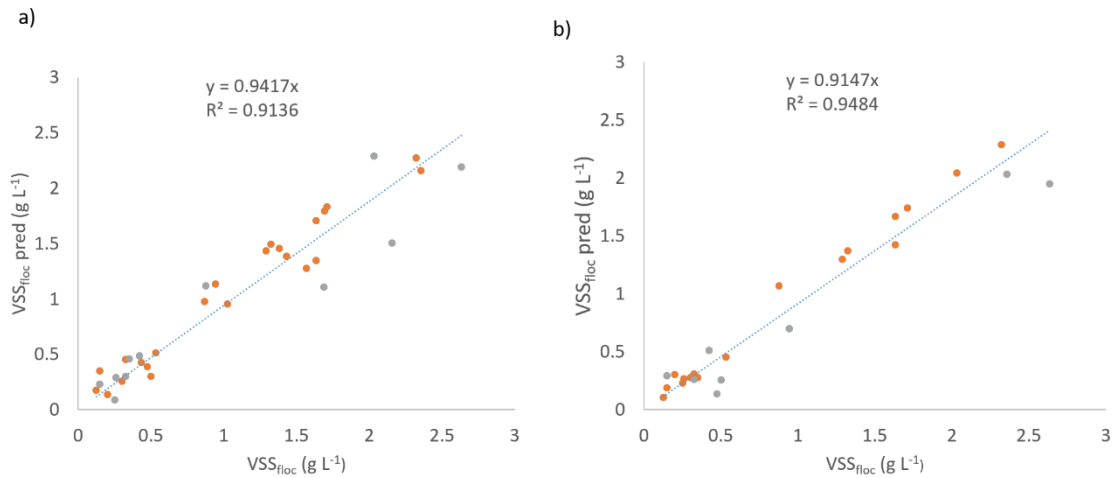


Figure 33 Correlations between the observed and predicted VSS for the suspended fraction. a) using the mature AGS dataset b) using the biomass density dataset.

Regarding the TSS of the suspended fraction, using the mature AGS dataset, a R^2 value of 0.905 (p-value<0.01, RMSE of 0.243 g L⁻¹ (9.0% of the studied range) and RPD of 3.28) was obtained for the prediction model presented in Equation 4, based on the overall and small flocs contents, small, intermediate and large flocs size, and overall and large flocs morphology.

$$TSS_{floc} = -11.9 + 1.085 \times 10^{-4} (TA_{floc}) + 6.98 \times 10^{-5} (Area_{F1})^2 + 7.36 (Rob_{floc}) - 0.001054 (TA_{F1}) - 0.001031 (Area_{F2}) + 0.153 (Diam_{F2}) + 6.079 \times 10^{-6} (Area_{F3}) + 1.57 (Ecc_{F3})^2 \quad (\text{Eq. 4})$$

Again, the TSS of the suspended fraction was also predicted using the biomass density dataset, with the most important parameters being related to the overall and large flocs contents, overall and intermediate flocs size, and overall flocs morphology. The obtained results are presented in Equation 5 and revealed a R^2 value of 0.922 (p-value<0.01, RMSE of 0.219 g L⁻¹ (8.2% of the studied range) and RPD of 3.89).

$$TSS_{floc} = 1.13 + 1.203 \times 10^{-4} (TA_{floc}) + 3.25 \times 10^{-7} (Area_{floc})^2 - 9.21 \times 10^{-9} (Area_{F2})^2 - 3.53 \times 10^{-10} (Nb_{F3}) - 0.00161 (Conv_{floc})^2 \quad (\text{Eq. 5})$$

The obtained correlations between the observed and predicted floccular TSS, both using the biomass density or the mature AGS datasets, are presented in Figure 34.

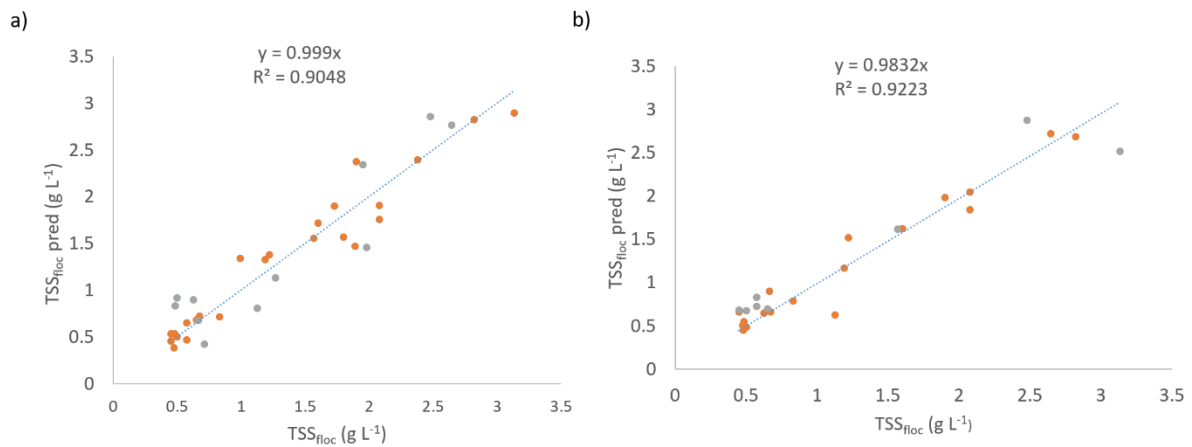


Figure 34 Correlations between the observed and predicted floccular TSS values. a) using the mature AGS dataset b) using the biomass density dataset.

As expected, the floccular TSS and VSS models show a high similitude, and a direct dependency on the overall flocs' contents and regularity. Indeed, it could be inferred that higher floccular VSS and TSS values were (mostly) positively correlated with more regular flocs, in accordance with the PCA results. It could also be inferred that the use of the biomass density data (and exclusion of the mature AGS data), in both VSS and TSS predictions for the floccular fraction, resulted in an increase in the models quality, taking in consideration the higher R^2 and RPD values, and lower RMSE, when the biomass density was included. The obtained RPD values, being above 3 in all cases, confirm the models' adequateness for screening purposes, with error (RMSE) values around or below 9.0% (8.2% for the inclusion of the biomass density data).

Regarding the VSS prediction for the granular fraction using the mature AGS dataset, a R^2 value of 0.927 (p -value<0.01, RMSE of 1.989 g L⁻¹ (8.9% of the studied range) and RPD of 3.61) was obtained for the prediction model shown in Equation 6, based on the small and large granules contents, intermediate granules size and overall and small granules morphology.

$$VSS_{gran} = -42.9 + 0.0448 (TV_{G3}) - 0.008202 (Diam_{G2}) + 71.264 (Rob_{G1}) + 4.98 \times 10^{-4} (Diam_{G2})^2 + 89.3 (TV_{G1}) - 37.7 (Ecc_{gran})^2$$

(Eq. 6)

In a similar way to the floccular fraction predictions, the granular fraction VSS was also predicted using the biomass density dataset, presented in equation 7, leading to a smaller R^2 value of 0.867 (p -

value < 0.01 RMSE of 1.593 g L⁻¹ (8.3% of the studied range) and RPD of 2.84). These results showed that the biomass density, overall and intermediate granules contents, and intermediate and small granules size were found to be crucial for the prediction.

$$VSS_{gran} = -53.3 + 0.137 (Nb_{gran}) + 0.05057 (Dens) + 0.292 (Diam_{G1}) + 0.385(Nb_{G3}) - 2.34 \times 10^{-9} (Vol_{G2}) \quad (Eq. 7)$$

The correlations between the VSS predicted and observed values for the AGS granular fraction, both using the biomass density or the mature AGS datasets, are presented in Figure 35.

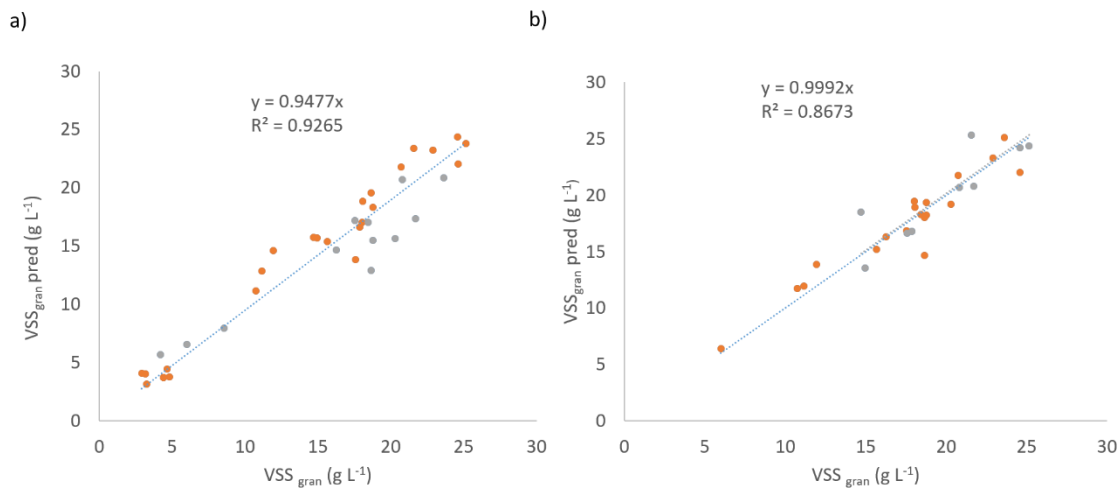


Figure 35 Correlations between the observed and predicted granular VSS. a) using the mature AGS dataset b) using the biomass density dataset.

With respect to the granular TSS, using the mature AGS dataset, a R² value of 0.915 (p-value<0.01, RMSE of 2.183 g L⁻¹ (9.6% of the studied range) and RPD of 3.44) was obtained for the prediction model presented in Equation 8, based on the overall and large granules contents, large granules fraction and morphology and small granules size.

$$TSS_{gran} = 1500 + 0.1948 (Nb_{gran}) + 0.001732 (\%Vol_{G3}) - 5.330 \times 10^{-6} (Vol_{G1}) + 8.818 \times 10^{-4} (Diam_{G1})^2 + 3.755 \times 10^{-5} (TV_{G3}) - 4510 (Ecc_{G3}) + 3251 (Ecc_{G3})^2 \quad (Eq. 8)$$

Regarding the TSS prediction for the AGS granular fraction, when the biomass density dataset was used (Equation 9), a decrease on the model prediction ability was perceived (R² value of 0.862, p-value<0.01, RMSE of 1.633 g L⁻¹ (8.7% of the studied range) and RPD of 2.75). It was found that the

biomass density, overall, large, intermediate and small granules contents, and small granules size were crucial for the prediction.

$$TSS_{gran} = -121.2 + 0.9901 (Nb_{gran}) + 0.05788(Dens) + 0.2268 (Diam_{G1}) - 2536 (TV_{G1})^2 + 93.52 (Rob_{G3}) - 0.7856 (Nb_{G2}) - 0.01556 (Nb_{G3})^2 \quad (Eq. 9)$$

The correlations between the observed and predicted granular TSS values, both when the mature AGS or biomass density datasets were used, are presented in Figure 36.

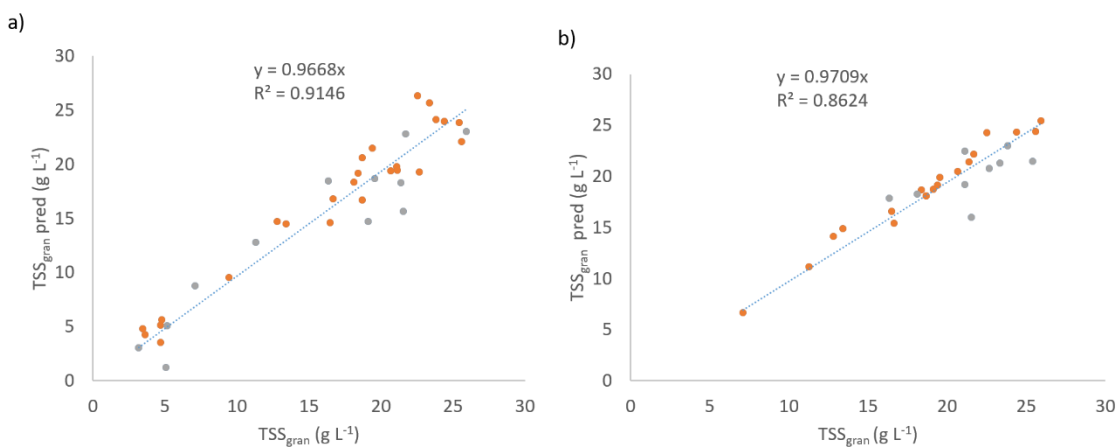


Figure 36 Correlations between the observed and predicted granular TSS. a) using the mature AGS dataset b) using the biomass density dataset.

As expected, the granular VSS and TSS models show a high similitude, and a direct dependency on the overall or dominant large granules contents. Furthermore, it could be inferred that higher granular VSS and TSS values were positively correlated with the biomass density, in accordance with the PCA results. Interestingly, these results revealed an opposite behavior when compared to the floccular fraction. Thus, it could be inferred that the exclusion of the mature AGS data decreased the prediction ability for both granular VSS and TSS. The obtained RPD values, being above 3 for the use of the mature AGS dataset, confirm these models' adequateness for screening purposes, with error (RMSE) values around or below 9.6%. However, when the mature AGS data was excluded, the RPD values dropped slightly below 3 (around 2.8), although the error (RMSE) values did not surpass a maximum of 8.7%.

Opposite to the previous analysis, the biomass density and SVI_5 were predicted including the ensemble suspended and granular fractions. Regarding the biomass density prediction (based on TSS)

a R^2 value of 0.886 (p-value<0.01, RMSE of 11.6 g TSS L⁻¹ biomass (8.8% of the studied range) and RPD of 3.02) was obtained for the prediction model shown in equation 10, based on the granular biomass and intermediate granules contents, large granules fraction and both large granules and flocs morphology. The obtained correlations between the observed and predicted density values (based on TSS) are presented in Figure 37a.

$$\text{Density (TSS)} = 658.9 + 0.1643 (\text{TSS}_{\text{gran}})^2 - 3.288 (\text{Nb}_{\text{G2}}) + 1341(\text{Conv}_{\text{F3}})^2 - 1233(\text{Conv}_{\text{F3}}) - 0.01495 (\% \text{Nb}_{\text{G3}})^2 - 459.26 (\text{Rob}_{\text{G3}})^2$$

(Eq. 10)

Similar results were obtained for the density prediction when based on VSS, presenting a R^2 value of 0.861 (p-value<0.01, RMSE of 11.6 g VSS.L⁻¹ biomass (8.7% of the studied range) and RPD of 2.95) for the prediction model shown in equation 11, based on the granular biomass and intermediate granules contents, small granules fraction and large flocs morphology. The obtained correlations between the observed and predicted density values (based of VSS) are presented in Figure 37b.

$$\text{Density (VSS)} = 337.1 + 0.1275(\text{VSS}_{\text{gran}})^2 - 0.06588(\text{Nb}_{\text{G2}})^2 + 1320(\text{Conv}_{\text{F3}})^2 - 1232(\text{Conv}_{\text{F3}}) + 0.02672(\% \text{Nb}_{\text{G1}})^2$$

(Eq. 11)

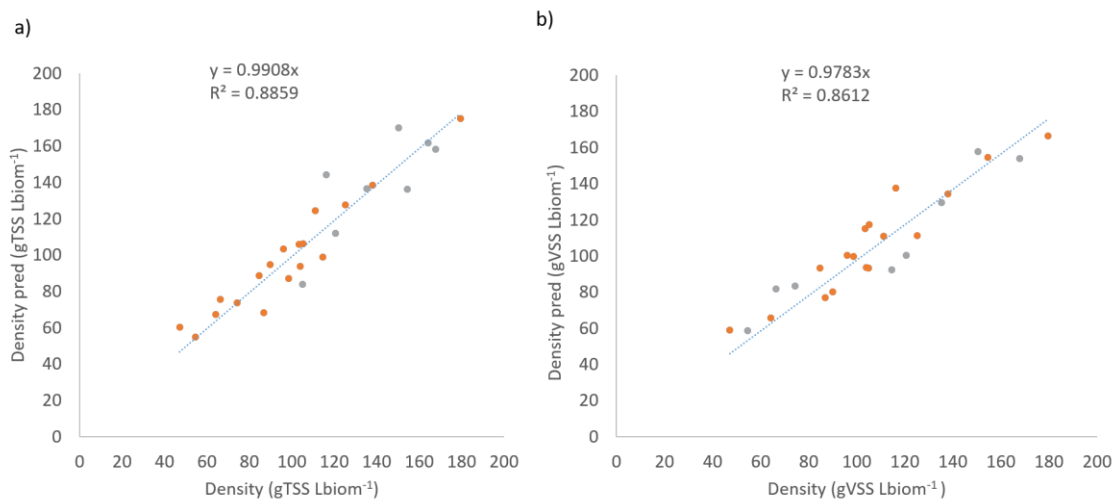


Figure 37 Correlations between observed and predicted density values. a) based on TSS b) based on VSS.

As could be expected, the density prediction model based on either the VSS or TSS show a high similitude. Given the above results it can be inferred that the biomass density can be predicted based upon the overall granular biomass (directly dependent), intermediate granules (inversely dependent) contents and granules regularity (inversely dependent), as already shown in the PCA analysis.

Furthermore, the flocs regularity was also found to be a key factor on the biomass density prediction. The obtained RPD values, around 3 in both cases, are on the threshold of confirming the models' adequateness for screening purposes, with error (RMSE) values around or below 8.8%.

The AGS settling properties, in terms of the SVI_5 , could also be successfully predicted, by the use of either VSS or TSS. In the former case, the use of the biomass density dataset allowed for a R^2 value of 0.990 (p-value<0.01, RMSE of 0.761 mL g⁻¹ VSS (3.2% of the studied range) and RPD of 8.42) for the prediction model shown in equation 12. The main parameters that allowed for the SVI_5 prediction were related to the granular (and overall) contents, overall and apparent granular density, filamentous bacteria contents, overall flocs size and intermediate granules morphology. The obtained correlations between the observed and predicted SVI_5 (based on VSS and using the biomass density dataset) are presented in Figure 38a.

$$SVI_5 (VSS) = 94.97 - 5.979 (VSS_{gran}) + 0.1519(VSS_{total})^2 - 1.882 \times 10^8 \left(\frac{VSS_{gran}}{TV_{gran}} \right)^2 - 0.02475(Dens) - 1.435 \times 10^{-6} (Area_{floc})^2 - 1.932 \left(\frac{TL}{TA_{floc}} \right) + 0.5577 \left(\frac{TL}{VSS_{floc}} \right) - 21.22(Ecc_{G2})^2 \quad (Eq. 12)$$

On the other hand, with the use of the mature AGS dataset, the SVI_5 prediction ability decreased to a R^2 value of 0.962 (p-value<0.01, RMSE of 2.373 mL g⁻¹ VSS (4.6% of the studied range) and RPD of 5.38) for the prediction model shown in equation 13. The main parameters that allowed for this prediction ability included the granular and intermediate granules contents, apparent floccular density, intermediate flocs fraction, overall flocs size, large granules and intermediate flocs morphology. The obtained correlations between the observed and predicted SVI_5 values (based on VSS and using the mature AGS dataset) are presented in Figure 38b.

$$SVI_5 (VSS) = 148.8 - 2.154 (VSS_{gran}) + 0.020024 (\%Nb_{F2})^2 - 1.323 \times 10^7 \left(\frac{VSS_{floc}}{TA_{floc}} \right) - 299.7 (Conv_{G3}) - 0.023058 (Area_{floc})^2 + 0.02608(Nb_{G2})^2 + 481.3(Conv_{F2}) - 284.2 (Conv_{F2})^2 \quad (Eq. 13)$$

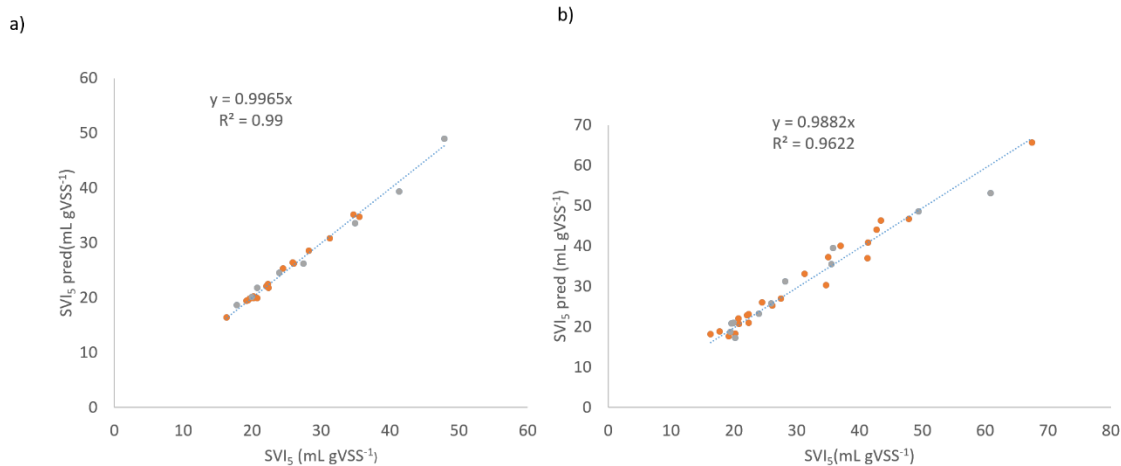


Figure 38 Correlations between observed and predicted SVI_5 values. a) using the biomass density dataset b) using the mature AGS dataset.

Regarding the SVI_5 predictions based on TSS, the use of the biomass density dataset, shown in equation 14, presented a R^2 value of 0.983 (p -value<0.01, RMSE of 0.720 mL g TSS⁻¹ (3.0% of the studied range) and RPD of 8.87). The most important parameters for the prediction were found to be related with the overall and granular biomass contents, overall biomass and apparent granular density, flocs and large granules size and large granules morphology. The correlations between the predicted and observed SVI_5 (based on TSS and using the biomass density dataset) are presented in Figure 39a.

$$SVI_5(TSS) = 55.33 - 2.629 (TSS_{gran}) + 0.054106 (TSS_{total})^2 - 2.201 \times 10^8 \left(\frac{TSS_{gran}}{TV_{gran}} \right)^2 - 0.2122 (Dens) + 68.97 (Rob_{G3})^2 + 7.805 \times 10^{-4} (Dens)^2 + 0.008118 (Diam_{G3}) - 0.005254 (Diam_{floc})^2 \quad (\text{Eq. 14})$$

The SVI_5 prediction, based on TSS, was also performed using the mature AGS dataset, shown in equation 15, with the main parameters found to be the granular biomass contents, overall flocs and filamentous bacteria contents, overall granules, overall and large flocs size. This model presented a R^2 value of 0.930 (p -value<0.01, RMSE of 3.32 mL g TSS⁻¹ (6.5% of the studied range) and RPD of 3.84). The correlations between the predicted and observed SVI_5 (based on TSS and using the mature AGS dataset) are presented in Figure 39b.

$$SVI_5(TSS) = 41.93 - 2.165 (TSS_{gran}) + 1.217 (TL)^2 + 1.850 \times 10^{-10} (Area_{F3})^2 - 2.215 \left(\frac{TL}{TSS_{floc}} \right) + 9.610 \times 10^{-10} (Vol_{gran}) + 6.0073 \times 10^{-4} (TA_{floc}) + 0.03494 (TSS_{gran})^2 - 1.318 \times 10^{-6} (Area_{floc})^2 \quad (\text{Eq. 15})$$

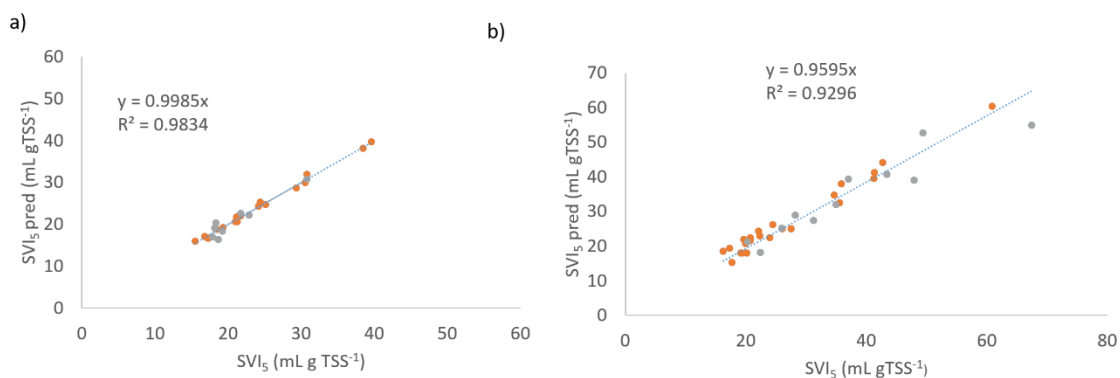


Figure 39 Correlations between the observed and predicted SVI_5 based on TSS a) using the biomass density dataset b) using the mature AGS dataset.

Given the above results it can be inferred that the obtained models were quite similar to each other, and that the AGS settling properties, in terms of the SVI_5 , can be predicted based upon the overall (and apparent) biomass density, granular contents and flocs size (all inversely dependent) and even granules and flocs regularity and filamentous bacteria contents. It should also be stressed that the determined relationships further strengthen the conclusions windthrown by the PCA analysis, namely regarding the inverse relationship between the settling ability with the biomass density and granular biomass contents.

The models result also revealed that the use of the biomass density data (excluding the mature AGS data) led to better SVI_5 prediction abilities, taking in consideration the obtained higher R^2 and RPD values, and lower RMSE. On the other hand, no significant difference could be found regarding the use of either VSS or TSS data. The obtained RPD values, largely above the value 3, confirm the models' adequateness for screening purposes, with error (RMSE) values around or below 6.5% (3.2% for the inclusion of the biomass density data).

6.4. *PhAC monitoring and identification*

6.4.1. *Use of Discriminant Analysis*

Likewise PCA, DA was also performed for the PhACs (E2, EE2 and SMX) dataset, including the mature AGS (CONT) experiment when feasible, addressing the SBR-AGS main physical properties and the morphological and structural parameters obtained by QIA. Again, the DA were performed both with and without the biomass density, due to the fact that no data regarding this parameter could be obtained for the mature AGS experiment.

The DA performed with the AGS physical and QIA data, using the mature AGS dataset, for the operational periods discrimination is presented in Figure 40.

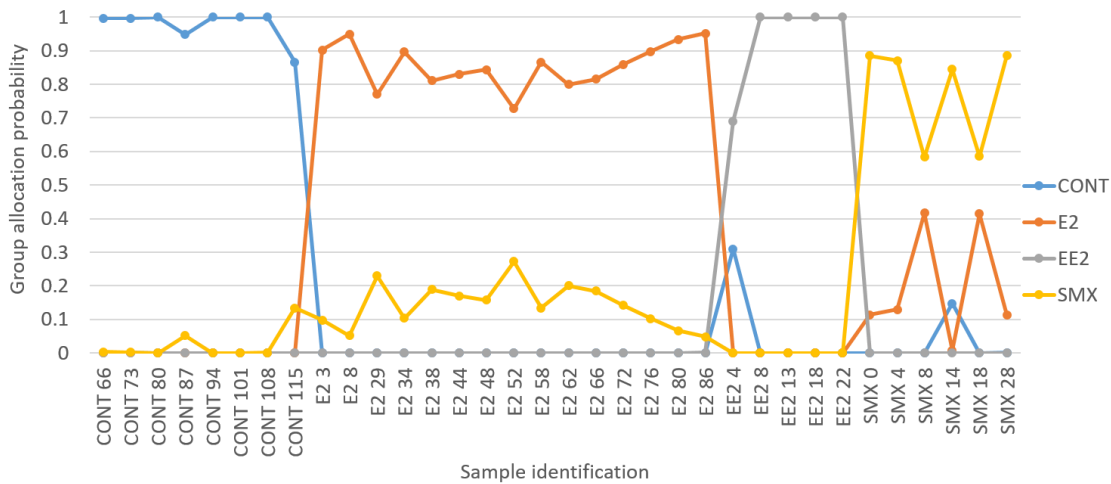


Figure 40 DA with AGS and QIA data, using the mature AGS dataset, for the operational periods discrimination.

Taking into consideration the obtained results, the CONT, E2, EE2 and SMX operational periods could be fully identified (recognition percentage of 100%) by the use of the flocs apparent density ($(VSS/TA)_{floc}$), with the E2 experiment presenting the larger values and the CONT experiment the smaller values, and the intermediate granules contents (G2-TV), with the EE2 experiment presenting the larger values. Although the different PhAC and mature AGS operational periods could be fully discriminated, differences could be seen regarding the samples' allocation probability within the respective group. The clearest discrimination was obtained for the mature AGS (CONT) and EE2 experiments, with an allocation probability larger than 90% for almost all samples. On the other hand, the E2 and SMX experiments presented lower allocation probabilities ranging from 72% to 95% (E2) and 58% to 89% (SMX). Furthermore, these two experiments presented the least separation ability between all pairs of experiments within the performed DA.

Based on the same dataset, another DA was performed aiming to discriminate the samples with and without PhAC addition (undiscriminating the E2, EE2, SMX and CONT experiments), with the main results presented in Figure 41.

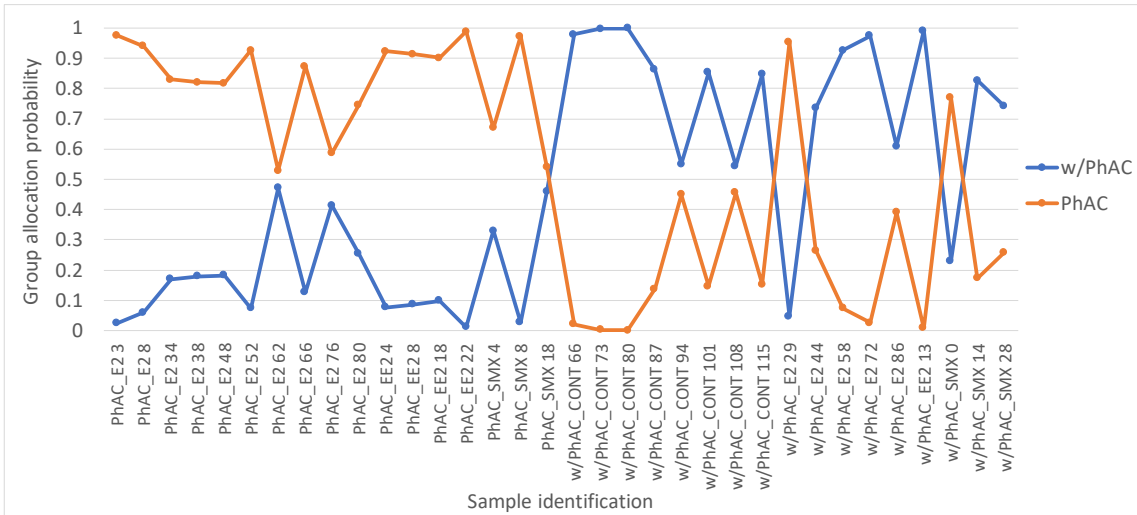


Figure 41 DA with AGS and QIA data, using the mature AGS dataset, for PhAC addition discrimination.

The obtained results revealed an overall discrimination of 94.1% between the operational days with and without PhAC addition, reflecting a 100.0% accuracy for the samples with PhAC addition and 92.0% without. The most important variables were found to be related to the filamentous bacteria presence (TL and TL/TSS), settling ability (SVI₅), small and intermediate granules fraction (G2-%V and G1-%Nb) and small flocs contents (F1-Nb). Indeed, significant differences were found for most of these parameters between the two operational periods, particularly for the EE2 and SMX experiments, with the PhAC addition leading to higher SVI and lower intermediate granules fraction and filamentous bacteria contents.

Again, a second DA was performed with the AGS physical and QIA data, by the use of the biomass density dataset, for the operational periods discrimination and is presented next in Figure 42.

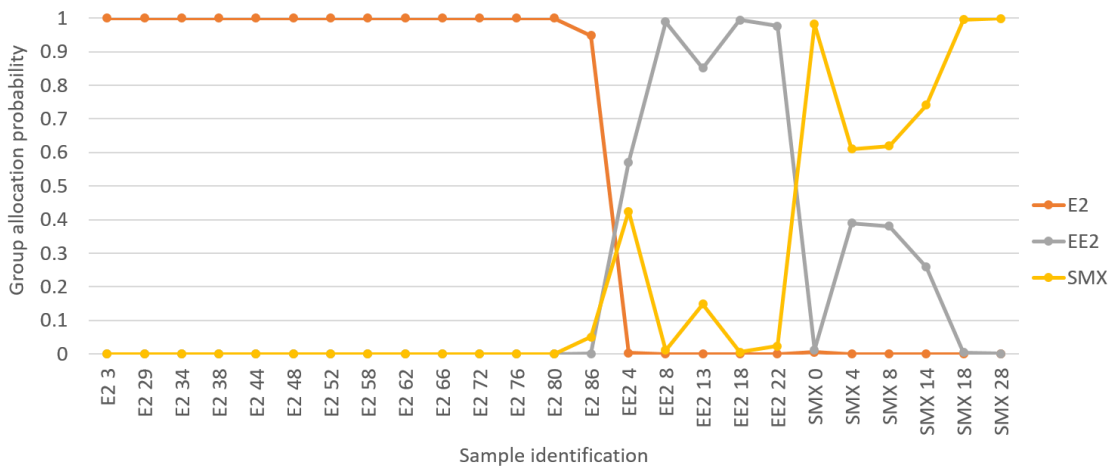


Figure 42 DA with AGS and QIA data, using the biomass density dataset, for the operational periods discrimination.

The obtained results allowed for a fully successful identification (recognition percentage of 100%) of the E2, EE2 and SMX operational periods samples, by the use of the small granules fraction (G1-%Nb),

with the EE2 experiment presenting the smaller values, and large granules contents (G3-Nb), with the E2 experiment presenting the smaller values. Interestingly, with the absence of the CONT samples, the flocs apparent density lost some significance regarding the allocation importance. Again, although the different PhAC operational periods could be fully discriminated, differences could be seen regarding the samples' allocation probability within the respective group. In this sense, the E2 experiment samples were the most clearly discriminated, presenting the larger allocation probabilities (100% except for one sample), while the EE2 experiment allocation probabilities were slightly lower (ranging from 85.1% to 99.5%, except for one sample). On the other hand, some of the SMX experiment samples, despite being successfully identified, presented relatively lower allocation probabilities (ranging from 61.0% to 99.9%), and close to being misclassified as EE2 in some samples. These results could be explained by the somewhat similar behavior of the biomass morphology in both EE2 and SMX experiments, also corroborated by previous results showed in PCA.

In a similar way to the previous DA study, and based on the current dataset, another DA was performed aiming to isolate the samples with and without PhAC addition (undiscriminating the E2, EE2 and SMX experiments), being presented in Figure 43.

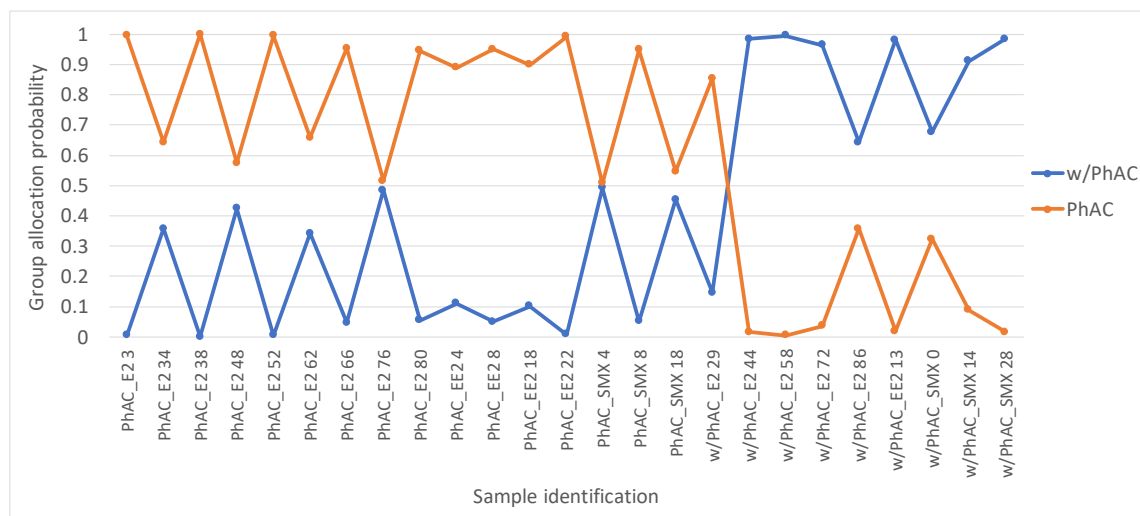


Figure 43 DA with AGS and QIA data, using the biomass density dataset, for PhAC addition discrimination.

The obtained results showed an overall discrimination of 96.0% between the operational days with and without PhAC addition, reflecting again a 100.0% accuracy for the samples with PhAC addition and 93.8% without. The most important variables were found to be related to the filamentous bacteria contents (TL), settling properties stability (SVI_{30}/SVI_5), large granules regularity (G3-Conv) and small granules contents (G1-Nb). These results can be explained by the lower filamentous bacteria and small granules contents in the PhAC addition experiments.

In a similar way to the PCA analysis, another set of DA analyses were performed to evaluate the importance of the different data groups with: the sludge physicochemical parameters i) including and ii) excluding the biomass density; the QIA based morphology and structural parameters of the AGS for the iii) floccular fraction and iv) granular fraction. These analysis were performed with the objective of identifying the operational periods (Figure 44) and PhAC containing samples (Figure 45).

The use of solely the sludge physicochemical parameters, with the mature granules dataset, allowed for a nearly perfect identification of the CONT and E2 operational periods, although the distinction between the EE2 and SMX periods was quite less evident, resulting in a 94.1% overall recognition percentage. The parameters found to contribute to these results were the $SVI_{5,}$ $TSS_{floc,}$ TSS_{gran} and VSS/TSS . Furthermore, when the biomass density dataset was used, the distinction between the EE2 and SMX operational periods improved, in line with the recognition percentage (96.0%), through the use of the density, TSS_{gran} and VSS_{gran} . On the other hand, the use of the granular biomass parameters (G3-Nb, G1-%Nb and G3-D) allowed for the best distinction between the EE2 and SMX periods, as well as overall (100%), just above (97.1%) the use of the floccular biomass data (F1-A, F2-Rob, F-Rob and $(TSS/TA)_{floc,}$). Most of the parameters found to contribute to the identification of the operational periods in the partial DA have already been found important in previous discussions.

Regarding the identification of the samples with, or without, PhAC addition, an 84.0% overall recognition percentage was obtained for the physicochemical parameters including the biomass density (density, $SVI_{5,}$ $SVI_{30,}$ TSS_{floc} and VSS_{floc}) and 85.3% excluding ($SVI_{5,}$ $SVI_{30,}$ $SVI_{30}/SVI_{5,}$ TSS_{floc} and TSS_{gran}). On the other hand, the use of the AGS morphology and structural parameters resulted in improved recognition percentages, namely of 91.2% for the floccular fraction (TL, F1-Nb, F3-Conv, F-A) and 88.2% for the granular fraction (G1-D, G1-Nb, G2-V and G3-D). Again, a significant fraction of the parameters found to contribute to the identification of the samples with, or without, PhAC addition in the partial DA have already been found relevant in previous discussions. Interestingly the PhAC addition samples presented an opposite recognition ability regarding the operational periods identification. These results highlight the importance of both AGS fractions in terms of process control and monitoring in the presence of the studied PhAC.

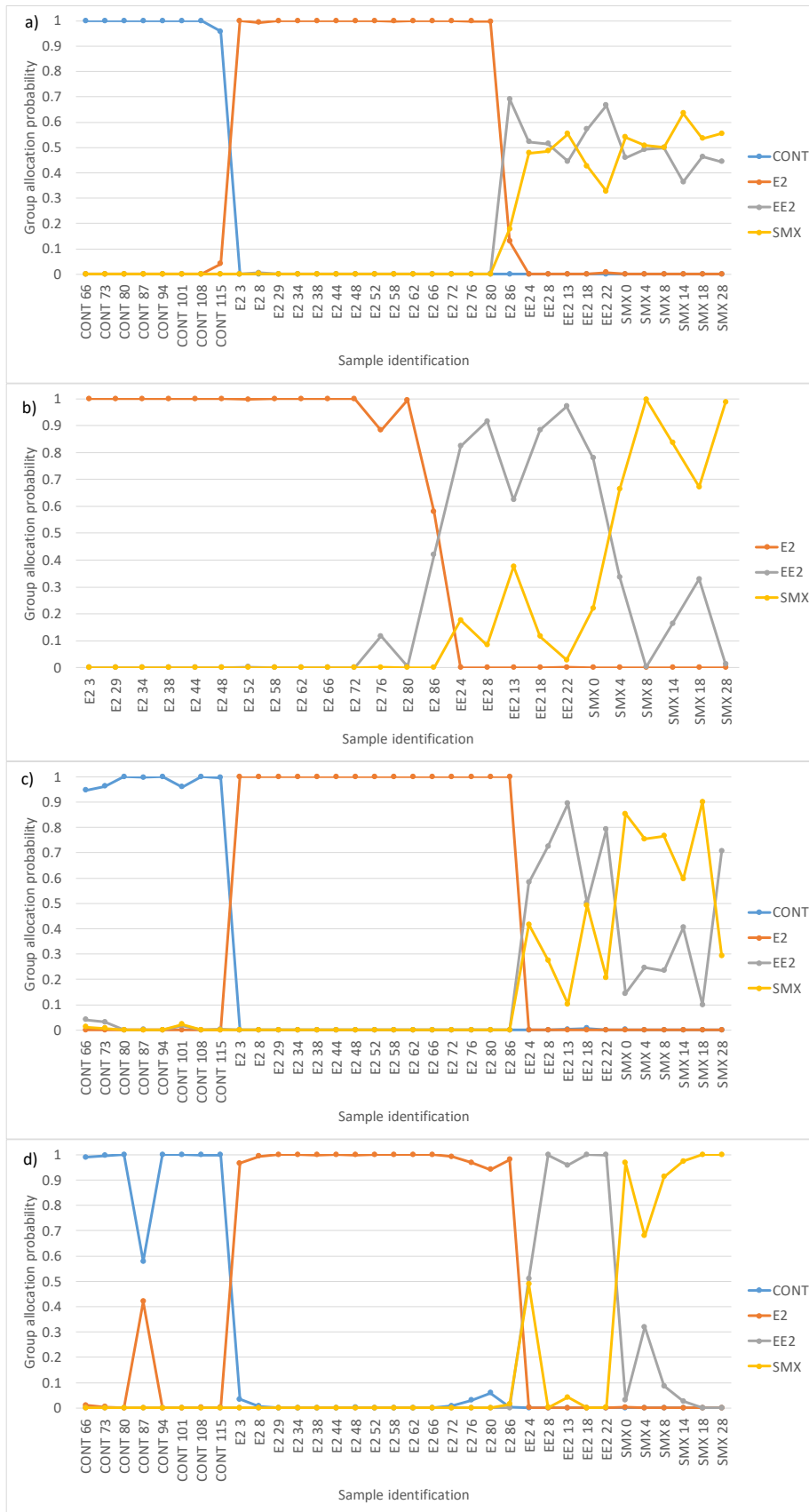


Figure 44 DA for operational periods identification with the: sludge physicochemical parameters a) including and b) excluding the biomass density; QIA based morphology and structural parameters of the AGS for the c) floccular fraction and d) granular fraction.

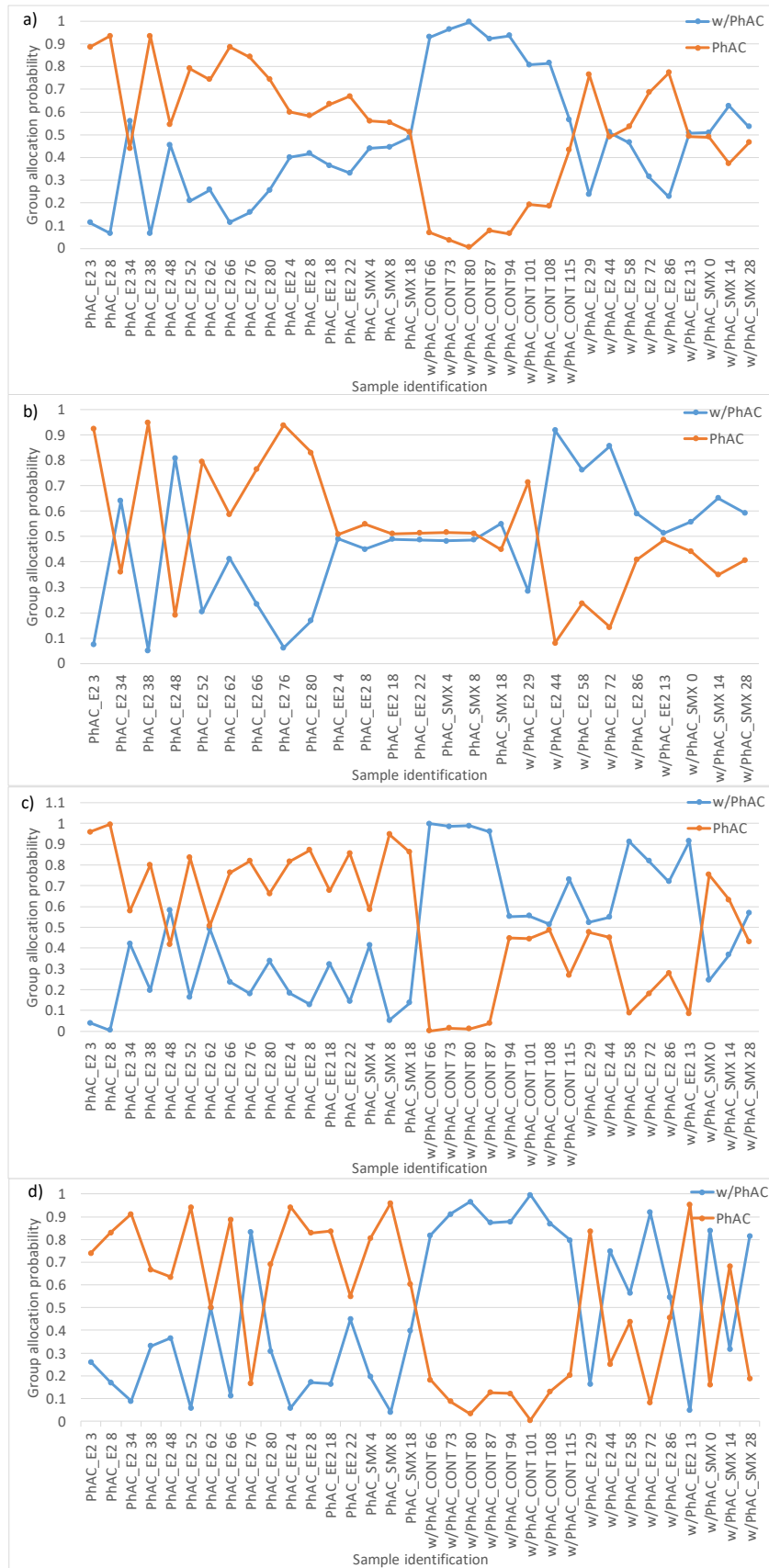


Figure 45 DA for PhAC addition discrimination with the: sludge physicochemical parameters a) including and b) excluding the biomass density; QIA based morphology and structural parameters of the AGS for the c) floccular fraction and d) granular fraction.

6.4.2. Use of Decision Trees

With a similar purpose to DA, DT were performed aiming to discriminate the different CONT, E2, EE2 and SMX operational periods, on one hand, and between the samples with and without PhAC addition, on the other. For that purpose, the SBR-AGS main physical properties, either using the biomass density or the mature AGS datasets, and QIA morphological and structural parameters were used.

In the first DT analysis, employing the mature AGS dataset, the CONT, E2, EE2 and SMX operational periods were successfully identified (recognition percentage of 100%) by the use of the filamentous bacteria presence (TL/TA_{floc}), settling ability (SVI_5) and the small granules fraction ($G1-\%Nb$). The TL/TA_{floc} parameter was found to be crucial for the E2 samples identification, presenting values below 0.354 mm/mm^2 . The second threshold for discriminating between experiments was the SVI_5 , allowing to identify the CONT samples which presented values larger than $30.1 \text{ mL gTSS}^{-1}$. Additionally, these values could be also correlated with the higher floccular fraction (presenting filamentous bacteria) in that period. Finally, the third ($G1-\%Nb$) threshold allowed to discriminate between the EE2 (below 10.6%) and SMX (above 10.6%) samples (further corroborated by the SMX granules visual inspection).

On the other hand, the discrimination of the monitoring periods with and without PhAC addition attained 97.1% of success, reflecting a 94.1% accuracy for the samples with PhAC addition and 100.0% without. The parameters found responsible for the discrimination were the large granules contents ($G3-TV$), settling ability (SVI_5), small flocs contents ($F1-Nb$) and intermediate flocs irregularity ($F2-Ecc$). Indeed, the samples reflecting the PhAC addition were characterized by $G3-TV$ values above $115.5 \text{ mm}^3 \text{ mL}^{-1}$, SVI_5 values above $18.5 \text{ mL gTSS}^{-1}$, $F1-Nb$ values below $7.74 \times 10^6 \text{ mL}^{-1}$ and $F2-Ecc$ values above 0.700.

In the second DT analysis, using the biomass density dataset, the E2, EE2 and SMX operational periods were successfully identified (recognition percentage of 100%) using the filamentous bacteria presence (TL/TA_{floc}) and small granules fraction ($G1-\%Nb$). Likewise the first DT analysis, the TL/TA_{floc} was found to be crucial for the E2 samples identification (values below 0.354 mm/mm^2) and the $G1-\%Nb$ to discriminate between the EE2 (below 10.6%) and SMX (above 10.6%) samples. Given that no CONT data was included in this analysis, no need for the SVI_5 parameter was found. As occurred in the first DT, as well as the majority of the previous chemometric analysis, the EE2 and SMX samples were the most related among the different experiments and, thus, were the last to be separated by the DT analysis.

Regarding the discrimination of the monitoring periods with and without PhAC addition a 96.0% successful percentage was obtained, reflecting a 93.8% accuracy for the samples with PhAC addition and 100.0% without. The parameters found to allow for the discrimination were the settling ability (SVI_5), small flocs contents (F1-Nb) and intermediate flocs irregularity (F2-Ecc). In accordance with the first DT analysis, the samples reflecting the PhAC addition were characterized by SVI_5 values above 18.5 mL gTSS⁻¹, F1-Nb values below 7.74×10^6 mL⁻¹ and F2-Ecc values above 0.700. The main results of DT are presented in Figure 46.

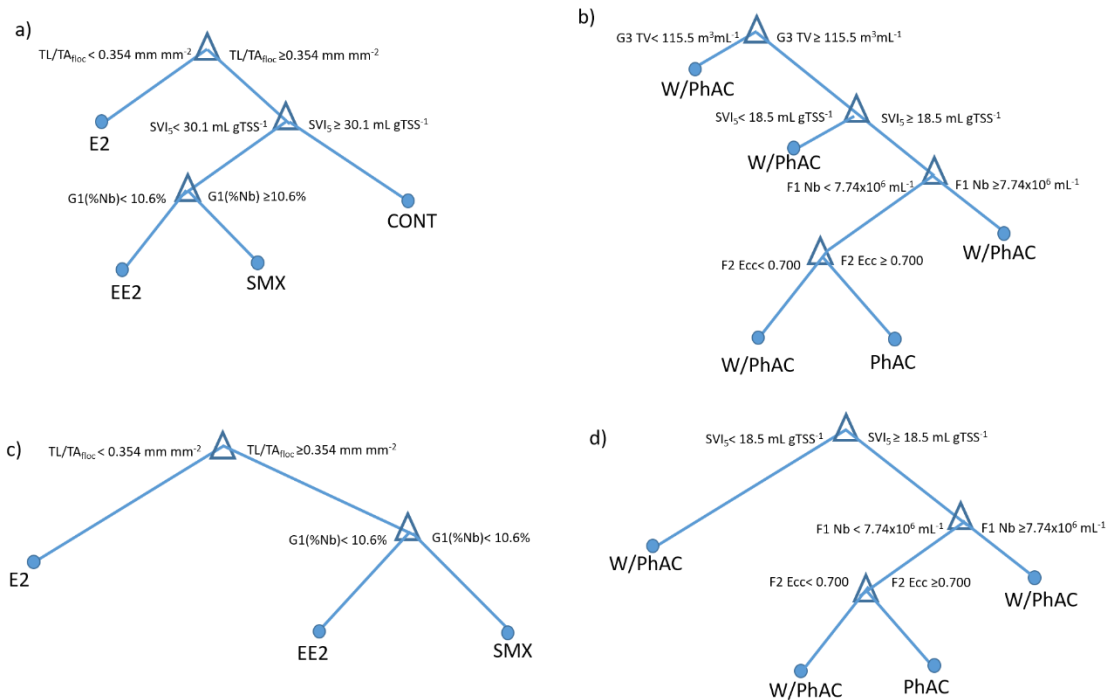


Figure 46 DT performed using the mature AGS dataset identification of a) operational periods and b) samples with, or without, PhAC addition; and using the biomass density dataset identification of c) operational periods and d) samples with, or without, PhAC addition

With the same objective of the previous partial PCA and DA, another set of DT analyses were performed to evaluate the importance of the different data groups with: the sludge physicochemical parameters i) including and ii) excluding the biomass density; the QIA based morphology and structural parameters of the AGS for the iii) floccular fraction and iv) granular fraction. The DT analysis with the different data groups is presented in Figure 47.

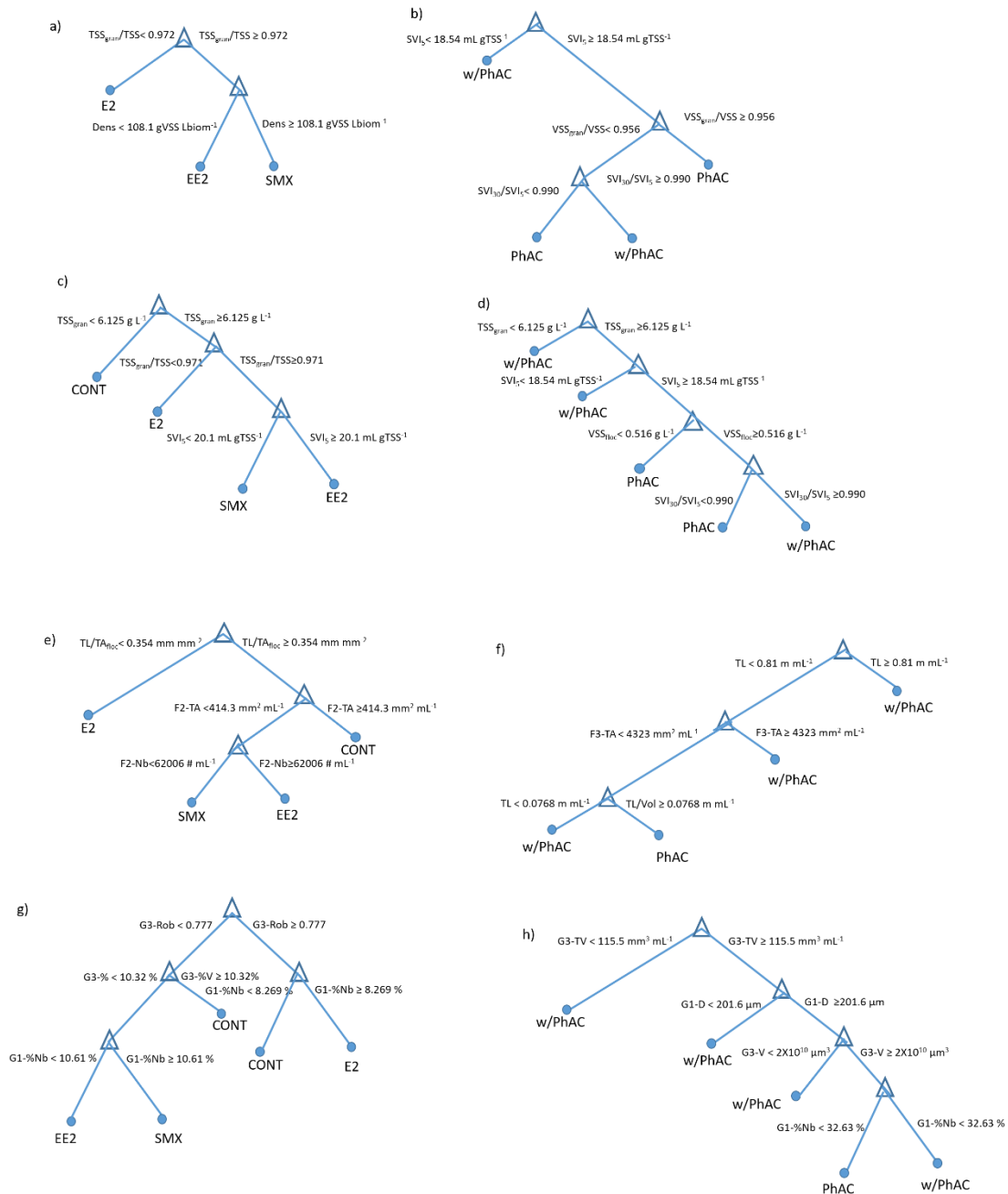


Figure 47 DT for identification operational periods and samples with, or without, PhAC addition a) operational periods with physicochemical parameters including density; b) samples with, or without, PhAC addition with physicochemical parameters including density; c) operational periods with physicochemical parameters excluding density; d) samples with, or without, PhAC addition with physicochemical parameters excluding density; e) Operational periods with floccular fraction QIA parameters; f) Samples with, or without, PhAC addition with floccular fraction QIA parameters; g) Operational periods with granular fraction QIA parameters; h) Samples with, or without, PhAC addition with with floccular fraction QIA parameters.

The use of the biomass density dataset in the physicochemical data (Figure 47a,b) revealed, in general, a slightly decrease in the DT discrimination ability, both in the operational periods and PhAC addition recognition, when compared with the use of the mature granules dataset (Figure 47c,d) (decreasing from 94.1% to 92.0% and from 91.2% to 88.0%, respectively). The parameters found to

contribute to the operational periods identification were the TSS_{gran} , TSS_{gran}/TSS and SVI_5 , whereas for the PhAC addition were the TSS_{gran} , SVI_5 , VSS_{floc} , VSS_{gran}/VSS and SVI_{30}/SVI_5 .

Furthermore, the DT identification ability based on the granular data (Figure 47g,h) was slightly higher than on the floccular data (Figure 47e,f) (overall identification of 97.1%, against 94.1%, for the operational periods, and 94.1%, against 88.2%, for the samples with, or without, PhAC addition. In that respect, the key parameters were found to be the TL/TA_{floc} , F2-Nb and F3-TA (floccular data) and the G1-%Nb, G2-%V and G3-Rob (granular data) for the operational periods and the TL and F3-TA (floccular data) and the G1-D, G1-%Nb, G3-V and G3-TV (granular data) for the PhAC addition. Given the above results, the granular dataset allowed for the best overall identification, with full identification of the operational periods (except for the EE2 with 80.0%) and of the samples without PhAC addition (88.2% accuracy for the PhAC addition samples). In contrast, the floccular dataset allowed for a full identification of the EE2 period, which corroborate the previous DA and PCA results recognizing the importance of the AGS floccular fraction, in addition to the granular fraction, in the process monitoring.

6.5. Conclusions

AGS processes stability is quite dependent on the balance between suspended and granular biomass contents, and the assessment of their contents, settling and density properties is of major interest. In this sense, the prediction of parameters such as density, SVI_5 , VSS and TSS of mature AGS, as well as in the presence of PhACs (E2, EE2 and SMX), was successfully studied by MLR techniques using data obtained by QIA. As a result, good prediction models were obtained for the SVI_5 (R^2 of 0.990), flocs VSS (R^2 of 0.948), granules VSS (R^2 of 0.927), flocs TSS (R^2 of 0.922) and granules TSS (R^2 of 0.915). On the other hand, the results obtained for the density prediction revealed solely a satisfactory correlation between the predicted and experimentally determined values (R^2 of 0.886). The main results of MLR predictions also revealed that the use of the biomass density data (excluding the mature AGS data) increased the prediction abilities of the floccular fraction suspended solids (VSS and TSS) and the AGS settling ability (SVI_5 based on either VSS or TSS). Interestingly, the predictions regarding the granular fraction VSS and TSS, revealed an opposite behavior with a decrease in the prediction ability by the exclusion of the mature AGS data.

The PCA allowed to clearly distinguish, in the PC1 – PC2 space, the four operational periods with the E2 experiment being the most far apart, related to the high flocs contents (at the expense of the granules contents) and overall flocs regularity. On the other hand, the EE2 and SMX were the two closest groups, which can be explained by the high biomass granular contents, with the main

differences being the SMX higher granules apparent density and sludge settling ability. The PCA also revealed a positive relationship between the biomass density, sludge settling ability, overall and granular biomass contents, granulation properties, granular biomass fraction and large granules fraction and size. Regarding the floccular biomass, the results showed a close relationship with the flocs contents, size and regularity, and opposing the biomass organic fraction, granular biomass fraction and filamentous bacteria contents. Furthermore, the small flocs fraction and large flocs regularity seem to also play a positive role in the biomass density, contrary to the intermediate (and overall) granules regularity, which seem to have unfavored the sludge settling ability. A partial PCA analysis stressed the importance of the granular fraction structure enlightenment to characterize the different operational periods, although the physicochemical data seem crucial to separate the mature granules period and the floccular fraction data to separate the E2 period.

The performed DA, either using the biomass density dataset or the mature AGS dataset, allowed for a 100% successful identification of the mature AGS (when applicable), E2, EE2 and SMX operational periods samples, by the use of the flocs apparent density, small granules fraction and intermediate and large granules contents. On the other hand, the use of the biomass density dataset (excluding the mature AGS data) allowed for a slightly higher discrimination ability (96% recognition) between the operational days with (100%) and without (93.8%) PhAC addition. Overall, the most important variables were found to be related to the filamentous bacteria contents, sludge settling ability, settling properties stability, large granules regularity, granules stratification and small flocs and granules contents. Following a partial DA analysis, it could be found that the use of the sludge physicochemical data, with the mature granules dataset, allowed for a nearly perfect identification of the CONT and E2 operational periods. On the other hand, the use of the granular biomass data allowed for the best distinction between the EE2 and SMX periods. On the other hand, with respect to the identification of the samples with, or without, PhAC addition the floccular biomass data allowed for the best results.

Comparable results were obtained with DT for the classifications of samples from different operational periods and samples with and without PhAC addition. Both the use of the mature AGS and of the biomass density datasets allowed to identify the different PhACs operational (and mature AGS) periods with a fully successful (100%) recognition percentage, by the use of the filamentous bacteria contents, settling ability and the small granules fraction. Moreover, the discrimination of the monitoring periods with and without PhAC addition attained 97.1% of success, reflecting a 94.1% accuracy for the samples with PhAC addition and 100.0% without. The parameters found to allow for the discrimination were the large granules contents, settling ability, small flocs contents and intermediate flocs irregularity.

Upon the analysis of the DT results, and comparing with the DA analysis, the use of the filamentous bacteria contents, small granules fraction, settling ability and small flocs contents for discriminating between the different PhAC experiments and/or the presence or absence of PhAC becomes reinforced. The partial DT analysis identified the granular dataset as allowing for the best overall identification, with full identification of the operational periods except for the EE2 period and of the samples without PhAC addition. In contrast, the floccular dataset allowed for a full identification of the EE2 period.

The obtained results proved that QIA, coupled to chemometric tools, is suitable for AGS systems monitoring in the presence of E2, EE2 and SMX, clearly illustrating the advantage of employing these techniques in full-scale WWTP and contributing to the process management and optimization.

Chapter 7 – Final conclusions and suggestions

7.1. Conclusions

The stability of AGS systems is dependent on the balance between the suspended (floccular) and granular sludge fractions. Taking this into consideration it seems imperative that an analysis on the relevance of both fractions in the studied SBR-AGS systems is envisaged. For that purpose, a QIA methodology, based on the SBR-AGS biomass sampling, microscopy monitoring, and image acquisition and processing, was employed given its advantage in terms of speed, objectiveness and quantitative analysis. To that effect, a new methodology for AGS sampling, and biomass fractions separation, was proposed and validated for the proposed QIA assessment, both in the absence and in the presence of PhACs (E2, EE2 and SMX). The compliance of the sample volumes, the fraction sieving methodology and the triplicates acquisition procedure could be corroborated for AGS characterization purposes.

In accordance, the granular and suspended (floccular) biomass fractions were monitored in all experiments, which led to the determination of a predominant granular biomass fraction, throughout the monitoring period of all experiments (both with and without PhAC addition). Furthermore, it could be determined a clear predominance of the large granules (above 2.5 mm in diameter) followed by the intermediate granules (diameter from 0.25 to 2.5 mm), presenting a robust and stable structure with good settling abilities. Regarding the floccular biomass, it could be established a predominance of the intermediate flocs (diameter from 25 to 250 μm) throughout the entire monitoring period, followed by the large flocs (above 250 μm in diameter). The organic fraction predominated over the inorganic counterpart and no evidence of bulking events was detected by monitoring the SVI, nor inferred by the filamentous bacteria contents within the reactor.

The addition of the studied PhACs to the SBR-AGS system, presented better performances in removing the organic matter than the inorganic. Indeed, a more pronounced effect could be established for both the TIN (especially regarding the SMX) and TP (quite poor during all experiments) removal efficiencies. Both estrogens, led to a small decrease in the settling ability, accompanied by a small decrease in the aggregates' density, by the end of the experiment, although presenting still good settling properties. On the contrary, the SMX experiment led to an increase on the sludge density, while maintaining a high settling ability. For all PhACs experiments, the granular fraction clearly predominated, though the E2 experiment seemed to cause a small decrease in that respect towards the end of the experiment. As already stated, the large granules clearly predominated (with the SMX experiment presenting the larger ones), with the small granules (below 0.25 mm in diameter) being

negligible. Regarding the floccular biomass, the large flocs predominated (followed by the intermediate ones) and no filamentous (or otherwise) bulking evidence was detected.

The PCA allowed to isolate the different operational periods (CONT, E2, EE2 and SMX), with the E2 experiment being the most far apart, related to the high flocs contents and overall flocs regularity. On the other hand, the EE2 and SMX were the two closest groups, which can be explained by the high biomass granular contents, with the main differences being the SMX higher granules apparent density and sludge settling ability. A positive relationship was found between the biomass density, sludge settling ability, overall and granular biomass contents, biomass stability properties, granular biomass fraction and large granules fraction and size. Interestingly, the floccular biomass showed an opposing trend towards the filamentous bacteria contents. The granular fraction was found crucial to characterize the different operational periods, though the physicochemical data was paramount to separate the mature AGS period and the floccular fraction data to separate the E2 period.

The use of a MLR technique further allowed to model the prediction of the biomass contents (both in terms of the granular and floccular fractions), density and settling ability (in terms of the SVI_5) based on the AGS ensemble (floccular and granular) morphological and structural parameters for mature granules and in the presence of the studied PhAC. Reasonable to good coefficients of determination were obtained for the floccular fraction VSS (0.948) and TSS (0.922), granular fraction VSS (0.927) and TSS (0.915), biomass density (0.886 by TSS and 0.861 by VSS) and SVI_5 (0.990 by the use of the biomass density dataset and 0.962 by the use of the mature AGS dataset). The analysis of the sludge parameters influencing the most the obtained models allowed to further reinforce the conclusions windthrown by the PCA.

The DA both using the biomass density or the mature AGS datasets revealed a successful identification (recognition percentage of 100%) of the mature AGS (when applicable), E2, EE2 and SMX operational periods samples, by the use of the flocs apparent density, granules stratification and contents. The inclusion of the biomass density allowed for a slightly higher discrimination ability (96%) between the operational days with and without PhAC addition. Overall, the most important variables were found to be related to the filamentous bacteria contents, sludge settling ability and stability, granules regularity, stratification and contents and flocs contents. The use of the sludge physicochemical data allowed for a nearly perfect identification of the mature granules and E2 operational periods, whereas the use of the granular biomass data allowed for the best distinction between the EE2 and SMX periods. With respect to the identification of the samples with, or without, PhAC addition, the floccular biomass data allowed for the best results.

The results of the DT allowed to fully identify the different PhACs (and mature AGS) operational periods, by the use of the filamentous bacteria contents, settling ability and small granules fraction. Moreover, the discrimination of the monitoring periods with or without PhAC addition attained 97.1% of success. In this case, the settling ability, granules and flocs contents, and flocs regularity parameters were found important for identification. The obtained DT results, reinforced the use of the filamentous bacteria contents, settling ability, granules stratification, and flocs contents for discriminating between the different PhAC operational periods and/or the presence or absence of PhAC addition, contributing to process optimization and management in the presence of the studied PhACs. The granular dataset allowed for the best overall identification, with full identification of the operational periods except for the EE2 period and of the samples without PhAC addition. In contrast, the floccular dataset allowed for a full identification of the EE2 period.

The application of QIA for sludge characterization is based on sample collection, microscopy survey, image acquisition and processing stages. In the current research work, the use of this methodology, coupled with chemometric tools for biomass contents, settling ability and density prediction in AGS, took around 4 h of man-work (in average) encompassing the sample collection and preparation, image acquisition and processing, and further extraction and treatment of the quantitative data. Thus, the application of such models can reduce the time of analysis when compared to traditional methods for VSS and TSS (reaching a constant dry weight usually takes quite longer than the 4 h of the presented methodology), and SVI and density determination (dependent on the TSS determination), contributing to the process optimization.

In this sense, the proposed QIA methodology, coupled to the use of CT, could be considered a valuable tool, in a daily basis operation of full-scale WWTP monitoring, for timely diagnosis of dysfunctions related to biomass' morphological features. Indeed, the obtained results in this work brought new insights on the effect of PhACs like E2, EE2 and SMX on the morphology and structure of AGS and may contribute to process optimization under dysfunctions caused by the presence of such substances.

7.2. Suggestions for future work

The main suggestions for future work include the study of: (i) strategies to avoid PhAC degradation in the feeding system, alternative (and more sensitive) analytical techniques for PhAC analytical determination and more effective control strategies; (ii) different operational strategies in SBR-AGS operation and use of alternative biological WWT systems in the presence of PhAC; (iii) the effect of

different PhAC (both standing alone and in mixture) in SBR-AGS systems and the adsorption and degradation processes impact; (iv) characterization and identification of the AGS microbial communities under PhAC presence, evaluation of the biomass Gram status and viability and assessment of toxicity, bioaccumulation and biomagnification potential in AGS biomass; (v) optimization strategies for the QIA methodology and extension of QIA and CT applications.

(i) Strategies to avoid PhAC degradation in the feeding system, alternative (and more sensitive) analytical techniques for PhAC analytical determination. In fact, this could be considered a critical issue regarding the PhAC monitoring purposes, especially regarding the concentrations lowest ranges of these compounds ($\mu\text{g L}^{-1}$ and ng L^{-1}). The use of more sensitive equipment (Liquid Chromatography coupled to Mass Spectrometry – LC-MS, etc.) on a regular basis could improve the monitoring ability, and consequently extend the knowledge about the studied compounds' behavior in AGS systems, including the analysis of metabolites and parent compounds. Also, the study of more effective control strategies for pH, redox potential and dissolved oxygen, among others, during the SBR cycles, would allow for a better performance regarding these WWT systems. Moreover, the operation in multiple reactors in parallel, for control purposes, could be another approach for assessing AGS systems.

(ii) Different operational strategies and configurations in SBR-AGS in the presence of PhAC and the study of alternative biological WWT systems is paramount. A large fraction of PhAC is very difficult to remove and combining different systems (Hybrid systems) could be relevant to address in further research. These combined systems could include activated carbon adsorption, membrane filtration and photocatalysis coupled to SBR-AGS.

(iii) The evaluation of different PhAC, both standing alone and in mixture, in SBR-AGS systems could also contribute for the scientific knowledge addressing the PhAC presence in WWT systems. In fact, studies encompassing PhAC mixtures, evaluating possible synergic effects and methodology validation, with real wastewater from full-scale WWTP with AGS systems (e.g., hospital or pharmaceutical industries wastewater) could be of interest. Furthermore, the study of the adsorption and degradation processes impact with respect to PhAC in AGS could increase the knowledge about the fate of these compounds, particularly in the biomass phase.

(iv) Further assessments in terms of molecular characterization and identification (Polymerase Chain Reaction – PCR techniques coupled to Fluorescent in situ Hybridization – FISH) of the AGS microbial communities, especially under stress caused by PhAC presence could bring new insights in AGS microbial assessment. Also, the evaluation of the granular biomass Gram status (positive, negative or variable) and viability, by QIA coupled to fluorescent staining and epifluorescence microscopy

monitoring and image acquisition could be useful to determine the contents of different bacteria groups present and understand their behavior when SBR-AGS are operated in the presence of PhAC. Further studies regarding the viability assessment of aerobic granules (e.g., Live Dead SYTO9 fluorescent staining) would be of interest in the context of PhAC presence in AGS. This should increase the knowledge on how PhAC selectively affect different bacteria within the granules. Furthermore, the use of toxicity tests for the AGS microbial community is paramount to increase the knowledge on the microorganisms' ability to sustain the presence of PhAC. Moreover, the bioaccumulation and biomagnification potential of these compounds through different trophic levels are crucial to understand the environmental impact of the discharge of PhAC containing treated wastewaters.

(v) The study of optimization strategies for the QIA methodology. Taking into consideration that the proposed methodology has been conducted for lab-scale biomass samples, further optimization studies should be considered for the application in pilot and full-scale AGS reactors. To that effect, further work should still be performed regarding both the sieving and sampling process, evaluating its adequateness to full-scale SBR-AGS biomass monitoring, alongside the continuous improvement and optimization of the QIA based methodology, assessing the robustness of the collected sample volume, number of monitored aggregates (both granular and floccular) and employed magnification (mainly regarding the granular biomass) in such systems. It is also expected that future applications of CT with QIA based AGS morphological and structural parameters could be used to estimate reactors performance in terms of COD, TIN and TP removal.

In a near future, it is also expectable that quantitative discharge limits and stringent legal requirements result from the extensive research in the PhACs field contributing for water resources management and sustainable development.

REFERENCES

- Ab Halim, M.H., Nor Anuar, A., Abdul, J.N.S., Azmi, S.I., Ujang, Z., and Bob, M.M. (2016) Influence of High Temperature on the Performance of Aerobic Granular Sludge in Biological Treatment of Wastewater. *Journal of Environmental Management* 184, 271–280.
- Abba, S.I., and Elkiran, G. (2017) Effluent Prediction of Chemical Oxygen Demand from the Wastewater Treatment Plant Using Artificial Neural Network Application. *Procedia Computer Science* 120, 156–163.
- Abreu, A.A., Costa J.C, Araya-Kroff, P., Ferreira E.C., and Alves M.M. (2007) Quantitative Image Analysis as a Diagnostic Tool for Identifying Structural Changes During a Revival Process of Anaerobic Granular Sludge. *Water Research* 41 (7), 1473–1480.
- Adav, S.S., Lee, D.J., and Lai, J.Y. (2010) Potential Cause of Aerobic Granular Sludge Breakdown at High Organic Loading Rates. *Applied Microbiology and Biotechnology* 85 (5), 1601–1610.
- Adeel, M., Song, X., Wang, Y., Francis, D., and Yang, Y. (2017) Environmental Impact of Estrogens on Human, Animal and Plant Life: A Critical Review. *Environment International* 99, 107–119.
- Afonso-Olivares, C., Sosa-Ferrera, Z., and Santana-Rodríguez. J.J. (2017) Occurrence and Environmental Impact of Pharmaceutical Residues from Conventional and Natural Wastewater Treatment Plants in Gran Canaria (Spain). *Science of the Total Environment* 599–600, 934–943.
- Ahmed, M.B., Zhou, J.L., Ngo, H.H., Guo, W., Thomaidis, N.S., and Xu, J. (2017) Progress in the Biological and Chemical Treatment Technologies for Emerging Contaminant Removal from Wastewater: A Critical Review. *Journal of Hazardous Materials* 323, 274–298.
- Amaral, A.L., C. Baptiste, C., Pons, M.N., Nicolau, A., Lima, N., Ferreira E.C., Mota M., and Vivier, H. (1999) Semi-Automated Recognition of Protozoa by Image Analysis. *Biotechnology Techniques* 13 (2), 111–118.
- Amaral, A.L., and Ferreira E.C. (2005) Activated Sludge Monitoring of a Wastewater Treatment Plant Using Image Analysis and Partial Least Squares Regression. *Analytica Chimica Acta* 544, 246–253.
- Amaral, A.L., Ginoris, Y.P., A. Nicolau, A., Coelho, M.A.Z., and Ferreira, E.C. (2008) Stalked Protozoa Identification by Image Analysis and Multivariable Statistical Techniques. *Analytical and*

Bioanalytical Chemistry 391 (4), 1321–1325.

Amaral, A.L., Da Motta, M., Pons, M.N., Vivier, H., Roche, N., Mota, M., and Ferreira, E.C. (2004) Survey of Protozoa and Metazoa Populations in Wastewater Treatment Plants by Image Analysis and Discriminant Analysis. *Environmetrics* 15 (4), 381–390.

Amaral, A.L., Leal, C.S., Vaz, A.I., Vieira, J.C., Quinteiro, A.C., Costa, M.L., and Castro, L.M. (2018) Use of Chemometric Analyses to Assess Biological Wastewater Treatment Plants by Protozoa and Metazoa Monitoring. *Environmental Monitoring and Assessment* 190 (497).

Amaral, A.L. (2003) Image Analysis in Biotechnological Processes: Applications to Wastewater Treatment. PhD Dissertation, University of Minho.

Amaral, A.L., Abreu, H., Leal, C., Mesquita, D.P., Castro, L.M. and Ferreira, E.C. (2017) Quantitative Image Analysis of Polyhydroxyalkanoates Inclusions from Microbial Mixed Cultures under Different SBR Operation Strategies. *Environmental Science and Pollution Research* 24 (17), 15148–15156.

Amaral, A.L., Mesquita, D.P., Ferreira, E.C. (2013) Automatic Identification of Activated Sludge Disturbances and Assessment of Operational Parameters. *Chemosphere* 91 (5), 705–710.

Amorim, C.L., Alves, M., Castro, P.M.L. and Henriques, I. (2018) Bacterial Community Dynamics within an Aerobic Granular Sludge Reactor Treating Wastewater Loaded with Pharmaceuticals. *Ecotoxicology and Environmental Safety* 147, 905–912.

Anderson, P.D., Johnson, A.C., Pfeiffer, D., Caldwell, D.J., Hannah, R., Mastrocco, F., Sumpter, J.P., and Williams, R.J. (2012) Endocrine Disruption Due to Estrogens Derived from Humans Predicted to Be Low in the Majority of U.S. Surface Waters. *Environmental Toxicology and Chemistry* 31(6), 1407-1415.

Andreozzi, R., Marotta, R., and Paxéus, N. (2003) Pharmaceuticals in STP Effluents and Their Solar Photodegradation in Aquatic Environment. *Chemosphere* 50 (10), 1319–1330.

Aqeel, H., Weissbrodt, D., Cerruti, M., Wolfaardt, G.M., Wilén, B.-M., and Liss, S.N. (2019) Drivers of Bioaggregation from Flocs to Biofilms and Granular Sludge. *Environmental Science Water Research & Technology* 5, 20172.

- Arcand-Hoy, L.D., and Benson, W.H. (1998) Fish Reproduction: An Ecologically Relevant Indicator of Endocrine Disruption. *Environmental Toxicology and Chemistry* 17 (1): 49–57.
- Asensi, E., Zambrano, D., Alemany E., and Aguado, D. (2019) Effect of the Addition of Precipitated Ferric Chloride on the Morphology and Settling Characteristics of Activated Sludge Flocs. *Separation and Purification Technology* 227, 115711.
- Aubertheau, E., Stalder, T., Mondamert, L., Ploy, M.C., Dagot, C., and Labanowski, J. (2017) Impact of Wastewater Treatment Plant Discharge on the Contamination of River Biofilms by Pharmaceuticals and Antibiotic Resistance. *Science of the Total Environment* 579, 1387–1398.
- Avberšek, M., Šömen, J., and Heath, E., (2011) Dynamics of Steroid Estrogen Daily Concentrations in Hospital Effluent and Connected Waste Water Treatment Plant. *Journal of Environmental Monitoring* 13 (8), 2221–2226.
- Avella, A.C., Görner, T., Yvon, J., Chappe, P., Guinot-Thomas, P., and de Donato, P. (2011) A Combined Approach for a Better Understanding of Wastewater Treatment Plants Operation: Statistical Analysis of Monitoring Database and Sludge Physico-Chemical Characterization. *Water Research* 45 (3), 981–992.
- Awang, N.A., and Shaaban, M.G. (2016) Effect of Reactor Height/Diameter Ratio and Organic Loading Rate on Formation of Aerobic Granular Sludge in Sewage Treatment. *International Biodeterioration and Biodegradation* 112, 1–11.
- Balest, L., Lopez, A., Mascolo, G., and Di Iaconi, C. (2008) Removal of Endocrine Disrupter Compounds from Municipal Wastewater Using an Aerobic Granular Biomass Reactor. *Biochemical Engineering Journal* 41 (3), 288–294.
- Baronti, C., Curini, R., D'Ascenzo, G., Di Corcia, A., Gentili, A., and Samperi, R. (2000) Monitoring Natural and Synthetic Estrogens at Activated Sludge Sewage Treatment Plants and in a Receiving River Water. *Environmental Science and Technology* 34 (24), 5059–5066.
- Bassin, J.P., Kleerebezem, R., Dezotti, M., and van Loosdrecht, M.C.M. (2012) Simultaneous Nitrogen and Phosphate Removal in Aerobic Granular Sludge Reactors Operated at Different Temperatures. *Water Research* 46 (12), 3805–3816.
- Batt, A.L., Kim, S., and Aga, D.S. (2007) Comparison of the Occurrence of Antibiotics in Four Full-Scale Wastewater Treatment Plants with Varying Designs and Operations. *Chemosphere* 68 (3), 428–

435.

- Bengtsson, S., de Blois, M., Wilén, B-M., and Gustavsson D. (2019) A Comparison of Aerobic Granular Sludge with Conventional and Compact Biological Treatment Technologies. *Environmental Technology* 40 (21), 2769–2778.
- Berg, L., Kirkland, C.M., Seymour, J.D., Codd, S.L., Van Loosdrecht, M.C.M., and de Kreuk, M.K. (2020) Heterogeneous Diffusion in Aerobic Granular Sludge. *Biotechnology and Bioengineering* 117 (12), 3809–3819.
- Besha, A.T., Gebreyohannes, A.Y., Tufa, R.A., Bekele, D.N., Curcio, E., and Giorno, L. (2017) Removal of Emerging Micropollutants by Activated Sludge Process and Membrane Bioreactors and the Effects of Micropollutants on Membrane Fouling: A Review. *Journal of Environmental Chemical Engineering*. 5(3), 2395–2414.
- Beun, J.J., Van Loosdrecht, M.C.M., and Heijnen, J.J. (2002) Aerobic Granulation in a Sequencing Batch Airlift Reactor. *Water Research* 36 (3), 702–712.
- Bila, D.M., and Dezotti, M. (2007) Desreguladores Endócrinos No Meio Ambiente: Efeitos e Consequências. *Química Nova* 30 (3), 651–666.
- BIO Intelligence Service. (2013) Study on the Environmental Risks of Medicinal Products, Final Report Prepared for Executive Agency for Health and Consumers.
- Birnbaum, L.S., and Fenton, S.E. (2003) Cancer and Developmental Exposure to Endocrine Disruptors. *Environmental Health Perspectives* 111 (4), 389–394.
- Bradley, J.V. (1968) *Distribution-Free Statistical Tests*. Prentice-H. Englewood Cliffs, NJ.
- Braga, O., Smythe, G.A., Schäfer, A.I., and Feitz, A.J. (2005) Fate of Steroid Estrogens in Australian Inland and Coastal Wastewater Treatment Plants. *Environmental Science and Technology* 39 (9), 3351–3358.
- Breiman, L., Friedman, J., Olshen R., Stone C. (1984) *Classification and Regression Trees*. Edited by Wadsworth. Belmont.
- Byliński, H., Sobiecki, A., and Gebicki, J. (2019) The Use of Artificial Neural Networks and Decision

- Trees to Predict the Degree of Odor Nuisance of Post-Digestion Sludge in the Sewage Treatment Plant Process. *Sustainability* 11 (16), 4407.
- Caldwell, D.J., Mastrocco, F., Anderson, P.D., Länge, R., and Sumpter, J.P. (2012) Predicted-No-Effect Concentrations for the Steroid Estrogens Estrone, 17 β -Estradiol, Estriol, and 17 α -Ethinylestradiol. *Environmental Toxicology and Chemistry* 31 (6), 1396–1406.
- Caluwé, M., Dobbeleers, T., D'aes, J., Miele, S., Akkermans, V., Daens, D., Geuens, L., Kiekens, F., Blust, R., and Dries, J. (2017) Formation of Aerobic Granular Sludge during the Treatment of Petrochemical Wastewater. *Bioresource Technology* 238, 559–567.
- Campbell, K., Wang, J., and Daigger, G.T. (2020) Filamentous Organisms Degrade Oxygen Transfer Efficiency by Increasing Mixed Liquor Apparent Viscosity: Mechanistic Understanding and Experimental Verification. *Water Research* 173, 115570.
- Campbell, K., Wang, J., and Daniels, M. (2019) Assessing Activated Sludge Morphology and Oxygen Transfer Performance Using Image Analysis. *Chemosphere* 223: 694–703.
- Campo, R., Sguanci, S., Caffaz, S., Mazzoli, L., Ramazzotti, M., Claudio Lubello, C., and Lotti, T. (2020) Efficient Carbon, Nitrogen and Phosphorus Removal from Low C/N Real Domestic Wastewater with Aerobic Granular Sludge. *Bioresource Technology* 305, 122961.
- Carabin, A., Drogui, P., and Robert, D. (2015) Photo-Degradation of Carbamazepine Using TiO₂ Suspended Photocatalysts. *Journal of the Taiwan Institute of Chemical Engineers* 54, 109–117.
- Carrera, P., Mosquera-Corral, A., Méndez, A.R., Campos, J.L., and Val del Rio, A. (2019) Pulsed Aeration Enhances Aerobic Granular Biomass Properties. *Biochemical Engineering Journal* 149, 107244.
- Carroll, S. P., Dawes, L., Hargreaves, M., and Goonetilleke, A. (2009) Faecal Pollution Source Identification in an Urbanising Catchment Using Antibiotic Resistance Profiling, Discriminant Analysis and Partial Least Squares Regression. *Water Research* 43 (5), 1237–1246.
- Castellanos, R.M., Dias, J.M.R., Bassin, I.D., Márcia Dezotti, M., and Bassin, J.P. (2021) Effect of Sludge Age on Aerobic Granular Sludge: Addressing Nutrient Removal Performance and Biomass Stability. *Process Safety and Environmental Protection* 149, 212–222.

- Kirkland, C. M., Krug, J.R., Vergeldt, F.K., van den Berg, L., Van As Aldrik H., Velders, H., Seymour, J.D., Codd, S.L., de Kreuk, M.K. (2020) Characterizing the Structure of Aerobic Granular Sludge Using Ultra-High Field Magnetic Resonance. *Water Sci. Technol* 82 (4), 627–639.
- Cavallucci, S. (2007) What's Topping the Charts in Prescription Drugs This Year? *Pharmacy Practice* 23 (12), 25–32.
- Chen, Q.-Q., Wu, W.-D., Zhang, Z.-Z., Xu, J.-J. and Jin, R.-C. (2017) Inhibitory Effects of Sulfamethoxazole on Denitrifying Granule Properties: Short- and Long-Term Tests. *Bioresource Technology* 233, 391–398.
- Cheng, Y., Xuan, X., Zhang, L., Zhao, J., and Long, B. (2018) Storage of Aerobic Granular Sludge Embedded in Agar and Its Reactivation by Real Wastewater. *Journal of Water and Health* 16 (6), 958–969.
- Choerudin, C., Harimawan, A., and Setiadi, T. (2018) The Comparison of Different Nutrient Sources in Development of Aerobic Granular Sludge. *MATEC Web of Conferences* 156, 1–6.
- Choquet-Kastylevsky, G., Vial, T., and Descotes, J. (2002) Allergic Adverse Reactions to Sulfonamides. *Current Allergy and Asthma Reports* 2 (1), 16–25.
- Coleman, H.M., Abdullah, M.I., Eggins, B.R., and Palmer, F.L. (2005) Photocatalytic Degradation of 17 β -Oestradiol, Oestriol and 17 α -Ethinylloestradiol in Water Monitored Using Fluorescence Spectroscopy. *Applied Catalysis B: Environmental* 55 (1), 23–30.
- Combalbert, S., and Hernandez-Raquet, G. (2010) Occurrence, Fate, and Biodegradation of Estrogens in Sewage and Manure. *Applied Microbiology and Biotechnology* 86 (6), 1671–1692.
- Corsino, S.F., Campo, R., Di Bella, G., Torregrossa, M., and Viviani, G. (2015) Cultivation of Granular Sludge with Hypersaline Oily Wastewater. *International Biodeterioration and Biodegradation* 105, 192–202.
- Corsino, S.F., Campo, R., Di Bella, G., Torregrossa, M., and Viviani, G. (2018) Aerobic Granular Sludge Treating Shipboard Slop: Analysis of Total Petroleum Hydrocarbons Loading Rates on Performances and Stability. *Process Biochemistry* 65, 164–171.
- Corsino, S.F., Campo, R., Di Bella, G., Torregrossa, M., and Viviani, G. (2016). Fate of Aerobic Granular

- Sludge in the Long-Term: The Role of EPSs on the Clogging of Granular Sludge Porosity. *Journal of Environmental Management* 183. 543–550.
- Costa, J.C., Alves, M.M., and Ferreira, E.C. (2009a) Principal Component Analysis and Quantitative Image Analysis to Predict Effects of Toxics in Anaerobic Granular Sludge. *Bioresource Technology* 100 (3), 1180–1185.
- Costa, J.C., Alves, M.M., and Ferreira, E.C. (2010) A Chemometric Tool to Monitor High-Rate Anaerobic Granular Sludge Reactors during Load and Toxic Disturbances. *Biochemical Engineering Journal* 53 (1), 38–43.
- Costa, J.C., Moita, I., Ferreira, E.C., and Alves, M.M. (2009b). Morphology and Physiology of Anaerobic Granular Sludge Exposed to an Organic Solvent. *Journal of Hazardous Materials* 167 (1–3), 393–398.
- Cripe, G.M, Hemmer, B.L., Goodman L.R., Fournie, J.W., Raimondo, S., Vennari, J.C., Danner R.L., Smith, K., Manfredonia, B.R., Kulaw, D.H., Hemmer, M.J. (2009) Multigenerational Exposure of the Estuarine Sheepshead Minnow (*Cyprinodon Variegatus*) to 17 β -Estradiol. I. Organism-Level Effects Over Three Generations. *Environmental Toxicology and Chemistry* 28 (11), 2397–2401.
- Cui, C.W., Ji, S.L., and Ren, H.Y. (2006) Determination of Steroid Estrogens in Wastewater Treatment Plant of a Contraceptives Producing Factory. *Environmental Monitoring and Assessment* 121 (1–3), 407–417.
- Cydzik-Kwiatkowska, A., Bernat, K., Zielińska, M., Bułkowska, K., and Wojnowska-Baryła, I. (2017) Aerobic Granular Sludge for Bisphenol A (BPA) Removal from Wastewater. *International Biodeterioration & Biodegradation* 122, 1–11.
- Cydzik-Kwiatkowska, A., Podlasek, M., Nosek, D., and Jaskulska, B. (2018) Treatment Efficiency and Characteristics of Biomass in a Full-Scale Wastewater Treatment Plant with Aerobic Granular Sludge. *Journal of Ecological Engineering* 19 (4): 95–102.
- Cydzik-Kwiatkowska, A., Wojnowska-Baryła, I., Szatkowski, M., and Smoczyński, L. (2013) Biochemical Conversions and Biomass Morphology in a Long-Term Operated SBR with Aerobic Granular Sludge. *Desalination and Water Treatment* 51 (10–12), 2261–2268.
- Czarnota, J., Masłoń, A., Zdeb, M., and Łagód, G. (2020) The Impact of Different Powdered Mineral

- Materials on Selected Properties of Aerobic Granular Sludge. *Molecules* 25 (2), 386.
- D'Ascenzo, G., Antonio Di Corcia, A., Gentili, A., Mancini, R., Mastropasqua, R., Nazzari, M., and Samperi, R. (2003) Fate of Natural Estrogen Conjugates in Municipal Sewage Transport and Treatment Facilities. *Science of the Total Environment* 302 (1–3), 199–209.
- Dahalan, F.A., Abdullah, N., Yuzir, A., Olsson, G., Salmiati, Hamdzah, M., Din, M.F.M., Ahmad, S.A., Khalil, K.A., Nor Anuar, A., Noor, Z.Z., and Ujang, Z. (2015) A Proposed Aerobic Granules Size Development Scheme for Aerobic Granulation Process. *Bioresource Technology* 181, 291–296.
- Danner, M.C., Robertson, A., Behrends, V., and Reiss, J. (2019) Antibiotic Pollution in Surface Fresh Waters: Occurrence and Effects. *Science of the Total Environment* 664, 793–804.
- Daston, G. P., Gooch, J.W., Breslin, W.J., Shuey, D.L., Nikiforov, A.I., Fico, T.A., and Gorsuch, J.W. (1997) Environmental Estrogens and Reproductive Health: A Discussion of the Human and Environmental Data. *Reproductive Toxicology* 11 (4), 465–481.
- Deepnarain, N., Nasr, M., Kumari, S., Stenström, T.A., Reddy, P., Pillay, K., and Bux, F. (2019) Decision Tree for Identification and Prediction of Filamentous Bulking at Full-Scale Activated Sludge Wastewater Treatment Plant. *Process Safety and Environmental Protection* 126, 25–34.
- Drugbank. 2016a. The Drugbank Database. Estradiol. 2016. <https://www.drugbank.ca/%0A drugs/DB00783> [visited at 12/02/2016].
- Drugbank. 2016b. The Drugbank Database. Ethinyl Estradiol. 2016. <https://www.drugbank.ca/drugs/DB00977> [visited at 12/02/2016].
- Ebrahimi, M., Gerber, E.L., and Rockaway, T.D. (2017) Temporal Performance Assessment of Wastewater Treatment Plants by Using Multivariate Statistical Analysis. *Journal of Environmental Management* 193, 234–246.
- Einax J.W., Zwanziger, H.W., and Geiss, S. (1997) *Chemometrics in Environmental Analysis*. Edited by VCH Verlagsgesellschaft. Weinheim.
- Estrada-Arriaga, E.B., Cortés-Muñoz, J.E., González-Herrera, A., Calderón-Mólgora, C.G., Rivera-Huerta, M. de L., Ramírez-Camperos, E., Montellano-Palacios, L., Gelover-Santiago, S.L., Pérez-Castrejón, S., Cardoso-Vigueros L., Martín-Domínguez, A., and García-Sánchez, L. (2016). Assessment of

- Full-Scale Biological Nutrient Removal Systems Upgraded with Physico-Chemical Processes for the Removal of Emerging Pollutants Present in Wastewaters from Mexico. *Science of the Total Environment* 571, 1172–1182.
- Etterer, T., and Wilderer, P.A. (2001) Generation and Properties of Aerobic Granular Sludge. *Water Science and Technology* 43, 19–26.
- Fan, W., Yuan, J.L., and Li, Y. (2019) CFD Simulation of Flow Pattern in a Bubble Column Reactor for Forming Aerobic Granules and Its Development. *Environmental Technology* 40 (27), 3652–3667.
- Farooqi, I. H., and Basheer, F. (2017) Treatment of Adsorbable Organic Halide (AOX) from Pulp and Paper Industry Wastewater Using Aerobic Granules in Pilot Scale SBR. *Journal of Water Process Engineering* 19, 60–66.
- Fearn, T. (2002) Assessing Calibrations: SEP, RPD, RER and R2. *NIR News* 13 (6), 12–13.
- Ferreira, V.R .A., Amorim, C.L., Cravo, S.M., Tiritan, M.E., Castro, P.M.L. and Afonso. C.M.M. (2016) Fluoroquinolones Biosorption onto Microbial Biomass: Activated Sludge and Aerobic Granular Sludge. *International Biodeterioration and Biodegradation* 110, 53–60.
- Figuerola, M., Mosquera-Corral, A, Campos, J.L, Mendéz, R. (2008) Treatment of Saline Wastewater in SBR Aerobic Granular Reactors. *Water Sci Technol* 58 (2), 479–485.
- Flores-Alsina, X., Gallego, A., Feijoo, G., and Rodriguez-Roda, I. (2010) Multiple-Objective Evaluation of Wastewater Treatment Plant Control Alternatives. *Journal of Environmental Management* 91 (5), 1193–1201.
- Fonseca, A. P., Cardoso, M., Esteves, V. (2013) Determination of Estrogens in Raw and Treated Wastewater by High-Performance Liquid Chromatography-Ultraviolet Detection. *Journal of Environmental & Analytical Toxicology* 04 (01), 1–5.
- Franca, R.D.G., Pinheiro, H.M., van Loosdrecht, M.C.M., and Lourenço, N.D. (2018) Stability of Aerobic Granules during Long-Term Bioreactor Operation. *Biotechnology Advances* 36 (1), 228–246.
- Franca, R.D.G., Vieira, A., Mata, A.M.T., Carvalho, G.S., Pinheiro, H.M., Lourenço. N.D. (2015) Effect of an Azo Dye on the Performance of an Aerobic Granular Sludge Sequencing Batch Reactor Treating a Simulated Textile Wastewater. *Water Research* 85, 327–336.

- Gao, D., Liu, L., Liang, H., and Wu, W.M. (2011) Aerobic Granular Sludge: Characterization, Mechanism of Granulation and Application to Wastewater Treatment. *Critical Reviews in Biotechnology* 31 (2), 137–152.
- Gao, P., Mao, D., Luo, Y., Wang, L., Xu, B., and Xu, L. (2012) Occurrence of Sulfonamide and Tetracycline-Resistant Bacteria and Resistance Genes in Aquaculture Environment. *Water Research* 46 (7), 2355–2364.
- Gao, S., He, Q., and Wang, H. (2020) Research on the Aerobic Granular Sludge under Alkalinity in Sequencing Batch Reactors: Removal Efficiency, Metagenomic and Key Microbes. *Bioresour. Technology* 296, 122280.
- Garcia-Alvarez, D., Fuente, M.J., Vega, P., and Sainz, G. (2009) Fault Detection and Diagnosis Using Multivariate Statistical Techniques in a Wastewater Treatment Plant *IFAC Proceedings Volumes*. Vol. 42. IFAC.
- Geissen, V., Mol, H., Klumpp, E., Umlauf, G., Nadal, M., vander Ploeg M, van de Zee S.E.A.T.M., and Ritsema, C.J. (2015). Emerging Pollutants in the Environment: A Challenge for Water Resource Management. *International Soil and Water Conservation Research* 3 (1), 57–65.
- Ginoris, Y.P., Amaral, A.L., Nicolau, A., Coelho, M.A.Z., and Ferreira, E.C. (2007a) Raw Data Pre-Processing in the Protozoa and Metazoa Identification by Image Analysis and Multivariate Statistical Techniques. *Journal of Chemometrics* 21, 156–164.
- Ginoris, Y.P., Amaral, A.L., Nicolau, A., Coelho, M.A.Z., and Ferreira, E.C. (2007b) Development of an Image Analysis Procedure for Identifying Protozoa and Metazoa Typical of Activated Sludge System. *Water Research* 41 (12): 2581–2589.
- Ginoris, Y.P., Amaral, A.L., Nicolau, A., Coelho, M.A.Z., and Ferreira, E.C. (2007c) Recognition of Protozoa and Metazoa Using Image Analysis Tools, Discriminant Analysis, Neural Networks and Decision Trees. *Analytica Chimica Acta* 595 (1-2), 160–169.
- Göbel, A., McArdell, C.S., Joss, A., Siegrist, H., and Giger, W. (2007) Fate of Sulfonamides, Macrolides, and Trimethoprim in Different Wastewater Treatment Technologies. *Science of the Total Environment* 372 (2–3), 361–371.
- Göbel, A., Thomsen, A., McArdell, C.S., Joss, A., and Giger, W. (2005) Occurrence and Sorption Behavior of Sulfonamides, Macrolides, and Trimethoprim in Activated Sludge Treatment.

Environmental Science and Technology 39 (11), 3981–3989.

Gong, H. (2018) Artificial Neural Network Modeling for Organic and Total Nitrogen Removal of Aerobic Granulation. Master dissertation, University of Calgary.

de Graaff, D.R., van Dijk, E.J.H., van Loosdrecht, M.C.M., and Pronk, M. (2018) Strength Characterization of Full-Scale Aerobic Granular Sludge. *Environmental Technology* 41(13), 1–11.

de Graaff, M.S., Vieno, N.M., Kujawa-Roeleveld, K., Zeeman, G., Temmink, H., and Buisman, C.J.N. (2011) Fate of Hormones and Pharmaceuticals during Combined Anaerobic Treatment and Nitrogen Removal by Partial Nitrification-Anammox in Vacuum Collected Black Water. *Water Research* 45 (1), 375–383.

Grandclément, C., Seyssiecq, I., Piram, A., Wong-Wah-Chung, P., Vanot, G., Tiliacos, N., and Roche Doumenq, N. (2017). From the Conventional Biological Wastewater Treatment to Hybrid Processes, the Evaluation of Organic Micropollutant Removal: A Review. *Water Research*, 297–317.

Gray, L.E. (1998) Xenoendocrine Disrupters: Laboratory Studies on Male Reproductive Effects. *Toxicology Letters* 102–103, 331–335.

Grijpspeerdt, K., and Verstraete, W. (1997) Image Analysis to Estimate the Settleability and Concentration of Activated Sludge. *Water Research* 31 (5), 1126–1134.

Guo, T., Ji, Y., Zhao, J., Horn, H., Li, J. (2020) Coupling of Fe-C and Aerobic Granular Sludge to Treat Refractory Wastewater from a Membrane Manufacturer in a Pilot-Scale System. *Water Research* 186, 116331.

Haaksman, V A, Mirghorayshi, M., Van Loosdrecht, M.C.M., and Pronk, M. (2020) Impact of Aerobic Availability of Readily Biodegradable COD on Morphological Stability of Aerobic Granular Sludge. *Water Research*, 187, 116402.

Hamscher, G., Pawelzick, H.T., Sczesny, S., Nau, H., and Hartung, J. (2003). Antibiotics in Dust Originating from a Pig-Fattening Farm: A New Source of Health Hazard for Farmers? *Environmental Health Perspectives* 111 (13), 1590–1594.

He, Q., Wang, H., Chen, L., Gao, S., Zhang, W., Song, J., and Yu, J. (2020) Elevated Salinity

- Deteriorated Enhanced Biological Phosphorus Removal in an Aerobic Granular Sludge Sequencing Batch Reactor Performing Simultaneous Nitrification, Denitrification and Phosphorus Removal. *Journal of Hazardous Materials* 390, 121782.
- He, Q., Xie, Z., Fu, Z., Wang, M., Xu, P., Yu, J., Ma, J., Gao, S., Chen, L., Zhang, W., Song, J., and Wang H. (2021) Interaction and Removal of Oxytetracycline with Aerobic Granular Sludge. *Bioresource Technology* 320 124358.
- Hirsch, R., Ternes, T., Haberer, K., and Kratz, K.L. (1999) Occurrence of Antibiotics in the Aquatic Environment. *Science of the Total Environment* 225 (1–2), 109–118.
- Hjorth, N., and Roed-Petersen, J. (1980) Allergic Contact Dermatitis in Veterinary Surgeons. *Contact Dermatitis* 6 (1), 27–29.
- Hruska, K., Franek, M. (2012) Sulfonamides in the Environment: A Review and a Case Report. *Veterinarni Medicina* 57 (1), 1–35.
- Huang, P., Mukherji, S.T., Wu, S., Muller, J., and Goel, R. (2016) Fate of 17 β -Estradiol as a Model Estrogen in Source Separated Urine during Integrated Chemical P Recovery and Treatment Using Partial Nitritation-Anammox Process. *Water Research* 103, 500–509.
- Huang, Q., Bu, Q., Zhong, W., Shi, K., Cao, Z., Yu, G. (2018) Derivation of Aquatic Predicted No-Effect Concentration (PNEC) for Ibuprofen and Sulfamethoxazole Based on Various Toxicity Endpoints and the Associated Risks. *Chemosphere* 193, 223–229.
- Isanta, E., Suárez-Ojeda, M.E., Val del Río, A., Morales, N., Pérez, J., and Carrera, J. (2012) Long Term Operation of a Granular Sequencing Batch Reactor at Pilot Scale Treating a Low-Strength Wastewater. *Chemical Engineering Journal* 198–199: 163–170.
- IWW. (2014) Pharmaceuticals in the Environment: Occurrence, Effects, and Options for Action. Research Project Funded by the German Federal Environment Agency (UBA) within the Environmental Research Plan No. 3712 65 408.
- Jahn, L., Saracevic, E., Svoldal, K., and Krampe, J. (2019) Anaerobic Biodegradation and Dewaterability of Aerobic Granular Sludge. *Journal of Chemical Technology and Biotechnology* 94 (9), 2908–2916.

- Jang, A., Yoon, Y.H., Kim, I.S., Kim, K.S., and Bishop, P.L. (2003) Characterization and Evaluation of Aerobic Granules in Sequencing Batch Reactor. *Journal of Biotechnology* 105 (1–2), 71–82.
- Jemaat, Z., Suárez-Ojeda, M.E., Pérez, J., and Carrera, J. (2013) Simultaneous Nitritation and P-Nitrophenol Removal Using Aerobic Granular Biomass in a Continuous Airlift Reactor. *Bioresource Technology* 150, 307–313.
- Jenné, R., Banadda, E.N., Philips, N., and Van Impe, J.F. (2003) Image Analysis as a Monitoring Tool for Activated Sludge Properties in Lab-Scale Installations. *Journal of Environmental Science and Health* (10), 2009–2018.
- Gaffney, V.J., Cardoso, V.V., Cardoso, E., Teixeira, A.P., Martins, J., Benoliel M.J., and Almeida, C.M.M. (2017) Occurrence and behaviour of pharmaceutical compounds in a Portuguese wastewater treatment plant: Removal efficiency through conventional treatment processes. *Environmental Science and Pollution Research* 24 (17), 14717–14734.
- Jing-Feng, W., Zhi-Gang, Q., Zhi-Qiang, C., Jun-Wen, L., Yi-Hong, Z., Xuan, W., and Bin, Z. (2012) Comparison and Analysis of Membrane Fouling between Flocculent Sludge Membrane Bioreactor and Granular Sludge Membrane Bioreactor. *PLoS ONE* 7 (7), 1–7.
- Johnson, A.C., and Sumpter, J.P. (2001) Removal of Endocrine-Disrupting Chemicals in Activated Sludge Treatment Works. *Environmental Science & Technology* 35 (24), 4697–4703.
- Johnson, A.C., and Williams, R.J. (2004) A Model To Estimate Influent and Effluent Concentrations of Estradiol Sewage Treatment Works. *Environmental Science & Technology* 38 (13), 3649–3658.
- Joss, A., Andersen, H., Ternes, T., Richle, P.R., and Siegrist, H. (2004) Removal of Estrogens in Municipal Wastewater Treatment under Aerobic and Anaerobic Conditions: Consequences for Plant Optimization. *Environmental Science and Technology* 38 (11), 3047–3055.
- Joss, A., Zabczynski, S., Göbel, A., Hoffmann, B., Löffler, D., Mcardell, C.S., Ternes, T.A., Thomsen, A., and Siegrist, H. (2006). Biological Degradation of Pharmaceuticals in Municipal Wastewater Treatment: Proposing a Classification Scheme. *Water Research* 40 (8), 1686–1696.
- Jun, B. H. (2011) Fault Detection Using Dynamic Time Warping (DTW) Algorithm and Discriminant Analysis for Swine Wastewater Treatment. *Journal of Hazardous Materials* 185 (1), 262–268.

- Kang, A.J., Brown, A.K., Wong, C.S., Huang, Z., and Yuan, Q. (2018a) Variation in Bacterial Community Structure of Aerobic Granular and Suspended Activated Sludge in the Presence of the Antibiotic Sulfamethoxazole. *Bioresource Technology* 261, 322–328.
- Kang, A.J., Brown, A.K., Wong, C.S., Huang, Z., and Yuan, Q. (2018b) Removal of Antibiotic Sulfamethoxazole by Anoxic/Anaerobic/Oxic Granular and Suspended Activated Sludge Processes. *Bioresource Technology* 251, 151–157.
- Kassotaki, E., Pijuan, M., Joss, A., Borrego, C.M., Rodriguez-Roda, I., and Buttiglieri, G. (2018) Unraveling the Potential of a Combined Nitritation-Anammox Biomass towards the Biodegradation of Pharmaceutically Active Compounds. *Science of the Total Environment* 624, 722–731.
- Katipoglu-Yazan, T., Merlin, C., Pons, M.N., Ubay-Cokgor, E., and Orhon, D. (2016) Chronic Impact of Sulfamethoxazole on the Metabolic Activity and Composition of Enriched Nitrifying Microbial Culture. *Water Research* 100: 546–555.
- Kent, J., and Tay, J.W. (2019) Treatment of 17 α -ethinylestradiol, 4-nonylphenol, and Carbamazepine in Wastewater Using an Aerobic Granular Sludge Sequencing Batch Reactor. *Science of the Total Environment* 652, 1270–1278.
- Khan, M.B., Nisar, H., and Aun, N.G. (2014) Segmentation Assessment of Activated Sludge Floccs for Wastewater Treatment. *2014 IEEE International Conference on Control System, Computing and Engineering, 28 - 30 November 2014, Penang, Malaysia Segmentation*, no. 06, 18–23.
- Khan, M.B., Nisar, H., and Aun, N.G., Lo, P.K., and Yap, V.V. (2018) Generalized Classification Modeling of Activated Sludge Process Based on Microscopic Image Analysis. *Environmental Technology* 39 (1), 24–34.
- Khanam, T., Syuhada W.N., Ata, W., Rashedi, A. (2016) Particle Size Measurement in Waste Water Influent and Effluent Using Particle Size Analyzer and Quantitative Image Analysis Technique. *Advanced Materials Research* 1133, 571–575.
- Kidd, K.A., Blanchfield, P.J., Mills, K. H.V., Palace, P., Evans, R.E., Lazorchak, J. M., and Flick, R.W. (2007) Collapse of a Fish Population after Exposure to a Synthetic Estrogen. *Proceedings of the National Academy of Sciences* 104 (21), 8897–8901.
- Kim, M., Guerra, P., Shah, A., Parsa, M., Alaei, M., and Smyth, S.A. (2014) Removal of Pharmaceuticals and Personal Care Products in a Membrane Bioreactor Wastewater Treatment

- Plant. *Water Science and Technology* 69 (11), 2221–2229.
- Kim, S.D., Cho, J., Kim, I.S., Vanderford, B.J., and Snyder, S.A. (2007) Occurrence and Removal of Pharmaceuticals and Endocrine Disruptors in South Korean Surface, Drinking, and Waste Waters. *Water Research* 41 (5), 1013–1021.
- Kim, Y. J., Choi, S. J., Bae, H., and Kim, C.W. (2011) Sludge Settleability Detection Using Automated SV30 Measurement and Its Application to a Field WWTP. *Water Science and Technology* 64 (8), 1743–1749.
- Kishida, N., Kono, A., Yutaka Yamashita, Y., and Tsuneda, S. (2010) Formation of Aerobic Granular Sludge in a Continuous-Flow Reactor - Control Strategy for the Selection of Well-Settling Granular Sludge *Journal of Water and Environment Technology* 8 (3), 251–258.
- Klein, E.Y., Van Boeckel, T.P., Martinez, E.M., Pant, S., Gandra, S., Simon A. Levin, S.A., Goossens, H., and Laxminarayan, R. (2018) Global Increase and Geographic Convergence in Antibiotic Consumption between 2000 and 2015. *Proceedings of the National Academy of Sciences of the United States of America* 115 (15), E 3463–470.
- Koba, O., Grabicova, K., Cervený, D., Turek, J., Kolarova, J., Randak, T., Zlabek, V., and Grabic, R. (2018) Transport of Pharmaceuticals and Their Metabolites between Water and Sediments as a Further Potential Exposure for Aquatic Organisms. *Journal of Hazardous Materials* 342, 401–407.
- Koczura, R., Mokracka, J., Taraszewska, A., and Lopacinska, N. (2016) Abundance of Class 1 Integron-Integrase and Sulfonamide Resistance Genes in River Water and Sediment Is Affected by Anthropogenic Pressure and Environmental Factors. *Microbial Ecology* 72 (4), 909–916.
- Koh, Y.K.K., Chiu, T.W., Boobis, A.R., Scrimshaw, M.D., Bagnall, J.P., Soares, A., Pollard, S., Cartmell, E., and Lester, J.N. (2009). Influence of Operating Parameters on the Biodegradation of Steroid Estrogens and Nonylphenolic Compounds during Biological Wastewater Treatment Processes. *Environmental Science & Technology* 43 (17), 6646–6654.
- Kolodziej, E.P., Harter, T., and Sedlak, D.L. (2004) Dairy Wastewater, Aquaculture, and Spawning Fish as Sources of Steroid Hormones in the Aquatic Environment. *Environmental Science and Technology* 38 (23), 6377–6384.
- Kolpin, D., Furlong, E., Meyer, M., Thurman, E., Zaugg, S., Barber, L., and Herbert, B. (2002) Pharmaceuticals, Hormones, and Other Organic Wastewater Contaminants in U.S. Streams,

- 1999-2000: A National Reconnaissance. *USGS Staff - Published Research*. 68.
<https://digitalcommons.unl.edu/usgsstaffpub/68>.
- Kotkar, V., and Gharde, S.S.(2013) Review of Various Image Contrast Enhancement. *International Journal of Innovative Research in Science, Engineering and Technology* 2 (7), 2786–2793.
- de Kreuk, M.K., Heijnen, J.J., and Van Loosdrecht, M.C.M. (2005) Simultaneous COD, Nitrogen, and Phosphate Removal by Aerobic Granular Sludge. *Biotechnology and Bioengineering* 90 (6), 761–769.
- Krzywinski, M., Altman, N. (2017) Classification and Regression Trees. *Nature Methods* 14, 757–758.
- Kümmerer, K. (2003) Significance of Antibiotics in the Environment. *Journal of Antimicrobial Chemotherapy* 52 (1), 5–7.
- Kwak, J., Khang, B., Kim, E., and Kim, H. (2013) Estimation of Biochemical Oxygen Demand Based on Dissolved Organic Carbon, UV Absorption, and Fluorescence Measurements. *Journal of Chemistry* Article ID 243769, 9 pages, 2013.
- Lang, L., Wan, J., Zhang, J., Wang, J., and Wang, Y. (2015) Interaction between Phosphorus Removal and Hybrid Granular Sludge Formation under Low Hydraulic Selection Pressure at Alternating Anaerobic/Aerobic Conditions. *Environmental Technology* 36 (21), 2746–2754.
- Lashkarizadeh, M. (2015) Operating pH and feed composition as factors affecting stability of aerobic granular sludge. Master Dissertation, University of Manitoba.
- Laurenson, J.P., Bloom, R.A., Page, S., and Sadrieh, N. (2014) Ethinyl Estradiol and Other Human Pharmaceutical Estrogens in the Aquatic Environment: A Review of Recent Risk Assessment Data. *The AAPS Journal* 16 (2), 299–310.
- Leal, C., Amaral, A.L., and Costa, M.L. (2016) Microbial-Based Evaluation of Foaming Events in Full-Scale Wastewater Treatment Plants by Microscopy Survey and Quantitative Image Analysis. *Environmental Science and Pollution Research* 23 (15), 15638–15650.
- Leal, C.S., Mesquita, D.P., Amaral, A.L., Amaral, A.M., and Ferreira, E.C. (2020a). Environmental Impact and Biological Removal Processes of Pharmaceutically Active Compounds: The Particular Case of Sulfonamides, Anticonvulsants and Steroid Estrogens. *Critical Reviews in Environmental*

Science and Technology 50 (7), 698–742.

- Leal, C., Val del Río, A., Mesquita, D.P., Amaral, A.L., Castro, P.M.L., and Ferreira, E.C. (2020b) Sludge Volume Index and Suspended Solids Estimation of Mature Aerobic Granular Sludge by Quantitative Image Analysis and Chemometric Tools. *Separation and Purification Technology* 234, 116049.
- Lee, S.P., Min, S.Y., Kim, J.S., Park, J.U., and Kim, M.S. (2014) A Study on the Influence of a Sewage Treatment Plant's Operational Parameters Using the Multiple Regression Analysis Model. *Environmental Engineering Research* 19 (1), 31–36.
- Lemaire, R., Webb, R.I., and Yuan, Z. (2008) Micro-Scale Observations of the Structure of Aerobic Microbial Granules Used for the Treatment of Nutrient-Rich Industrial Wastewater. *ISME Journal* 2 (5), 528–541.
- Leung, H.W., Jin, L., Wei, S., Tsui, M.M.P., Zhou, B., Jiao, L., Cheung, P.C., Chun, Y.K., Murphy, M.B., and Lam, P.K.S. (2013) Pharmaceuticals in Tap Water: Human Health Risk Assessment and Proposed Monitoring Framework in China. *Environmental Health Perspectives* 121 (7), 839–846.
- Li, J., Cai, A., Wang, D., Chen, C., and Ni, Y. (2014) Structure Analysis of Aerobic Granule from a Sequencing Batch Reactor for Organic Matter and Ammonia Nitrogen Removal. *International Journal of Environmental Research and Public Health* 11 (3), 2427–2436.
- Li, Z. H., Kuba, T., and Kusuda, T. (2006) Selective Force and Mature Phase Affect the Stability of Aerobic Granule: An Experimental Study by Applying Different Removal Methods of Sludge. *Enzyme and Microbial Technology* 39 (5), 976–981.
- Li, Z.-H., Zhu, Y.-M., Zhang, Y.-L., Zhang, Y.-R., and He, C.-B., and Yang, C.-J. (2019) Characterization of Aerobic Granular Sludge of Different Sizes for Nitrogen and Phosphorus Removal. *Environmental Technology* 40(27), 3622–3631.
- Liao, J., Liu, C., Liu, L., Li, J., Fan, H., Ye, J., and Zeng, Z. (2019) Influence of Hydraulic Retention Time on Behavior of Antibiotics and Antibiotic Resistance Genes in Aerobic Granular Reactor Treating Biogas Slurry. *Frontiers of Environmental Science and Engineering* 13 (3), 1–9.
- Lin, T., Chen, Y., and Chen, W. (2013) Impact of Toxicological Properties of Sulfonamides on the Growth of Zebrafish Embryos in the Water. *Environmental Toxicology and Pharmacology* 36 (3), 1068–1076.

- Lipman, A.G. (1993) *Martindale – the Extra Pharmacopoeia*. Edited by JEF Reynolds. 30th ed. London: The Pharmaceutical Press.
- Liu, F., Ying, G.-G., Tao, R., Zhao, J.-L., Yang, J.-F., and Zhao, L.-F. (2009) Effects of Six Selected Antibiotics on Plant Growth and Soil Microbial and Enzymatic Activities. *Environmental Pollution* 157 (5), 1636–1642.
- Liu, H., Xiao, H., Huang, S., Ma, H., and Liu, H. (2014) Aerobic Granules Cultivated and Operated in Continuous-Flow Bioreactor under Particle-Size Selective Pressure. *Journal of Environmental Sciences* 26 (11), 2215–2221.
- Liu, L., You, Q., Fan, H., Huang, X., Wei, L., and Liu, C. (2019) Behavior of Antibiotics and Antibiotic Resistance Genes in Aerobic Granular Reactors: Interrelation with Biomass Concentration. *International Biodeterioration and Biodegradation* 139, 18–23.
- Liu, S., Zhan, H., Xie, Y., Shi, W., and Wang, S. (2017) Rapid Cultivation of Aerobic Granular Sludge by Xanthan Gum in SBR Reactors. *Water Science and Technology* 2017 (2), 360–369.
- Liu, Y.Q., and Tay, J.H. (2007) Characteristics and Stability of Aerobic Granules Cultivated with Different Starvation Time. *Applied Microbiology and Biotechnology* 75 (1), 205–210.
- Liu, Y.Q., and Tay, J.H., and Moy, B.Y.P. (2006) Characteristics of Aerobic Granular Sludge in a Sequencing Batch Reactor with Variable Aeration. *Applied Microbiology and Biotechnology* 71 (5), 761–766.
- Liawska-Bizukojc, E., Klepacz-Smółka, A., and Andrzejczak, O. (2014) Variations of Morphology of Activated Sludge Flocs Studied at Full-Scale Wastewater Treatment Plants. *Environmental Technology* 36 (9–12), 1123–1131.
- Long, B., Xuan, X., Yang, C., Zhang, L., Cheng, Y., and Wang, J. (2019) Stability of Aerobic Granular Sludge in a Pilot Scale Sequencing Batch Reactor Enhanced by Granular Particle Size Control. *Chemosphere* 225, 460–469.
- Luo, Y., Mao, D., Rysz, M., Zhou, Q., Zhang, H., Xu, L., and Alvarez, P.J.J. (2010) Trends in Antibiotic Resistance Genes Occurrence in the Haihe River, China. *Environmental Science and Technology* 44 (19), 7220–7225.

- Madureira, T.V., Rocha, M.J., Cruzeiro, C., Rodrigues, I., Monteiro, R.A.F., and Rocha, E. (2012) The Toxicity Potential of Pharmaceuticals Found in the Douro River Estuary (Portugal): Evaluation of Impacts on Fish Liver, by Histopathology, Stereology, Vitellogenin and CYP1A Immunohistochemistry, after Sub-Acute Exposures of the Zebrafish Model. *Environmental Toxicology and Pharmacology* 34 (1), 34–45.
- Majewsky, M., Wagner, D., Delay, M., Bräse, S., Yargeau, V., and Horn, H. (2014) Antibacterial Activity of Sulfamethoxazole Transformation Products (TPs): General Relevance for Sulfonamide TPs Modified at the Para Position. *Chemical Research in Toxicology* 27 (10), 1821–1828.
- Manas, A., Sperandio, M., Decker, F., Biscans, B. (2012) Location and Chemical Composition of Microbially Induced Phosphorus Precipitates in Anaerobic and Aerobic Granular Sludge *Environmental Technology*, 33(19), 2195-2209.
- Manickum, T., and John. W. (2014) Occurrence, Fate and Environmental Risk Assessment of Endocrine Disrupting Compounds at the Wastewater Treatment Works in Pietermaritzburg (South Africa). *Science of the Total Environment*.(468-469). 584-597.
- Badia-Fabregat, M., Oller, I., and Malato, S. (2017) Overview on Pilot-Scale Treatments and New and Innovative Technologies for Hospital Effluent. In *The Handbook of Environmental Chemistry*, 1–22.
- Martinez, J.L. (2008) Antibiotics and Antibiotic Resistance Genes in Natural Environments. *Science* 321 (5887), 365–367.
- Maszenan, A M, Liu, Y., Jern, W. (2011) Bioremediation of Wastewaters with Recalcitrant Organic Compounds and Metals by Aerobic Granules. *Biotechnology Advances* 29 (1), 111–123.
- McAndrew, A. (2005) An Introduction to Digital Image Processing with Matlab Notes for SCM2511 Image Processing 1. *Image Rochester NY* 1 (1), 1–13.
- McAvoy, K. (2008) Occurrence of Estrogen in Wastewater Treatment Plant and Waste Disposal Site Water Samples. *Clearwaters*,: 28–34.
- McSwain, B.S., Irvine, R.L., Hausner, M., and Wilderer, P.A. (2005) Composition and Distribution of Extracellular Polymeric Substances in Aerobic Flocs and Granular Sludge. *Applied and Environmental Microbiology* 71 (2), 1051–1057.

- Barros, A.R.M., Argenta, T.S., de Carvalho, C.A., Oliveira, F.S., Firmino, P.I.M., and dos Santos, A.B. (2021) Effects of the Antibiotics Trimethoprim (TMP) and Sulfamethoxazole (SMX) on Granulation, Microbiology, and Performance of Aerobic Granular Sludge Systems. *Chemosphere* 262, 127840.
- Mery-Araya, C., Lear, G., Perez-Garcia, O., Astudillo-Garcia, C., and Singhal, N. (2019) Using Carbon Substrate as a Selection Pressure to Enhance the Potential of Aerobic Granular Sludge Microbial Communities for Removing Contaminants of Emerging Concern. *Bioresource Technology* 290, 121705.
- Mesquita, D.P., Amaral, A.L., and Ferreira, E.C. (2011a) Characterization of Activated Sludge Abnormalities by Image Analysis and Chemometric Techniques. *Analytica Chimica Acta* 705 (1–2), 235–242.
- Mesquita, D. P., Amaral, A.L., and Ferreira, E.C (2011b) Identifying Different Types of Bulking in an Activated Sludge System through Quantitative Image Analysis. *Chemosphere* 85 (4), 643–652.
- Mesquita, D. P., Dias, O., Amaral, A.L., and Ferreira, E.C. (2009) Monitoring of Activated Sludge Settling Ability through Image Analysis: Validation on Full-Scale Wastewater Treatment Plants. *Bioprocess and Biosystems Engineering* 32 (3), 361–367.
- Mesquita, D. P., Dias, O., Amaral, A.L., and Ferreira, E.C. (2010a) A Comparison between Bright Field and Phase-Contrast Image Analysis Techniques in Activated Sludge Morphological Characterization. *Microscopy and Microanalysis* 16 (2), 166–174.
- Mesquita, D., Dias, O., Elias, R.A.V., Amaral, A.L., and Ferreira, E.C. (2010b) Dilution and Magnification Effects on Image Analysis Applications in Activated Sludge Characterization, *Microscopy and Microanalysis* 16(5), 561–568.
- Mesquita, D.P., Dias, O., Amaral, A.L., and Ferreira, E.C. (2008) Relationship Between Sludge Volume Index and Biomass Structure Within Activated Sludge Systems . Proceedings of the XVII Congresso Brasileiro de Engenharia Química, Recife, 7 p. CD-ROM.
- Mesquita, D. (2010) Image Analysis and Chemometric Tools to Characterize Aggregated and Filamentous Bacteria in Activated Sludge Process. PhD Dissertation, University of Minho.

- Mesquita, D.P., Amaral, A.L., and Ferreira, E.C. (2013) Activated Sludge Characterization through Microscopy: A Review on Quantitative Image Analysis and Chemometric Techniques. *Analytica Chimica Acta* 802, 14–28.
- Mesquita, D.P., Amaral, A.L., Leal, C., Carvalheira, M., Cunha, J.R., Oehmen, A., Reis, M.A.M., and Ferreira, E.C. (2014) Monitoring Intracellular Polyphosphate Accumulation in Enhanced Biological Phosphorus Removal Systems by Quantitative Image Analysis. *Water Science and Technology* 69 (11), 2315–2323.
- Mesquita, D.P., Amaral, A.L., Leal, C., Oehmen, A., Reis, M.A.M., and Ferreira, E.C. (2015) Polyhydroxyalkanoate Granules Quantification in Mixed Microbial Cultures Using Image Analysis: Sudan Black B versus Nile Blue A Staining. *Analytica Chimica Acta* 865 (1), 8–15.
- Mesquita, D.P., Leal, C., Cunha, J.R., Oehmen, A., Amaral, A.L., Reis, M.A.M., and Ferreira, E.C. (2013) Prediction of Intracellular Storage Polymers Using Quantitative Image Analysis in Enhanced Biological Phosphorus Removal Systems. *Analytica Chimica Acta* 770, 36–44.
- Meyer, R. L., Saunders, A.M., Zeng, R.J., Keller, J., and Blackall, L.L. (2003) Microscale Structure and Function of Anaerobic-Aerobic Granules Containing Glycogen Accumulating Organisms. *FEMS Microbiology Ecology* 45 (3), 253–261.
- Michael, I., Rizzo, L., Mc Ardell, C.S., Manaia, C.M., Merlin, C., Schwartz, T., Dagot, C., Fatta-Kassinos, D. (2013) Urban Wastewater Treatment Plants as Hotspots for the Release of Antibiotics in the Environment: A Review. *Water Research* 47 (3), 957–995.
- Miège, C., Choubert, J.M., Ribeiro, L., Eusèbe, M., and Coquery, M. (2009) Fate of Pharmaceuticals and Personal Care Products in Wastewater Treatment Plants - Conception of a Database and First Results. *Environmental Pollution* 157 (5), 1721–17226.
- Mihciokur, H., and Oguz, M. (2016) Removal of Oxytetracycline and Determining Its Biosorption Properties on Aerobic Granular Sludge. *Environmental Toxicology and Pharmacology* 46, 174–182.
- Milobeldzka, A., Witeska, A., and Lski, A.M. (2016) Factors Affecting Population of Filamentous Bacteria in Wastewater Treatment Plants with Nutrients Removal. *Water Science and Technology* 73 (4), 790–797.
- Mohapatra, D.P., Brar, S.K., Tyagi, R.D., Picard, P., and Surampalli, R.Y. (2014) Analysis and Advanced

Oxidation Treatment of a Persistent Pharmaceutical Compound in Wastewater and Wastewater Sludge-Carbamazepine. *Science of the Total Environment* 470–471, 58–75.

Molina, M.A., Acuña Pérez, C.A., and Leiva, C.A. (2020) Characterization of Filamentous Floccs to Predict Sedimentation Parameters Using Image Analysis. *Journal of Sensors* Article ID 5248509, 8 pages, 2020.

Mosquera-Corral, A., De Kreuk, M.K., Heijnen, J.J., and Van Loosdrecht, M.C.M. (2005) Effects of Oxygen Concentration on N-Removal in an Aerobic Granular Sludge Reactor. *Water Research* 39 (12), 2676–2686.

da Motta, M. Pons, M. N., Vivier, H., Amaral, A.L., Ferreira, E.C., Roche, N., and Mota, M. (2001) The Study of Protozoa Populations in Wastewater Treatment Plants by Image Analysis. *Brazilian Journal of Chemical Engineering* 18 (01), 103–111.

Mückter, H. (2006). Antibiotika-Rückstände im Trinkwasser. 47. Arbeitstagung des Arbeitsgebiets Lebensmittelhygiene, Garmisch-Partenkirchen.

Muñoz-Palazon, B., Pesciaroli, C., Rodriguez-Sanchez, A., Gonzalez-Lopez, J., and Gonzalez-Martinez, A. (2018) Pollutants Degradation Performance and Microbial Community Structure of Aerobic Granular Sludge Systems Using Inoculums Adapted at Mild and Low Temperature. *Chemosphere* 204, 431–441.

Nancharaiah, Y.V., Reddy G.K.K. (2018) Aerobic Granular Sludge Technology: Mechanisms of Granulation and Biotechnological Applications. *Bioresource Technology* 247, 1128–1143.

Nancharaiah, Y. V., and Sarvajith, M. (2019) Aerobic Granular Sludge Process: A Fast Growing Biological Treatment for Sustainable Wastewater Treatment. *Current Opinion in Environmental Science and Health* 12, 57–65.

Nereda ® (2020) Nereda Sewage Treatment Plants on 5 Continents. Accessed December 21, 2020. <https://www.royalhaskoningdhv.com/Nereda>.

Nguyen Quoc, B., Wei, S., Armenta, M., Bucher, R., Sukapanpotharam, P., Stahl, D.A., Stensel, H.D., and Winkler, M.K.H. (2021) Aerobic Granular Sludge: Impact of Size Distribution on Nitrification Capacity. *Water Research* 188, 116445.

- Nor Anuar, A., Ujang, Z., van Loosdrecht, M.C.M. and de Kreuk, M.K. (2007) Settling Behaviour of Aerobic Granular Sludge. *Water Science and Technology* 56 (7), 55–63.
- Nor Anuar, A., Ujang, Z., Dahalan, F.A., van Loosdrecht M.C.M. and Olsson, G. (2008). Physical Strength of Aerobic Granular Sludge (AGS). *Int. Conf & Expo on Environmental Management and Technologies*, Kuala Lumpur, Malaysia
- Pal, A., Gin, K.Y.-H., Lin, A.Y.-C., and Reinhard, M. (2010) Impacts of Emerging Organic Contaminants on Freshwater Resources: Review of Recent Occurrences, Sources, Fate and Effects. *Science of the Total Environment* 408 (24), 6062–6069.
- Pandolfi, D., and Pons, M.N. (2004) Gram-Staining Characterisation of Activated Sludge Filamentous Bacteria by Automated Colour Analysis. *Biotechnology Letters* 26 (24), 1841–1846.
- Panter, G.H., Thompson, R.S., Beresford, N., and Sumpter, J.P. (1999) Transformation of a Non-Oestrogenic Steroid Metabolite to an Oestrogenically Active Substance by Minimal Bacterial Activity. *Chemosphere* 38 (15): 3579–3596.
- Park, M., Anumol, T., and Snyder, S.A. (2015) Modeling Approaches to Predict Removal of Trace Organic Compounds by Ozone Oxidation in Potable Reuse Applications. *Environmental Science: Water Research and Technology* 1 (5), 699–708.
- Paulo, A.M.S., Amorim, C.L., Costa, J., Mesquita, D.P., Ferreira, E.C., and Castro, P.M.L. (2021) Long-Term Stability of a Non-Adapted Aerobic Granular Sludge Process Treating Fish Canning Wastewater Associated to EPS Producers in the Core Microbiome. *Science of The Total Environment* 756, 144007.
- Pawlowski, S., Van Aerle, R., Tyler, C.R., and Braunbeck, T. (2004) Effects of 17 α -Ethinylestradiol in a Fathead Minnow (*Pimephales Promelas*) Gonadal Recrudescence Assay. *Ecotoxicology and Environmental Safety* 57 (3), 330–345.
- Petrie, B., Barden, R., and Kasprzyk-Hordern, B. (2014) A Review on Emerging Contaminants in Wastewaters and the Environment: Current Knowledge, Understudied Areas and Recommendations for Future Monitoring. *Water Research* 72, 3–27.
- Pishgar, R., Dominic, J.A., Tay, J.H., and Chu, A. (2020) Pilot-Scale Investigation on Nutrient Removal Characteristics of Mineral-Rich Aerobic Granular Sludge: Identification of Uncommon Mechanisms.

Water Research 168, 115151.

- Platikanov, S., Rodriguez-Mozaz, S., Huerta, B., Barceló, D., Cros, J., Batle, M., Poch, G., and Tauler, R. (2014) Chemometrics Quality Assessment of Wastewater Treatment Plant Effluents Using Physicochemical Parameters and UV Absorption Measurements. *Journal of Environmental Management* 140, 33–44.
- Polesel, F., Andersen, H.R., Trapp, S., and Plósz, B.G. (2016). Removal of antibiotics in biological wastewater treatment systems – A critical assessment using the Activated Sludge Modelling framework for Xenobiotics (ASM-X). *Environmental Science and Technology* 50, 10316–10334.
- Pomati, F., Castiglioni, S., Zuccato, E., Fanelli, R., Vigetti, D., Rossetti, C., and Calamari, D. (2006) Effects of a Complex Mixture of Therapeutic Drugs at Environmental Levels on Human Embryonic Cells. *Environmental Science and Technology* 40 (7), 2442–2447.
- Pronk, M., Bassin, J. P., De Kreuk, M. K., Kleerebezem, R., and Van Loosdrecht, M.C.M. (2014) Evaluating the Main and Side Effects of High Salinity on Aerobic Granular Sludge. *Applied Microbiology and Biotechnology* 98 (3), 1339–1348.
- Pronk, M., de Kreuk, M.K., de Bruin, B., Kamminga, P., Kleerebezem, R., and van Loosdrecht, M.C.M. (2015) Full Scale Performance of the Aerobic Granular Sludge Process for Sewage Treatment. *Water Research* 84, 207–217.
- Pronk, M., Neu, T.R., van Loosdrecht, M.C.M., and Lin, Y.M. (2017) The Acid Soluble Extracellular Polymeric Substance of Aerobic Granular Sludge Dominated by *Deffluviicoccus* Sp. *Water Research* 122, 148–158.
- Purba, L.D.A., Ibiyeye, H.T., Yuzir, A., Mohamad, S.E., Iwamoto, K., Zamyadi, A., and Abdullah, N. (2020) Various Applications of Aerobic Granular Sludge: A Review. *Environmental Technology and Innovation* 20, 101045.
- Qin, L., Liu, Y., and Tay J.H. (2004) Effect of Settling Time on Aerobic Granulation in Sequencing Batch Reactor. *Biochemical Engineering Journal* 21 (1), 47–52.
- Quintelas, C., Mesquita, D.P., Ferreira, E.C., and Amaral, A.L. (2019) Quantification of Pharmaceutical Compounds in Wastewater Samples by near Infrared Spectroscopy (NIR). *Talanta* 194, 507–513.

- Racz, L.A., and Goel, R.K. (2010) Fate and Removal of Estrogens in Municipal Wastewater. *Journal of Environmental Monitoring* 12 (1), 58–70.
- Radjenović, J., Petrović, M., and Barceló, D. (2009) Fate and Distribution of Pharmaceuticals in Wastewater and Sewage Sludge of the Conventional Activated Sludge (CAS) and Advanced Membrane Bioreactor (MBR) Treatment. *Water Research* 43 (3), 831–841.
- Ranzinger, F., Matern, M., Layer, M., Guthausen, G., Wagner, M., Derlon, N., and Horn, H. (2020) Transport and Retention of Artificial and Real Wastewater Particles inside a Bed of Settled Aerobic Granular Sludge Assessed Applying Magnetic Resonance Imaging. *Water Research* 177, 100050.
- Rodriguez-Sanchez, A., Margareto, A., Robledo-Mahon, T., Aranda, E., Diaz-Cruz, S., Gonzalez-Lopez, J., Barcelo, D., Vahala, R., and Gonzalez-Martinez, A. (2017) Performance and Bacterial Community Structure of a Granular Autotrophic Nitrogen Removal Bioreactor Amended with High Antibiotic Concentrations. *Chemical Engineering Journal* 325, 257–269.
- Rusanowska, P., Cydzik-Kwiatkowska, A., Świątczak, P., and Wojnowska-Baryła, I. (2019) Changes in Extracellular Polymeric Substances (EPS) Content and Composition in Aerobic Granule Size-Fractions during Reactor Cycles at Different Organic Loads. *Bioresource Technology* 272, 188–193.
- Russ, J.C. (2002) *The Image Processing Handbook*. Fourth edi. Boca Raton: CRC Press.
- Sacher, F., Lange, F.T., Brauch, H.-J., and Blankenhorn, I. (2001). Pharmaceuticals in groundwaters: analytical methods and results of a monitoring program in BadenWuerttemberg, Germany. *Journal of Chromatography A* 938 (1–2): 199–210.
- Salgado, R., Marques, R., Noronha, J. P., Carvalho, G., Oehmen, A., and Reis, M.A.M. (2012) Assessing the Removal of Pharmaceuticals and Personal Care Products in a Full-Scale Activated Sludge Plant. *Environmental Science and Pollution Research* 19 (5), 1818–1827.
- Santos, J.L., Aparicio, I., Callejón, M., and Alonso, E. (2009) Occurrence of Pharmaceutically Active Compounds during 1-Year Period in Wastewaters from Four Wastewater Treatment Plants in Seville (Spain). *Journal of Hazardous Materials* 164 (2–3), 1509–1516.
- Sarma, S.J., and Tay, J.H. (2018) Aerobic Granulation for Future Wastewater Treatment Technology: Challenges Ahead. *Environmental Science: Water Research and Technology* 4 (1), 9–15.

- Sarmah, A.K., Northcott, G.L., Leusch, F.D.L., and Tremblay, L.A. (2006a) A Survey of Endocrine Disrupting Chemicals (EDCs) in Municipal Sewage and Animal Waste Effluents in the Waikato Region of New Zealand. *Science of the Total Environment* 355 (1–3), 135–144.
- Sarmah, A.K., Meyer, M.T., and Boxall, A.B.A. (2006b) A Global Perspective on the Use, Sales, Exposure Pathways, Occurrence, Fate and Effects of Veterinary Antibiotics (VAs) in the Environment. *Chemosphere* 65 (5), 725–759.
- Seki, M., Fujishima, S., Nozaka, T., Maeda, M., and Kobayashi, K. (2006) Comparison of Response to 17 β -Estradiol and 17 β -Trenbolone among Three Small Fish Species. *Environmental Toxicology and Chemistry* 25 (10), 2742–2752.
- Sheng, G.P., Li, A.J., Li, X.Y., and Yu, H.Q. (2010) Effects of Seed Sludge Properties and Selective Biomass Discharge on Aerobic Sludge Granulation. *Chemical Engineering Journal* 160 (1), 108–114.
- Shi, Y.J., Wang, X.W., Qi, Z., Diao, M.H., Gao, M.M., Xing, S.F., Wang, S.G., and Zhao, X.C., (2011) Sorption and Biodegradation of Tetracycline by Nitrifying Granules and the Toxicity of Tetracycline on Granules. *Journal of Hazardous Materials* 191 (1–3), 103–109.
- Shin, S.G., Ahn, Y., Park, C., Choi, Y.K., Cho, H.M., and Cho, S.K., 2019. Size and Morphological Analyses of Ultrasonicated Hydrogen-Producing Granules Using a Simple Method. *International Journal of Hydrogen Energy* 44 (4), 2246–2252.
- Singh, K.P., Malik, A., Mohan, D., Sinha, S., and Singh, V.K. (2005) Chemometric Data Analysis of Pollutants in Wastewater - A Case Study. *Analytica Chimica Acta* 532
- Sodré, F.F., Locatelli, M.A.F., Montagner, C.C., and Jardim, W.F. (2007) Origem E Destino De Interferentes Endócrinos Em Águas Naturais. *Caderno Temático*. Vol. 06. Campinas.
- Solomon, G.M., and Schettler, T. (2000) Environment and Health: 6. Endocrine Disruption and Potential Human Health Implications. *Cmaj* 163 (11), 1471–1476.
- Soto, A.M., Justicia, H., Wray, J.W., and Sonnenschein, C. (1991) P-Nonyl-Phenol: An Estrogenic Xenobiotic Released from modified Polystyrene. *Environmental Health Perspectives* 92, 167–173.
- APWA (2017). *Standard Methods for the Examination of Water and Wastewater, 23rd Edition*. American

Public Health Association, American Water Works Association, Water Environment Federation.

Straub, J.O. (2016) Aquatic Environmental Risk Assessment for Human Use of the Old Antibiotic Sulfamethoxazole in Europe. *Environmental Toxicology and Chemistry* 35 (4), 767–779.

Stumpe, B., and Marschner, B. (2007) Long-Term Sewage Sludge Application and Wastewater Irrigation on the Mineralization and Sorption of 17 β -Estradiol and Testosterone in Soils. *Science of the Total Environment* 374 (2–3), 282–291.

Sulthana, A., Latha, K.C., Rathan, R., Sridhar, R., and Balasubramanian, S. (2014) Factor Analysis and Discriminant Analysis of Wastewater Quality in Vidyanayapuram Sewage Treatment Plant, Mysore, India: A Case Study. *Water Science and Technology* 69 (4), 810–818.

Svenson, A., Allard, A.S., and Ek, M. (2003) Removal of Estrogenicity in Swedish Municipal Sewage Treatment Plants. *Water Research* 37 (18), 4433–4443.

Swan, S.H., Liu, F., Overstreet, J.W., Brazil, C., and Skakkebaek, N.E. (2007) Semen Quality of Fertile US Males in Relation to Their Mothers' Beef Consumption during Pregnancy. *Human Reproduction* 22 (6), 1497–1502.

Świątczak, P., and Cydzik-Kwiatkowska, A. (2018) Performance and Microbial Characteristics of Biomass in a Full-Scale Aerobic Granular Sludge Wastewater Treatment Plant. *Environmental Science and Pollution Research* 25 (2), 1655–1669.

Tassew, F.A., Wenche Hennie Bergland, W.H., Dinamarca, C., and Bakke, R. (2019) Settling Velocity and Size Distribution Measurement of Anaerobic Granular Sludge Using Microscopic Image Analysis. *Journal of Microbiological Methods* 159, 81–90.

Tay, J.-H., Liu, Q.-S. and Liu, Y. (2001) Microscopic Observation of Aerobic Granulation in Sequential Aerobic Sludge Blanket Reactor. *Journal of Applied Microbiology* 91 (1), 168–175.

Ternes, T.A., Stumpf, M., Mueller, J., Haberer, K., Wilken, R.D., and Servos, M. (1999) Behavior and Occurrence of Estrogens in Municipal Sewage Treatment Plants - I. Investigations in Germany, Canada and Brazil. *Science of the Total Environment* 225 (1–2), 81–90.

Ternes, T.A., Andersen, H., Gilberg, D., and Bonerz, M. (2002) Determination of Estrogens in Sludge and Sediments by Liquid Extraction and GC/MS/MS. *Analytical Chemistry* 74 (14), 3498–3504.

- Ting, Y.F., and Praveena, S.M. (2017) Sources, Mechanisms, and Fate of Steroid Estrogens in Wastewater Treatment Plants: A Mini Review. *Environmental Monitoring and Assessment* 189 (4), 178.
- Tiwari, B., Sellamuthu, B., Ouarda, Y., Drogui, P., Tyagi, R.D., and Buelna, G. (2017) Review on Fate and Mechanism of Removal of Pharmaceutical Pollutants from Wastewater Using Biological Approach. *Bioresource Technology* 224, 1–12.
- Truong, H.T.B., Nguyen, P.T.T., and Bui, H.M. (2018a) Integration of Aerobic Granular Sludge and Membrane Filtration for Tapioca Processing Wastewater Treatment: Fouling Mechanism and Granular Stability. *Journal of Water Supply: Research and Technology - AQUA* 67 (8), 846–857.
- Truong, H.T.B., Van Nguyen, P., Nguyen, P.T.T and Bui, H.M. (2018b) Treatment of Tapioca Processing Wastewater in a Sequencing Batch Reactor: Mechanism of Granule Formation and Performance. *Journal of Environmental Management* 218, 39–49.
- Uslu, M.O., Jasim, S., Arvai, A., Bewtra, J., and Biswas, N. (2013) A Survey of Occurrence and Risk Assessment of Pharmaceutical Substances in the Great Lakes Basin. *Ozone: Science and Engineering* 35 (4), 249–262.
- Val del Río, A., Figueroa, M., Arrojo, B., Mosquera-Corral, A., Campos, J.L., García-Torriello, G., and R. Méndez, R. (2012) Aerobic Granular SBR Systems Applied to the Treatment of Industrial Effluents. *Journal of Environmental Management* 95, 88–92.
- Verawaty, M., Pijuan, M., Yuan, Z., and Bond, P. L. (2012) Determining the Mechanisms for Aerobic Granulation from Mixed Seed of Floccular and Crushed Granules in Activated Sludge Wastewater Treatment. *Water Research* 46 (3), 761–771.
- Verawaty, M., Tait, S., Pijuan, M., Yuan, Z., and Bond, P.L. (2013) Breakage and Growth towards a Stable Aerobic Granule Size during the Treatment of Wastewater. *Water Research* 47 (14), 5338–5349.
- Verbinnen, R.T., Nunes, G.S., and Vieira, E.M., 2010. Determinação de Hormônios Estrógenos Em Água Potável Usando CLAE-DAD. *Quimica Nova* 33 (9), 1837–1842.
- Vystavna, Y., Frkova, Z., Marchand, L., Vergeles, Y., and Stolberg, F. (2017) Removal Efficiency of Pharmaceuticals in a Full Scale Constructed Wetland in East Ukraine. *Ecological Engineering* 108, 50–58.

- Wan, X., Gao, M., Ye, M., Wang, Y.K., Xu, H., Wang, M., and Wang, X.H. (2018) Formation, Characteristics and Microbial Community of Aerobic Granular Sludge in the Presence of Sulfadiazine at Environmentally Relevant Concentrations. *Bioresource Technology* 250, 486–494.
- Wang, J., Lin, H., Sun, W., Xia, Y., Ma, J., Fu, J., Zhang, Z., Wu, H., and Qian, M. (2016). Variations in the Fate and Biological Effects of Sulfamethoxazole, Norfloxacin and Doxycycline in Different Vegetable-Soil Systems Following Manure Application. *Journal of Hazardous Materials* 304, 49–57.
- Wang, N., Guo, X., Xu, J., Hao, L., Kong, D., and Gao, S. (2015) Sorption and Transport of Five Sulfonamide Antibiotics in Agricultural Soil and Soil-Manure Systems. *Journal of Environmental Science Health B* 50 (1), 23–33.
- Wang, X.C., Shen, J.M. Chen, Z.L. Hao, X., and Xu, H. (2016) Removal of Pharmaceuticals from Synthetic Wastewater in an Aerobic Granular Sludge Membrane Bioreactor and Determination of the Bioreactor Microbial Diversity. *Applied Microbiology and Biotechnology* 100 (18), 8213–8223.
- Wang, X., Shen, J., Kang, J., Zhao, X., and Chen, Z. (2019) Mechanism of Oxytetracycline Removal by Aerobic Granular Sludge in SBR. *Water Research* 161, 308–318.
- Wang, Xi., Ratnaweera, H., Holm, J.A., and Olsbu, V. (2017) Statistical Monitoring and Dynamic Simulation of a Wastewater Treatment Plant: A Combined Approach to Achieve Model Predictive Control. *Journal of Environmental Management* 193, 1–7.
- Watkinson, A.J., Murby, E.J., and Costanzo, S.D. (2007) Removal of Antibiotics in Conventional and Advanced Wastewater Treatment: Implications for Environmental Discharge and Wastewater Recycling. *Water Research* 41 (18), 4164–4176.
- Watkinson, A.J., Murby, E.J., Kolpin, D.W., and Costanzo, S.D. (2009) The Occurrence of Antibiotics in an Urban Watershed: From Wastewater to Drinking Water. *Science of the Total Environment* 407 (8), 2711–2723.
- Wei, D., Zhang, K., Wang, S., Sun, B., Wu, N., Xu, W., Du, B., and Wei, Q. (2017) Characterization of Dissolved Organic Matter Released from Activated Sludge and Aerobic Granular Sludge Biosorption Processes for Heavy Metal Treatment via a Fluorescence Approach. *International Biodeterioration and Biodegradation* 124, 326–333.
- Weissbrodt, D.G., Neu, T.R., Kuhlicke, U., Rappaz, Y., and Holliger, C. (2013) Assessment of Bacterial

- and Structural Dynamics in Aerobic Granular Biofilms. *Frontiers in Microbiology* 4, 1–18.
- Wilén, B.M., Liébana, R., Persson, F., Modin, O., and Hermansson, M. (2018) The Mechanisms of Granulation of Activated Sludge in Wastewater Treatment, Its Optimization, and Impact on Effluent Quality. *Applied Microbiology and Biotechnology* 102 (12), 5005–5020.
- Winkler, M.K.H., Meunier, C., Henriot, O., Mahillon, J., Suárez-Ojeda, M.E., Del Moro, G., De Sanctis, M., Di Iaconi, C., and Weissbrodt, D.G. (2018) An Integrative Review of Granular Sludge for the Biological Removal of Nutrients and Recalcitrant Organic Matter from Wastewater. *Chemical Engineering Journal*, 336 489–502.
- Xia, Z., Xiao-Chun, W., Zhong-Lin, C., Hao, X., and Qing-Fang, Z. (2015) Microbial Community Structure and Pharmaceuticals and Personal Care Products Removal in a Membrane Bioreactor Seeded with Aerobic Granular Sludge. *Applied Microbiology and Biotechnology* 99 (1), 425–433.
- Xu, J., He, J., Wang, M., and Li, L. (2018) Cultivation and Stable Operation of Aerobic Granular Sludge at Low Temperature by Sieving out the Batt-like Sludge. *Chemosphere* 211: 1219–1227.
- Xue, W., Hao, T., Mackey, H.R., Li, X., Chan, R.C., and Chen, G. (2017) The Role of Sulfate in Aerobic Granular Sludge Process for Emerging Sulfate-Laden Wastewater Treatment. *Water Research* 124, 513–520.
- Yan, Q., Gao, X., Chen, Y.P., Peng, X.Y., Zhang, Y.X., Gan, X.M., Zi, C.F., and Guo, J.S. (2014) Occurrence, Fate and Ecotoxicological Assessment of Pharmaceutically Active Compounds in Wastewater and Sludge from Wastewater Treatment Plants in Chongqing, the Three Gorges Reservoir Area. *Science of the Total Environment* 470–471: 618–630.
- Yao, W.Y., Yang, G.J., Lu, C., Xu, T., Yuan, K., and Yang, S.S. (2014) The Characteristics of Biological Nutrient Removal in a SBR through Aerobic Granular Sludge. *Applied Mechanics and Materials* 522–524, 161–67.
- Yergeau, E., Lawrence, J.R., Waiser, M.J., Korber, D.R., and Greer, C.W. (2010) Metatranscriptomic Analysis of the Response of River Biofilms to Pharmaceutical Products, Using Anonymous DNA Microarrays. *Applied and Environmental Microbiology* 76 (16): 5432–5439.
- Yergeau, E., Sanschagrin, S., Waiser, M.J., Lawrence, J.R., and Greer, C.W. (2012) Sub-Inhibitory Concentrations of Different Pharmaceutical Products Affect the Meta-Transcriptome of River Biofilm Communities Cultivated in Rotating Annular Reactors. *Environmental Microbiology Reports*

4 (3), 350–359.

- Ying, G., Kookana, R.S., and Kumar, A. (2008). Fate of Estrogens and Xenoestrogens in Four Sewage Treatment Plants with Different Technologies. *Environmental Toxicology and Chemistry* 27 (1), 87–94.
- Ying, G.G., Kookana, R.S., and Ru, Y.J. (2002) Occurrence and Fate of Hormone Steroids in the Environment. *Environment International* 28 (6), 545–551.
- Yu, Z., Zhang, Y., Zhang, Z., Dong, J., Fu, J., Xu, X., Zhu, L. (2020) Enhancement of PPCPs Removal by Shaped Microbial Community of Aerobic Granular Sludge under Condition of Low C/N Ratio Influent. *Journal of Hazardous Materials* 394 (866), 122583.
- Yuan, S., Gao, M., Zhu, F., Afzal, M.Z., Wang, Y.K., Xu, H., Wang, M., Wang, S.G., and Wang, X.H. (2017) Disintegration of Aerobic Granules during Prolonged Operation. *Environmental Science: Water Research and Technology* 3 (4), 757–766.
- Zhang, C., Zhang, H., and Yang, F. (2015) Diameter Control and Stability Maintenance of Aerobic Granular Sludge in an A/O/A SBR. *Separation and Purification Technology* 149, 362–369.
- Zhang, Q.-Q., Bai, Y.-H., Wu, J., Xu, L.-Z., J., Zhu, W.-Q., Tian, G.-M., Zheng, P., Xu, X.-Y. and Jin, R.-C., 2019. Microbial Community Evolution and Fate of Antibiotic Resistance Genes in Anammox Process under Oxytetracycline and Sulfamethoxazole Stresses. *Bioresource Technology* 293, 122096.
- Zhao, B.-H., Sun, Q., Chen, J., Zhang, J., Zhang, X.-Y., Liu, B.J., and Li. J., (2020) 17 Beta-Estradiol Biodegradation by Anaerobic Granular Sludge: Effect of Iron Sources. *Scientific Reports* 10 (7777)
- Zhao, X., Chen, Z., Wang, X., Li, J., Shen, J., and Xu, H. (2015) Remediation of Pharmaceuticals and Personal Care Products Using an Aerobic Granular Sludge Sequencing Bioreactor and Microbial Community Profiling Using Solexa Sequencing Technology Analysis. *Bioresource Technology* 179, 104–112.
- Zheng, X.-Y., He, Y.-J., Chen, W., Wang, M.-Y., Cao, S.-L., Ni, M., and Chen, Y. (2016) A Comparative Adsorption Study: 17 β -Estradiol onto Aerobic Granular Sludge and Activated Sludge. *Environmental Technology* 37 (1), 136-144.

- Zheng, X., Sun, P., Lou, J., Fang, Z., Guo, M., Song, Y., Tang, X., and Jiang, T. (2013) The Long-Term Effect of Nitrite on the Granule-Based Enhanced Biological Phosphorus Removal System and the Reversibility. *Bioresource Technology* 132, 333–341.
- Zheng, Y.-M., Yu, H.-Q., Liu, S.-J., and Liu, X.-Z. (2006) Formation and Instability of Aerobic Granules under High Organic Loading Conditions. *Chemosphere* 63 (10), 1791–1800.
- Zhou, J.-H., Zhang, Z.-M., Zhao, H., Yu, H.-T., Alvarez, P.J.J., and Xu, X.-Y. (2016) Optimizing Granules Size Distribution for Aerobic Granular Sludge Stability : Effect of a Novel Funnel-Shaped Internals on Hydraulic Shear Stress. *Bioresource Technology* 216 (866), 562–570.
- Zhou, Y., Zha, J., Xu, Y., Lei, B., and Wang, Z. (2012) Occurrences of Six Steroid Estrogens from Different Effluents in Beijing, China. *Environmental Monitoring and Assessment* 184 (3), 1719–1729.
- Zhu, L., Yu, Y., Dai, X., Xu, X., and Qi, H. (2013) Optimization of Selective Sludge Discharge Mode for Enhancing the Stability of Aerobic Granular Sludge Process. *Chemical Engineering Journal* 217, 442–446.
- Zhu, L., Zhou, J., Yu, H., and Xu, X. (2015) Optimization of Hydraulic Shear Parameters and Reactor Configuration in the Aerobic Granular Sludge Process. *Environmental Technology* 36(13) 1605–1611.
- Zou, H., Du, G.-C., Ruan, W.-Q., and Chen, J. (2006) Role of Nitrate in Biological Phosphorus Removal in a Sequencing Batch Reactor. *World Journal of Microbiology and Biotechnology* 22 (7), 701–706.
- Zuccato, E., Castiglioni, S., Bagnati, R., Melis, M., and Fanelli, R. (2010) Source, Occurrence and Fate of Antibiotics in the Italian Aquatic Environment. *Journal of Hazardous Materials* 179 (1–3), 1042–1048.

SCIENTIFIC OUTPUT

Articles in international Journals with peer-review

- Sludge volume index and suspended solids estimation of mature aerobic granular sludge by quantitative image analysis and chemometric tools (Cristiano S. Leal, Ángeles Val del Río, Daniela P. Mesquita, António L. Amaral, Paula M.L. Castro, Eugénio C. Ferreira). *Separation and Purification Technology* 234(116049), 2020.
- Environmental impact and biological removal processes of pharmaceutically active compounds: The particular case of sulfonamides, anticonvulsants and steroid estrogens (Cristiano S. Leal, Daniela P. Mesquita, António Luís Amaral, Almerinda M. Amaral & Eugénio C. Ferreira). *Critical Reviews in Environmental Science and Technology*, 50:7, 698-742 2020.
- Validation of a quantitative image analysis methodology for the assessment of the morphology and structure of aerobic granular sludge in the presence of pharmaceutically active compounds (Cristiano Leal, Ángeles Val del Río, Eugénio Ferreira, Daniela Mesquita, António Amaral) submitted.
- Assessment of an aerobic granular sludge system in the presence of pharmaceutically active compounds by quantitative image analysis and chemometric techniques (Cristiano S. Leal, Mariana Lopes, Angeles Val del Río, Cristina Quintelas, Paula M.L. Castro, Eugénio C. Ferreira, A. Luís Amaral, Daniela P. Mesquita) submitted.
- Prediction of density and suspended solids of aerobic granular sludge in the presence of pharmaceutically active compounds by quantitative image analysis and chemometric tools (in preparation)

Abstract in international congress

- Density and sludge volume index estimation in mature aerobic granular sludge by quantitative image analysis and chemometrics tools (Leal, Cristiano; Val del Río, Angeles; Zlatkova, Anastasiya; Araújo, Bárbara; Mesquita, Daniela P.; Amaral, A. Luís; Ferreira, Eugénio C)- CHEMPOR 2018 - 13th International Chemical and Biological Engineering Conference (Book of Extended Abstracts). Aveiro, Portugal, (02-04/10/2018), 238-239, 2018.

APPENDICES

Section 1 Chemical properties and metabolic pathways of the studied PhAC

In this section 1 will be presented the main chemical properties and metabolic pathways of the studied PhAC.

Table I Main chemical properties and metabolic pathways of E2

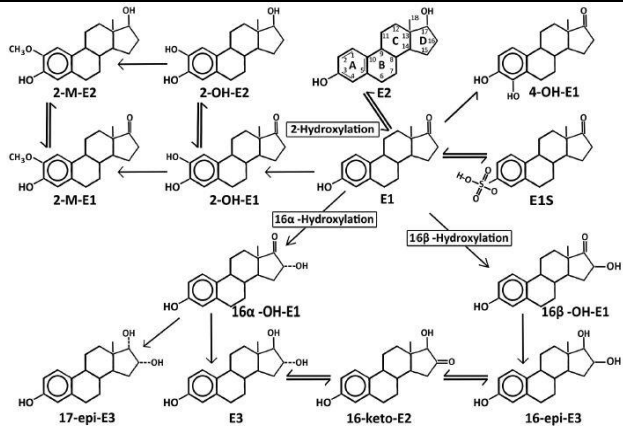
E2	
Formula, CAS number and molecular weight	$C_{18}H_{24}O_2$; 50-28-2; 272.4 g mol ⁻¹
Water solubility	13mg L ⁻¹ (20 °C) (Ying <i>et al.</i> , 2002)
Log Kow (octanol–water)	3.94 (Ying <i>et al.</i> , 2002)
pKa	10.6 (Adeel <i>et al.</i> , 2017)
Elimination half-life	-
Excretion	Urine and feces (Laurenson <i>et al.</i> , 2014)
Metabolites found in wastewater	Estradiol-17-glucuronide; 17β-estradiol-3-glucuronide; 17β-estradiol-3-sulphate (Johnson <i>et al.</i> , 2004)
Metabolic pathways of E2 in humans (Mattison <i>et al.</i> 2014)	 <p>The diagram illustrates the metabolic pathways of estradiol (E2) in humans. E2 is converted to estrone (E1) via 17β-hydroxylation. E1 is then metabolized through several pathways: 2-hydroxylation to 2-OH-E1, which can be further methylated to 2-M-E1; 16α-hydroxylation to 16α-OH-E1, which can be further hydroxylated to 16-keto-E2 and 16-epi-E3; and 16β-hydroxylation to 16β-OH-E1, which can be further hydroxylated to 16-epi-E3. E2 is also converted to estradiol-4-OH (4-OH-E1) via 4-hydroxylation. The diagram shows the chemical structures of E2, E1, 2-OH-E1, 2-M-E1, 4-OH-E1, 16α-OH-E1, 16-keto-E2, 16-epi-E3, and 16β-OH-E1, along with the enzymes involved in these transformations.</p>
Dosage	-
Other information	-

Table II Main chemical properties and metabolic pathways of EE2

EE2	
Formula, CAS number and molecular weight	$C_{20}H_{24}O_2$; 57-63-6; 296.4 g mol ⁻¹
Water solubility	4.8 mg L ⁻¹ (at 20 °C) (Ying <i>et al.</i> , 2002)
Log Kow (octanol–water)	4.14 (Ying <i>et al.</i> , 2002)
pKa	10.4 (Adeel <i>et al.</i> , 2017)
Elimination half-life	-
Excretion	Urine and feces (Laurenson <i>et al.</i> 2014)
Metabolites found in wastewater	17α-ethinylestradiol-3-glucuronide; 17α-ethinylestradiol-3-sulphate (Jonhson <i>et al.</i> , 2004)

EE2	
Major metabolic pathways of EE2 in humans (Li <i>et al.</i> , 1999)	
Dosage	30-35 $\mu\text{g day}^{-1}$ (Johnson <i>et al.</i> , 2004)
Other information	-

Table III Main chemical properties of SMX and metabolic pathways

SMX	
Formula, CAS number and molecular weight	$\text{C}_{10}\text{H}_{11}\text{N}_3\text{O}_3\text{S}$; 723-46-6; 253.276 g mol^{-1}
Usage	Antimicrobial
Water solubility	610 mg L^{-1} (37 °C) (Drugbank 2016c)
Log Kow (octanol–water)	0.89 (Toxnet (2018))
pKa	$\text{pKa}_1 = 1.6$; $\text{pKa}_2 = 5.7$ (Boreen <i>et al.</i> , 2004)
Elimination half-life	-
Excretion	Urine and feces (Göbel <i>et al.</i> , 2005)
Metabolites in urine	(N4-acetyl-SMX); (SMX-N1-Glu, SMX-2-Glu) (Polesel <i>et al.</i> 2016)
Percentage of oral administration	50-75% (Polesel <i>et al.</i> , 2016)
Metabolic pathways of SMX in humans (Polesel <i>et al.</i> , 2016)	
Dosage	-
Other information	It is also used in Human and Veterinary medicine in combination with Trimethoprim (Raz <i>et al.</i> , 2002; Campbell <i>et al.</i> , 1999)

Section 2 Size descriptors obtained by QIA

The different QIA parameters determined for the AGS monitoring are presented below in table IV.

Table IV QIA parameters obtained for AGS monitoring purposes,

Variable	Definition	Calculation
<i>Global parameters</i>		
TL	Total filamentous bacteria length (per volume)	<i>n.a.</i>
Nb_{fil}	Total filamentous bacteria number (per volume)	<i>n.a.</i>
TL/TA_{floc}	Total filamentous bacteria length per total flocs area	$\frac{TL}{TA_{floc}}$
TL/TSS_{floc}	Total filamentous bacteria length per suspended TSS	$\frac{TL}{TSS_{floc}}$
TL/VSS_{floc}	Total filamentous bacteria length per suspended VSS	$\frac{TL}{VSS_{floc}}$
TA_{floc}	Total flocs area (per volume)	<i>n.a.</i>
Nb_{floc}	Total flocs number (per volume)	<i>n.a.</i>
TV_{gran}	Total granules volume (per volume)	<i>n.a.</i>
Nb_{gran}	Total granules number (per volume)	<i>n.a.</i>
<i>Parameters for each "i" class</i>		
Deq	Equivalent diameter	$De = 2\sqrt{A/\pi}$
P	Perimeter	<i>n.a.</i>
L	Major axis length ($Fmax$)	<i>n.a.</i>
W	Minor axis length ($Fmin$)	<i>n.a.</i>
$Area$	Floc area	<i>n.a.</i>
Vol	Granule volume	$Vol = \frac{\pi \times Width^2 \times Length}{6}$
FF	Form factor	$FF = \frac{P^2}{4\pi A}$
$Conv$	Convexity	$Conv = \frac{P}{P_{Conv}}$
$Comp$	Compactness	$Comp = \frac{\sqrt{4\pi/A}}{Fmax}$
$Round$	Roundness	$Round = \frac{4\pi A}{P_{Conv}^2}$
$Solid$	Solidity	$Sol = \frac{A}{A_{Conv}}$
Ext	Extent	$Ext = \frac{A}{Wbb \times Lbb}$
Ecc	Eccentricity	$Ecc = \frac{(4\pi)^2(M2x - M2y)^2 + 4M^2 2xy}{A^2}$
Rob	Robustness	$Rob = \frac{2er_{obj}}{\sqrt{A}}$
$Concav$	Concavity index	$MaiorConc = \frac{2er_{comp}}{\sqrt{A}}$
$RelArea$	Ratio between holes and object area	$Rel\ area = \frac{A_H}{A}$

Variable	Definition	Calculation
%Nb	Aggregates number percentage	$\% Nb = \frac{\sum_{i=1}^{N_{class}} N_i}{TNb}$
%Area	Flocs area percentage	$\% Area = \frac{\sum_{i=1}^{N_{class}} A_i}{TA}$
%Vol ^{..}	Granules volume percentage	$\% Vol = \frac{\sum_{i=1}^{N_{class}} Vol_i}{TVol}$
Nb	Total aggregates number (per volume)	n.a.
TA	Total flocs area (per volume)	n.a.
TV ^{..}	Total granules volume (per volume)	n.a.

n.a.; Not applicable

[·] The subscript "i" refers to F1, F2, F3, G1, G2 or G3.

^{..} These variables were only determined for the granules fraction

Pconv is the convex perimeter; Aconv is the convex area; Fmax is the maximum Feret diameter; A_i is the holes area; M2x and M2y are the central second moments with respect to x-axis and y-axis respectively, Wbb is the bounding box width; Lbb is the bounding box length; er_{obj} is the number of erosions needed to delete an object; er_{comp} is the number of erosions needed to delete the complement of an object in relation to its convex envelope; A_i is the Area of each aggregate belonging to the i size class; N_i is number of each aggregate belonging to the i size class; V_i is the volume of each aggregate belonging to the i size class.

Section 3 SBR-AGS physical and chemical parameters of synthetic wastewater, mixed liquor, and bed volume of sludge

Figure I presents the evolution of the temperature, pH (synthetic wastewater entering the SBR-AGS, aerobic phase and treated effluent) and bed volume of sludge during the different operational periods.

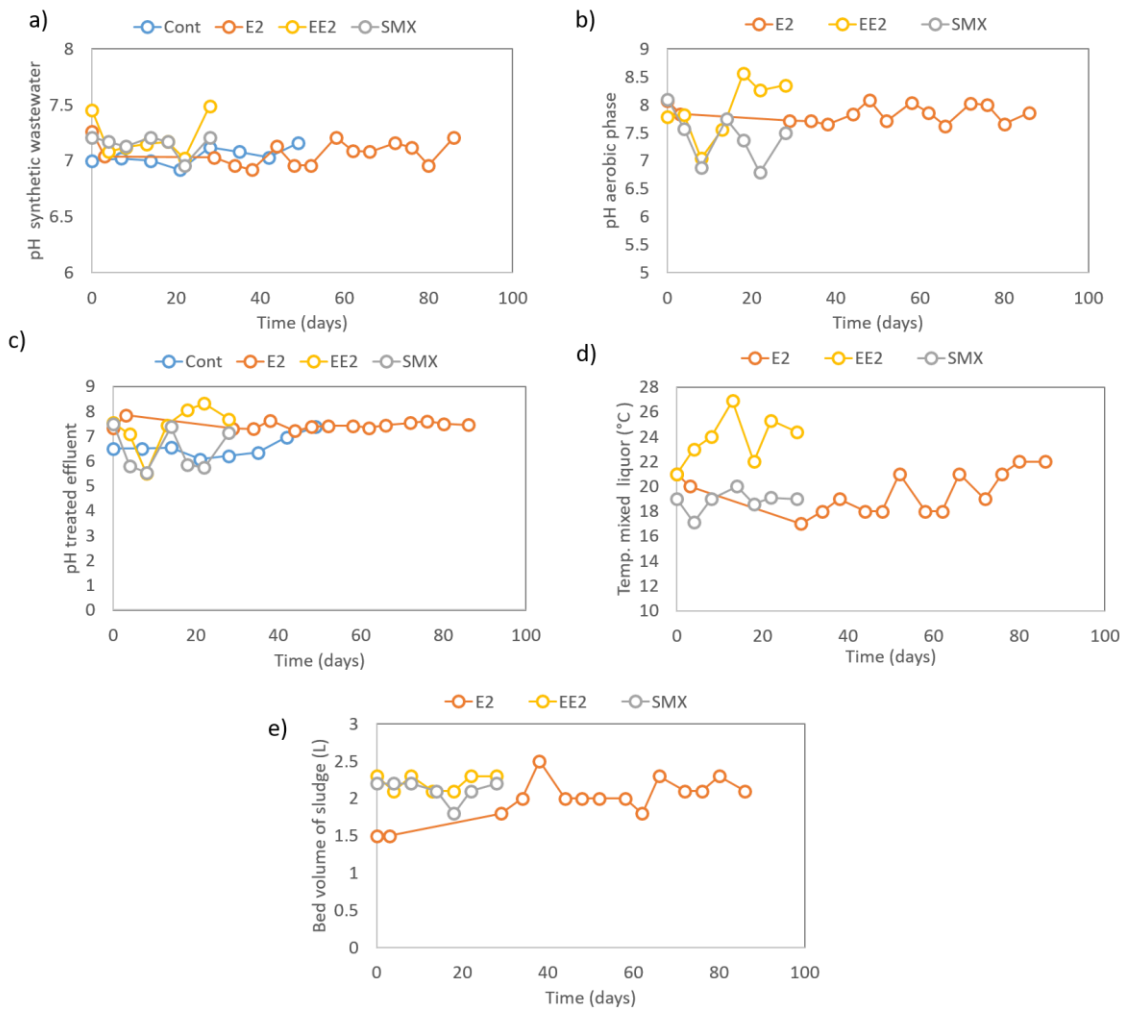


Figure I Evolution of pH and temperature of the SBR-AGS in the different operational periods a) pH of synthetic wastewater; b) pH at the beginning of aerobic phase; c) pH of treated wastewater; d) Temperature of mixed liquor; e) bed volume of sludge.

The evolution of the suspended solids (VSS and TSS) in the treated effluent and the nitrification capacity (% of NH_4^+ oxidation), during the different operational periods, is presented in Figure II.

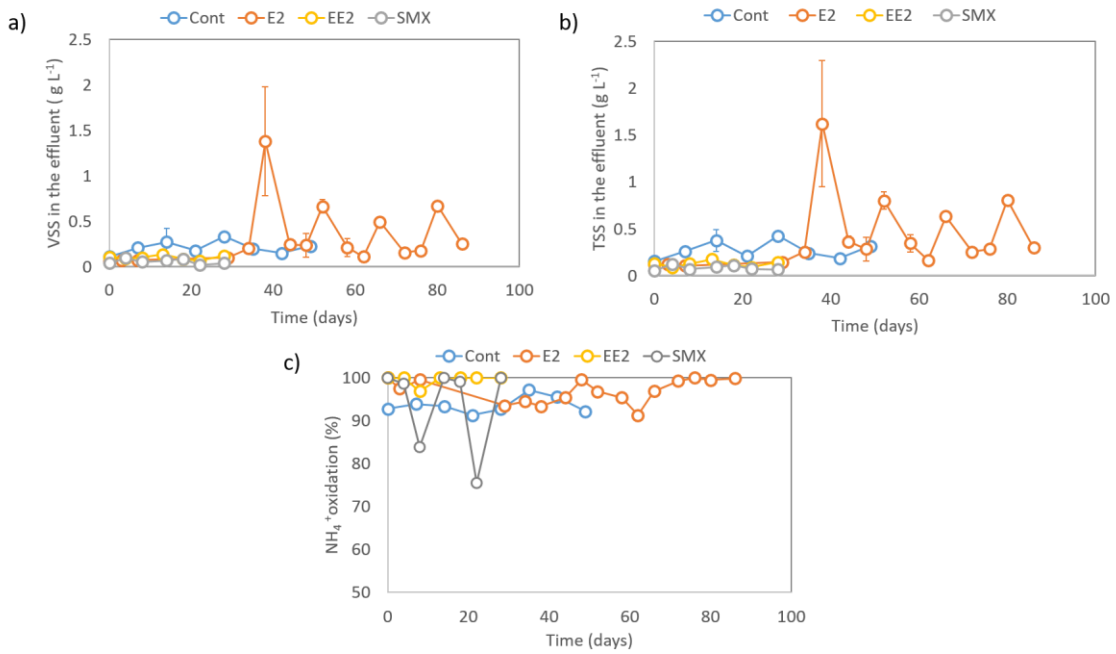


Figure II Evolution of suspended solids in the treated effluent during the different operational periods a) VSS b) TSS c) % of NH₄⁺ oxidation.

Section 4 Evolution of morphological and structural parameters during the monitoring period

In this section the evolution of relevant morphological and structural parameters of the sludge floccular and granular fractions, not introduced in the thesis body, will be presented. The evolution of the granule's and floc's apparent density during the different operational periods is presented in Figure III.

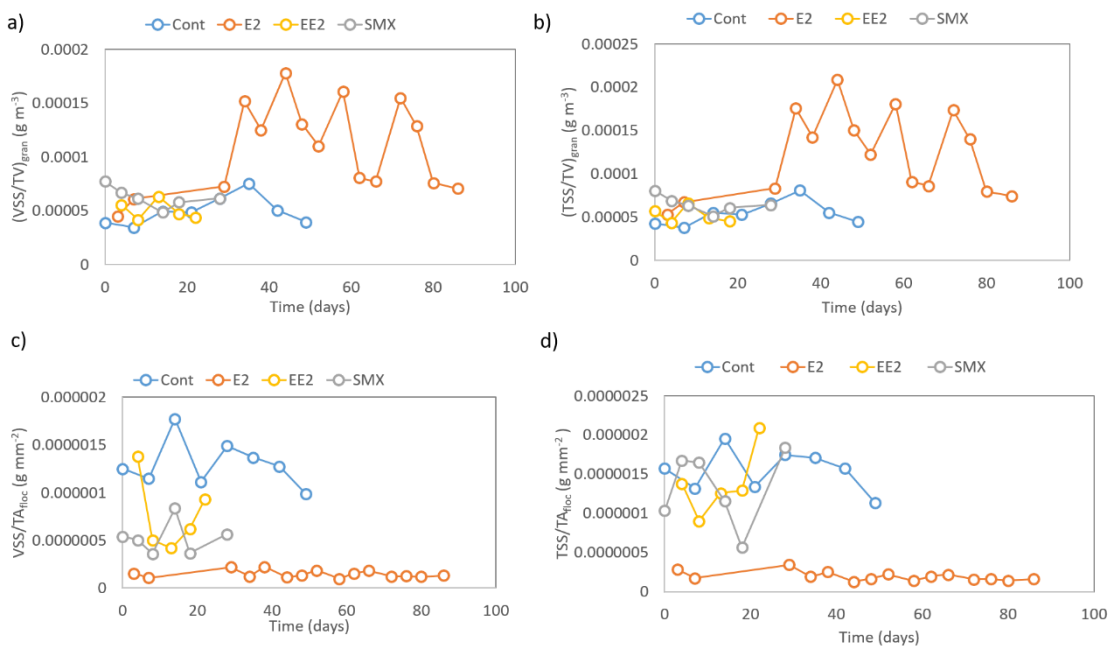


Figure III Evolution of the apparent density during the different operational periods a) granular fraction based on VSS b) granular fraction based on TSS c) floccular fraction based on VSS d) floccular fraction based on TSS.

The evolution of the aggregates (F1, F2, F3, G1 G2 and G3) contents (number) and relative percentages is presented in Figure IV.

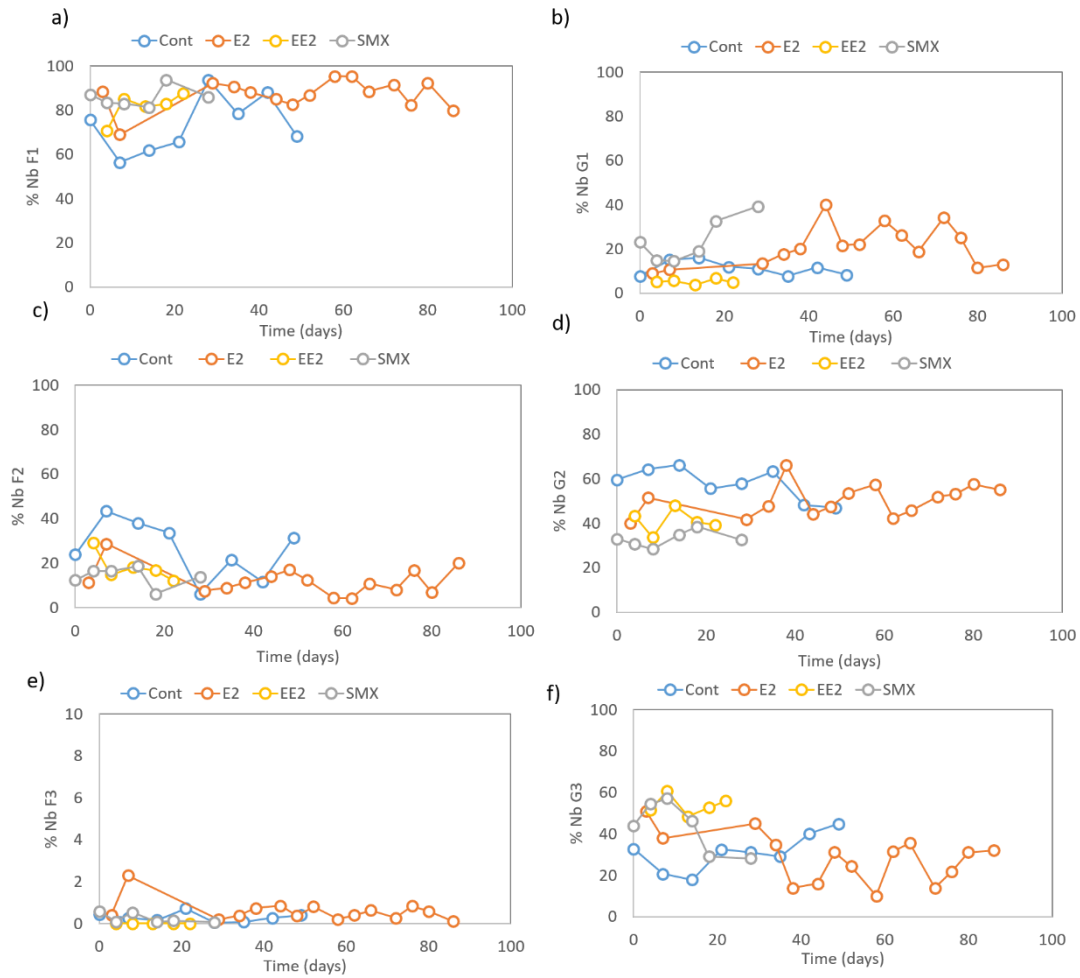


Figure IV Evolution of the aggregates relative percentages. a) F1 b) G1 c) F2 d) G2 e) F3 f) G3.

The evolution of the aggregates (overall, F1, F2, F3, G1 G2 and G3) size (diameter) is presented in Figure V

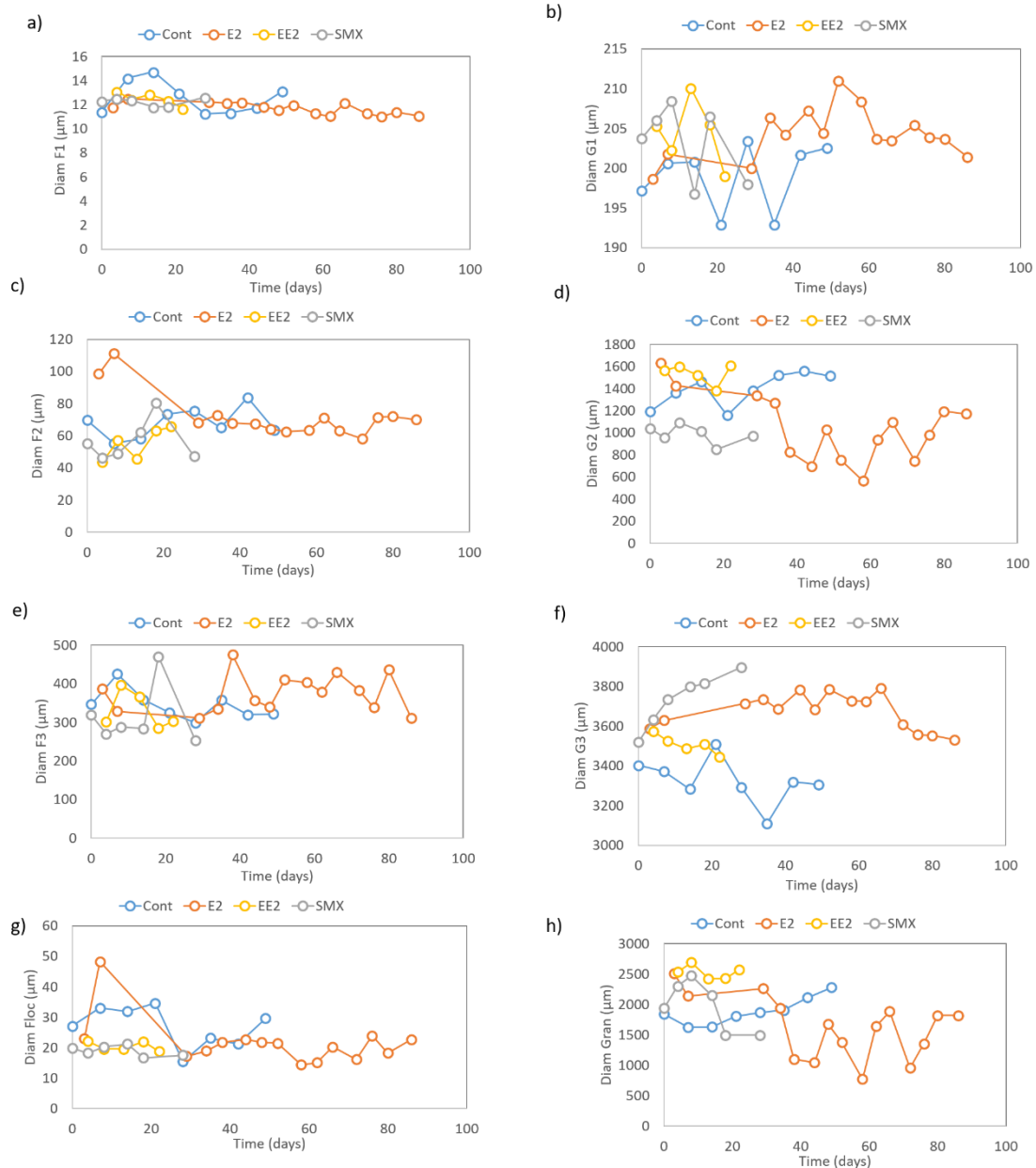


Figure V Evolution of the aggregates diameter. a) F1 b) G1 c) F2 d) G2 e) F3 f) G3 g) overall floc h) overall granules.

The evolution of the floccular fraction aggregates (overall, F1, F2 and F3) size (area) is presented in Figure VI.

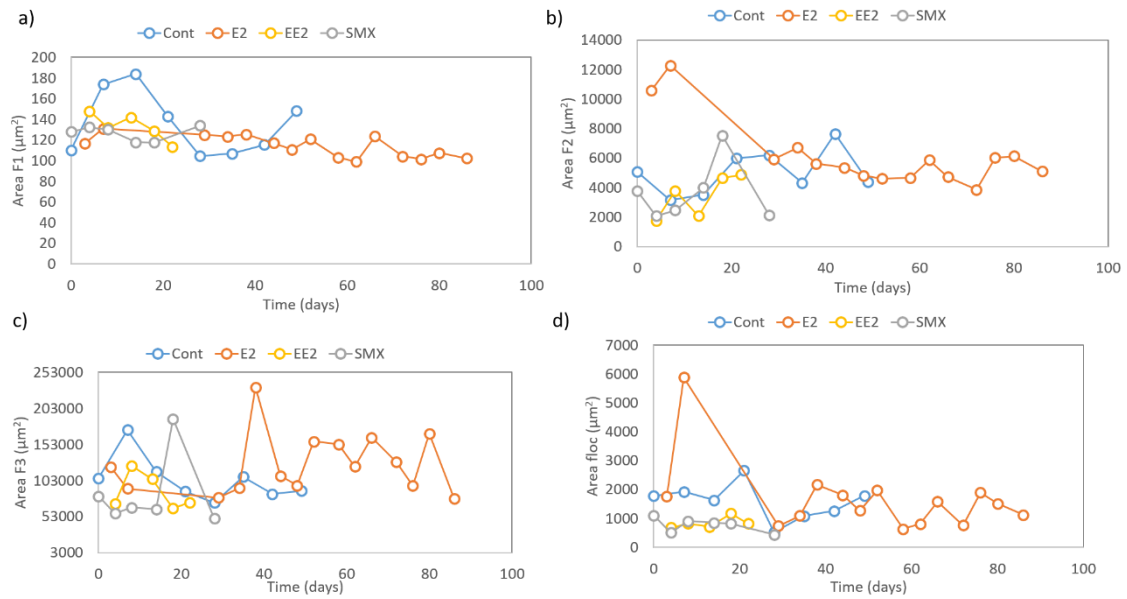


Figure VI Evolution of the floccular fractions aggregates area. a) F1 b) G1 c) F2 d) overall floccs.

The evolution of the granular fraction aggregates (overall, G1, G2 and G3) size (volume) is presented in Figure VII.

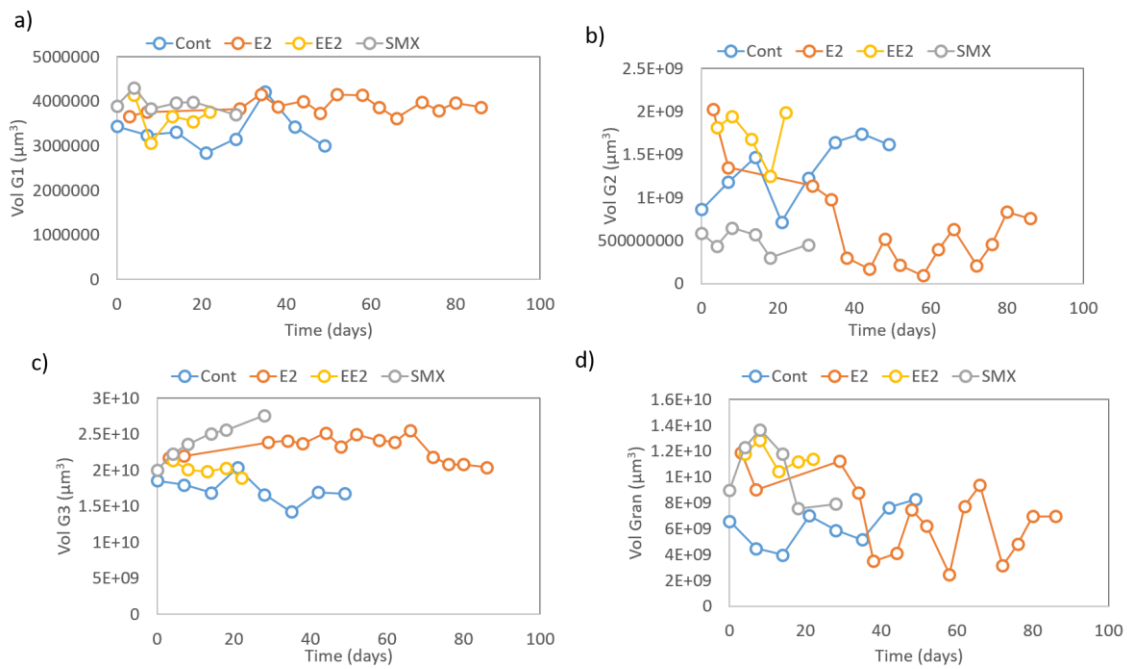


Figure VII Evolution of the granular fraction aggregates volume. a) G1 b) G2 c) G3 d) overall granules.

The evolution of the granules TV and number (nb) for the G1, G2 and G3 is presented in Figure VIII.

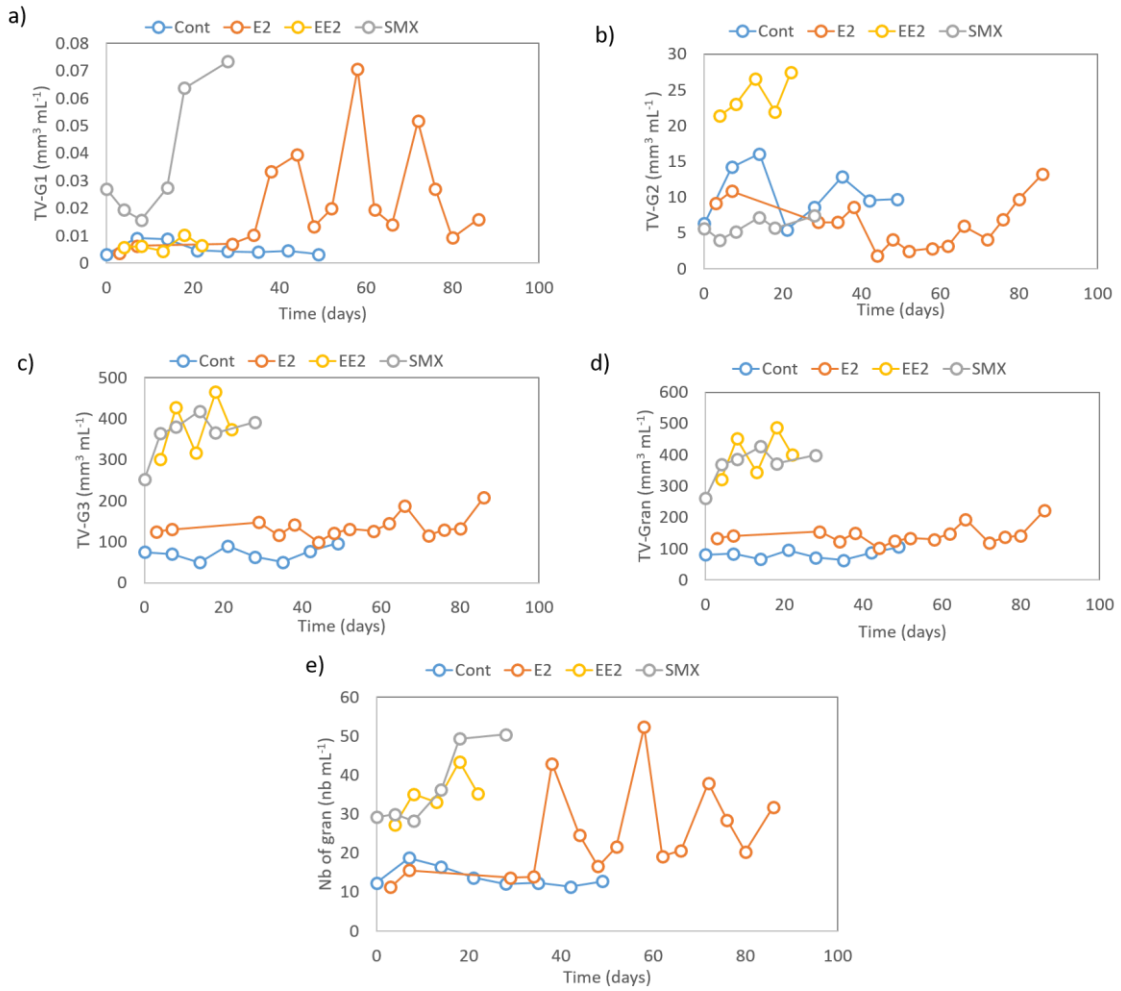


Figure VIII Evolution of the granular fraction TV (mm³ mL⁻¹) and contents (nb mL⁻¹). a) G1 b) G2 c) G3 d) overall granules e) Nb-G.

The evolution of the floccular fraction total aggregates area (TA) and number (Nb) is presented in Figure IX.

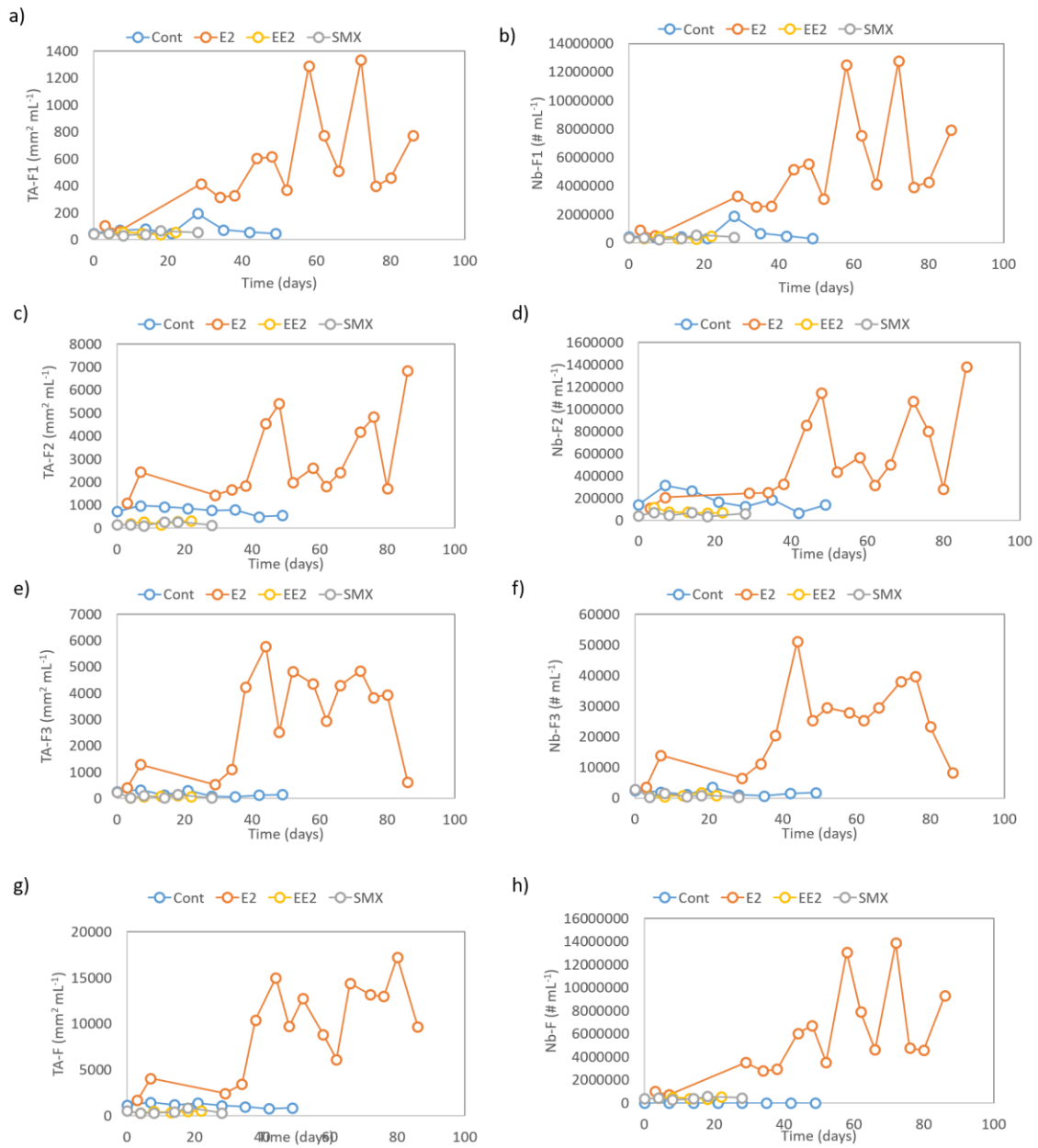


Figure IX Evolution of the floccular fraction TA and Nb. a) TA-F1 b) Nb-F1 c) TA-F2 d) Nb-F2 e) TA-F3 f) Nb-F3 g) TA-F h) Nb-F.